Poly(vinyl alcohol) and Methylglyoxal Hybrid Fibres for Antibacterial Wound Dressing Materials

Sophie Elizabeth Louise Bulman

Submitted in accordance with the requirements for the degree of

Doctor of Philosophy

The University of Leeds

School of Design

October 2015

The candidate confirms that the work submitted is her own, except where work which has formed part of jointly-authored publications has been included. The contribution of the candidate and the other authors to this work has been explicitly indicated below. The candidate confirms that appropriate credit has been given within the thesis where reference has been made to the work of others.

The work in Chapter 5 of the thesis has appeared in publications as follows:

Bulman Sophie E L, Goswami Parikshit, Tronci Giuseppe, Russell Stephen J and Carr Chris. Investigation into the potential use of poly(vinyl alcohol)/methylglyoxal fibres as antibacterial wound dressing components. Journal of Biomaterials Applications. 2015;29(8):1193-1200.

Sophie Elizabeth Louise Bulman was solely responsible for performing the experiments and doing the analysis. The other authors, Prof. Stephen J Russell, Dr. Parikshit Goswami, Dr. Giuseppe Tronci and Prof. Chris Carr, assisted with the reading, reviewing and planning the layout of the paper.

Acknowledgments

Firstly I would like to thank both of my supervisors, Professor Stephen J Russell and Dr. Parikshit Goswami for their continued support, enthusiasm and guidance throughout this PhD. This work would not have been possible without them. Secondly I would like to thank the Clothworkers' Foundation for the financial contribution and assistance in the experimental procedures during this research.

I would also like to thank, Dr. Jane Freeman, Mr. Peter Parnell, Mr. Paul Verity and Ms.Sally Pilling in the Infection control centre at the Leeds Pathology department for their constant friendly and helpful advice.

I would also like to thank Dr. Giuseppe Tronci of the Nonwovens Research Group and Dr.Algy Kazlauciunas from the School of Chemistry for their academic advice, help and support.

A special thanks to my dearest friends, Lauren Elizabeth Tidball, Caroline Suzanne Hemingray and Katy Stevens for keeping me sane and focused. I also wish to thank Lissie Dufton, Birthe Lange and Angela Bradshaw for their kind words of encouragement.

Finally I wish to express my deepest appreciation and love to my parents, David Nicholas Bulman and Ann Bulman, my sister Lucy Ann Elaine Bulman and my loving boyfriend Thomas Brian Lewis Bradshaw. Their inspiration, encouragement, reassurance and endless love has kept me strong and motivated.

Abstract

Various bioactive wound dressing materials exist on the market that are designed to aid recovery and comfort of patients with chronic wounds. However, one of the persistent issues is the control of bacterial activity in the wound, which can influence infection rates, efficacy of wound healing and odour generation. A key requirement of a wound dressing is to facilitate a moist wound-healing environment and simultaneously control the growth of bacteria using an antibacterial agent. Manuka honey is currently utilised in bioactive wound dressing materials as an antibacterial agent via the direct impregnation or coating of honey onto a suitable material. It provides a unique antibacterial potency, attributable to one of its constituents, methylglyoxal (MGO). Commercially, there have been relatively few examples of electrospun fabric components being integrated into advanced wound care products. However, many studies have explored the potential of electrospun webs as part of a novel wound dressing material, due to their inherent nano and micro-fibrous structure, which provides a high surface area available for active delivery.

In this research, synthetic MGO was evaluated for its effectiveness as a novel antibacterial agent, when encapsulated into an electrospun poly(vinyl alcohol) (PVA) hydrogel forming web. In the first phase of this research, the antibacterial activity of both Manuka honey and synthetic MGO when applied as a topical coating to a nonwoven fabric was assessed via two British standard methods using Gram positive and Gram negative bacteria *in-vitro*. BS EN ISO 20743:2007 was employed as a quantitative method to establish if Manuka honey and synthetic MGO provided an antibacterial effect at equivalent MGO concentrations. It was found that concentrations of 0.0054 mg cm^{-2} of MGO in the form of Manuka honey and synthetic MGO was sufficient to achieve 100% reduction in bacteria for both Gram positive and Gram negative strains. Further tests were then carried out using BS EN ISO 20645:2004, which assessed the zone of inhibition using a seeded bacteria agar plate. In this case, higher concentrations between 0.0170 mg cm^{-2} and 0.1 mg cm^{-2} were required to facilitate a good antibacterial effect. The minimum inhibitory concentration (MIC) and minimum bactericidal concentration (MBC) was also assessed for MGO in liquid form against the three most prevalent wound pathogens, *Staphylococcus. aureus, Pseudomonas. aeruginosa and Enterococcus. faecalis*. Concentrations similar to that found in the literature, between and 128 mg L^{-1} and 1024 mg L^{-1} were shown to provide either a bacteriostatic or bactericidal effect. Most importantly, the MIC and MBC of MGO against *Enterococcus. faecalis* was reported for the first time.

The encapsulation of synthetic MGO in electrospun PVA fibres was explored using both needle and free surface (needleless) electrospinning technologies, with a successful outcome. It was found that an 11.22 wt % MGO solution with 16% (w/v) PVA was most favourable for producing fibres free from beads when using needle electrospinning. A higher PVA concentration of 20% (w/v) was required to achieve bead free fibres using free surface electrospinning. Two different collector materials were utilised during free surface electrospinning, where an aluminium foil collector was found to produce a smaller mean fibre diameter when compared with a less conductive polypropylene spundbond substrate. Characterisation of the as-spun webs was determined via Fourier transform infrared spectroscopy (FTIR) and proton nuclear magnetic resonance (NMR), where the presence of MGO in the PVA webs was confirmed by the characteristic carbonyl groups associated with MGO's keto-aldehyde groups. A continuation of the zone of inhibition method highlighted that concentrations of MGO between 1.14 mg cm^{-2} and 1.50 mg cm^{-2} were required to have an antibacterial effect *in-vitro*.

Finally the release behaviour of MGO from the electrospun webs was investigated using high performance liquid chromatography (HPLC). Crosslinking of the PVA/MGO webs with glutaraldehyde (GA), in the form of a vapour and a novel plasma technique showed promising results for controlling the release rate of MGO from the fibres. Prior to crosslinking, 93.7% of the MGO was released from the PVA fibres within 30 minutes. After crosslinking the amount of MGO released was considerably reduced over a period of 24 h, with a maximum of 75% released. The novel plasma crosslinking technique was further confirmed using FTIR and it is believed this is the first time this technique has been employed.

Contents

List of Tables

List of Figures

Chapter 1 Introduction

Textile materials are commonly used as health care and medical products, in applications such as blood filtration, infection control, implantable materials, tissue regeneration, drug delivery and wound care. (1). With the global population set to rise to 9.6 billion by 2050 (2), and an increase in the number of people aged 65 and above (3), it is expected that demand for improved health care products will continue to grow. Owing to the ageing population, growing rates of diabetes and obesity, chronic wounds are an increasing problem. Such wounds are extremely burdensome to health care providers and to patients because they do not heal in a progressive manner and can persist for months or even years. Wound care is estimated to account for about 3% of the NHS expenditure, equivalent to £2.3 - £3.1 billion, largely because of the nursing staff costs. Chronic wounds in particular represent a large portion of the cost, and affect around 200,000 patients (4). Pressure ulcers, venous leg ulcers, diabetic foot ulcers and arterial insufficiency ulcers are all known as chronic wounds (5). They cause patients serious discomfort and delayed healing as a result of infection from numerous strains of bacteria and bacteria biofilms, including Methicillin-resistant *Staphylococcus aureus* (*MRSA*), *Escherichia coli* (*E.Coli*), *Pseudomonos aeruginosa* (*P.aeruginosa*) and *Enterococcus faecalis* (*E.faecalis*) (6). As bacteria start to show resistance to antibiotics (7, 8) the use of topical bioactive wound dressings are increasingly being used in the treatment of infected chronic wounds (9). The excessive use of silver-based antimicrobials, used for the treatment of infected wounds, has recently been highlighted as a potential concern owing to potential toxic effects within the human body (argyria) (10), cyctotoxic effects on cells required for wound healing (11, 12) and bacterial resistance (13, 14). As a result, despite the widespread use of silver in commercial dressings, alternatives are being actively sought, particularly by the large manufacturers in Europe. It is for this reason that the controlled delivery of new topical antimicrobials in wound care, is of interest in the development of new wound dressings (15, 16).

1.1 Bioactive wound dressing materials

"*Bioactive dressings are dressings which deliver substances active in wound healing; either by delivery of bioactive compounds or constructed from materials having endogenous activity*". This type of dressing belongs to the Food and Drugs Administration (FDA) category of interactive dressings (17). In 1962 and 1963 the work by George Winter contributed to a significant advancement in wound care. He demonstrated that when the wound surface of a pig was kept moist with a polythene film, healing was more rapid when compared to a wound left exposed to the air. This is because a moist wound environment encourages epithelisation to be twice as fast and reduces the formation of scarring (18, 19). Present theories of modern wound care are based on maintaining a moist wound environment, the ability to promote healing, absorb wound exudate, provide mechanical protection against microorganisms and the removal of a dressing without pain or trauma (20). The majority of current bioactive dressings are able to fulfil these requirements by the use of biopolymers. Hydrogels and hydrocolloids are two types of bioactive dressings, which fall into this category. Hydrocolloids contain gel-forming agents, such as carboxymethylcellulose, gelatin or pectin (21). These materials absorb the wound fluid (exudates) and transform into a jelly-like state, which keeps the wound hydrated and enables a low adherent wound contact layer. Normally these materials are combined with elastomers or adhesives in the form of a foam or film carrier material to produce an occlusive or semi-occlusive dressing (22). Hydrogels are semi-occlusive and composed of hydrophilic synthetic and natural polymers, such as poly(methacrylates), polyvinylpyrrolidine and alginates. They contain large amounts of water (70-90%) and are able to absorb moderate amounts of wound exudates (21). Hydrogels are able to provide a soothing and cooling effect and can be useful in treatment of burns and painful wounds (22). As well as hydrating the wound, a bioactive dressing may incorporate agents active in wound healing, including cleansing or debriding agents for removing necrotic tissue, growth agents to aid tissue regeneration and antimicrobials to prevent or combat infection (21).

1.2 Topical antimicrobials in wound care

Antimicrobials in the form of systemic antibiotics or topical therapies are frequently used in the treatment of infected chronic wounds. Topical antimicrobials are chemicals which are used to either kill or inhibit the growth of microorganisms on the wounds surface (23). All wounds contain microorganisms, though not all microorganisms cause infection and healing can occur successfully without intervention. In this case the bioburden of the wound and the patient's immune system are in balance. However, when the bioburden of the wound is impaired due to multiplication of microorganisms (24) resulting in 'critical colonisation' (25), direct intervention is required. Systemic antibiotic treatment is usually prescribed as the first course

of treatment, however as the resistance to systemic antibiotic continues, topical antimicrobial (8) therapy is increasingly utilised in chronic wound care (25, 26). Traditionally topical antimicrobials have been formulated as ointments or creams (26), but recent advancements have seen the incorporation of antimicrobial agents into dressings (17) including chlorhexidine, iodine, silver, polyhexamethylenebiguanide (PHMB), honey and glucose oxidase enzyme systems (27). The ultimate goal of a topical antimicrobial agent is to control and prevent the growth of microorganisms to the stage of critical colonisation where infection prevails (28). It is important that a balance is found by reducing the bioburden while avoiding cytotoxicity to cells. An ideal topical antimicrobial should have broad spectrum activity against bacterial organisms, minimal systemic absorption, no impedance to wound healing, have good eschar penetration, be painless and inexpensive (29). Furthermore the dressing should be contained in contact with the wound for 12 hours or more allowing the antimicrobial agent to remain active for the duration of wear time (27). Silver, the predominant antimicrobial agent currently used in the treatment of chronic infections is available in many forms, including ionic, metallic and nanocrystalline (29). Silver has been proven to have antimicrobial activity against a broad range of microorganisms (30) and contribute towards the healing of infected chronic wounds (31). Durafiber (Smith and Newphew) is an example of a nonwoven product that combines gel forming fibres, in this case cellulose ethyl sulphonate, with ionic silver to create both cooling and antimicrobial effects when in contact with the wound. The silver ions start to kill bacteria after 30 minutes post application, with sustained release for up to 7 days (32). Although the benefits of silver have been extensively reported in the wound care community (33), some scepticism exists because of concerns about cytotoxicity and bacterial resistance (34). Consequently, alternative topical antimicrobial agents continue to be an active area of current research.

1.3 Honey as a topical antimicrobial in wound care

Natural products and remedies have been used for many years in wound care and recently there has been an increased interest in identifying appropriate antimicrobial compounds. Many natural products are known to provide antimicrobial, astringent, anti-inflammatory and bio stimulant properties (35). In 1999 an editorial in 'Advances in Wound Care', suggested that "*unproven complementary and alternative medicine strategies and opinions provide us with a tremendous opportunity to re-examine old treatments and apply them in the current environment*" (36). In the last two decades honey, which is an ancient wound treatment, has been reintroduced as a traditional and natural remedy in the treatment of chronic wounds (37, 38). Honey is known to have antibacterial properties and an ability to assist in debridement and deodorisation of wounds as well as having anti-inflammatory properties and an ability to stimulate tissue growth (37). Manuka honey in particular has received considerable attention

owing to its antibacterial properties compared to conventional honeys. This characteristic known as the Unique Manuka Factor (UMF) has been linked to the presence of methylglyoxal (MGO) (39). MGO or MG contains ketone and aldehyde functional groups and is present as a metabolite in the human body and various food and drink sources. Numerous studies have reported beneficial effects of MGO in the treatment of numerous pathogens and diseases including cancers (40-42), viruses (43, 44) and bacterial pathogens found in wounds (45-47). Currently Manuka honey dressings are manufactured by the direct impregnation of the honey onto fibres in preformed fabrics via processes such as coating. This can make the dressing very sticky and impractical for clinicians or patients to handle. When applied to exuding wounds the honey can also become unevenly liquefied, which can lead to it running off the wound (17). To overcome this problem, a potential alternative is to encapsulate MGO within the fibres during the spinning process. It is common practice to suspend or dissolve an antimicrobial compound or drug into a polymer solution, which is then used to produce fibres (48). Using such an approach, when the dressing is in contact with the wound exudates, the antimicrobial agent could be potentially released from the fibre at a controlled rate of delivery.

1.4 Electrospun polymeric webs as delivery vehicles for antimicrobial compounds

In the last decade electrospinning of sub-micron and nanofibres has attracted much attention for biomedical applications, including implantable scaffolds for tissue engineering (49, 50), controlled drug delivery (51, 52) and wound dressings (53-57). The properties of electrospun fibres make them desirable materials in the biomedical field. There is the ability to control the fibre diameter in the nanometre range, enabling fabrics to be produced with very large surface areas. Also when the diameter of fibres is in the nanometre range, there is the ability to closely mimic the scale of collagen fibres found in the extracellular matrix (ECM) of the skin (58). The topographical nature of electrospun matrices play an important role in cell proliferation and adhesion (59). The high surface to volume ratio allows for cell attachment and the tuneable porosity aids in nutrient support. The fibres also have a malleability to conform to various shapes and sizes (51). Another beneficial property includes the optimisation of fibre morphology for controlled drug delivery. Due to the high surface to volume ratio, nanofibres have the ability to overcome mass transfer limitations observed in other polymer drug delivery systems and can also offer greater drug loading (58).

Electrospun polymeric webs provide a suitable matrix for the controlled release of antimicrobials and the inclusion within a composite wound dressing. The local delivery of an antimicrobial agent sustained for about one week, in a chronic wound, can help solve and minimise the problem of frequent dressing change (21). The sustained release also improves

the effectiveness of drug targeting and optimum concentrations at the wound site. This avoids the need for high systemic dosages of antibiotics (21, 54, 60).

Electrospinning offers great potential in selecting materials for wound dressings and drug delivery. Poly(vinyl alcohol) (PVA) is a well known polymer that is approved by the FDA for medical use in humans (61) It has many beneficial properties including biocompatibility with tissue and blood (62), non-carcinogenicity and biodegradability (54). It has received significant attention in the literature for use as a hydrogel material (61, 63, 64) and for use in wound care (65, 66). Numerous studies have reported on the electrospinning of PVA alone (67) or the combined effect with other polymers for controlled drug release (54, 66). Biodegradable or non-biodegradable polymers can be used to control drug release via diffusion alone or diffusion and the biodegradation of the polymeric webs (58). Drug release from polymeric materials for wound healing is also controlled by one or more physical processes, whereby the polymer is hydrated by the wound exudate, which in turn results in the formation of a gel and the swollen gel then facilitates the release of the antimicrobial into the wound bed (21).

1.5 Aims and Objectives

The purpose of this work is to evaluate a new wound contact layer in which methylglyoxal (MGO) found in manuka honey is incorporated as a novel antibacterial compound within a poly(vinyl alcohol) (PVA) hydrogel polymer matrix formed in to fibres. The aim of this research is to study the production and properties of electrospun polymeric webs made from PVA incorporating MGO within the polymer matrix. In this study, two different electrospinning techniques are investigated, needle electrospinning and free surface (needleless) electrospinning.

The specific objectives of the study are:

- To study the antibacterial efficiency of Manuka honey and synthetic methylglyoxal (MGO) with equivalent MGO concentrations.
- To investigate the feasibility of incorporating MGO as an antimicrobial agent in PVA electrospun fibre webs.
- To analyse the physical and antibacterial properties of polymeric webs containing MGO.
- To determine the main effects and interactions of different manufacturing conditions on the properties of the experimental materials.
- To study the kinetics of antimicrobial release from the new fabric and the influence of crosslinking.

It is intended that the outcome of the study may ultimately contribute towards the development of new topical antimicrobial dressings for wound care.

Chapter 2 Literature Review

2.1 Introduction

The purpose of this chapter is to critically review aspects of the science and technology relevant to the experimental work that follows. Accordingly, to provide contextual background, a brief review of wounds and wound healing is presented, including the role of antimicrobials, followed by a discussion of salient aspects of honey in relation to wound healing. Finally, aspects of electrospinning relevant to the experimental work are discussed.

2.1.1 Types of Wounds

A wound is defined as "a break in the epidermis or dermis that can be related to trauma or to pathological changes within the skin or body" (68). A wound can be caused intentionally or accidentally or it may be part of a skin disease (69). Physical trauma will cause a tear, cut or puncture to the skin and surgical procedure may also contribute to these breaks in skin. Wounds may be classified as acute or chronic, open or closed and by the way in which the wound is closed, either primary or secondary intention.

2.1.1.1 Acute wounds

An acute wound was defined by the Wound Healing Society (WHS) as "*one that proceeds through an orderly and timely reparative process to establish sustained anatomic and functional integrity*" (70). A simpler definition is "*a recent wound that has yet to progress through the sequential stages of wound healing*" (71). An acute wound may be a result of surgery, such as an incision or excision and will usually heal faster than a chronic wound as a result of primary intention.

2.1.1.2 Chronic wounds

The WHS defined a chronic wound as "*one that has failed to proceed through an orderly and timely reparative process to produce anatomic and functional integrity or that has proceeded through the repair process without establishing a sustained anatomic and functional result*" (70). A simpler definition is "*a wound that has remained unhealed for more than six weeks"*. Venous leg ulcers, pressure ulcers, diabetic foot ulcers and arterial ulcers are key examples of chronic wounds (5). Chronic wounds are typically healed by secondary intention.

2.1.2 Wound Healing

Wound healing is a very complex process, in which a series of independent and overlapping stages occur. It is important for medical professionals to understand each of these stages in order to recognise any abnormalities which may cause prolonged healing and to select and change the appropriate dressing during the different stages. Healing occurs either by; primary,

secondary or tertiary intention. These categories are based on the anticipated nature of the repair process or how the wound is closed (72).

2.1.2.1 Stages in Wound Healing

The wound healing process takes place in a series of stages (Fig. 2.1). There are some contradicting views on the number, duration and names of each stage (73-76), but for the purpose of this study four stages referred to below are briefly discussed:

- Haemostasis
- Inflammation
- Proliferation
- Maturation

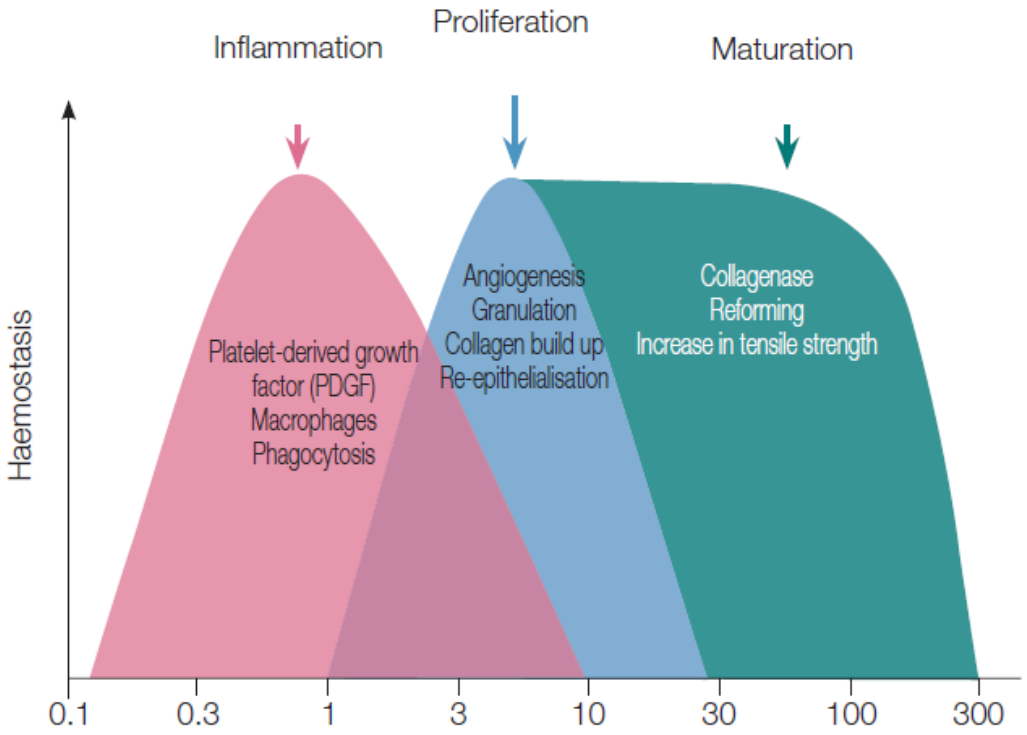

Figure 2.1: Time scale of stages in wound healing (77).

Haemostasis is the control or the arrest of bleeding (68, 77), and after wounding is the normal physiological response of the body. The injured surface of the skin and blood vessels expose connective tissue, and platelets are attracted to the site of injury. The platelets come into contact with the collagen present in the walls of the damaged blood vessels (77). Interaction between the platelets and damaged tissue generates cytokines and the biochemical cascade forms thrombin. Thrombin converts fibrinogen to fibrin, which activates the platelets to clot and this forms the physical plug that stops bleeding. Cytokines and growth factors such as, thromboxane A-2 and serotonin are released from the activated platelets causing vasoconstriction. The

platelet derived growth factor (PDGF) and transforming growth factor (TGR) are activated (78) prompting clotting to begin. Blood flow is reduced to the damaged cells giving the skin surrounding the wound a pale appearance. In contradicting cases it is claimed that haemostasis is achieved within 10 minutes after injury (77), others suggest that this process may take 2 to 4 hours (5).

Inflammation is an emergency response reaction to damaged tissue and bacterial invasion (75) which will not show any obvious signs of healing for about twelve hours (79). The signs that inflammation is taking place include redness to the surrounding area of the wound, heat which is created by a large amount of warm blood and heat energy produced by metabolic reactions, swelling and pain (75). The inflammation stage may last 3 to 5 days in acute wounds (77, 79). However, it is also suggested that it may last between 5 to 7 days (5). In chronic wounds non-resolving inflammation is a key characteristic. It is this unresolved process that significantly delays the healing process in chronic wounds and no time limit can be anticipated (76). There is evidence to show that the impaired inflammation stage is due to bacteria biofilms, which harbour on the surface on the wound and can show a resistance to antibiotic and chronic inflammation (80-84). The importance of biofilms is discussed later in section 2.2.3.

After the second or third day, proliferation begins and continues for up to 3 to 4 weeks (5). Overlapping of phases takes part in this stage, including granulation tissue formation, angiogenesis and epithelialisation.

Granulation Tissue Formation

Fibroblasts are cells which are responsible for collagen and elastin synthesis (68). They are also responsible for the extra-cellular matrix (ECM), visually seen as granulation tissue (75). They start to appear in the wound within the third to the fourth day of injury and reach their peak numbers on the seventh day (85). As the number of macrophages is reduced, fibroblasts begin to produce growth factors such as the fibroblast growth factor (FGF), the transforming growth factor (TGF) and the platelet derived growth factor (PDGF). Keratinocyte and insulin growth factors are also produced. The collagen produced gives the wound its tensile strength (77), where cells involved in angiogenesis and ECM attach to and grow (5). Granulation tissue that appears bright red in colour and moist to touch is classed as healthy. Unhealthy tissue may bleed easily and will appear darker in colour (77). Fibroblasts are also involved in the process of contraction (73, 75). Specialist fibroblasts known as myofibroblasts, gather around the wound edge pulling them together (77).

Angiogenesis

Defined as "*the production of new blood vessels*", angiogenesis gives the skin a healthy red colour (68). Vascular endothelial cells are the major cells involved in this process. They arise from undamaged blood vessels, pushing through the ECM. New vessels develop and form capillary loops which are transformed into arteries and veins, establishing new blood flow in the wound (5, 73, 85).

Epithelialisation

This is the stage in which epithelial cells migrate across the wound forming new epithelial tissue that appear pink and pale in colour (68). This process occurs in the following way: Keratinocytes found at the wound edges are simulated by the epidermal growth factor (EGF) released by macrophages. They synthesise fibronectin, forming a temporary matrix, where epithelial cells can migrate along (75). The cells move over the surface in a leap frog motion, where one cell migrates over the top of another and provides a base for other cells to climb over. When the cells meet in the middle they stop and migration ceases. This is known as contact inhibition (68, 75). When the cells stop migrating the basement membrane is rebuilt, which is essential for the epidermis to fix with the dermis (75). Iocono et al. claims that epithelialisation may begin within the first 12 to 24 hours after injury (86). However, Dealy states that this will start in the second day (75).

Maturation often termed the 'remodelling' stage (77), involves the remodelling of collagen into an organised structure, where it is laid down at right angles to the wound margins (75, 77). The newly organised collagen structure contributes to the increased tensile strength (85). The vascularity of the wound decreases owing to the paler colour of the scar tissue (77). This process of maturation may take up to 2 years, depending on the size and severity of the wound (5).

2.1.3 Factors Affecting Wound Healing

2.1.3.1 Moist Environment

In 1962, Winter (18) discovered that wounds in a moist environment heal faster than those in a dry environment. He discovered that wounds covered with an occlusive vapour permeable film dressing, encouraged epithelialisation to be twice as fast. The moist environment allowed the epithelial cells to migrate freely across the wound surface. In contrast if the wound was left in the open air where a scab had formed, the epithelial cells would migrate deep under the dried exudate and cells to find an area of moisture to allow cell movement (18). The work by Winter was not taken into consideration until the 1980s, when Eaglestein (87), compared the healing rate of a wound covered with a gauze dressing and a wound in a moist environment. He found that the healing rate was reduced by 40% when using a gauze dressing in comparison to a wound in a moist environment (87). The advantages of a moist wound environment are summarised as follows (88):

- Assists epidermal migration
- Promotes alterations in the pH and oxygen levels
- Maintains an electrical gradient
- Retains wound fluid on the wound surface

It was also reported that the benefits of a moist wound environment reduce the pain for the patient, as the wound is submerged in the natural bodily fluids fewer bacteria may exist compared to dry scab and eschar tissue which harbours microorganisms. The removal of a dressing will also cause less distress to the patient, as it is unlikely that the dressing will adhere to moist tissue (89). Autolytic debridement (the skins ability to remove dead necrotic tissue through the use of enzymes) is more likely to occur in a moist wound environment (68).

2.1.3.2 Nutrition

The nutrients required for healing and their advantages can be seen in Table 2.1. Water is not mentioned, but may be considered the most important of all. It aids in hydration to the wound site and in oxygen perfusion. Vitamins, minerals, glucose and amino acids all need water as a solvent to enable diffusion into and out of cells. It also transports vital materials to cells and carries waste away (90). A patient's nutritional balance must be monitored by a recognised nutritional screening tool, such as the Malnutritional Screening Tool (MUST) (British Association for Parenteral and Enteral Nutrition [BAPEN], 2005) to ensure they are receiving the correct nutritional balance (91).

Table 2.1: Nutrients required for healing (5, 92, 93).

Nutrient	RDA	Food Source	Contribution
Carbohydrates	1600-3350 kcals	Wholemeal bread, wholegrain cereals, potatoes (refined carbohydrates are seen as empty calories)	Energy for leuocyte, macropahge and fibroblast function
Proteins	42-84g	Meat, fish, eggs, cheese, pulses, wholegrain cereals	Immune response phagocytosis, angiogenesis, fibroblast proliferation, collagen sysnthesis and wound remodelling
Fats	1-2% kcals	Dairy products, vegetable oil, oily fish, nuts	Provision of energy, formation of new cells
Vitamin A	750 µg	Carrots, spinach, broccoli, apricots, melon	Collagen synthesis and cross-linking, tensile strength of wound
B Complex	3 mg	Meat (especially liver) diary products, fish	Immune response, collagen cross-linking, tensile strength
Vitamin C	30 mg	Fruit and vegetables (but easily lost in cooking)	Collagen synthesis, wound tensile strength, neutrophil function, macrophage migration, immune response
Vitamin E	n/a	Vegetable oils, cereals, eggs	Appears to reduce tissue damage from free radical formation
Vitamin K	n/a	Green leafy vegetables	Aids in haemostasis
Copper	n/a	Shellfish, liver, meat, bread	Collagen synthesis, leucocyte formation
Iron	10-12 mg	Meat (especially offal), eggs, dried fruit	Collagen synthesis, oxygen delivery
Zinc	12-15 mg	Oysters, meat, whole cereals, cheese	Enhance cell proliferation, increases epithelialisation

2.1.3.3 Infection

Infection is the most common cause of delayed healing in wounds (5). Several definitions exist, including "*the presence of multiplying organisms which overwhelm the body's immune system resulting in spreading cellulitis*" (inflammation of the tissues) (94). Two simpler definitions include "*infection is the invasion of living tissue by microorganism"*' (95) and "*the deposition and multiplication of organisms in a tissue with an associated host reaction*" (96). The important thing for health care professionals to distinguish is the difference between wound colonisation and infection. All wounds are contaminated with microorganisms (91). Wound contamination is the presence of organisms on the surface of a wound. Contamination can occur in many different ways, including the transference of normal body bacteria (97). The skin hosts resident bacteria such as *Staphylococcus aureus* (*S.aureus*) and *Staphylococcus epidermidis* (*S.epidermidis*). This bacteria, is also referred to as normal body flora and lives quite happily on the skin without causing any harm and may also protect against more harmful or pathogenic organisms (98). If, however, the skin becomes broken, perhaps during surgery or through accidental or intentional injury, the resident bacteria may enter the wound and begin to cause complications (91).

Wound colonisation can be characterised by the multiplication of microorganisms on the wound surface with no immune response from the host. Similar to contamination, colonisation does not cause ill health, delayed healing or disease and does not imply wound infection (91, 99). It is only when the wound becomes 'critically' colonised (23) with microorganisms that infection prevails (88). At this point the microorganisms invade the tissue below the wound surface and attack viable tissue, triggering the host responses (99). Wound infection can be identified by the following characteristics (91, 99):

- Increase in pain
- Wound breakdown
- Spreading cellulitis

If the wound continues to look inflamed after the initial 3 to 5 day period of inflammation, then cellulitis may be assumed. However, distinguishing infection in acute wounds is often easier to identify when compared to chronic wounds (99).

2.1.3.4 Other factors

Ageing can cause a decrease in the immune response (91), resulting in the prolonged infection of wounds. The collagen that is produced is weaker and more susceptible to trauma (73) and underlying health conditions are often associated with the elderly which may also affect the healing process (91). Medical conditions such as arthritis, renal disease, cancer, heart disease, immune disorder, blood disorders, lung disease and diabetes all affect the wound healing

process (5). Poorly controlled glucose levels delays the wound healing rate of elderly diabetic patients up to three times that of non-diabetic elderly patients (100). Medication such as chemotherapy and long-term steroid therapy can lower the immune response, allowing bacteria to replicate in the wound, which will subsequently increase the potential for wound infection (101). Anti-inflammatory, immunosuppressive, anticoagulant and cytotoxic drugs interrupt cell division and clotting factors causing a reduction in the healing rate (5, 102). Obesity has shown some risks in the development of infection in surgical wounds (103). The deep layers of fat tissue can often make surgical procedures more technical and complicated, particularly when trying to avoid the tearing of blood vessels. If this does occur, reduced blood supply to the wound during the healing process may cause a delay (91, 104). A review on the effects of smoking on wound healing, found that nicotine inhibits the epithelisation, macrophage activity and wound contraction (105). Smoking was also found to reduce the synthesis of type 1 collagen (106). Psychological factors such as stress and anxiety have also been shown to contribute to a delay in healing (107, 108).

2.2 Bacteria

Bacteria are a type of microorganism, unicellular and prokaryotic in type, they exist in nearly all places in the environment (109, 110). Bacteria can be classified into two groups; domain bacteria and domain archaea. However, the domain archaea contain only a small number of organisms, including species that live in extreme habitats with elevated temperatures and high salinity (109). This type of bacteria does not apply to the bacteria found in common environments, such as hospitals and so does not apply to this study.

Bacteria are responsible for some major and minor diseases and infection. However, bacteria can live on the human body without causing any harm and in most cases are useful to man. Some of these uses include: biological washing powders, crop pesticides/insecticides, the production of cheese, yoghurt and butter and biodegradable plastics (109), these are only a few of the processes bacteria are involved in. For the purpose of this study bacterial pathogens will be discussed.

Any microorganism which initiates disease is known as a pathogen. Bacteria which live on the human body known as microflora, are not known as pathogens, but can sometimes cause disease when the host is disturbed and are referred to as opportunist pathogens (91, 109). This may be through injury or surgery when the microflora migrate to places in the body that are not usual. Table 2.2, represents the microflora found on the human body. The bacteria frequently found in wounds, which may lead to infection, are discussed in section 2.2.3.

Table 2.2.: Microflora found on the human body (111).

Location	Species
Colon	*Bacteroids, Clostridium, Escherichia, Proteus*
Ear (conjunctivia)	*Corynebacterium, Mycobacterium, Staphylococcus*
Eye	*Staphylococcus (coagulase-negative), Corynebacterium, Propionibacterium*
Mouth	*Actinomyces, Bacteroids, Streplococcus*
Nasal passages	*Staphylococcus, Corynebacterium*
Nasopharnyxn	*Streplococcus, Haemophilus (e.g. H. influenzae)*
Skin	*Propionibacterium, Staphylococcus, Others (according e.g. to personal hygiene and environment)*
Uretha	*Acinetobacter, Escherichia, Staphylococcus*
Vagina (adult pre-menopausal)	*Acinetobater, Cornyebacterium, Lactobacillus, Staphylococcus*

2.2.1 Types of Bacteria

Bacteria can be classified into gram negative and gram positive. The difference is determined by the structure of the cell wall. Gram negative bacteria possess an outer membrane (110) (Fig. 2.2). Typical gram negative and Gram positive bacteria used commonly in testing are *Escherichia Coli* (*E.Coli*) and *Staphylococcus aureus* (*S.aureus*) respectively (91). Bacteria can also be classified via the reactions they employ to generate growth and other activities. They are classified as either; aerobic, anaerobic or facultative. Aerobic bacteria require oxygen and cannot grow in its absence. In contrast, oxygen is toxic to anaerobic bacteria and they cannot grow in its presence (112). Both aerobic and anaerobic bacteria reside in wounds which may lead to infection. *S.aueus, E.coli* and *Klebsiella pneumoniae* are some types of aerobic bacteria while *Peptostreptococcus* and *Prevotella*, Clostridium species are anaerobic, all of which may reside in wound environments (113).

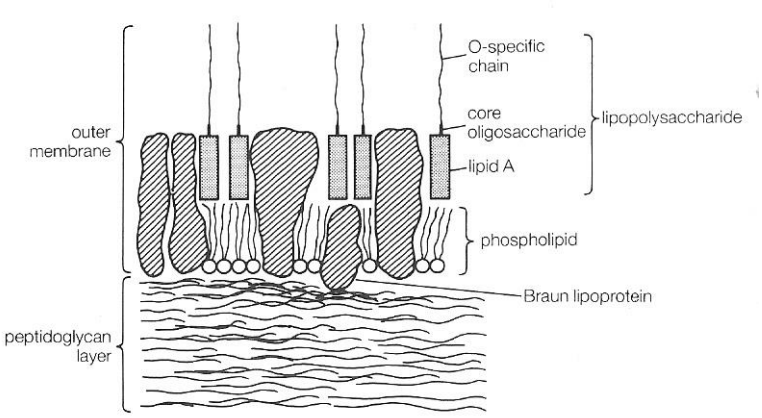

Figure 2.2: A Gram negative bacteria cell (114).

2.2.2 Bacteria involved in wound infections

Wounds are host to an extensive range of bacterial species. A study published in 2006 examined the chronic wounds of 46 patients with venous leg ulcers (6). A total of 37 species of bacteria were found. All of the ulcers contained more than one bacterial species, with a mean number of 6.3 species per ulcer. The most common species isolated was *S.aureus*, which was found in 93.5% of ulcers. *Enterococcus faecalis* (*E.faecalis*) was found in 71.7% of all ulcers and *Pseudomonos aeruginosa* (*P.aeruginosa*) was found in 52.2% (6). An earlier study in 1999 (113) investigated the aerobic and anaerobic bacteria of infected and non-infected leg ulcers. 57 bacteria species were cultured from both infected and non-infected wounds, 24 aerobic and 33 anaerobic. The mean number of aerobe and anaerobe species from infected wounds was 2.6 and 2.5 respectively. In comparison the non-infected wounds had a lower mean number of anaerobes at 1.3 and aerobes at 2.3. Numerous anaerobic species were more prevalent in the infected ulcers compared with the non-infected wounds. *Peptostreptococcus* and *Prevotella* species accounted for 37% of the total microbial population in infected wounds compared with 26% in non-infected wounds. *S.aureus*, an aerobic species, was more prominent in non-infected wounds at 53% compared with infected ulcers at 43% (113). Bacteria biofilms are particularly troublesome in chronic wounds and play a significant role in the delay of healing, this is discussed in section 2.2.3.

2.2.3 Bacteria Biofilms

Bacteria are present as free floating entities in a planktonic state (115). However in clinical and natural environments, bacteria can grow as sessile communities, where the bacteria group together on a surface or air/liquid interface and are embedded within a matrix of extracellular polymeric substances (EPS), this is known as a biofilm (115-117). The EPS are composed of proteins, lipids, polysaccharides and DNA (115, 118), which act as a scaffold for the biofilm to quarantine and preserve enzymes and metal ions, all of which are thought to support its stability, aiding in survival (117). Biofilms also differ from planktonic bacteria in that they have an

altered phenotype with respect to growth rate and gene transcription (119). The control of gene expression is thought to support and prepare bacteria biofilms for prompt adaption during external hostile conditions (117). The defences of a biofilm make them resistant to antibiotics (120), antiseptics (121) and the human immune response (122). It was reported that up to 17 million new biofilm infections arise in the US and 550 000 people die from these infections annually (123).

Both acute and chronic wounds are susceptible to bacteria biofilms (115), however it is chronic wounds which make up a large percentage of this. James et al. used scanning electron microscopy to study the existence of biofilms in patients with chronic and acute wounds. The results showed that 30 out of 50 chronic wounds had a biofilm existence compared with only 1 out of 16 acute wounds (124). A chronic wound environment encourages the spread and growth of key opportunist pathogens already living on the intact skin. It is therefore likely that a chronic wound environment will promote propagation and collection of opportunist bacteria populations which will lead to a delay in healing and increased risk of infection from biofilms (125). One of the main reasons postulated why chronic wounds such as diabetic foot ulcers, venous leg ulcers and pressure ulcers fail to heal is because of biofilms (82). The wound becomes stuck in the inflammatory stage, which is characterised by a persistent influx of polymorphonuclear neutrophils (PMNs), which release cytotoxic enzymes and oxygen free radicals causing prolonged and detrimental damage to the host tissue (82, 88). The importance for understanding biofilms in wounds, is their inherent tolerance to antimicrobials and inflammatory reactions to the host (118). This is discussed in section 2.3.1.

2.3 Antimicrobials

Antimicrobials are agents which may kill or inhibit microbes such as bacteria, fungi or viruses. An antibacterial refers to an agent that specifically targets bacteria and falls into two general categories, bacteriostatic and bactericidal. Bacteriostatic refers to an agent's ability to prevent the growth of bacteria, it keeps the bacteria in a stationary phase. Bactericidal means that the agent will kill the bacteria (102, 126).

Antimicrobial is as an 'umbrella' term that includes: disinfectants, antiseptics and antibiotics. Chemical agents or biocides, such as hyperchlorite or glutaraldehyde are used to inhibit or kill microbes on inanimate objects and are referred to as disinfectants. Antiseptics are biocides used on a wound or intact skin to inhibit or kill micro-organisms (127, 128). These may also be referred to as an antibacterial. Hospitals and other health care settings use antiseptics and disinfectants extensively to aid in infection control practices. In general antiseptics target a broader spectrum of bacteria with multiple target sites (128). Antibiotics act differently to antiseptics, in that they employ a toxic effect against selective bacteria (128, 129). They are

naturally occurring or synthetic organic substances that are used predominantly for the treatment of infections in humans and animals (129). Antiseptics and antibiotics use different mechanisms of action to kill or inhibit bacteria. The mechanistic role of antibiotics are well documented, however the function of an antiseptic is less understood (130). Table 2.3 highlights the basic mechanisms employed in the bacteriostatic or bactericidal action of an antibiotic or an antiseptic.

Table 2.3: Antibiotic and antiseptic mechanisms (130).

Antibiotic mechanisms against bacteria	Antiseptic mechanisms against bacteria
Act as inhibitors to peptidoglycan synthesis	Interact with bacterial cell wall or envelopes
Protein synthesis	Produce changes in cytoplasm membrane integrity
Nucleic acid synthesis by interrupting nucleotide metabolism	Dissipate the proton-motive force
Inhibiting RNA polymerase	Inhibit membrane enzymes
Inhibiting DNA gyrase	Act as alkylating, crosslinking and intercalating agents
Interfere with membrane integrity*	Interact with identifiable groups within the cell

*Only select antibiotics act in this way

2.3.1 Bacteria and biofilm resistance to antibiotics and antiseptics in wound care

Chronic wounds are polymeric in nature and this provides an appropriate environment for the genetic mutation of bacteria (8). The first two cases of vancomycin (an antibiotic) resistant *S.aureus* were first reported to have come from chronic wounds in the USA (131). An analysis of antibiotic susceptibilities of skin wound flora in hospitalised dermatology patients found that more than half of *S.aureus* isoltaes from leg ulcers were *MRSA* and more than one third of *P.aeruginosa* were resistant to ciprofloxacin. The ulcers also appeared to be significantly larger in terms of area than ulcers which were not infected (132). The polysaccharide (Psl) in *P.aeruginosa* biofilms has been shown to provide a physical barrier against various antibiotics at the beginning stages of biofilm development. Psl was found to sequester antibiotics to the matrix via electrochemical interaction, which therefore limited their effectiveness (120). Another study compared the antimicrobial effect of silver sulphadiazine and tobramycin against *P.aeruginosa* biofilms. It found that 340 µg ml^{-1} of tobramycin had no effect against mature biofilms. In contrast only 5 µg ml^{-1} of silver sulphadiazine was able to destroy the biofilm. However the amount of silver available in three commercial dressings via extraction, was found

to be considerably lower, including 0.033 µg ml^{-1}, 2.2 µg ml^{-1} and 0.93 µgml^{-1} and showed no effect towards the established biofilms (121).

The emergence of silver resistant bacteria has been documented since the 1970s where it was first reported in Massachusetts General hospital in Boston, USA. Burn victims suffering from *Salmonella typhimurium* were treated with a standard 0.5% silver nitrate ($AgNO_3$) solution. Resulting swab cultures reported persistent resistance to $AgNO_3$ and was transmissible to susceptible strains of *E.coli* and *Salmonella typhimurium* (133). Following this, other studies reported that various strains of gram negative bacilli showed resistance to silver sulphadiazine (134). Similarly burn patients with bacteria infections from *P.aeroginosa* showed resistance to treatment by $AgNO_3$ (135) and silver sulphadiazine (136). A Canadian burns unit also documented that isolates of *Enterobacter cloacae* (*E.cloacae*), *Proteus mirabilis* (*P.mirabilis*) and *Klebsiella pneumonaie* (*K.pneumonaie*) showed resistance to $AgNO_3$ (137).

Bacterial resistance to silver is thought to arise through mutation or acquisition of plasmids or transposons, as an intrinsic natural property or via epigenetic mechanisms (change not modulated by genetic expression) (14). The silver resistant strain of Salmonella typhimurium has provided in depth insight into the mechanisms of silver resistance in bacteria. The following Sil gene products are said to be attributable for action of silver resistance to Salmonella typhimurium (138):

- SilE, a small silver binding protein located on the bacterial cell surface
- SilS, a regulatory kinase membrane receptor protein
- SilR, a transcriptional responder protein that regulates mRNA transcription in silver resistance
- SilCBA, a complex three protein membrane protein dependant silver and hydrogen ion anti-porter
- SilP, a P-type efflux ATPase.

Multi-species bacteria biofilms are now highly resistant to most antimicrobial agents, including silver. The mechanisms of biofilm resistance to silver have been documented and the principal features of resistance are anticipated to be (13, 139):

- Modified nutrient requirements and suppression of growth
- Direct interactions between the polysaccharide and its constituents with the active moiety of the antibiotic, namely silver
- Lack of penetration and diffusion of the antibiotic into the polysaccharide matrix
- Development of specific biofilm/attachment phenotypes within the biofilm

With the growing rise in planktonic and bacteria biofilm resistance to antibiotics and topical silver treatment, biofilm based wound care (BBWC) strategies are being implemented, which involves the physical debridement of necrotic tissue and the use of topical treatments (122). The search for new and novel antiseptics are also being explored, including natural remedies like Manuka honey. Manuka honey dressings are in use, as there has been limited evidence to show biofilm resistance (140, 141). The role of Manuka honey in wound care is discussed in section 2.4.3.2.

2.4 Topical antimicrobials in wound dressings

Antimicrobial wound dressings contain an antiseptic agent which has been incorporated within the dressing, this does not include products which contain antibiotics. Antimicrobial dressings offer many benefits over antibiotics, which include (24):

- Relatively easy to use
- Widely available
- Frequently cost less than antibiotics
- Available without prescription
- Have less risk of resistance

Antimicrobial dressings are applied topically to the wound. They differ to antibiotics, in that they exert an extensive spectrum of non-selective antibacterial action and act at multiple sites within microbial cells, this reduces the likelihood of bacteria developing resistance. Antibiotics however, are selective against the bacteria they inhibit or kill and are usually administered systemically, although it is possible to apply them topically which is not recommended. Silver, honey, cadexomer iodine and polyhexamethyl biguanide (PHMB) are among the most common antiseptics utilised within a dressing (24). Silver and honey are traditional antiseptics which have been used throughout the centuries for the treatment of wounds (127). They are both highly regarded as being effective in the treatment of infected chronic wounds with numerous publications highlighting their antibacterial performance. For the purpose of this study silver and honey will be discussed.

2.4.1 Silver (Ag)

In today's medicine silver has received much attention and has been utilised in advanced wound care for the past 40 years (142). There are many papers reporting on the antibacterial efficiency against a range of bacteria, including both gram positive and gram negative (30) and its use in the treatment of patients suffering from chronic wound infections (31). The range of silver dressings is extensive, including film, foam (143), hydrocolloid (25), hydrogels (144) and dressings incorporating a Hydrofibre® technology (145). A variety of silver compounds are

available within a dressing, as indicated in Table 2.4 and the methods for incorporating these consist mainly of the following (96):

- Coating of the base fabric or fibres with metallic silver
- Attachment of silver ions to the base material through ion exchange
- Blending fine silver particles with the base layer
- Blending silver containing fibres with other non-silver fibres
- Incorporation into fibres

Table 2.4: Silver compounds used in dressings (96).

Manufacturer	Name of the Dressing	Silver Compound
Argentum	Silverlon	Metallic Silver
Smith and Nephew	Acticoat	Metallic Silver
Mediline	SilvaSorb	Silver Chloride
Convatec	Aquacel Ag	Silver Chloride
Mediline	Arglase	Silver Calcium Phosphate
Coloplast	Contreet	Silver Annomium Complex
Johnson and Johnson	Actisorb Silver 220	Silver Carbon

The amount of silver content within commercially available dressings have been found to be considerably different. These differences were highlighted in two studies in 2003 by Thomas and McGubbin (146, 147). Both of the studies compared the antimicrobial properties of commercially available silver containing wound dressings and reported the total extractable content observed by optical emission spectroscopy, as seen in Table 2.5.

Table 2.5: Silver content in commercial dressings (146).

Dressing	Silver content (mg 100 cm^{-2})
Silverlon	546
Calgitrol Ag	141
Acticaot	101
Contreet Ag	47
Contreet H	32.4
Aquacel Ag	8.3
Silvasorb	5.3
Actisorb Silver 220	2.9
Avance	1.6

2.4.1.1 Toxic and cytotoxic effects of silver

Argyria is a non-life threatening condition, where a blue to grey discolouration of the skin has occurred in systemic or localised forms (10, 148). The condition is also referred to as Argyriasis, Argyrism and Argyrosis and is predominantly a condition affecting the skin and its limbs, attributable to minute particles of metallic silver, silver sulfide or silver selenide containing granules in the connective tissues of the dermis (149-151). It can occur in a variety of circumstances and be localised via the implantation of silver-loaded acupuncture needles, or generalised throughout the body where discolouration to the eyes (Argyrosis) or the internal organs may occur (149, 150, 152). Argyria may be defined as "*a permanent or long-lasting grey or blue-grey discolouration of the skin attributable to prolonged exposure to metallic silver or ionisable silver salts*" (10). Fig. 2.3 depicts an image of a 65 year old woman's chest ulcer, which was treated with silver sulfadiazine cream. A blue to grey discolouration of the non-healing ulcer can be seen. The patient reported that the discoloration did not change appreciably over a 3 year period (148). The increasing use of silver (metallic or Ag^{+}) can be introduced directly into the circulation via a coating or impregnate on materials used in implantable or in-dwelling devices such as catheters, bone cements and prostheses, dental materials, cardiovascular valve sewing cuffs and stents (10). Topical treatment with silver sulfadiazine in burn wound therapy has shown cases where side effects including hypersensitivity reactions, allergic contact dermatitis, erythema multiforme, and systemic Argyria have occurred (148). Although the condition is visually undesirable, it must be regarded as a cosmetic condition at most (10). There is minimal evidence that even in severe cases an overdose of silver is fatal. Where death has been recorded, pre-existing health problems unrelated to silver have been the cause (153).

The cytotoxicity of silver in cells required for healing including fibroblasts and keratinocytes has been highlighted in few studies (11, 12). One study evaluated the cytotoxicity of six commercially available dressings, including Acticoat, Aquacels Ag, Contreet foam, PolyMem silver, Urgotuls SSD and Aquacel (a control sample with no silver available). The method of investigation involved the seeding of both keratinocytes and fibroblasts separately into six well plates at a density of 1 x 10^5/well and 5 x 10^4/well respectively. Upon three to four days culture, separate dressing pieces measuring 1 x 1 cm^2, were soaked with 0.8 ml of deionized water, saline and fetal bovine serum (FBS) separately before being added to the plate well for culture. The three solutions were also tested separately as a control. It was found that Acticoat, Aquacels Ag, and Contreet foam, had the most cytotoxic effects on keratinocytes and fibroblasts after 24 h, while PolyMem Silver and Urgotul SSD were found to be the least cytotoxic. All silver dressings resulted in a significant delay of reepithelialisation and Acticoat and Contreet foam indicated a strong inhibition of wound reepithelialisation (12). Table 2.6 and Table 2.7 show the percentage cell death for both the keratinocytes and fibroblasts, respectively after 24 h.

Figure 2.3: Argyria on a non-healing ulcer, after treatment with silver sulfadiazine cream (148).

Table 2.6:Percentage (%) of keratinocyte cell death after dressing treatments.

	Pre-treatment		
	Deionized water	**Saline**	**FBS**
Dressing	**Percentage (%) of keratinocyte cell death after 24 h**		
Aquacel (control)	12	25	Comparable to control solutions
Acticoat	80	80	50
Aquacel Ag	47	91	80
Contreet Foam	90	50	95
Poly Mem silver	Shown to enhance the cell proliferation in all cases		
Urgotul SSD	Comparable to the control sample (Aquacel)		

Table 2.7: Percentage (%) of fibroblast cell death after dressing treatments.

	Pre-treatment		
	Deionized water	**Saline**	**FBS**
Dressing	**Percentage (%) of keratinocyte cell death after 24 h**		
Aquacel (control)	Comparable to the control solutions		
Acticoat	75	< 50	< 30
Aquacel Ag	<25	<25	<25
Contreet foam	50	25	30
PolyMem silver	Initially all pre-treatments showed a mild cytotoxic effect after 6 h. After 24 h, all cells began to proliferate		
Urgotul SSD	Comparable to PolyMem silver		

2.4.2 Honey

Honey is produced in the hive, by bees who convert the natural sugars from nectar, a thin, sweet and spoiled solution to a highly viscous, high energy food (154). Honey was defined by the British Pharmacopoeia in 1993 as being "*obtained by purification of the honey from the comb of the bee, Apis mellifera L, and other species of Apis*" (155). The composition of honey is mainly 80 wt % sugars and 17 wt % water (17). However, the plant source, season and production of honey will vary the chemical composition (156). The main constituents include carbohydrates, proteins, amino acids, vitamins, minerals and antioxidants (154, 157). The carbohydrates present are the monosaccharides, fructose (38%) and glucose (31%), (17, 157). The disaccharides include a smaller percentage of (~9%) sucrose, maltose, isomaltose, maltulose, turanose and kojibiose. There are also some oligosaccharides present approximately 4.0%, including erlose, theanderose and panose, which are formed from the incomplete breakdown of the higher saccharides present in nectar and honeydew (157).

2.4.2.1 History of Medicinal Use

Honey has been used for thousands of years for its medicinal and nutritional effects. It has been cited as far back as 2100-2000 BC, where honey was mentioned as a drug and ointment treatment on a clay tablet (158), and in Chinese literature dating back to 2000 BC (159). There are Egyptian records from 1550 BC which include 147 prescriptions for the external application of honey, used for treating eyes. Honey treatment for wounds and diseases of the gut was used by the Ancient Egyptians, Assyrians, Chinese, Greeks and Romans (160). There are also reports that using cotton wool soaked in honey and lemon juice, was used as a contraceptive. Around 300 BC a study by Herophilus, founder of the medical school in Alexandria, discovered techniques used by the Egyptians for treating wounds. This included applying a salve made of either honey and animal fat or honey and aromatic resins, with an adhesive linen tape (161). The therapeutic properties of honey are known to act as an antimicrobial and anti-inflammatory, as well as having the ability to debride, deodorise, simulate tissue growth, manage pain and minimise scarring (162).

2.4.2.2 Antimicrobial action of honey

In 1937 the work by by Dold, Du and Dzaio (163), discovered that honey when diluted with water had superior antibacterial activity against certain bacteria. This discovery was later confirmed in 1962 when White, Subers and Schepartz concluded that hydrogen peroxide (H_2O_2) found in honey is responsible is for its antibacterial action. It was found that when honey is diluted, hydrogen peroxide is produced (164). Originally H_2O_2 is produced by the interaction of the honey bee when it releases an enzyme known as invertase, converting the sucrose found in pollen into glucose and fructose. A small amount of the glucose is then converted by a second enzyme known as glucose oxidase, which converts the glucose into gluconic acid and H_2O_2

(165). It is believed that the function of H_2O_2 prevents the damage of unripe honey when the sugar concentration has not yet reached levels able to prevent microbial growth. The enzyme glucose oxidase is deactivated throughout the ripening of honey. However it reclaims its activation on dilution of honey (166). H_2O_2 is responsible for a broad range of activity against bacteria, in particular gram positive bacteria. It serves as an oxidising agent, affecting the cellular elements of the bacteria by producing free radicals which react with lipids, proteins and nucleic acids. A 3% H_2O_2 solution is often used as an antiseptic and disinfectant (96, 167). H_2O_2 has been reported as the main constituent responsible for the bacteriostatic effect of honey (168, 169).

The osmolarity has also been reported to play an important role in the biocidal activity of honey. Due to honeys super saturated sugar and low water content, it has very high osmolarity (170), with an osmotic pressure estimated to be 2000 mosm. This environment makes it very difficult for micro-organisms to grow in. The acidity of honey has also been shown to contribute to the resistance of spoilage by bacteria (171), with an average pH of 3.9. However, although the low acidity was presumed to have a relationship to honey's antibacterial activity, it has since been reported that no correlation between the acidity and antibacterial activity has been found (170).

2.4.3 Manuka Honey

Manuka honey is derived from the floral source '*Leptospernum scoparium',* in New Zealand. It is known to possess a distinctive antibacterial characteristic known as the Unique Manuka Factor (UMF) (172). The UMF activity of Manuka honey was established by Molan and Russell in 1988 to test the non-peroxide antibacterial activity of Manuka honey (173). The method of assay was later altered by Allen et al. in 1991 (174) and is now used widely in honey laboratory's in New Zealand to establish the UMF of Manuka honey for therapeutic use (175).

The production of Manuka honey has grown over the last decade due to the desire for therapeutic use (175) and it is now widely recognised in wound management (37) where it has been accepted by regulatory health authorities in the European Union member states, Australia and Canada (38), Hong Kong and North America (127). In 2006 it was reported that the annual Manuka honey harvest was said to be approximately 1500-2000 tonnes. The geographical location of the plant is also known to affect the low or high levels of the UMF and the north and east of New Zealand's north island are found to produce the most prominent UMF activity.

2.4.3.1 Non-peroxide antibacterial activity in Manuka honey

The work by Russell et al. in 1983 highlighted Manuka's enhanced antibacterial activity was unrelated to the osmolarity, acidity and H_2O_2 commonly found in all honeys (176). Following this discovery the properties of Manuka honey have been extensively researched by Professor

Molan and his team at the University of Waikato in New Zealand. In 1988 a study reported the antibacterial comparison of 19 honeys of differing floral sources from numerous geographical locations in New Zealand. They were tested against the common gram positive bacteria *S.aureus* and the zone of inhibition was measured for varying diluted concentrations of honey. The average results expressed in mean weighted sum (mm^2) highlighted that three honeys, Kanuka, Manuka and Penny Royal were most active, with values of 28.24, 14.64 and 5.12 respectively. However the small number of samples tested for Kanuka and Penny Royal cast doubt on the reliability of the results and so it was concluded that Manuka honey showed the most promising results for therapeutic treatments (177).

Further studies by Molan and his team were conducted to determine if Manuka honey showed any signs of antibacterial activity on the removal of hydrogen peroxide. Upon dilution of the Manuka honey with an enzyme catalase to remove the hydrogen peroxide, zones of inhibition against *S.aureus* were still evident. However after dilution to the lone hydrogen peroxide solution with the enzyme catalase to resemble that of the Manuka honey dilutions, no zone of inhibition was observed. These results concluded that another compound must play a significant part in the antibacterial activity of Manuka honey (173).

Several attempts have been made to distinguish the unique antibacterial compound in Manuka honey. Using thin layer chromatography Molans team was able to isolate a number of aromatic acid derivatives, including syringic acid and phenyllatic acid, which were found to have an antibiotic activity towards a range of bacteria (178). This was later confirmed by Wilkins et al. who found these aromatic acids to be the most abundant phytochemicals found in Manuka honey (179). However these acids are also plentiful in other honey from Europe (180). Weston et al. also confirmed the presence of syringic acid in over 45% of the total extract of Manuka honey, however after testing Manuka honey and inactive honeys against *S.aureus*, the degree of inhibition was found to be the same for both honeys and so syringic acid cannot be solely responsible for the antibacterial activity of Manuka honey (181).

In 2004 Weigel et al. found that honey contains varying amounts 1,2-dicarbonyl compounds including glyoxal (GO), methylglyoxal (MGO), 3-deoxyglucosulose (3-DG) and 5-hydroxymethylfurfural (HMF) (182). Following this work, Henle and his team at the University of Dresden conducted a study to determine if the 1,2-dicarbonyl compounds could be responsible for the unique antibacterial activity in Manuka honey. The study looked at total of 50 honeys from various origins, plus six Manuka honey samples labelled as ‘active’ or with increasing UMF. It was found that GO, MGO and 3-DG were present in all honey samples, however much higher concentrations of MGO were recorded in the Manuka honey samples, up to 100 fold higher when compared to conventional honeys. The antibacterial activity of GO,

MGO and 3-DG was also evaluated using minimum inhibitory concentration (MIC) values and compared with honey samples. An antibacterial effect was observed for all 1,2-dicarbonyl compounds and honeys, however 3-DG showed no antibacterial effect until a MIC concentration of 60 mM was achieved. GO showed much lower MIC values of 6.9 mM for E. coli and 4.3 mM for *S. aureus*. A pronounced antibacterial effect was found for MGO, with a low MIC value of 1.1 mM (79.3µg ml^{-1}) (183) for both bacteria strains. No antibacterial activity was observed for the conventional honeys with dilutions below 80% (w/v), however Manuka honey samples showed an antibacterial effect with dilution to 15% (w/v). Henle and his team believe this work conclusively provided evidence that MGO is directly responsible for the unique antibacterial effect of Manuka honey (172). Following the work by Henle's team, Molan conducted a study to determine the origin of MGO in Manuka honey. It was concluded that MGO is derived in New Zealand Manuka honey by the non-enzymatic conversion of dihydroxyacetone in the nectar. Although it is not yet understood why this occurs (184).

2.4.3.2 Manuka honeys antimicrobial effectiveness in wound care

The use of Manuka honey in wound healing is now widely accepted with numerous studies showing the benefits to heal various types of chronic wounds, including leg ulcers (185-189), diabetic foot ulcers (190, 191), burns (192) and forelimbs of horses (193). A study of particular interest reported the treatment of a surgical infected wound which had not responded to treatment for 36 months. Several treatment options were tried, including antibiotics and topical silver, sulphadiazine, silver nitrate and povidone-iodine. After the failure of all these options, the patient requested to try a honey dressing. A noticeable improvement in the appearance of the wound was observed within 1 week. After four months following initial closure of the wound, the patient discontinued the honey dressing and experienced no further problems (194).

With the growing rise in bacterial resistance to antibiotics (8, 129, 130) and concern to find alternative treatments (130, 195), the antibacterial activity of Manuka honey is of growing interest and well documented with reference made to the antibacterial potency. Manuka honey inhibits the growth of clinically important pathogens and biofilms found in wounds, including Methicillin-resistant *Staphylococcus aureus* (*MRSA*) (196, 197), *E.coli* (198), *Proteus mirabilis* and *Enterobacter cloacae* (199), *P.aeruginosa* (200, 201) and *Streptococcus pyogenes* (202). Gastrointestinal pathogens (203) and oral infections (204) have also shown susceptibility to Manuka honey.

The anti-biofilm formation of Manuka honey was evaluated for its effectiveness to inhibit the *in-vitro* development of important gram negative bacteria. Activon Manuka honey, developed by Advancis Medical was used in a study and tested against methicillin-sensitive *S.aureus* (*MSSA*), *MRSA* and vancomycin-resistant *Enterococcus faecalis* (*VRE*). Concentrations of

honey ranging from 1% (w/v) to 20% (w/v) in increments of 1% (w/v) were evaluated. It was observed that for both *MSSA* and *MRSA* concentrations of honey from 2% (w/v) upwards began to show reduction in the biofilm formation. No depletion of *VRE* was seen below a 5% (w/v) concentration. At concentrations above 10% (w/v) the biofilm growth was completely inhibited for all three test organisms. A further experiment looked at the survival of each bacteria organism over a period of 24 h with a Manuka honey concentration of 40% (w/v) and compared this with a control. It was found that each biofilm mass was significantly reduced in comparison to the control, decreasing over the 24 h period (197).

In comparison another study also investigated the effect of Activon Manuka honeys anti-biofilm properties against *MRSA* at different concentrations over a period of 24 h and compared this against a manmade artificial honey which was tested with and without the addition of 614 mg kg^{-1} of MGO. The concentration of MGO added to the artificial honey was thought appropriate for a 10% (w/v) sample of Manuka honey. The results showed that 10% (w/v) artificial honey, 2.5% (w/v) Manuka honey and the control sample had a generation time of 30 min, with colony forming units reaching up to 8.5 (log_{10} cfu ml^{-1}) after 24 hours. The Manuka honey samples with a concentration of 5% (w/v) to 20% (w/v) and the artificial honey containing MGO showed a loss in the colony forming units after 30 min, which continued to fall to 3.5 (log_{10} cfu ml^{-1}) after 24 h for all the Manuka honey samples. The extent of inhibition after 24 h was less for the artificial honey containing MGO, which fell to 5 (log_{10} cfu ml^{-1}) (196).

A very recent study used Woundcare™ 18+Active Manuka honey to establish the potency against Clostridium difficile biofilms. The results highlighted that there was a dose-response relationship between the concentration of Manuka honey and the depletion of the biofilm. Concentrations below 20% (w/v) had little or no effect against the established biofilm however, at concentrations between 20% (w/v) to 50% (w/v) the amount of biofilm decreased during a 24 h period (205).

There has been limited or no evidence to show biofilm resistance to Manuka honey until recently, when an experiment highlighted for the first time that *P.aeruginosa* strains were resistant to Manuka honey with a MIC of 30.6% (w/v) (206). This is not surprising, owing to *P.aeruginosa* reputation to provide a physical barrier to other antibiotics and antiseptics (120, 121, 132).

2.4.3.3 Manuka honey dressings

At present Manuka honey wound dressings are manufactured through the direct impregnation of honey into the fabric or as a hydrogel. Currently some of the medically approved honey dressings include Medihoney by Derma Science (207), the Advancis Medical range (208) and

L-Mesitran (209). The Medihoney range includes Medihoney Calcuim Alginate dressing (a nonwoven fabric impregnated with 95% content of Manuka honey) and Medihoney Hydrocolloid dressing (80% content Manuka honey). Within the Advancis Medical range are Activon Tulle (a knitted viscose mesh, impregnated with 100% Manuka honey), Algivon (a soft nonwoven alginate dressing impregnated with 100% Manuka honey) and Actilite (a light viscose net dressing coated with Manuka honey and Manuka oil). L-Mesitran offer two dressings types including a hydro active dressing (a thin honey hydrogel dressing) and a net dressing (a hydro-active hydrogel honey coated dressing with an open weave mesh).

2.5 Methylglyoxal

Methylglyoxal (MGO) also termed 2-oxopropanol, pyruvaldehyde, pyruvic aldehyde, 2-ketoproinoaldehyde, acetylformaldehyde, propandendione or propioaldehyde is a yellow liquid found in Manuka honey (210). It has a strong distinctive odour (211). Chemically it is a keto-aldehyde (Fig. 2 4), is hygroscopic and polymerises readily (210). MGO has been identified in a range of beverages and foods including wine, beer (212), bread (213), soya, coffee, teas (214) and Manuka honey (184). MGO is also a metabolite found in the human body, where it is formed endogenously via enzymatic and non-enzymatic reactions (210). In water MGO is available in the mono and dehydrate forms, the non-hydrated form of MGO is available only in trace amounts (215). The reactivity of MGO in cells and tissues can be strongly influenced by the presence of some organic compounds which are dependent on temperature and amount of water (216).

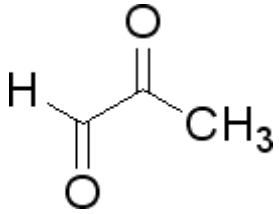

Figure 2.4: Chemical structure of Methylglyoxal (217).

2.5.1 Methylglyoxal as a therapeutic agent

A number of studies have looked at the beneficial effects of MGO in the conquest of different diseases. As already discussed, MGO is present in Manuka honey and is thought to be the unique antibacterial compound responsible for killing or inhibiting bacteria in wounds (172). However the antiviral activities of glyoxals were first reported in 1957, where two of these studies looked at the antiviral effect of 95 glyoxals against influenza and Newcastle disease virus when administered to an embryotic egg (43, 44, 218). Following these studies the anti-cancer properties of MGO were first reported in 1958 by French and Freelander, who investigated the carcinostatic action of polycarbonyl compounds. Although MGO was not the

sole focus of the study it was reported that an effective response against leukaemia cells was apparent with MGO (219).

A later report in 1993 concluded that MGO had the anti-proliferative effects on leukaemia cells *in-vitro* (41); however, a recent report has described the opposite effect *in-vivo* highlighting the activation of macrophages and lymphophocytes by MGO against tumour cells (220). It is thought that the apoptosis mechanisms of MGO responsible for cell death to include inhibition of DNA synthesis, RNA synthesis and protein synthesis (221). Two earlier reports also discovered the high success rate of MGO as an anti-cancer treatment against mice who were intraperitoneally injected with ascites cancers. In the first study mice were subjected to either lymphosarcoma or leukaemia. It was found that a five or six day dosage of 70 mg kg^{-1} to 80 mg kg^{-1} of MGO given once each day resulted in 90% to 99% inhibition of cancer growth (42). On the contrary, in the other study, mice were divided into four groups, where treatment began after 1, 4, 24 and 48 h respectively. Over a ten month period mice were treated with 18 injections daily, which amounted to 22 mg of MGO. In the first group, 15 mice remained free from ascites, in the second group, 13 remained free, in the third group 7 and in the fourth group, 4 (222).

A clinical trial of MGO in cancer patients has been reported with significant results. The study evaluated the performance of MGO against different types of cancer in fourty-six patients over a period of four months to five years. The cancers included, but not limited to brain tumours, head and neck cancer, gastrointestinal, lung, gynecological, breast, urological, hematological, prostate, gall bladder, and pancreatic cancer. The treatment consisted of an 8 ml solution of 0.45 M MGO diluted in 60 ml of water followed by a chewable tablet of vitamin C containing 400 mg of sodium ascorbate. The treatment was administered four times a day at regular intervals. The results highlighted the positive effects of MGO treatment with 78% of patients greatly benefited. 39% of patients had complete remission, while another 39% were classed as having partial remission or stable, 17% of patients were progressive and 2% was not stated. Patients during the study who had no sign of the disease after treatment strongly desired to continue the treatment for fear of recurrence. The significant finding of this study is that MGO is effective against a wide variety of cancer, which is in sharp contrast to other anticancer drugs now widely used. It also highlighted no adverse effects on glucose levels, which have been reported in other studies (40).

More recent studies have experimented with the idea of introducing MGO into hydrogel wound dressings (45, 46) and polymer based nano-formulations for drug administration (47). The former study investigated the liquid and hydrogel formulations of MGO against two bacteria pathogens found in wounds; *S.aureus* and *S.epidermidis*. The hydrogel was prepared using

Carbopol as a gelling agent with an MGO concentration of 0.5% (w/w). Liquid concentrations of MGO were also prepared at 0.5% (w/w) and 0.8% (w/w) in water. A 70 µM solution of Methicillin was also formulated for testing. 150 µL of the liquid solutions and hydrogel were deposited into 9 mm wells cut in agar plates which were inoculated with each bacteria species. The plates were incubated overnight at 37ºC and then examined for a zone of inhibition. The results highlighted that the average zone of inhibition diameters ranged from 18 mm to 40 mm with an increasing concentration of MGO from 1.25 mg mL^{-1} to 15 mg mL^{-1}. No zone of inhibition was observed against Methicillin, proving the resistance that the bacteria have to this drug. The hydrogel performed equally as well as MGO in liquid form, with average zones of inhibition of 29.3 mm ± 0.4 mm, using the gel, and 29.5 mm ± 0.3 mm when using the liquids (45). Following this study the development of a topical hydrogel formulation containing MGO and hyaluronan was developed to access the activity against various wound pathogens. Hyaluronan was chosen as it is a naturally occurring glycosaminoglycan of the extracellular matrix and has been shown to promote wound healing and tissue regeneration in a recent study (223). *E. coli*, *S. aureus*, *P.aeruginosa*, *Proteus mirabilis* and *MRSE* were all included for testing using standard agar diffusion and dilution tests. Gel formulations were prepared with varying amounts of MGO from 0.1 wt % to 1 wt %. The results showed that MGO was found to inhibit and kill bacteria for all bacteria species with the minimum inhibitory (MIC) values between 1.05 mM and 4.22 mM and minimum bactericidal (MBC) values between 2.11 mM and 4.22 mM (46).

New developments for the use of MGO in drug delivery have recently been investigated using conjugated MGO based nano-formulations (47). MGO was successfully encapsulated in nanoparticles in an emulsification mediated crosslinking method using a chitosan polymer (NMG). A second process involved the physical loading within a dendrimer polymer matrix using an equilibrium dialysis method (DMG). The diameters of the particles were found to be between 68 nm ± 10 nm and 45 nm ± 5 nm respectively. These diameters are found to be acceptable for an encapsulated drug delivery technique *in-vivo*. The release behaviour of the MGO was studied using a dialysis bag. After 12 h 75% of the MGO content was released from the DMG particles compared to 43% of the MGO content being release from NMG particles. This is thought to be due to the crosslinking of the NMG particles with glutaraldehyde and the hydrophobic and hydrogen bonding interactions between the MGO and chitosan. Both the NMG and DMG particles were tested for their antibacterial activity against four bacterial strains including both gram negative and gram positive species; *E.coli*, *P.aeruginosa*, *S.aureus* and Bacillus subtilis respectively. NMG showed antibacterial activity against both positive and gram negative bacteria. However, the DMG demonstrated antibacterial activity against gram negative bacteria only. The values for NMG particles against gram positive bacteria displayed a strong activity, ranging from 0.4 µg mL^{-1} to 0.8 µg mL^{-1} MIC and 1.6 µg mL^{-1} to 2 µg mL^{-1} MBC. In

contrast the MIC and MBC values against gram-negative bacteria were 2 μg mL^{-1} to 6 μg mL^{-1} and 4 μg mL^{-1} to 8 μg mL^{-1} respectively. DMG particles exhibited a strong effect with MIC values of 0.8 μg mL^{-1} and MBC values of 1.6–2 μg mL^{-1} against gram negative bacteria; *P.aeruginosa* and *E.coli*, respectively in comparison to MIC values of NMG. The concentrations of MGO found to demonstrate a biocidal effect in this study, where nanoparticles are used, were shown be considerably lower when compared to another study which showed a concentration of 1.05mg mL^{-1} in a liquid form (172).

2.5.2 Potential complications of Methylglyoxal in diabetic patients

MGO has the ability to induce irreversible modifications in proteins under physiological conditions (224). It was shown that MGO was a potent protein glycating agent able to form advanced glycation end products (AGEs) (225). Numerous studies have indicated that AGEs have a pathogenic role in the progression of different oxidative-based diseases including diabetes (226-228). MGO is thought to be elevated in diabetic patients which may cause a variety of complications including nephropathy, retinopathy and cardiovascular disease (229). There are also reports that irreversible AGEs can disrupt the matrix remodelling of collagen (230). The treatment of diabetic foot ulcers with a Manuka honey dressing is also the subject of debate due to the speculation MGO may put patients as risk (231). However no study to date has reported any direct complications in diabetic patients treated with a Manuka honey dressing.

On the contrary one study which assessed the treatment of neuropathic diabetic ulcers with a Manuka honey dressing, showed that no complications arose during treatment. The results showed a comparison of healing time between a Medihoney tulle dressing and a saline soaked gauze dressing. An increased rate in healing was achieved with the Manuka honey, with a mean healing time of 31 ± 4 days compared with 43 ± 3 days for the saline dressing (191).

2.6 Polymeric materials as delivery vehicles for targeted drug delivery in wound care

Recent attempts in the area of drug delivery in wound care, include targeted drug delivery, where the antibacterial agent or drug shows activity at the wound site and limits systemic absorption (232). Controlling the release of a drug to a specific target, involves prolonging the action of the active drug, while maintaining a continual release. The use of polymers, such as PVA (233) show promising advantages for controlling the delivery, when compared to drug administration via injection or oral ingestion. These advantages include; 1) continuously maintained plasma drug levels in a therapeutically desired range, 2) harmful side effects from systemic administration are eliminated or reduced, 3) a continuous release of a small amount of a drug may be less painful than several large doses, 4) delivery via this method is potentially

less wasteful and expensive (60), 5) many polymers are readily biodegradable and can be washed off the wound surface once the drug has exerted the desired effect, 6) improvement of patient compliance, as there is less need for frequent dressing change if the delivery can be maintained for up to one week (21). An ideal drug delivery system should follow zero-order kinetics, where the concentration of the drug or antibacterial agent in the blood remains constant throughout the delivery period. The controlled delivery is most suited for non-healing chronic wounds such as diabetic ulcers, venous leg ulcers and decubitus ulcers. In these cases a bioactive compound is incorporated into a carrier material and the release rate may be dependent on the physiochemical properties of the carrier material, as well as the bioactive compound. It may also rely on the environmental conditions of the wound, including pH, ionic strength, temperature, enzymic concentration and degree of infection. Some dressings require the influence of the inflammatory enzymes or microbial proteases in the wound, in order for the drug release to take place. The polymer in the dressing is degraded by the enzymes, thereby releasing the drug from the polymer matrix (232).

In others systems, where hydrophilic polymers, such as hydrogels are used, the controlled release of a drug happens via one or more physical process, including; 1) hydration of the polymer by the wound exudate, 2) swelling of the polymer to form a gel, 3) diffusion of the drug through the gel matrix and 4) eventual biodegradation of the polymer gel (21). Hydrogels offer many unique characteristics as wound dressings for drug delivery systems, in that they can be easily tuned via crosslinking techniques to control the rate of swelling and subsequent diffusion of the drug into the wound. They are generally highly biocompatible since they provide a high water content and have similar physiochemical properties similar to the extracellular matrix of the skin (234). Hydrogels are discussed in more detail in section 2.7.1.1.

2.7 Wound dressing classification

Wound dressings can be classified into four main categories based on the required treatment, these include passive, interactive, advanced and bioactive. A passive dressing will provide protection to the wound from mechanical trauma and bacteria permeation. They are dry and will not control moisture levels in the wound. Examples of passive dressings include gauze, bandages and tulle materials (235). An interactive dressing will facilitate wound healing by alternating the environment and interacting with the wound surface to optimise the healing process (22). They are fabricated with polymeric films and foams which are permeable and transparent to water vapour and oxygen. They offer a protective environment from external organisms such as bacteria (235). An advanced dressing is capable of maintaining a moist environment around the wound. Hydrocolloids and alginates are classed as advanced dressings (235). However hydrocolloids and alginates have also been grouped into the class of bioactive dressings (17). A bioactive dressing delivers substances active in wound healing; either by

delivery of bioactive compounds or constructed by materials having endogenous activity (17). For the purpose of this study, bioactive dressings are of importance when considering the delivery method of antibacterials into the wound environment.

2.7.1 Bioactive wound dressings

Bioactive dressings should be able to provide all or some of the following characteristics (17, 235):

- Maintain a moist wound environment, while absorbing small amounts of wound exudate.
- Neutralise the wound alkalinity by restoring the natural pH of the wound and skin.
- Act as a drug delivery system to the wound site, while maintaining a controlled release rate.
- Act as a skin substitute to severe burns or chronic wounds, where a large portion of the skin is lost.

Within the classification of bioactive dressings, are specific types and structures, including hydrocolloids, hydrogels, alginates, chitin and chitosan derivatives and antibacterial dressings, such as honey and silver (17). As the work in this thesis is concerned with the hydrogel forming polymer PVA, a further discussion of hydrogels is given below in section 2.7.1.1. PVA is discussed in section 2.7.1.2.

2.7.1.1 Hydrogels

A hydrogel is known as ‘a water absorbing gel substance of varying rigidity (17)’. They are three-dimensional hydrophilic polymer networks, which are soluble in water (234, 236). Synthetic polymers such as poly(methacrylates), poly(vinylpyrrolidine (21) and poly(vinyl alcohol) (PVA) (237-239) are some common polymers used in hydrogel dressings. If the hydrogel has low rigidity it can be applied onto a wound via a syringe as an amorphous gel. These gels may require a second covering to avoid any movement. However, the more rigid hydrogels in the form of an elastic, solid sheet or film (240) are enclosed in a sealed sterile sachet which is opened upon direct application to the wound. The main role of a hydrogel is to hydrate the wound environment. Hydrogel dressings contain between 70–90% water which allows only a limited amount of exudate to be absorbed. Therefore hydrogels are more suited to light moderately exuding wounds (21). A hydrogel dressing may be used on necrotic, sloughy, granulating (241) and epithelializing wounds. If the hydrogel is used on a heavily exuding infected wound, the hydrogel must be changed daily, as there is the possibility the hydrogel will donate fluid into the wound causing maceration (236). Hydrogels have recently attracted attention with the objective of use as a properly controlled system to deliver drugs. The high

water content of a hydrogel promotes similarities to the physical and mechanical properties of the extracellular matrix, making them favourable materials in drug delivery (234).

2.7.1.2 Poly(vinyl alcohol) (PVA) as a hydrogel material

Poly(vinyl alcohol) (PVA) is a semi crystalline, hydrophilic polymer. It is known to have good chemical and thermal resistance and good physical properties (242, 243). Recently, PVA has become attractive for its use as a hydrogel in biomedical applications (238). PVA has been approved for medical use in humans by the FDA (61), where it has been used for several medical applications including transdermal patches, oral drugs, contact lenses, ophthalmic solutions such as synthetic tears (244), implants of artificial organs, cardiovascular devices and cartilage skin (245) . It has been shown to provide biocompatibility with tissue and blood, when combined with sodium alginate into a gel matrix (246) and in a study where a PVA hydrogel was used for the controlled release of antibiotic gentamicin when in contact with wound fluid (247) and the slow release of antibiotics into rats (63). PVA is also valued for its biodegradability (248).

Several studies have explored the potential of PVA as a hydrogel forming polymer when used alone or combined with other natural or synthetic materials. Of these studies, PVA and poly (acrylic acid) were blended with two biological polymers, collagen and hyaluronic acid to form a hydrogel which was loaded with growth hormones for drug delivery for bone and cartilage repair (245). Another study combined PVA with poly (N-vinyl prryolidone) and chitosan as medicated hydrogel dressings containing antibiotic ciprofloxacin (249). PVA/gelatin hydrogel membranes were also fabricated via esterification of the hydroxyl groups in PVA and the carboxyl group of gelatin. The hydrogel membranes were shown to be super absorbent and highly compatible with human blood (64). Another study investigated the controlled release of two antibiotics, tylosin and oxytetracycline via the use of a PVA hydrogel. The results indicated a slow release of up to five days with tylosin as detected in the kidneys and muscles (63). The preparation of PVA hydrogels via electrospinning has also been explored in many cases and is discussed in section 2.8.4.2.

2.7.1.3 Crosslinking of PVA

PVA has poor stability in water, resulting in the majority of studies crosslinking PVA via physical or chemical treatment in order to make PVA insoluble, improve the mechanical integrity and control the release of any additional agents (54). The different techniques previously used to crosslink PVA are discussed in detail in a review by Bolto et al. (250) and are shown in Table 2.8. One of most popular methods, glutaraldehyde crosslinking which has already been employed for potential hydrogel materials in wound care (66), is discussed below.

Table 2.8: Crosslinkers used on PVA (250).

Freeze thaw treatment	Maleic acid and anhydride
Heat treatment	Malic acid
Acid catalysed dehydration	Malonic acid
Irradiation	Fumaric acid
Persulphate treatment	Poly(acrylic acid)
Formaldehyde	Trimesic acid
Gluataraldehyde	Trimesoly chloride
Glyoxal	Toluene diisocyanate
Teraphthaldehyde	Glycidal acrylate
Acrolein	Divinly sulphone
Urea formaldehyde/H_2SO_4	Boric acid
Citric acid	1-2 Dibromoethane
ɣ-Glycidoxypropyltrimethoxysilane	Tetraethoxysilane
ɣ-Mercaptopropyltrimethoxysilane	

Gluataraldehyde has been employed as a crosslinking agent to PVA and PVA composite membranes in the form of a vapour (66), or a solution, where an acid catalysis is sometimes used (251, 252). It may also be included within polymer solutions during electrospinning (253). The crosslinking reaction between PVA and GA can be seen in Fig. 2.5 and can be attributed to the formation of acetal bridges between the hydroxyl groups in the PVA and the difunctional aldehyde molecule in GA (254, 255).

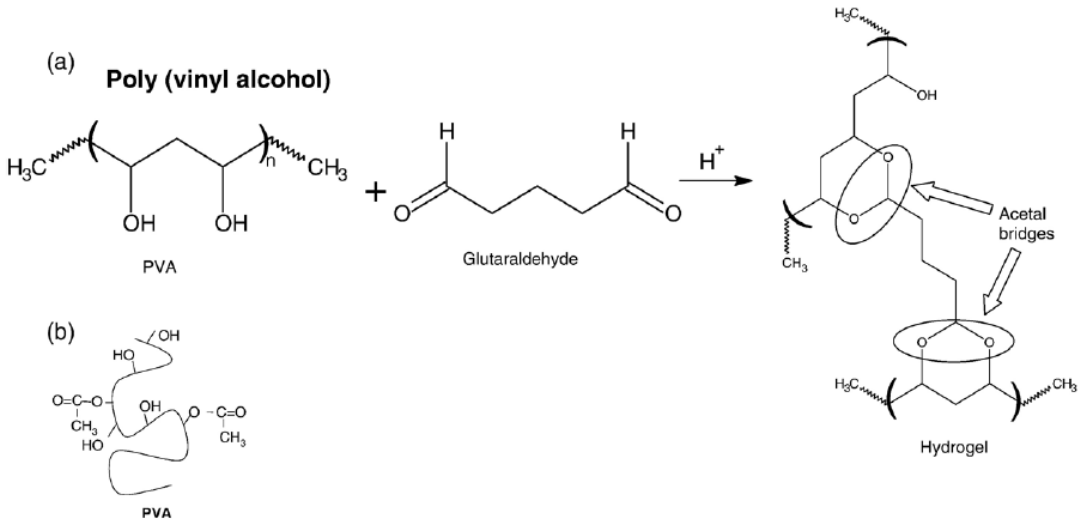

Figure 2.5: Chemical reaction of PVA polymer with Glutaraldehyde (256).

A study by Wang and Hseih (251) prepared a GA crosslinking solution by dissolving 50 wt % aqueous GA with 0.5 M aqueous sodium sulphate or ethanol to achieve a 0.2 M GA solution. PVA fibrous membranes were immersed into either GA solution for various lengths of time between 20 min to 2 days. The PVA membranes were then dried in a vacuum oven at 80ºC for 12 h. In both cases the crosslinking with both GA solutions proved successful in providing water stable hydrophilic PVA membranes.

In another study, nanofibre mats fabricated from chitosan, silver nanoparticles and PVA were exposed to a 25 wt % GA vapour for various lengths of time between 30 min to 120 min. Any unreacted GA vapour was removed via the incubation of the nanofibre mats in a vacuum oven at 70ºC for 24 h. The study showed that the cumulative amount of silver ions released over a 7 day period in distilled water at 32ºC, was greater after only 30 min crosslinking time when compared with 60 min and 120 min crosslinking time (66). Fig. 2.6 shows the release profile of the silver ions from the GA crosslinked PVA nanofibre mats.

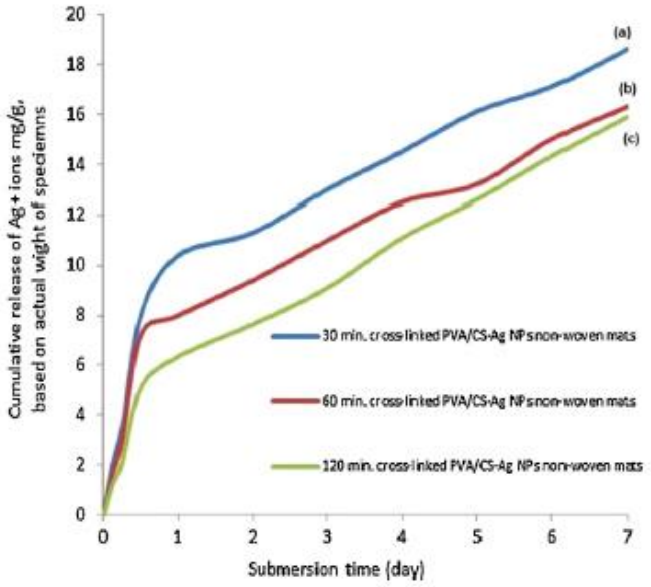

Figure 2.6: Cumulative release profile of silver ions released from the GA crosslinked PVA nanofibre mats for different crosslinking times (66).

A similar study by Destaye, Lin and Lee (254), examined the crosslinking of PVA electrospun mats. Four different GA molar concentrations between 0.5 and 2.56 were prepared and the PVA mats were exposed to the GA vapour for differing lengths of time between 6 h and 48 h. It was reported that the non crosslinked PVA mats were instantly soluble in water. After crosslinking via GA vapour, the PVA mats were rendered water insoluble. The higher molar concentrations of 2.0 and 2.56 showed no change in fibre morphology. At the lower molar concentrations of 0.5 and 1.0, with increasing crosslinking time, the fibres began to swell and flatten. This was explained by the higher water content at lower GA concentrations, which caused swelling in the fibres.

Tang et al. (253) reported a single step process of crosslinking PVA during electrospinning, by incorporating GA and a hydrochloric acid in appropriate portions in the polymer solution. Another study also employed a similar technique, using hydrochloric acid. PVA electrospun substrates were immersed in GA concentrations prepared between 15 mM to 60 mM and 0.01 N hydrochloric acid in an acetone solution for 24 h. It was found that the water uptake of the electrospun PVA substrates was reduced by approximately 6 g in weight when the GA concentration was lowered from 15 mM to 30 mM. Between a GA concentration of 30 mM and 60 mM a gradual decrease in the water uptake of 1.5 g in weight was observed (255). The release profile of raspberry ketone (RK) from a gelatin/PVA nanofibre matrix at concentrations of 2% and 5% after crosslinking with GA was also reported. The exact method of crosslinking was not given. GA crosslinking times of 0 h, 2 h and 5 h were employed. A weight of 0.2 g of fibre was placed into 80 ml of phosphate buffer solution at 37ºC and agitated at 100 rpm. 5 ml samples were taken from the buffer solution at times between 10 min and 300 min. The

cumulative amount of RK released in the buffer solution was detected using UV spectroscopy. The release profile can be seen in Fig. 2.7. In the first 2 h, a large initial burst between 70% and 80% KR was detected, before the profile levelled out. With an increase in crosslinking time the release rate was slowed down and the degree of fibre swelling was decreased (64).

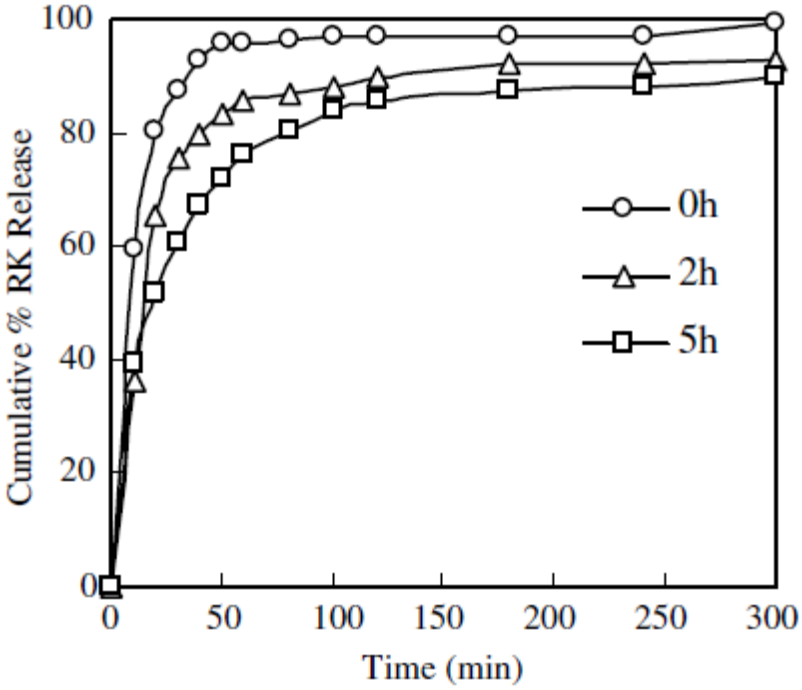

Figure 2.7: Cumulative release profile of raspberry ketone released from GA crosslinked gelatin/PVA nanofibres for different crosslinking times (64).

2.8 Electrospinning fundamentals

2.8.1 The principles of needle electrospinning

The ability to create fibres using an electrostatic field has been known since 1934, when Formhals patent on artificial filaments using a high electric field was published (257). This technique described the effect of an electrostatic force on a liquid droplet. A cone shape was formed at the tip of a capillary where small jets were formed when the charge density was high enough (257). The cone shape at the needle tip was later described as a Taylor cone by Geoffrey Taylor, where the disintegration of water droplets in an electric field was explored (258). Since these discoveries the basics of solution electrospinning in many laboratories has followed the basic set-up shown in Fig. 2.8.

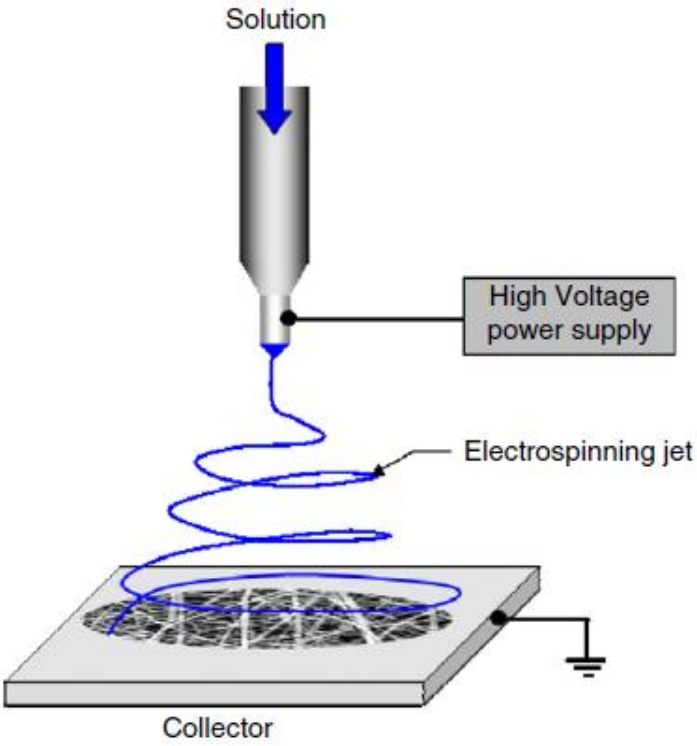

Figure 2.8: Basic solution electrospinning set-up (259).

The simple set-up consists of three major components, a high voltage power supply, a spinnerette (syringe and needle) and a grounded collector (260). A solution is held in the syringe, which is fed to the needle tip at a controlled rate. A high voltage, usually more than 5 kV (259), is supplied to the needle, this electrifies the drop of solution at the needle tip by both electrostatic repulsion between the surface charges and the Coulombic force exerted by the electrical field. As a result the drop of solution at the needle tip transforms into a conical shape known as the Taylor cone (258). When the electrostatic charges are great enough to overcome the surface tension of the solution, the ejection of polymer jets from the needle tip are initiated. The electrified jet undergoes a whipping action, during which it is elongated and stretched into a long thin polymer thread attracted by the grounded collector. During this phase, the solvent is evaporated and the charged fibre landing upon the collector is arranged in a randomly orientated state (260).

This basic electrospinning process where by only one electrospinning jet is formed, has some limitations when considering the productivity, with reports that one needle can only produce fibres up to 300 mg h^{-1} (261). Various other systems have since been explored, including multi-jets from a single needle, multi-jets from multiple needles and free surface (needleless) systems. However, the multi-needle systems usually require a large operating space, and the optimisation of the relative locations of needles, has to be considered to avoid the strong charge-repulsion

between the neighbouring solution jets. Regular cleaning has to be employed to each needle to prevent the blockage of the nozzles during spinning (262).

To solve these problems, several methods of free surface (needleless) electrospinning have been explored, where several polymer jets are launched from a free liquid surface. In this method, several potential benefits are available, including simplicity of design, lower operating and equipment costs, higher production rate, higher fibre and web uniformity, and higher fibre packing density (262). Elmarco s.r.o in the Czech Republic, are the first company to develop and patent (263) laboratory and commercial free surface (needleless) electrospinning equipment. In this study an Elmarco NS Lab was employed during experimental work and for the purpose of this literature survey, the technology of this equipment will be discussed in section 2.8.2.

2.8.2 Free surface (needleless) electrospinning - Nanospider

In this process a rotating electrode drum is dipped into a bath containing a polymer solution. A thin layer of the polymer is carried on the surface of the drum, which is exposed to a high voltage electrical field. When the voltage applied exceeds a critical value, electrospinning jets are formed along the electrode (264). These jets then rise upwards towards the grounded electrode, covered by a supporting substrate. Fig. 2.9 shows a schematic illustration of the free surface needleless electrospinning set-up using an Elmarco Nanospider. Fig. 2.10 shows the formation of jets along a spinning electrode (265). Until recently the theoretical description of free surface needleless electrospinning was not formulated.

In 2008, Lukas, Sarkar and Pokorny derived a hypothesis based on the process of multi-jet formation from a liquid surface in an electric field. The work showed that the process can be analysed based upon Euler's equation for liquid surface waves (265). From this equation, they developed another which explained the critical field strength value which must be met in order to initiate jet formation from the rotating electrode and one which explains the critical spatial period (wavelength- the average distance between jets generated from the surface) (264, 265).

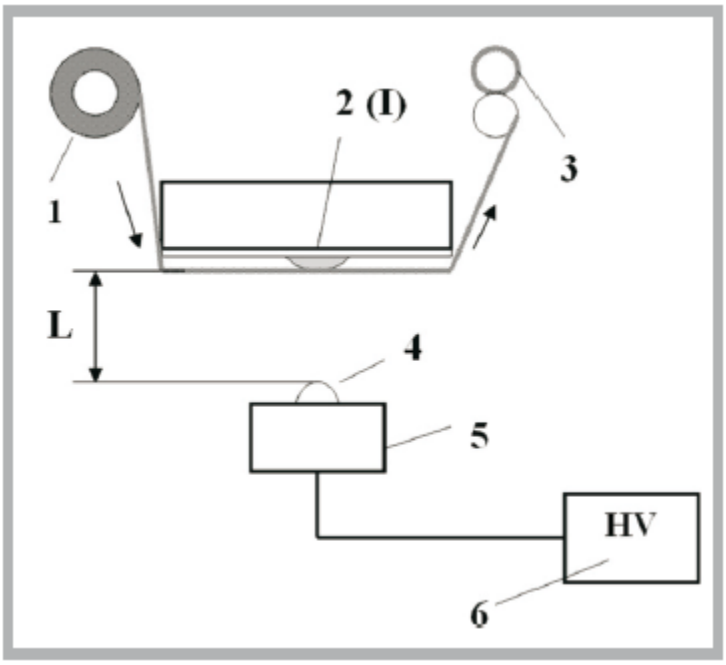

Figure 2.9: Set-up of the free surface (needleless) electrospinning process using a Nanospider (266). 1 = support material, 2 = grounded electrode, 3 = support material with a layer of fibres, 4 = bottom rotating electrode drum, 5 = tray with polymer solution, 6 = power supply with a positive polarity from 0-75 kV & L = the distance between bottom rotating electrode and support material (265).

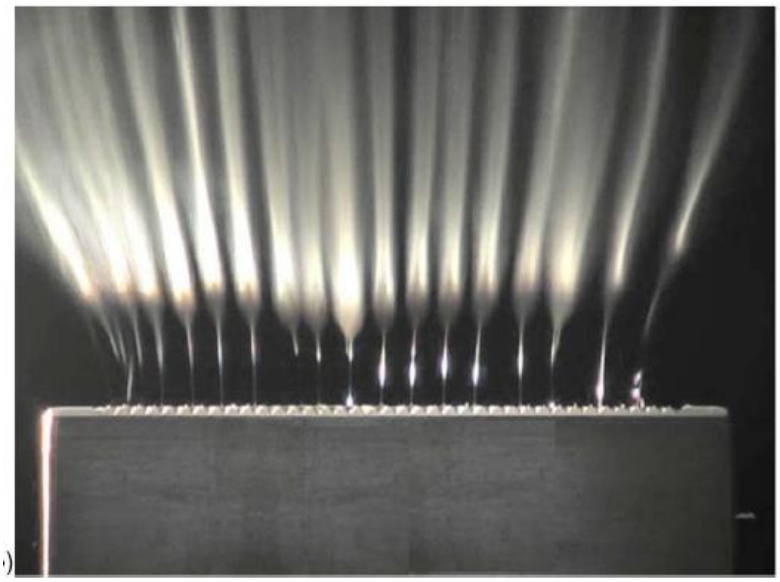

Figure 2.10: Formation of polymer jets rising from the rotating electrode drum (265)

2.8.3 Electrospinning Parameters

Polymer solution, processing conditions and ambient conditions are three factors which influence the morphology of electrospun fibres. Within each of these factors are numerous parameters which may be altered to achieve a desired fibrous structure. Table 2.9 refers to each of these parameters, some of which are discussed in further detail.

Table 2.9: Electrospinning parameters.

Solution Parameters	Processing Condition Parameters	Ambient Condition Parameters
Molecular weight	Voltage	Humidity
Concentration	Flow Rate*	Atmosphere
Viscosity	Collector	Pressure
Surface Tension	Diameter of Needle*	Temperature
Conductivity	Distance between tip/electrode and collector	

* Applies only to needle electrospinning

2.8.3.1 Polymer Solution Parameters

Molecular Weight/Viscosity/Concentration

The molecular weight (M_w) has a direct influence on the viscosity of a solution. When the M_w of a solution is higher, there will be greater entanglement of the polymer chains within the solution, resulting in a higher viscosity. An increase in concentration of a polymer will also increase the viscosity for the same reason (267). As an example, a study looked at the effect of varying M_w between 9000 and 186,000 g mol^{-1}, and solution concentrations between 6 wt % and 31 wt %, when using PVA. It was found that by varying the M_w and solution concentration of PVA in water, a significant effect was had upon the fibre morphology. At a concentration of 21 wt % and a M_w of 13,000-23,000 g mol^{-1}, the fibres appeared circular. As the concentration is increased to 27 wt % for the same M_w, the fibres become less round and appeared flat. When the PVA concentration was relatively low, at 6 wt %, a higher M_w between 50,000 and 186,000 g mol^{-1} produced round fibres. During the experiment a voltage of 30 kV was supplied and aluminium foil was used as the collector. No mention was given to the flow rate used (242).

Many studies have also shown that at low polymer concentrations and viscosities, beaded fibres are generally formed (268). A critical polymer chain entanglement is required in order to initiate the electrospinning jet and obtain fibres free from beads (269). If the viscosity becomes too high, in the case of needle electrospinning, the flow of polymer solution to the needle tip will be prohibited (270) and subsequent needle blockage may occur (268).

Surface Tension

For the electrospinning process to occur, the charge of the polymer solution must be high enough to overcome the surface tension of the solution. If the polymer solution has a high concentration of free solvent molecules, there is a possibility that the molecules will group together and create a spherical bead shape due to the surface tension. To overcome this problem an increase in viscosity will help to create a greater interaction between the solvent and polymer molecules. When the solution is stretched during electrical charging the solvent and polymer molecules are less likely to congregate into a spherical shape. Instead the solvent molecules will spread over the entangled polymer molecules (267). Fig. 2.11 illustrates this occurrence.

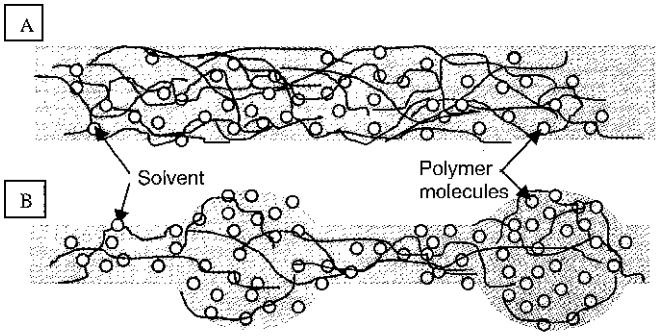

Figure 2.11: Bead formation during electrospinning, where (A) shows the solvent molecules distributed over the entangled polymer at a relatively high viscosity and (B) shows how the solvent molecules tend to congregate under the action of surface tension at a relatively low viscosity (267).

Conductivity

The electrospinning process can only occur when a solution gains sufficient charge so that the repulsive forces within the solution can overcome the surface tension. The ability for a solution to incur stretching and drawing also depends on how well the solution can carry charges (267). A number of studies have reported that a high solution conductivity yielded fibres free from beads (271-273). One study reported that the addition of salts to the electospinning solution resulted in a higher charge density on the electrospinning jet surface, which in turn increases the charges carried by the jet, causing higher elongation and fibres with fewer beads (268).

2.8.3.2 Processing Condition Parameters

Voltage

A high voltage is an essential element in the electrospinning process. A high voltage will induce the required charges on the polymer solution and together with the external electrical field an elctrospinning jet will emerge from the needle tip or rotating electrode when the electrostatic charge is high enough to overcome the surface tension of the solution (267). During the electrospinning process the viscoelastic solution will be stretched by the columbic repulsive

force in the jet. A higher voltage will increase the acceleration of the jet and stretch the polymer solution due to the increase in electrical charges (268). This may result is fibres with a smaller mean diameter, due to the stretching of the polymer jet (274, 275). However, if the acceleration is too fast the solvent will have less time to evaporate and will result in wet polymer fibres composed of mainly beads landing upon the collector (276).

Distance

It can be assumed that by increasing the distance the polymer solution has to travel, the stretching of the solution will be increased, resulting in a smaller fibre diameter. Increasing the distance also allows time for the solvent to evaporate before it reaches the collector (267). When the distance is too low, it may cause the fibres to merge, forming junctions (275), as shown in Fig. 2.12.

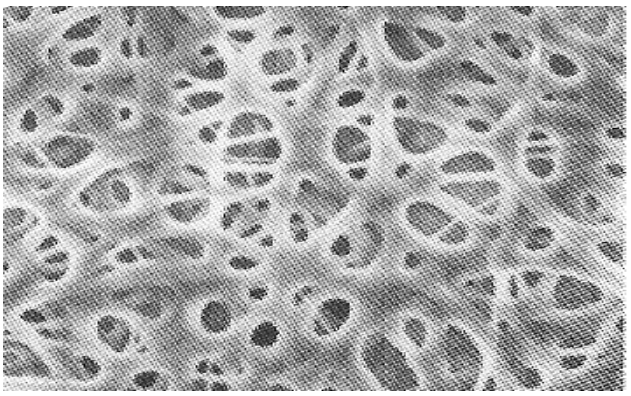

Figure 2.12: Nylon 6,6 . Merging fibres deposited at a distance of 0.5 cm from the collector (241).

Flow Rate

Flow rate refers to the amount of solution released from the needle tip. It can be assumed that if a greater volume is drawn away from the needle tip at a given voltage, the fibre diameter may be greater than a lower flow rate at the same voltage (268). However, a greater volume of solution will take longer for the solvent to evaporate and so the distance must be considered when finding optimum spinning conditions (277).

2.8.3.3 Ambient Condition Parameters

The temperature, humidity, atmosphere and pressure may also have an influential effect on the polymer solution during electrospinning. The humidity is of particular importance as water drops may condense on the surface of the fibres, disrupting the fibre morphology (267). A study on the effect of relative humidity (RH) on the electrospinning of poly (acrylonitrile) (PAN) and polysulfone (PSU) showed great variation in the diameter and mechanical strength of the fibres with varying RH between 0% to 60%. For example the average fibre diameter of PAN increased

from 150 nm at 0% RH to 630 nm at 60% RH while the average diameter of PSU fibres increased from 1.15 µm at 0% RH to 3.58 µm at 50% RH, all other parameter remained constant. PAN fibres were also shown to shift from a smooth surface to a rougher one with increasing RH. PSU exhibited varying changes in the surface morphology with increasing RH, from smooth to elongated pores and creases in the fibres (278).

A change in temperature is also known to affect the fibre morphology during electrospinning, due to the change in viscosity of the electrospinning solution and solvent evaporation (267). Polyurethane was shown to produce more uniform fibres, when electrospun at a higher temperature of approximately 70ºC, when compared with those spun at ambient room temperature. At the higher temperature several jets were produced from the tip of the needle, with a large angle between each jet. It was also observed that the deposition rate of the fibres was increased at a higher temperature, resulting in a thicker electrospun web (279).

2.8.4 Electrospun polymeric materials for wound care

Electrospun materials as medical dressings are still in their infancy, with many research institutions exploring new possibilities. These materials meet the majority of the requirements outlined for wound healing polymer devices, as their microfibrous and nanofibrous structures provide the nonwoven textile with desirable properties (280). The fibres produced from electrospinning are exceptionally small, with typical fibre diameters ranging from 5 nm to 500 nm (57). This offers many advantages including, a high surface area between 5 m^2 g^{-1} to 100 m^2 g^{-1} (281) and a high aspect ratio, where the length of the fibres can be as long as several kilometres due to the continuous process (260). The size of the fibres also provides an environment which closely mimics the extracellular matrix (ECM) required in healing (260). They also have a high porosity but small pore size, with reports of 93.6% porosity (280) and pore throat diameters ranging between 0.1 µm to 0.8 µm (282). These unique properties of electrospun webs provide the following benefits for materials in wound care and can be seen below in section 2.8.4.1.

2.8.4.1 Potential benefits of electrospun materials in wound care

Haemostatic effect: Due to the small interfaces and effective high surface area, haemostasis is promoted via the physical nature of the nanofibrous material without the need of a haemostatic agent (283, 284).

Absorption: The work by Dabney (285) showed that the water absorption of nanofibres of the same polymer, absorbed between 17.9% to 213% compared to a typical film dressing which only absorbed 2.3%. If a hydrophilic polymer is used, this will increase absorbability further, which is necessary for heavy exuding wounds.

Semi-permeability: The porous structure provides excellent respiration for the cells (284) and does not lead to wound desiccation (286). The small pore size allows for protection against bacteria, while allowing gas permeation (286).

Conformability: The ability of a dressing to conform to the contour of the wound is one of the parameters that needs to be clinically assessed. It is recognised that conformability of a textile material is closely related to the fineness of the fibres. In the case of electrospun fibres, the lower fibre diameter results in better coverage and protection from bacteria infection (284).

Functionality: Antibacterial agents or growth factors for promoting fibroblast or epithelisation can be incorporated into the carrier polymer during the electrospinning process, making the fibrous membranes bioactive. Multi layers can also be achieved to provide different functionality in each layer to attain desired objectives in wound healing (285). This allows for the decreased frequency in dressing change and the disturbance of tissue regeneration.

Reduction of Scar Tissue: Fibres produced via electrospinning can also provide a scaffold to promote cell growth, as the size of the fibres closely bio-mimics the proteins such as collagen found in the ECM (58). The topographical nature of the electrospun webs also plays an important role in cell attachment and proliferation (59). These features hope to aid in a wound free from scarring.

2.8.4.2 Electrospun poly(vinyl alcohol) webs for wound care

Electrospun hydrophilic polymer webs provide a convenient way of incorporating antibacterial agents or drugs into fibres, via suspending or dissolving the agent into a polymer solution prior to spinning (48). These webs offer potential means of delivering a drug or antibacterial agent to the wound site via diffusion alone or diffusion and scaffold degradation (58). PVA has many beneficial properties which make it a desirable polymer for use in wound care and drug delivery systems, as discussed previously in section 2.7.1.2. Several studies have explored the use of

electrospun PVA webs for potential wound dressing materials or transdermal patches. Of these studies PVA has been used alone (67, 159, 287-291) or combined with other natural and synthetic polymers such as sodium alginate (292), calcium alginate (293), poly(vinyl acetate) (54), polyurethane (PU) (294), polyethylene (295), chitosan (66, 296), gelatin (233), and silk fibroin (297).

Antibacterial agents or antibiotics, such as silver (67, 288, 292, 295), honey (287), gum tragacanth (298), ciprofloxacin HCL (54), gentamicin (294), ketoprofen (291), raspberry ketone (233) and non-steroidal anti-inflammatory drugs (289) have been incorporated within the PVA or copolymer matrix with the intention of providing a controlled delivery to the intended site or an antibacterial effect on bacterial organisms. In certain cases, the controlled release of the antibacterial agent or drug was achieved via crosslinking with GA (64, 66), as discussed in section 2.7.1.3. The release of antibacterials or drugs from PVA webs without crosslinking has also been reported. A study by Maleki et al. (287), assessed the release of dexamethasone sodium phosphate (Dex-P), an anti-inflammatory drug, from electrospun PVA/honey nanofibres, for the potential use in wound dressings. In this work, PVA/honey electrospun solutions were prepared at differing ratios in distilled water. Dex-P was added to the certain PVA/honey ratios at concentrations of 5, 10 and 15 wt %. PVA solutions without honey, containing Dex-P at equivalent concentrations were also prepared for electrospinning. The spinning solutions were electrospun using the syringe method at a voltage of 19 kV, a distance of 20 cm and flow rate of 1 ml h^{-1}. The release of Dex-P from the as-spun webs was assessed via immersing pre-weighed webs of both PVA/honey (ratio of 80/20) and PVA in phosphate buffer solution (PBS) at 37ºC in a shaking incubator. At scheduled intervals, 1 ml of the solution was taken and replaced by 1ml of fresh PBS. The amount of Dex-P present in the solution was measured by a UV-visible spectrometer and related to the premade calibration curves of Dex-P in in PBS. Figure 2.13 shows the cumulative release profile of Dex-P from both PVA/honey (Fig. 2.13B) and PVA webs (Fig. 2.13A) was similar. A large initial burst was firstly observed in the first 40 min. After this the amount release amount plateaued. The effect of Dex-P concentration also showed a limited effect, with the higher concentration of 15 wt % showing a slightly increased release percentage (287).

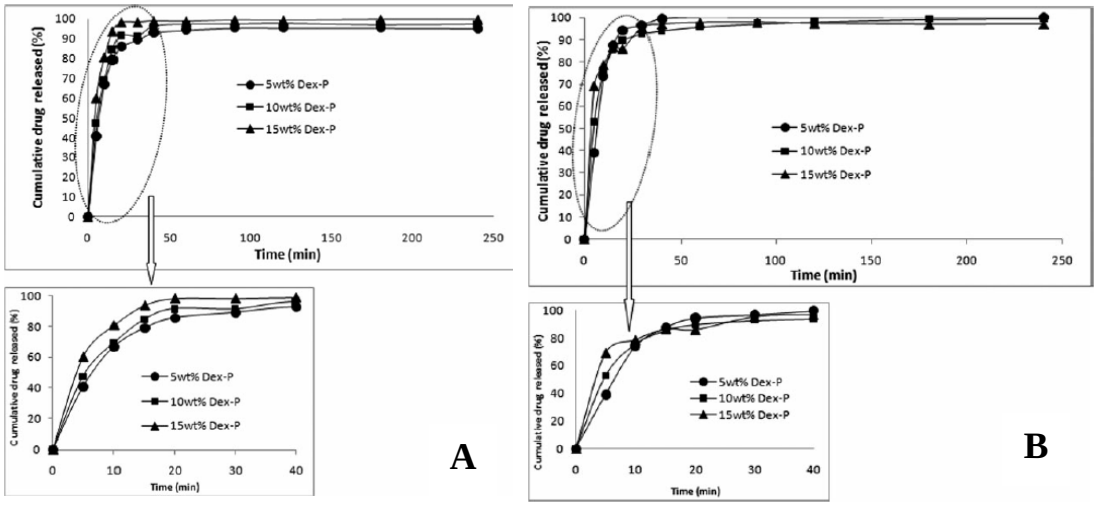

Figure 2.13: Cumulative release of Dex-P from PVA (A) and PVA/honey 80/20 (B) electrospun fibres (287).

The antibacterial effect of the electrospun PVA fibres, in the majority of cases is assessed via a common zone of inhibition method (292, 294). One study reported the effect of gentamicin on bacteria *S.aureus* and *P.aeruginosa* from a multi-layered electrospun composites prepared by nanospider technology (294). PU and PVA were electrospun separately in a layering process to build a novel composite structure. Within the PVA layer, gentamicin was added to the PVA electrospun mixture at a 10 wt % concentration. Thermal crosslinking was employed to the PVA layer at 145ºC for 15 min. A non-crosslinked sample was also prepared. To determine the antibacterial performance from the multi-layered structure, 6 mm discs were cut from the electrospun samples and placed on agar plates seeded with either *S.aureus* or *P.aeruginosa*. The plates were incubated at 37ºC for 1, 2 and 6 days. Pure gentamicin disks containing the same concentration were used as a control, as well as a multi-layered electrospun structure free from the drug. Clear inhibitory zones were observed with both strains around all of the gentamicin loaded samples, as seen in Fig. 2.14. The control samples showed no zone. This experiment proves that gentamicin survives the high electric field during electrospinning and high temperatures during thermal crosslinking (294).

Similarly two others studies also reported the antibacterial effect of sodium alginate/PVA/zinc fibres and PVA/silver fibres using the agar plate diffusion method, where zones of inhibition were reported in both cases (67, 292).

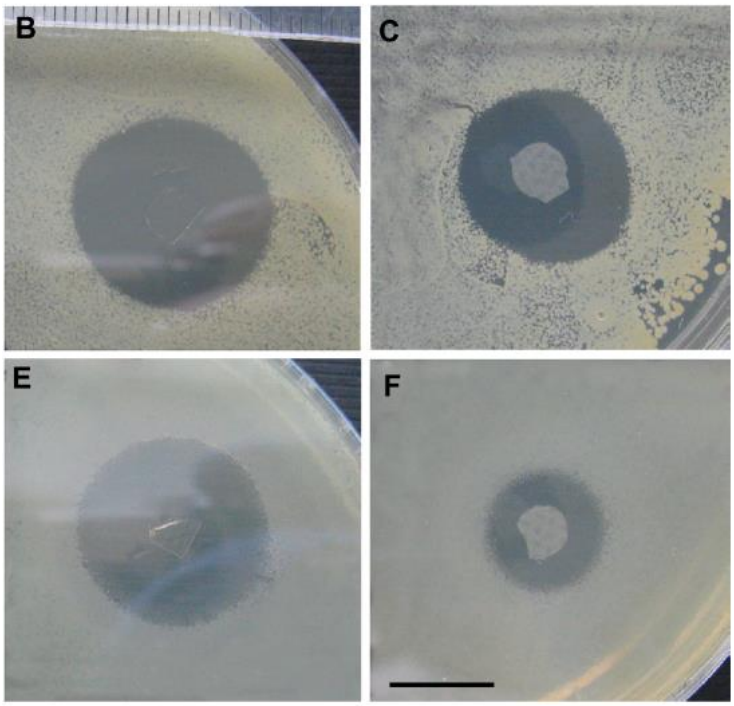

Figure 2.14: Zone of inhibition produced from non-crosslinked PU/PVA samples (B&E) and crosslinked PU/PVA samples (C&F) loaded with gentamicin for different bacterial strains. B&C = *S.aureus* and E&F = *P.aeruginosa* (294).

The antibacterial activity of chitosan/PVA nanofibre mats loaded with silver nanoparticles (Ag-NPs), was assessed using a different approach called a viable cell counting method (66). In brief, this system cultivated a known amount of *E.coli* colony forming units (CFU) per ml of nutrient broth. Several dilutions of this original solution were made to reach a desired concentration of bacteria. Electrospun PVA/chitosanAg-NPs and PVA/chitosan mats were prepared at varying ratios to determine the effect of chitosanAg-NPs or chitosan on the growth of *E.coli*. 100 g samples of the electrospun webs measuring 2.8 cm in diameter were added to 10 ml of the cultured bacteria broth and incubated in a shaker at 37ºC for 24 h. After this time, 100 µL of the bacterial solution was taken and spread onto nutrient agar containing plates. These plates were then incubated again at 37ºC for 24 h and the number of surviving bacteria colonies was counted. The results indicated that the PVA/chitosan webs were able to prevent the growth of *E.coli* at a ratio of 80:20, where the concentration of bacteria was at 7×10^5 CFU ml^{-1}. In comparison the PVA/chitosanAg-Nps at a ratio of 90:10 were able to prevent the growth of bacteria, as seen in Fig. 2.15.

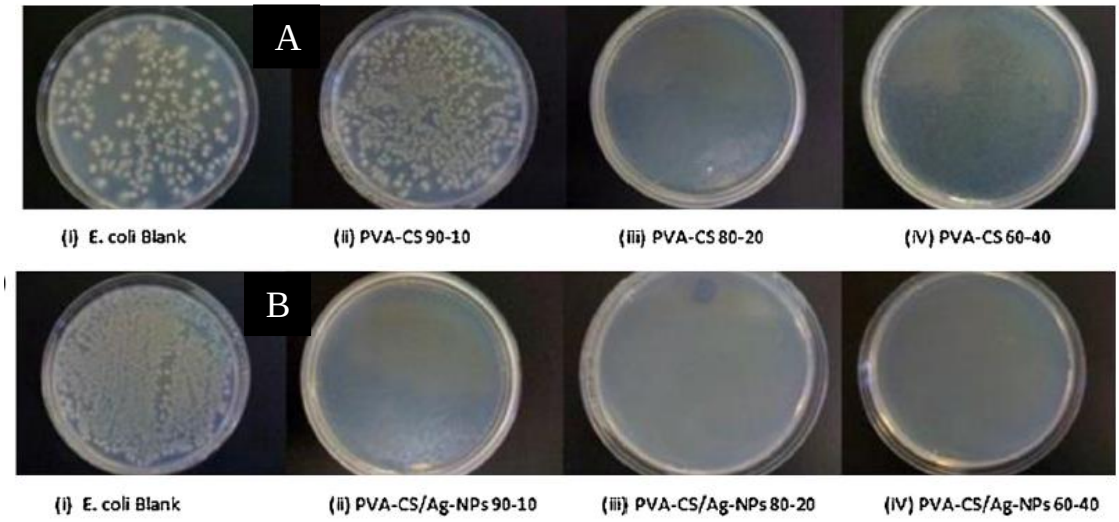

Figure 2.15: Effect of PVA/chitosan (A) and PVA/chitosanAg-NPs (B) electrospun webs at varying ratios on the growth of *E.coli* at a concentration of 7 x 10^5 CFU ml^{-1}(66).

2.9 Summary

There is substantial evidence to support the effective antibacterial properties of Manuka honey in chronic wound care, with several studies reporting on the improved healing of chronic wounds, after treatment with a Manuka honey dressing. In the majority of cases, MGO is reported to be the main constituent reason as to why these infected chronic wounds are healing. MGO as a lone compound was shown to inhibit the growth of *S.aureus*, *E. coli*, *P.aeruginosa*, *Proteus mirabilis* and *MRSE* when combined in hydrogel formulations *in-vitro*. The controlled delivery of MGO when encapsulated in nanoparticles was successfully demonstrated and the antibacterical effect against *E.coli*, *P.aeruginosa*, *S.aureus* and *Bacillus subtilis* was also reported in the same study. MGO has also shown ability to provide anti- carcinostatic activity, with successful outcomes both *in-vivo* and human trials.

The production of nano and submicron fibres via electrospinning, shows many beneficial properties for novel materials in wound care, including the ability to incorporate antibacterial agents or drugs. PVA has been effectively used in a number of electrospinning studies as a potential carrier material for the release of antibacterial agents or drugs, owing to its hydrogel form and biocompatibility with human tissue and blood. The controlled delivery of antibacterial agents and drugs from PVA hydrogels has been demonstrated with and without the need for crosslinking mechanisms.

The aim of the experimental study was therefore to determine the feasibility of producing a functional electrospun PVA hydrogel forming material, with the addition of MGO as antibacterial agent. Antibacterial studies were carried out to determine the minimum MGO

concentrations required to have an antibacterial effect *in-vitro*. The effect of crosslinking was also explored to understand the release kinetics of MGO from the PVA webs.

Chapter 3 Experimental Materials and Methods

3.1 Introduction

In this chapter a description of the raw materials, chemicals, experimental setup and the main experimental and characterisation techniques that were used in this research are discussed. Details of the experimental methodology are explained in the following chapters.

3.1.1 Stock Chemicals

Polymers and reagents used throughout this study and the individual suppliers are listed below in Table 3.1.

Table 3.1: Chemicals used in experiments.

Chemical	Supplier
Poly(vinyl alcohol) (31-50000 Mw, 98-99% hydrolysed)	Sigma Aldrich
Methylglyoxal (40% in H_2O)	Sigma Aldrich
Manuka honey (MGO 550 mg kg^{-1})	Wellbeing, UK
Glutaraldehyde (25% in H_2O)	Sigma Aldrich
Acetone (99.5%)	Sigma Aldrich
Distilled Water	Distilled in house
Deuterium Oxide (99.9% atom D)	Sigma Aldrich

3.1.2 Equipment

Equipment and materials used throughout this study and the individual manufacturers are listed in Table 3.2.

Table 3.2: Equipment for characterisation techniques.

Equipment	Model	Make
Optical Microscope		Watson Barnet
Viscometer	DV-E Viscometer	Brookfield LV
Conductivity meter	CON 2700	EUTECH
Tensiometer	K100	KRUSS
Fourier transform infra-red spectroscopy (FTIR)	Spectrum BX	Perkin Elmer
High Performance Liquid Chromatography (HPLC)	1290 Infinity	Agilent
HPLC column	Eclipse XDB-C8	Agilent
Plasma machine	Electronic diener	Pico
Scanning Electron Microscope	JSM-6610LV	Jeol

Scanning Electron Microscope	EVO MA15	Carl Zeiss
Field Emission Gun Scanning Electron Microscope (FEGSEM)	LEO 1530	Carl Zeiss
Field Emission Gun Scanning Electron Microscope (FEGSEM)	Quanta 200F	FEI
SEM Sample Coater	High resolution sputter coater	Agar
SEM Sample Coater	Model: SC500	Emscope
Proton NMR Spectrometer	500 MHz ^{1}H NMR	Bruker Avance
High voltage DCpower supplies	EH series 100 watt	Glassman High Voltage
Syringe pump	Model 200 series	Kd Scientific
Glass syringes	Fortuna Optima, 10 ml	Poulten & Graf, Barking
Syringe needle	21 gauge stainless steel	Sigma Aldrich Ltd
Digital Temperature and Humidity meter	N18FR	Precision GOLD
Free surface needleless electrospinning	Nanospider NS LAB	Elmarco
Aluminium foil		
Polypropylene spunbond (SPB)		Elmarco
Electronic scale	Sartorius CP225D	Sartorius AG
Electronic scale	EK -200G	AND
Hotplate/Magnetic stirrer	PC-351	Corning
Hotplate/Magnetic stirrer		Stuart Scientific
Shaker/Incubator	Orbital shaker-Incubator ES-20	Grant-bio
Shaker/Incubator	Orbital Incubator; S1500	Stuart Scientific
Incubator	IGS 180	Thermo Scientific
Water bath	BB2	Grant
Petri dishes	92x16 mm with cams	Sarstedt (AG & Co)
Desiccator		
Metal frame	10 cm diameter	

3.2 Materials and Methods

The preparation of individual electrospinning solutions is discussed in following chapters. To avoid repetition the methods used to characterise these spinning solutions throughout the experimental work are detailed in this section.

3.2.1 Viscosity of electrospinning solutions and Manuka honey

Electrospinning solutions were characterised by viscosity measurements to determine a relationship between the spin ability of the polymer solution and the viscosity. Details of the polymer solutions are provided in Table 3.3.

Table 3.3: Polymer solutions for viscosity, surface tension and electrical conductivity measurements.

Solvent	MGO concentration (wt %)	PVA concentration (% w/v)
Distilled water	0	8, 12, 14, 16, 18, 20
40 wt % MGO	40	
40 wt % MGO diluted with distilled water	21.57	
	14.76	
	11.22	

Rheology is the science of flow which describes the deformation of a body against a certain strain or force (299). Viscosity is the measure of a liquid against a forced motion (300). There are two methods for measuring viscosity; kinematic and dynamic viscosity. In the present study dynamic viscosity measurements were taken, as most polymers solutions are non-Newtonian and dependent on the shear rate. Dynamic viscosity provides the ability to control the shear rate during testing. Dynamic viscosity (η) is a measure of the shear stress (τ) divided by the shear rate (ɣ) of a liquid, seen in the following equation:

Eq. 3. 1

$$\eta = \tau/\gamma$$

The shear stress (τ) is the force applied to a specified unit area. As a result of this shear stress on the liquid, a shear rate (ɣ) (flowing liquid) is created. The shear rate describes the flow gradient between the spindle and sample chamber wall. The unit of measurement of viscosity is the poise (P). A liquid requiring a shear stress of one dyne per square centimetre to produce a shear rate of one reciprocal second, has a viscosity of one poise of 100 centipoise (cP) (301).

A Brookfield LV viscometer (DV-E) was used to measure the viscosity of the polymer solutions and Manuka honey (MGO 550). The viscosity measurements of all polymer solutions were measured using a removable sample chamber, at a temperature of 25ºC ± 2ºC. The Manuka honey was measured at a temperature of 25ºC ± 2ºC and 37 ºC ± 2ºC in order to determine the effect of temperature on the viscosity of Manuka honey. In order for the chamber and solution to reach the specific temperature required, 9.4 ml of the polymer solutions and 16.1 ml of the Manuka honey was decanted into the chamber and conditioned in an S1 500 Orbital Incubator at the required temperature for 24 h prior to testing. The spindle was also conditioned to the correct temperature. The speed (shear rate) and spindle were kept constant during all measurements (300, 302). For the polymer solutions, the speed was set at 6 r min^{-1} and a spindle size 34 was used. For the Manuka honey solutions a speed of 6 r min^{-1} and a spindle size of 18 was used.

3.2.2 Surface tension of electrospinning solutions

Electrospinning solutions were characterised by surface tension measurements to determine a relationship between the spinning ability of the polymer solution and the surface tension. Details of the solvents and conditions used to prepare each polymer solution are provided in Table 3.3.

Surface tension, also known as surface free energy is caused by the imbalance of liquid molecule forces at the surface of a liquid. In the bulk of a liquid each atom is surrounded by similar atoms, which are pulled equally in every direction by the neighbouring atom. This

results in a net zero force. At the surface of the liquid, the atoms are exposed and do not have neighbouring atoms surrounding them to provide a balanced force in equal directions. These atoms are pulled inwards by the atoms below, creating an internal pressure, which results in the liquid voluntarily contracting its surface area to maintain the lowest surface free energy (303).

The surface tension of electrospinning solutions was measured using the Wilhelmy plate method, using the KRUSS Tensiometer K100 (Fig. 3.1). The surface tension measurements of all polymer solutions were measured at 25ºC ± 2ºC. The polymer solution was contained in a sample vessel with a diameter of 66.5 mm and a depth of 35 mm, capable of holding 121.5 ml of solution. In order for the sample vessel and the solution to reach the specific temperature required, 100 ml of the polymer solution was decanted into the chamber and conditioned in a Grant bio ES-20 Orbital shaker incubator at 25ºC ± 2ºC for 24 hours prior to testing. A platinum plate of 19.9 mm in width, 0.2 mm thickness and 10 mm in height was used to carry out the measurements. The platinum plate was lowered vertically into the liquid solution. Upon contact with the surface a force (F) acts upon this plate and the surface tension (σ) can be calculated by the following equation:

Eq. 3. 2

$$\sigma = F / (L. \cos\theta)$$

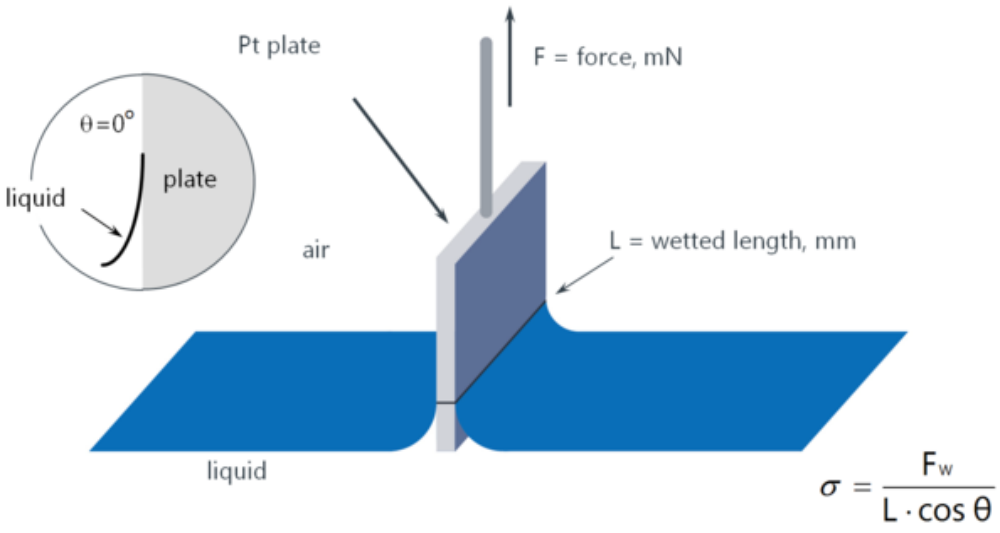

Figure 3.1: Wilhelmy plate method (304).

3.2.3 Electrical conductivity of electrospinning solutions

The conductivity of electrospinning solutions was determined to understand if there was a relationship between the spinning ability of the polymer solutions and conductivity. Details of the polymer solutions can be seen in Table 3.3.

Conductivity *is* defined as *"the ability of a substance to conduct electric current*" (305). Electrical conductivity in a liquid occurs by the migration of positive and negative ions through the liquid. When two electrodes are placed in a liquid and an electromotive force is connected to them, a current is supplied. An electric field between the positive and negative terminals causes the ions in the liquid to drift. The drift velocity and number of ions per unit volume influences the electrical conductivity of a liquid. The electric field intensity, the mass of the ion and other factors influences drift velocity of the ions. This means that the electrical conductivity of various liquids may be expected to have different values (306). Water molecules even at low temperatures tend to be in continuous motion. When two water molecules collide, the transfer of a hydrogen ion from one molecule to another occurs. The molecule that loses a hydrogen ion will become negatively charged hydroxide ion (OH^-) and the molecule that gains a hydrogen ion becomes positively charged hydrogen ion (H^+). This is a process known as self ionisation of water (307). At a room temperature of 25ºC the conductivity of water is around 0.05 µS cm^{-1}. The amount of H^+ and OH^- ions are approximately the same. However, in other solutions the concentrations of these ions will be unequal (306).

The conductivity of the prepared electrospinning solutions was measured using a EUTECH CON 2700 conductivity meter, fitted with a probe capable of measuring conductivity in the range of 0-500 µS cm^{-1}. The conductivity measurements of all polymer solutions were measured at 25ºC ± 2ºC. Each solution was contained in a 40 ml measuring vessel in an incubator at 25ºC ± 2ºC for 24 hours prior to testing. The conductivity probe was also conditioned to the required temperature. During testing the conductivity probe was positioned in the centre of this solution and left until a stable reading could be taken.

3.2.4 Electrospinning Procedures

Preparation of electrospinning solutions is discussed in detail in following chapters. The general procedures are described in this section.

3.2.4.1 Needle electrospinning

Electrospinning solutions were contained in a 10 ml syringe, fitted with a 21 gauge blunt needle. The syringe was connected to a dual head syringe pump set to run at a feed rate of 0.1 ml hr^{-1}. Details of the time spun are explained in the relevant experimental chapters. The voltage was supplied to the needle at its base via a copper electrode. A voltage between 7 kV and 18 kV and a distance between 5 cm to 15 cm from the tip of the needle to the collector was used. An aluminuium foil collector measuring 10 cm x 10 cm was secured on a non-conducting board opposite the needle and connected to a grounded cable. The electrospinning procedure was carried out inside a fume cupboard where continuous suction was available to evacuate any fumes. The ambient temperature was 25ºC ± 2ºC and the humidity was 49% ± 2%. Fig. 3.2 displays the needle electrospinning setup.

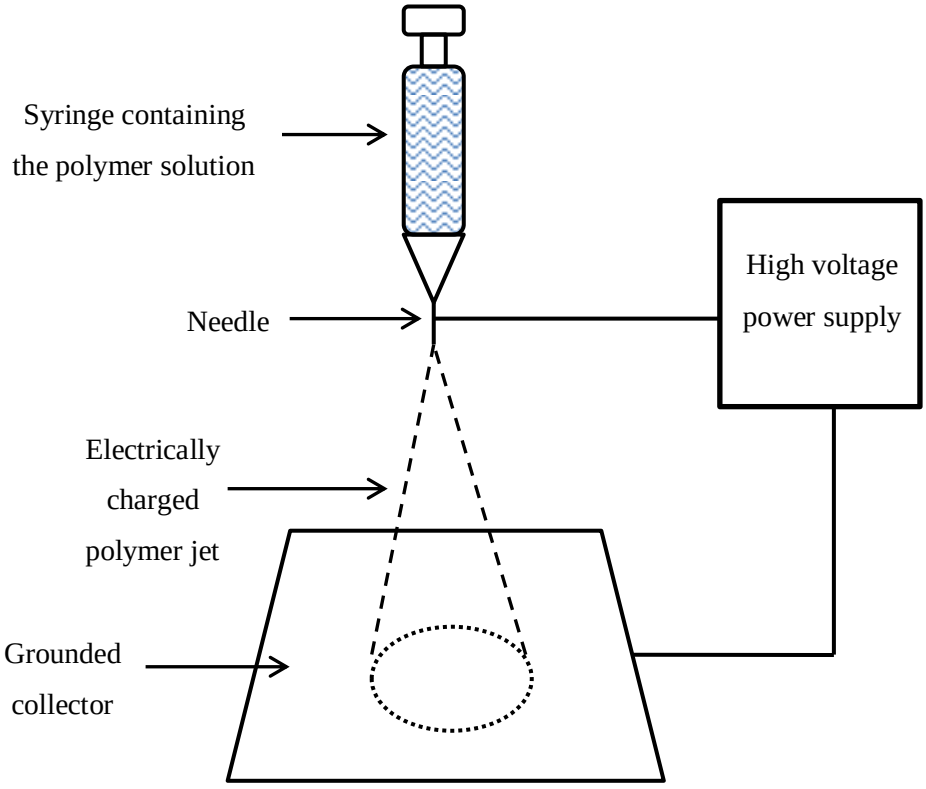

Figure 3.2: Needle electrospinning setup.

3.2.4.2 Free surface (needleless) electrospinning

An Elmarco Nanospider NS LAB was used to carry out free surface electrospinning. A spinning bath capable of holding quantities of liquid between 15 ml to 25 ml was fitted with a cylindrical wire roller electrode measuring 300 mm in length. The voltage was supplied to the electrode by means of internal wiring contained within the machine. A voltage between 65 kV to 75 kV and a distance between 163 mm to 183 mm from the electrode to the collector was used. The electrode speed was set to run at 6.0 r min^{-1}. Fig. 3.3 displays the free surface electrospinning setup. Fig. 3.4 shows an image of the spinning bath and cylindrical wire electrode. Both aluminium foil and polypropylene spunbond (SPB) collectors were utilised during the experiments. The following experimental chapters make reference to these where necessary.

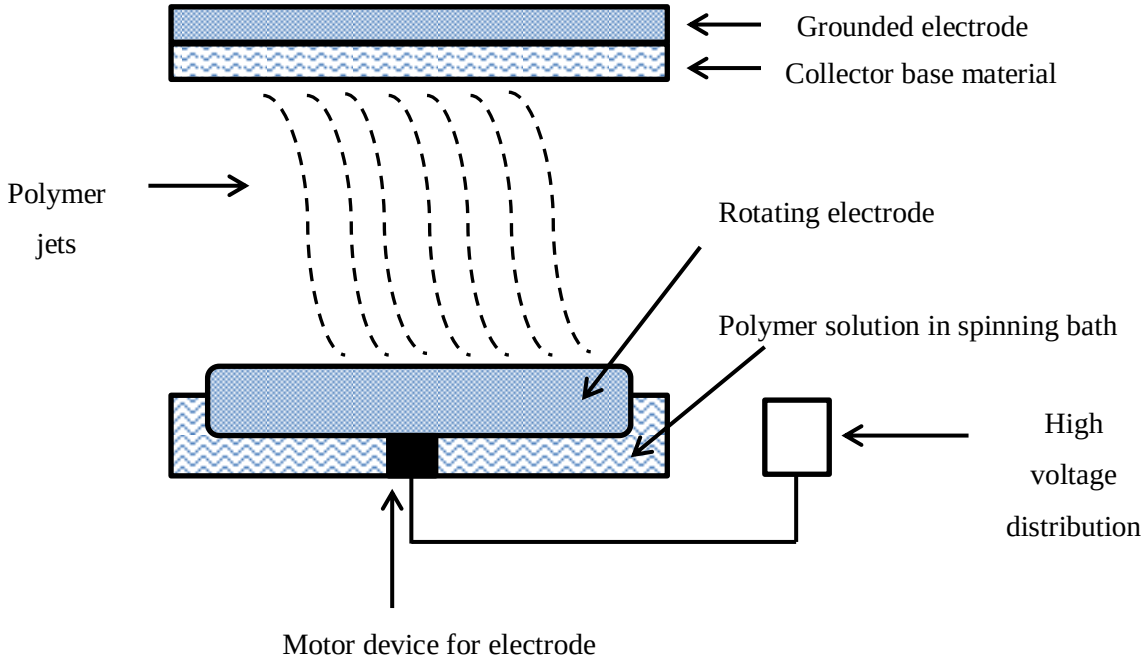

Figure 3.3: Free surface electrospinning set up using the Elmarco Nanospider NS Lab.

Figure 3.4: Free surface electrospinning bath with wire cylindrical electrode.

3.2.5 Scanning Electron Microscopy (SEM)

SEM was employed to elucidate details of fibre morphology, fibre diameter and the degree of bead formation. SEM has the advantage over optical microscopy, in that it is able to produce images with an increased depth of field and greater resolution. Prior to imaging, all samples were cut and mounted onto 25 mm aluminium stubs and sputter coated with gold in a vacuum of 0.05 torr for 4 minutes at 20 mA. Four different scanning electron microscopes were used during the course of this study, an EVO MA15 SEM, a LEO 1530 FEGSEM, a Jeol JSM 6610LV SEM and a Quanta 200F FEGSEM. A voltage between 5 kV and 15 kV and a vacuum pressure in the order of 10^{-6} mbar was achieved in the chamber. Magnifications between x200 and x6000 were used in order to record morphological features of individual fibres.

3.2.6 Fourier Transform Infra-Red (FTIR) Spectroscopy

FTIR is used for identifying the major functional groups in a compound (308). When a polymer sample is placed inside the IR machine wavelengths are passed through an interferometer and onto the sample. The sample absorbs all the different wavelength characteristics of its spectrum and this subtracts specific wavelengths from the interferogram. The atoms and bonds inside the molecule will vibrate and at different frequencies depending on the type of bond. A detector in the machine records the variation in energy versus time for all wavelengths simultaneously. Fourier transform analysis allows the conversion of the intensity vs. time spectrum into an intensity vs. frequency spectrum (309).

An FTIR Perkin Elmer Spectrum BX spotlight spectroscope was used in this study to detect the presence of specific compounds within the fibres. Solid polymer particles and solutions were measured with a diamond ATR attachment. Measurements of polymeric fibres were measured using a KBR disk. Fibres were cut into small pieces measuring approximately 1 cm^2 and ground with potassium bromide (KBr) granules to make sample pellets. Measurements were taken in the range between 4000 – 400 cm^{-1} with a resolution of 4 cm^{-1}. 64 scans were taken for each sample with the diamond ATR and 16 scans were performed for samples with the KBr pellets.

3.2.7 ^{1}H- Nuclear Magnetic Resonance (NMR) Spectroscopy

To quantify the presence of antibacterial compounds within electrospun fibres, nuclear magnetic resonance spectroscopy was utilised. NMR spectroscopy is frequently used as one of the most popular methods for characterisation of polymers in both solution and solid states. Solution NMR is regularly used due to its high resolution and sensitivity (310).

Nuclear magnetic resonance spectroscopy involves the absorption and emission of electromagnetic radiation by the nuclei in certain atoms when they are subjected to a magnetic field (311). The nuclei of an atom must possess a non-zero magnetic moment in order to absorb electromagnetic radiation. This is possible if the spin quantum number (I) is non-zero (311). If the atomic number and atomic mass are even, the nucleus will have no magnetic properties and a spin quantum number of I = 0. When the atomic number or atomic mass is odd or both are odd, the nucleus is said to be spinning. Hydrogen (^{1}H), the simplest atom found in most organic compounds is composed of a single proton and a single electron. Because the atomic number of hydrogen is odd, the nucleus of the hydrogen atom is spinning.

When a sample, typically liquid, is placed into a magnetic field (B0) whose units are tesla or T, the atoms have a preferred orientation as a compass needle has in the earth's magnetic field. Energy, supplied to the system along a direction designated as the z axis, will move the nuclei to a less preferred energy orientation. Nuclei with a spin of $\frac{1}{2}$, such as hydrogen atoms, can assume two orientations; lower energy, with the external magnetic field (+z) and higher energy (-z), against the magnetic field (312, 313). The nuclei will not align perfectly horizontally along the z axis and instead will move in a circular motion about the z axis called precession. The two directions of precession are referred to as + $\frac{1}{2}$ and - $\frac{1}{2}$. The precession motion of the magnetic moment occurs by angular frequency known as Larmor frequency (ω0). A second magnetic field (B1) is supplied in order to interconvert the two orientations. When the radio frequency of the B1 field is the same as the Larmor frequency of the nucleus, energy will flow between the newly applied field as absorption and emission. Absorption occurs as + $\frac{1}{2}$ nuclei become - $\frac{1}{2}$ nuclei and emission occurs as - $\frac{1}{2}$ nuclei become + $\frac{1}{2}$ nuclei. At the beginning of the experiment there is an excess of + $\frac{1}{2}$ nuclei and there is a net absorption of energy. This process is known as resonance and the absorption is detected electronically and displayed as frequency vs amount of energy absorbed (312, 313).

In this study a Bruker Avance spectrometer 500 MHz ^{1}H NMR was used to characterise and detect the presence of a compound. Prior to testing, 10 mg of each sample was dissolved in 1 ml of Deuterium oxide (99.9%) solvent which contains deuterons instead of protons. There are two reasons for this, firstly a protonated solvent would overwhelm the proton signal from the sample, secondly the deuterated solvent can be used for frequency locking to ensure magnetic field stability (310). H-NMR spectra were recorded with 1024 repetitions.

3.2.8 Antibacterial Testing

Three methods of testing were used to assess the antibacterial properties of the experimental fabrics or solutions. BS EN ISO 20743:2007 Textiles - Determination of antibacterial activity of antibacterial finished products (314), was carried out at Shirley Technology Ltd. BS EN ISO 20645:2004, Textile fabrics - Determination of antibacterial activity, agar diffusion plate test (315), was carried out at the Leeds Pathology and Microbiology department. The minimum inhibitory concentrations (MIC) and minimum bactericidal concentrations (MBC) were carried out at the Research and Development Laboratory of the Health Care Associated Infections group, Leeds Institute of Biomedical And Clinical Sciences (LIBACS), University of Leeds. Details of each test are described in the following sections.

3.2.8.1 BS EN ISO 20743:2007 Textiles - Determination of antibacterial activity of antibacterial finished products

A brief summary of the method of test performed at Shirley Technology is given below.

Preparation of bacterial culture

The bacterial cultures were prepared to concentrations between 1-3 x 10^5 per 10 ml in 1 in 20 nutrient broth.

Preparation of test specimens

Test pieces with a mass of 0.40 g ± 0.05 g were cut into suitable sizes for testing. Six control specimens and six antibacterial specimens were prepared.

Inoculation

The test specimens were placed in sterile jars and inoculated with 0.2 ml of bacterial suspension on several areas of the sample, taking care to prevent contact of the suspension with the jar surface. Immediately after inoculation, 20 ml of SCDLP medium (simulated wound exudate) was added to three of the control jars and three of the antibacterial sample jars. The jars were sealed with caps and shaken in an arc of approximately 30 cm by hand for 30 sec.

The number of bacteria recovered from the samples was then determined using a standard serial dilution and pour plate technique using peptone salt solution as the dilutant and enumeration agar. The remaining jars were incubated at 37ºC for 24 h.

Calculation of results

After the incubation period, the number of bacteria that could be recovered was determined using the following equation:

Eq.3.3

$$M = 20\ cB$$

where

M is the number of bacteria per specimen

cB is the bacteria concentration obtained

20 is the volume of shake out solution in ml

Calculation of percentage reduction

In this thesis, the average percentage reduction of bacteria after incubation for 24 h was calculated using the following equation.

Eq.3.4

$$100\ (CFUb - CFUa) / CFUb$$

where

CFUb is the average number of colony forming units before incubation

CFUa is the average number of colony forming units after incubation

3.2.8.2 BS EN ISO 20645:2004, Textile fabrics Determination of antibacterial activity agar diffusion plate test

In this study, two bacterial strains were used, including one gram positive and one gram negative; *Staphylococcus aureus* (*S.aureus*) and *Escherichia.coli* (*E.coli*) respectively. The selection of both strains are in accordance with the standard and are common pathogens found in infected wounds.

Preparation of bacteria inoculated agar plates

Separate agar plates were inoculated with *S.aureus* and *E.coli* bacterial species via streaking the plates with an inoculation loop from a solution containing 1-5 x 10^8 colony forming units per ml.

Preparation of Test Specimens

A circular specimen of fabric with a diameter of 25 ± 5 mm was cut from the test sample. Two specimens of the antibacterial fabric and two control specimens without addition of antibacterial treatment were prepared. The specimens were stored between 12 h to 24 h in sterilized petri dishes at room temperature.

Test Procedure

The test specimen was placed onto the bacterial inoculated agar surface using a sterilized pair of tweezers until the texture of the specimen was uniformly imprinted onto the agar. The petri dishes were placed in the incubator for 24 h at 37°C ± 1°C. Immediately after this period the petri dishes were examined for bacterial growth. If any zone of inhibition was formed around the test specimens, the diameter of the zone was measured using a pair of calibrated callipers. The microbial zone of inhibition was calculated using the following equation:

Eq.3.5

$$H = (D - d)/2$$

Where

H is the inhibition zone (mm)

D is the total diameter of specimen and inhibition zone (mm)

d is the diameter of specimen (mm)

After calculating the inhibition zone, the specimen was removed from the agar with a pair of tweezers. The contact zone under the specimen was examined for bacterial growth using a Watson Barnet x20 magnification optical microscope. Referring to Table 1 in section 10.4 of the test method, the antibacterial effect of the specimens was evaluated.

3.2.8.3 Minimum Inhibitory Concentrations (MIC) and Minimum Bactericidal Concentrations (MBC)

The MICs of synthetic MGO were determined against *S.aureus, Pseudomonas aeruginosa* (*P. aeruginosa*) and *Entrocuccus faecalis* (*E. faecalis*) isolates using a broth microdilution method. The method was based on the procedures recommended for broth microdilution determination of MICs by the Clinical and Laboratories Standards Institute (CLSI) (316).

The bacterial isolates used in MIC testing are listed in Table 3.4 and consisted of reference strains from the National Type Culture Collection (NTCC) (Public Health England) and clinical isolates obtained by the Leeds General Infirmary (LGI), following ethical approval.

Table 3.4: Bacterial isolates.

Bacterial isolate	Source
S. aureus NTCC29213	NTCC
S. aureus patient 1	LGI
S. aureus patient 2	LGI
P. aeruginosa NTCC27853	NTCC
P. aeruginosa patient 1	LGI
P. aeruginosa patient 2	LGI
E. faecalis NTCC29213	NTCC
E. faecium patient 1	LGI
E. faecium patient 2	LGI

Media and Diluents

The media and diltuents used in this method are listed in Table 3.5. All media and diluents were prepared according to the manufacturer's instructions, unless otherwise stated.

Table 3.5: Media and dilutents.

Medium/diluent	Supplier
Mueller Hinton Broth	Oxoid
0.9% saline	Sigma Aldrich

Preparation of MGO MIC broths

MGO 40 wt % from Sigma Aldrich was diluted in sterile distilled water to achieve a working stock solution of 4096 mg L^{-1}. A double strength dilution series was then prepared by diluting the working stock solution in Mueller Hinton broth to achieve a doubling dilution series from 2

mg L^{-1} to 2048 mg L^{-1}. The dilution series was dispensed across all rows of a 96-well microtitre tray (Fisher Scientific) in 50 µl amounts, as seen in Fig. 3.5.

Preparation of bacterial inocula

Each bacterial isolate was inoculated on to fresh blood agar (FBA) plates and incubated at 37^{o}C for 24 h. Single colonies of each bacterial isolate were removed from the FBA and resuspended in 5 ml Mueller Hinton Broth to a 0.5 MacFarland turbidity equivalent.

Test procedure

Starting with the non-MGO-containing growth control, and then working from the lowest to the highest MGO containing broth, duplicate rows of the 96 well MGO MIC plate were inoculated with each bacterial isolate. Inoculation of the MGO MIC plates occurred within 15 minutes of inoculum preparation. Lids were placed on each MGO MIC 96-well plate, and these were then incubated at 37^{o}C for 24 h.

Reading and interpretation of MIC results

The MIC was defined as the lowest concentration of MGO that completely inhibited the growth of the bacterial isolates, as detected by the unaided eye. This is assessed by placing a clear black line underneath the wells in the microtitre tray. If the black line is visible under the well, the concentration of MGO in that well shows an inhibitory effect. If the black line is not visible, this is due to the growth of bacteria in that well, creating a turbid solution. An example of this can be seen in Fig. 3.6A.

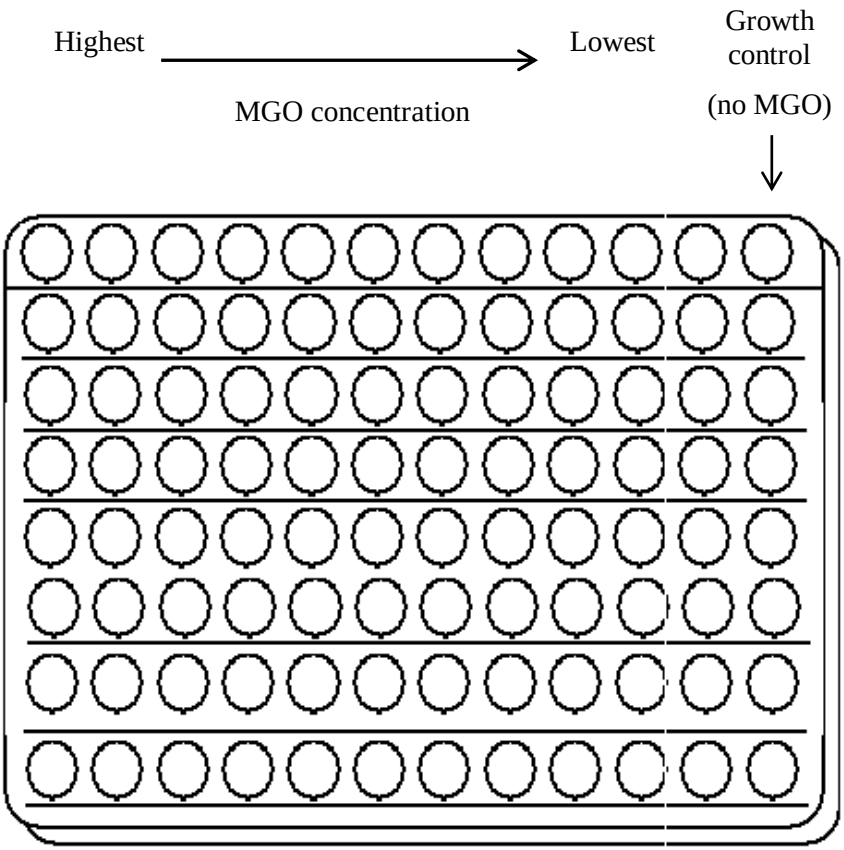

Figure 3.5: Preparation of the 96-well microtitre tray showing the placement of 50 µl of MGO, with the highest concentration starting at the left and finishing with the lowest concentration at the right. The final well is left blank as the control.

In order to determine whether the growth inhibition at any particular dilution was bactericidal or bacteriostatic, triplicate 20 µl aliquots were inoculated onto each of four quarters of a FBA plate and spread over the surface of the agar quarter with a sterile inoculating loop. Inoculated FBA plates were then incubated at 37^{o}C for 24 h. The MBC was defined as the lowest concentration at which there was no visible bacterial growth upon FBA. Fig. 3.6B shows an example of this.

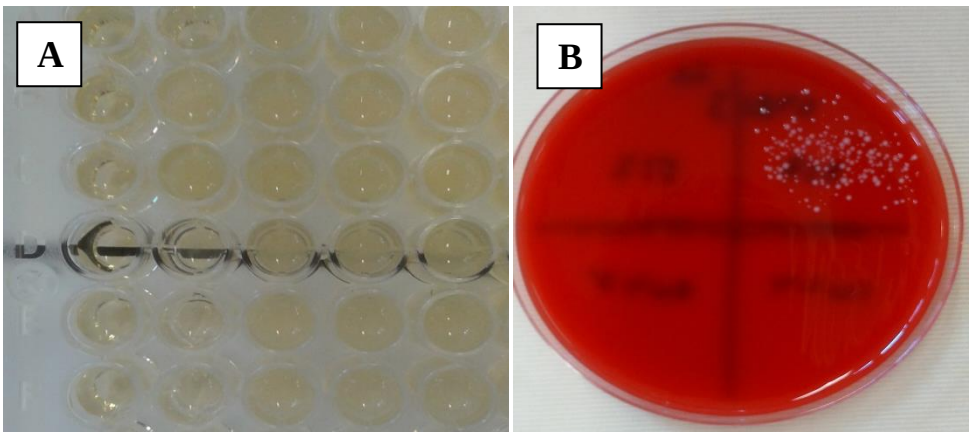

Figure 3.6: Determination of MIC via visibility of black line under the well in the microtitre tray (A) and determination of MBC via the regrowth of bacteria on FBA plates (B).

3.2.9 High Performance Liquid Chromatography (HPLC)

High performance liquid chromatography was used in this study to determine the release profile of MGO from the electrospun fibres.

High performance liquid chromatography (HPLC) is a physical technique used to separate a liquid sample into individual components (317, 318). The separation occurs by the interaction of the sample with a mobile and stationary phase. The mobile phase is the phase that moves in a definite direction and consists of the liquid sample in a solvent. When the mobile phase passes through the column the sample interacts with the stationary phase and is separated. There are many combinations of stationary and mobile phases that can be employed when separating a mixture. Based on each components affinity in the mobile phase, the components will migrate through the column at different rates. For example, if the components in the mobile phase are of different polarities, one component will migrate through the column faster than the other based on that component's affinity for either the mobile or stationary phase (317). Several modes of liquid chromatography exist. In this study reversed-phase liquid chromatography (RPLC) was employed. In RPLC the column is non-polar and the mobile phase is polar; this is the opposite to normal phase chromatography (319).

To detect the presence of MGO after the dispersion of the PVA/MGO fibres in a distilled water solution, an Agilent 1290 Infinity with a Diode UV Array detector was used. The machine was fitted with an Agilent Eclipse XDB-C8 column, measuring 150 mm x 4.6 mm and having a 5 um particle size. The flow rate was set at 0.5 ml min^{-1}. A binary pumping system allowed the mixing of two solvents as the mobile phase. Acetonitrile (solvent A) and water (solvent B) both containing 0.1% Trifluroacetic acid (TFA) were used. The acetonitrile and water were mixed by the pump in a linear gradient starting with 5% solvent A and 95% solvent B, increasing to 95% solvent A and 5% solvent B over 15 minutes. Peaks were detected by UV-absorbance at 280 nm.

3.2.10 Plasma treatment with GA as a crosslinking agent

Plasma is a collection of particles, including positive ions and electrons, ultraviolet radiation, free radicals and neutral species, which are created by supplying a high voltage to a gas or vapour. This is carried out at atmospheric pressure or in closed vessel at low pressure (low pressure temperature plasma technology) (320, 321). In this study, experiments were carried out with a low pressure low temperature plasma (LPLT). In LPLT systems the plasma state can be reached when the gas or vapour are subjected to a sufficiently low pressure, dependent on the frequency of the electromagnetic energy supplied (322, 323).

Textile materials that are subjected to plasma treatments undergo chemical changes in surface layers, changes in surface layer structure and changes in physical properties of the surface layers. Five major effects on the textile surfaces can occur, including surface cleaning, ablation or etching, activation of specific sites on the surface to give rise to chemical reactions, polymerisation and grafting (321, 323). In this study plasma technology was used with the intention of producing crosslinks between the hydroxyl groups on the surface of the electrospun PVA/MGO material and the aldehyde molecules of the GA when in a plasma state.

A Diener, PICO LPLT plasma system was employed for experiments in this study. Prior to plasma treatment, 100ml of 25 wt % GA solution was placed in a sealed bottle connected with a metal pipe to the machine (vaporiser). The electrospun samples were attached to a metal frame and placed inside the plasma chamber. A vacuum was created in the machine and allowed to reach a pressure of 0.5 mbar. At this point the GA vapour was supplied into the machine, where an electromagnetic energy was provided to convert the vapour to a plasma state. The valve connecting the vaporiser to the plasma chamber operates in a 10s time cycle where the opening time of the vaporiser could be varied. In this work, the opening time was varied from 20% (2s) to 80% (8s).

Chapter 4 Antibacterial Properties of Manuka Honey and Synthetic Methylglyoxal Coated Nonwovens

4.1 Introduction

As previously reported in sections 2.4.3.1 and 2.4.3.2, the antibacterial behaviour of Manuka honey is well documented with several studies reporting its effectiveness against numerous types of bacteria (196, 199, 200, 202, 204, 324) as well as its use in the treatment of wound infections (187, 191, 193, 194, 325). Methylglyoxal (MGO), the non-peroxide antibacterial compound found in Manuka honey (172), has also received significant attention because of its ability to act as a lone compound for the inhibition of bacterial growth. In these previous studies synthetic MGO has been studied in the form of a solution (45, 172), a hydrogel (45) and a polymer based formulation (47). All studies evaluated the effectiveness of MGO using an agar well diffusion method where the MIC (minimum inhibitory concentration) was reported. Comparison of the antibacterial performance of both Manuka honey and MGO was studied by Henle's team (172), where six different Manuka honeys were first analysed to determine the concentrations of MGO. The MGO concentrations were found to range between 38 to 761 mg kg^{-1}. Each of the honeys was diluted to concentrations ranging between 15% (w/v) and 80% (w/v). Synthetic MGO solutions were also prepared that corresponded to the MGO concentrations within the diluted Manuka honey solutions. It was established that five out of six of the Manuka honeys with concentrations ranging between 15% (w/v) to 30% (w/v) exhibited an antibacterial effect. The MGO concentration in these honeys ranged from 347 ± 20 mg kg^{-1} to 761 ± 25 mg kg^{-1}. These results correspond to synthetic MGO concentrations with a MIC value of 1.1 mM (79.3 µg ml^{-1}) (183) to 1.8 mM. To the author's knowledge no published work has evaluated and compared the antibacterial effects of Manuka honey and synthetic MGO when applied as a coating to a nonwoven fabric or reported the concentration per unit area. It was of interest to understand the degree to which synthetic MGO has an equivalent antibacterial effect to Manuka honey and could be used as an alternative to Manuka honey in an antibacterial dressing.

Accordingly, the aim of this chapter was firstly to compare and evaluate the antibacterial efficiency of both Manuka honey and synthetic MGO when applied as a coating to a nonwoven fabric at equivalent MGO concentrations. Two standard methods to determine the antibacterial effect of textile products were utilised in this study, including BS EN ISO 20743:2007 (314) and BS EN ISO 20645:2004 (315), outlined in sections 3.2.8.1 and 3.2.8.2 respectively. Previous studies that have reviewed the concentration of antibacterial compounds in a dressing have expressed the values in terms of mass per unit area (mg cm^{-2}) (146), therefore the concentration of MGO on the nonwoven fabric was determined in the same manner. Secondly, it was of interest to determine the antibacterial effect of MGO against three of the most common wound pathogens including *Staphylococcus aureus*

(*S.aureus*), *Peudomonas aeruginosa* (*P. aeruginosa*) and *Enterococcus faecalis* (*E. faecalis*) (6). The minimum inhibitory concentration (MIC) and minimum bactericidal concentration (MBC) of synthetic MGO in liquid form was evaluated against these three bacterial wound pathogens using a common laboratory protocol outlined in section 3.2.8.3.

4.2 Preparation of coatings and nonwoven samples

4.2.1 Formulation of the Manuka honey and synthetic MGO solutions for coating

Given that the work by Henle's team (172), in which five honeys with varying concentrations of MGO between 347 ± 20 mg kg^{-1} to 761 ± 25 mg kg^{-1} exhibited an antibacterial effect, a Manuka honey certified by the University of Dresden as having 550 mg kg^{-1} of MGO (Manuka honey MGO 550+) was used in the following experiments.

Solutions of Manuka honey and synthetic MGO were prepared to contain final equivalent concentrations of MGO in mg g^{-1}. A 20% (w/w) and a 60% (w/w) aqueous solution of Manuka honey was made by dissolving 100 g and 300 g of Manuka honey (MGO 550+) in distilled water made up to 500 g. The concentration of MGO within these two solutions was 0.11 mg g^{-1} and 0.33 mg g^{-1} respectively. The equivalent concentrations of synthetic MGO were made by diluting a 40 wt % MGO solution with distilled water.

4.2.2 Manufacture of nonwoven coated samples

Airlaid webs were produced from 100% lyocell (TENCEL®) fibre (short cut, 1.7 dtex/10 mm) using a sifting airlaying machine of the Kroyer type, to give a basis weight of 120 g m^{-2}. Webs were bonded by hydroentanglement (STL Hydrolace) with a 110 - 120 jet strip and a jet pressure of 50 bar on one side and 50 bar on the reverse. The hydroentangled webs were washed with warm water and fabric detergent to ensure any finish on the fabric was removed. The samples were then air dried at room temperature. The coatings were applied by immersing a pre-weighed sample into the prepared Manuka honey and synthetic MGO coating solutions for 10 min. A sample liquor ratio of 1:50 was used. The samples were then passed through a pad mangle at a pressure of 10 kg cm^{-2}, weighed and left to air dry at room temperature. A sample without coating was also prepared and used as a control. The amount of MGO per unit area (mg cm^{-2}) assumed to be absorbed onto the nonwoven coated samples was calculated using the MGO concentration in the coating solutions (mg g^{-1}), the amount of solution absorbed (g) and the area of the sample (cm^2). Conditions are summarised in Table 4.1.

Table 4.1: Nonwoven sample weight (g) before and after coating with Manuka honey and synthetic MGO solutions and the calculated concentration of MGO on the coated samples (mg cm^{-2}).

Coating on the nonwoven sample and concentration of MGO (mg g^{-1})	Original sample weight (g)	Sample area (cm^2)	Sample weight after coating (g)	Amount of solution absorbed (g)	Amount of MGO absorbed (mg)	Concentration of MGO per unit area (mg cm^{-2})
Nonwoven control	10.00	833	n/a	n/a	0	0
Manuka honey coating 0.11	10.00	833	53.02	43.02	4.73	0.0057
Manuka honey coating 0.33	10.03	836	52.74	42.72	14.09	0.0169
Synthetic MGO coating 0.11	9.97	831	50.56	40.58	4.46	0.0054
Synthetic MGO coating 0.33	9.95	829	52.75	42.80	14.12	0.0170

4.2.3 Antibacterial evaluation of the nonwoven coated samples

The antibacterial activity of the nonwoven coated samples was firstly evaluated using BS EN ISO 20743:2007 Textiles - Determination of antibacterial activity of antibacterial finished products, as outlined in section 3.2.8.1. This method has been previously used to evaluate commercial dressings containing silver where it is intended to simulate contaminated wound exudate that comes into contact with a dressing in a clinical situation (147). A quantitative result is obtained as a result of this test protocol. This method was initially used to give a reliable indication that Manuka honey and synthetic MGO had an antibacterial effect at equivalent MGO concentrations. In this method, the Manuka honey and synthetic MGO coated nonwovens, plus a nonwoven control (Table 4.1) were tested against Gram positive bacteria *S. aureus* and Gram negative bacteria *Klebsiella pneumonia* (*K. pneumonia*), according to standard requirements. The antibacterial effect was determined by determining the average count of bacteria colony forming units, immediately after inoculation and after 24 h in incubation. A percentage reduction of bacteria based on the difference between these two counts was calculated. Following the initial evaluation to

determine the antibacterial effect of Manuka honey and synthetic MGO as coatings on a nonwoven fabric, further experiments were carried out using BS EN ISO 20645:2004 Textile fabrics, determination of antibacterial activity, agar diffusion plate test, as outlined in section 3.2.8.2. Firstly the coated nonwoven samples tested using BS EN ISO 20743:2007 (Table 4.1), having MGO concentrations between 0.0054 mg cm^{-2} and 0.0170 mg cm^{-2} were assessed. Following tests at these concentrations, additional coated nonwoven test samples were prepared to give six new MGO concentrations between 0.1 mg cm^{-2} and 1.2 mg cm^{-2} using both Manuka honey and synthetic MGO. A 7 cm^2 circular sample of the pre-made nonwoven was placed in a weighing boat, put upon a balance and the reading was zeroed. The addition of Manuka honey or synthetic MGO was added to the nonwoven sample to equate to the required weight needed to give the new range of MGO concentrations between 0.1 mg cm^{-2} and 1.2 mg cm^{-2}. Prior to adding the Manuka honey 550+, the honey was heated in an incubator to 40ºC to allow it to soften and enable a homogeneous distribution over the nonwoven sample. The Manuka honey and synthetic MGO coated nonwovens, plus a nonwoven control were tested against Gram negative bacteria *Escherichia coli (E.coli)* and Gram positive bacteria *S. aureus* in accordance with standard requirement. The number of samples tested at each concentration was three. The antibacterial activity of the samples was assessed by the absence or presence of bacterial growth in the contact zone between the agar and the specimen and the appearance of an inhibition zone around the specimen. The calculated width of the inhibition zone was recorded based on *Eq. 3.5* outlined in section 3.2.8.2.

4.2.4 Results and Discussion

4.2.4.1 Antibacterial performance of the nonwoven coated samples using BS EN ISO 20743:2007

Table 4.2 and 4.3 give the results obtained from the BS EN ISO 20743:2007. The results indicate the average reduction of bacteria in colony forming units (CFU). Interestingly, a 99% reduction in bacteria was reported for the nonwoven control against *S.aureus*. A considerably reduced count of bacteria, (-252%) was also reported for the nonwoven control against *K.pneumonia*. The woven polyester control showed a high negative percentage reduction in both cases (-22438% and -5635%), which corresponds to heavy growth of bacteria in contact with the sample. For the Manuka honey coated and synthetic MGO coated nonwoven samples, 100% reduction in bacteria was achieved for all samples where the calculated concentration of MGO ranged from 0.0054 mg cm^{-2} to 0.0170 mg cm^{-2}. The 99% reduction in bacteria for the control samples may be attributed to cross contamination from the Manuka honey or synthetic MGO coatings. However, the lyocell fibres may also

have had some inherent antibacterial effect. A study by Lenzing, compared the bacterial growth of *S.aureus* against cellulosic and synthetic materials including polypropylene, polyester and polyacrylate. Using a similar method to BS EN ISO 20743:2007, *S.aureus* was cultured in a medium to simulate perspiration and a known number of bacteria were then transferred to the textile samples in a dilution where a moisture content of 50% was obtained and incubated at 37 ºC for 24 h. The results revealed that the synthetic samples exhibited 100 to 1000 times higher bacteria growth when compared with lyocell. The reduced growth on lyocell was attributed to the behaviour of the fibres in water. In the case of the synthetic fibres, the water has limited penetration into the fibres and sits mainly on the surface which is fully accessible to bacteria organisms. However, because of the nano-fibrillar structure of lyocell fibres, the water was absorbed into the micro capillaries inside the fibre, offering a reduced life sustaining environment for the bacteria to thrive (326).

Table 4.2: Average reduction in colony forming units (CFU) for *S.aureus*.

Concentration of MGO per unit area of the sample (mg cm^{-2})	Average CFU immediately after inoculation	Average CFU after 24 h in incubation	Average percentage reduction (%)
Nonwoven control	**2.64×10^4**	**8.60×10^2**	96.7
Woven polyester control	**1.30×10^5**	**2.93×10^7**	-22438
Manuka honey coating (0.0054)	**3.15×10^4**	**0**	100
Manuka honey coating (0.0169)	**3.90×10^4**	**0**	100
Synthetic MGO coating (0.0054)	**3.20×10^4**	**0**	100
Synthetic MGO coating (0.0170)	**3.05×10^4**	**0**	100

Table 4.3: Average reduction in colony forming units (CFU) for *K.pneumonia.*

Concentration of MGO per unit area of the sample (mg cm^{-2})	Average CFU immediately after inoculation	Average CFU after 24 h in incubation	Average percentage reduction (%)
Nonwoven control	**8.53×10^4**	**2.40×10^5**	-181
Woven polyester control	**6.80×10^4**	**3.90×10^6**	-5635
Manuka honey coating (0.0054)	**7.07×10^4**	**0**	100
Manuka honey coating (0.0169)	**8.60×10^4**	**0**	100
Synthetic MGO coating (0.0054)	**7.20×10^4**	**0**	100
Synthetic MGO coating (0.0170)	**9.93×10^4**	**0**	100

4.2.4.2 Antibacterial performance of the nonwoven coated samples using BS EN ISO 20645:2004

Table 4.4 and 4.5 display the results achieved for the nonwoven controls and nonwoven coated samples against *E.coli* and *S.aureus* respectively. The average zones of inhibition and standard deviations are shown, as well as the effect of the sample on the growth of each bacteria species and the assessment of the antibacterial activity in accordance with standard requirements. Fig. 4.1 and 4.2 give a visual representation of the effect of the nonwoven control samples and the nonwoven coated sample initial tests at MGO concentrations of 0.0054 mg cm^{-2} and 0.0170 mg cm^{-2}. Fig. 4.5 and 4.6 show a visual representation of the Manuka honey coated nonwoven samples and the synthetic MGO coated nonwoven samples where an inhibition zone was produced, respectively.

Table 4.4: Effect of MGO concentration on the growth of *E.coli* when applied as a coating.

	Manuka honey coatings			**Synthetic MGO coatings**		
MGO concentration (mg cm^{-2})	**Mean inhibition zone (standard deviation) (mm)**	**Growth under sample**	**Assessment**	**Mean inhibition zone (standard deviation) (mm)**	**Growth under sample**	**Assessment**
Control	0 (0)	Heavy	Insufficient	0 (0)	Complete	Insufficient
0.0054	0 (0)	Heavy	Insufficient	0 (0)	Moderate	Insufficient
0.0170	0 (0)	Slight	Limited efficiency	0 (0)*[1]	No growth	Good effect
0.10	0.42 (0.31)	No growth	Good effect	0 (0)*[1]	No growth	Good effect
0.15	0.75 (0.54)	No growth	Good effect	0 (0)*[1]	No growth	Good effect
0.20	1.58 (0.42)	No growth	Good effect	0 (0)*[1]	No growth	Good effect
0.40	n/a*[2]	n/a	n/a	1.00 (0.41)	No growth	Good effect
0.80	n/a*[2]	n/a	n/a	2.17 (1.30)	No growth	Good effect
1.20	n/a*[2]	n/a	n/a	4.50 (0.94)	No growth	Good effect

*[1] The absence of growth, even without an inhibition zone, may be regarded as a good effect, as the formation of such an inhibition zone may have been prevented by a low diffusion of the active substance (314).

*[2] It was not possible to prepare Manuka honey samples at concentrations above 0.2 mg cm^{-2} because nonwoven samples became heavily saturated.

Table 4.5: Effect of MGO concentration on the growth of *S. aureus* when applied as a coating.

	Manuka honey coatings			Synthetic MGO coatings		
MGO concentration (mg cm^{-2})	**Mean inhibition zone (standard deviation) (mm)**	**Growth under sample**	**Assessment**	**Mean inhibition zone (standard deviation) (mm)**	**Growth under sample**	**Assessment**
Control	0 (0)	Heavy	Insufficient	0 (0)	Heavy	Insufficient
0.0054	0 (0)	Heavy	Insufficient	0 (0)	Moderate	Insufficient
0.0170	0 (0)	Heavy	Insufficient	0 (0)	Slight	Limit of efficiency
0.10	0.17 (0.24)	No growth	Good effect	0 (0)*[1]	No growth	Good effect
0.15	1.58 (0.82)	No growth	Good effect	0 (0)*[1]	No growth	Good effect
0.20	3.08 (0.24)	No growth	Good effect	0 (0)*[1]	No growth	Good effect
0.40	n/a*[2]	n/a	n/a	0 (0)*[1]	No growth	Good effect
0.80	n/a*[2]	n/a	n/a	3.08 (0.62)	No growth	Good effect
1.20	n/a*[2]	n/a	n/a	4.50 (0.35)	No growth	Good effect

*[1] The absence of growth, even without an inhibition zone, may be regarded as a good effect, as the formation of such an inhibition zone may have been prevented by a low diffusibility of the active substance (314).
*[2] It was not possible to prepare Manuka honey samples at a concentration above 0.2 mg cm^{-2} because nonwoven samples became heavily saturated.

The results in Table 4.4 and 4.5 indicate that for the control samples, no zone of inhibition was achieved for *E.coli* and *S.aureus*. This is evident in Fig. 4.1A & 4.1C. Upon removal of the control samples from the surface of the agar, the contact zone between the sample and the agar presented heavy bacterial growth (Fig. 4.1B & 4.1D). This confirms that the control samples did not exhibit any antibacterial activity. The effect of equivalent MGO concentrations in the Manuka honey coatings and synthetic MGO coatings between 0.0054 mg cm^{-2} and 0.0170 mg cm^{-2} showed no zone of inhibition for *E.coli* and *S.aureus*, as is evident in Fig. 4.2. Upon removal of the Manuka honey coated samples from the agar, heavy growth was apparent at an MGO concentration of 0.0054 mg cm^{-2} for both *E.coli* and *S.aureus* (Fig. 4.2E2 & 4.2G2). At the equivalent MGO concentration in the synthetic MGO coatings, moderate growth was achieved for both *E.coli* and *S.aureus* (Fig. 4.2A2 & 4.2C2). With an MGO concentration of 0.0170 mg cm^{-2} for the Manuka honey coated samples (Fig. 4.2F2 & 4.2H2), moderate and heavy growth was observed for *E.coli* and *S.aureus*

respectively. However, for the synthetic MGO coatings with an equivalent MGO concentration of 0.0170 mg cm^{-2}, no growth and slight growth was evident against *E.coli* and *S.aureus* respectively (Fig. 4.2B2 & 4.2D2). These initial evaluations at a concentration of 0.0054 mg cm^{-2}, suggest an insufficient antibacterial effect was achieved for both Manuka honey and synthetic MGO coatings. At a concentration of 0.0170 mg cm^{-2}, limited efficacy was observed for the Manuka honey coatings. However, for the synthetic MGO coatings with an MGO concentration of 0.0170 mg cm^{-2}, the antibacterial effect was shown to improve slightly and a good antibacterial effect and a limit of efficiency was achieved for *E.coli* and *S.aureus* respectively.

Where no growth is seen and no zone is apparent, a good antibacterial effect is still regarded. This may be due to a low diffusion of the active compound from the fabric (315) and may be attributed to the affinity of the lyocell fibres for moisture. Lyocell fibres are hygroscopic in nature with a high water absorption capacity. This is influenced by the hydrophilic, crystalline nano-fibrils, which are arranged in a very regular manner. Water is absorbed in the capillaries between the fibrils, not into the fibres themselves (327). A single lyocell fibre will act as a wetting bundle of micro and nano-fibrils with pores in the nanometer range (327, 328). Fig. 4.3 shows images of the different cellulosic fibres and their ability to absorb water using a transmission electron microscope. The dark areas, which were stained with a dye, show the water containing pores in the fibres. It can clearly be discerned that TENCEL® (lyocell) has a large affinity for water, as the whole fibre appears dark. A higher resolution image of lyocell can be seen in Fig. 4.4, where the pore clusters within the fibre cross-section are revealed. Thus, in the present study the lyocell fibres may retain the synthetic MGO and honey coating within their structure thereby restricting the diffusion of MGO into the agar at these relatively low MGO concentrations (329).

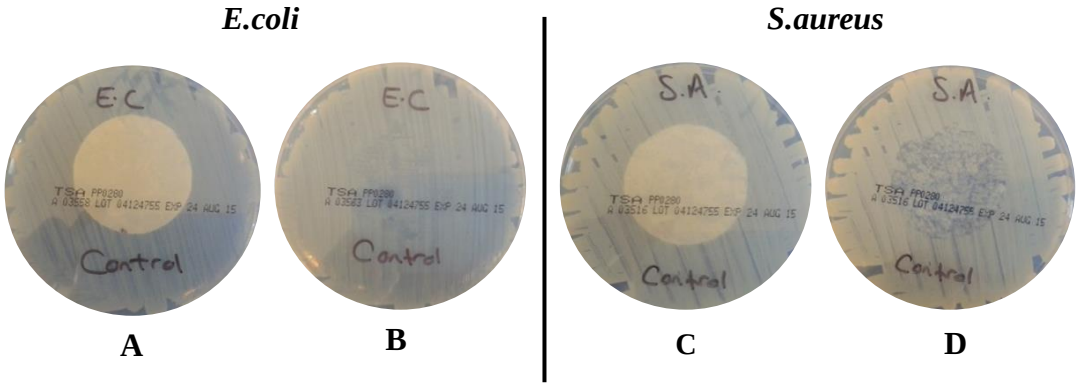

Figure 4.1: Effect of control samples on the growth of *E.coli*; A = no zone, B = heavy growth under sample & *S.aureus*; C = no zone and D = heavy growth under sample.

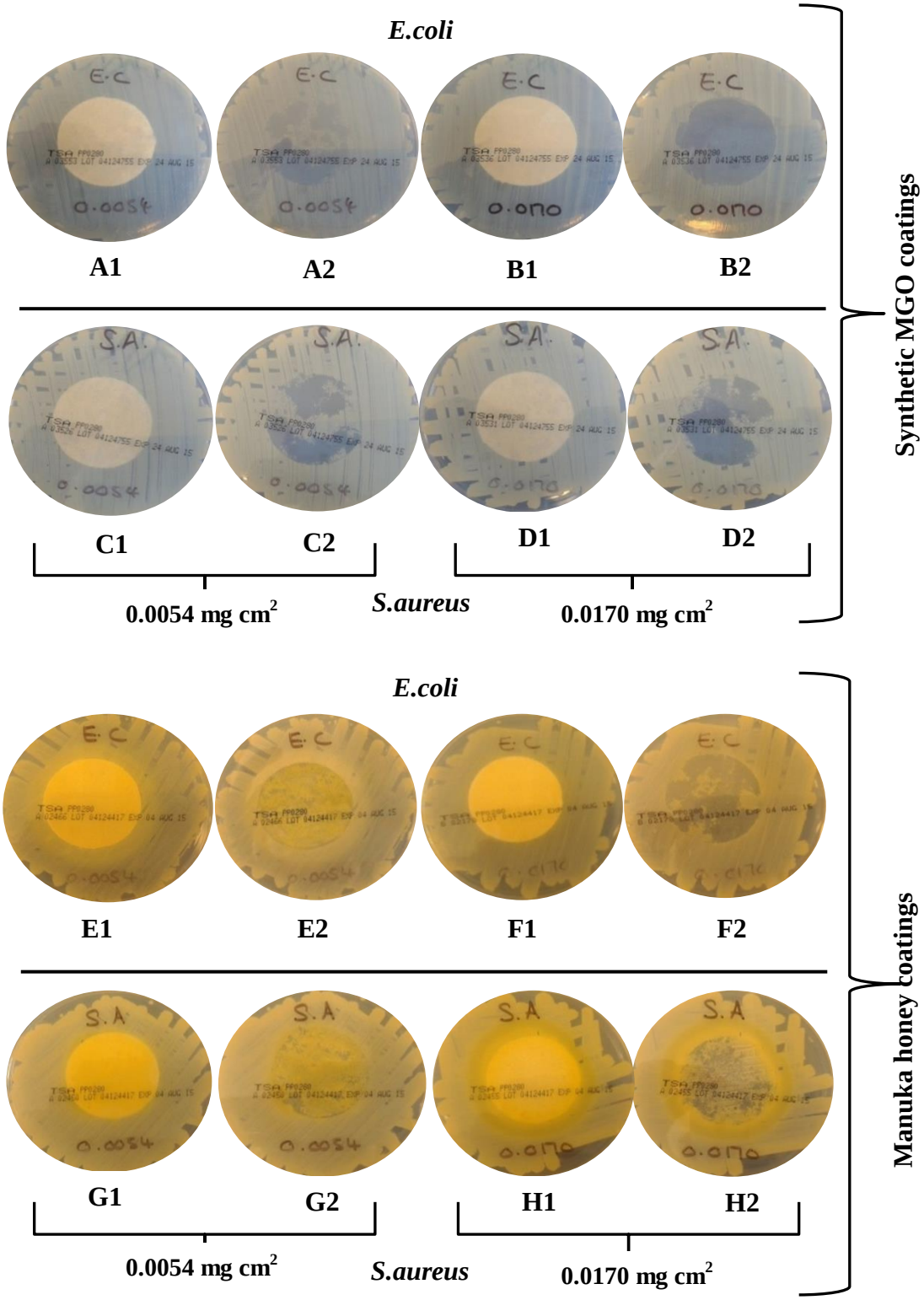

Figure 4.2: Effect of initial coated nonwoven MGO concentrations (0.0054 mg cm^2 and 0.0170 mg m^2 on the growth of *E.coli* and *S.aureus*). A to D show the effect of the synthetic MGO coatings. For *E. coli*, A1 & A2 = 0.0054 mg cm^2 (no zone and moderate growth respectively), B1 and B2 = 0.0170 mg cm^2 (no zone and no growth respectively). For *S. aureus*, C1 & C2 = 0.0054 mg cm^2 (no zone and moderate growth respectively), D1 & D2 = 0.0170 mg cm^2 (no zone and slight growth respectively). E to H show the effect of the Manuka honey coatings. For *E. coli*, E1 & E2 = 0.0054 mg cm^2 (no zone and heavy growth respectively), F1 & F2 = 0.0170 mg cm^2 (no zone and moderate growth respectively). For *S.aureus*, G1 & G2 = 0.0054 mg cm^2 (no zone and heavy growth respectively), H1 & H2 = 0.0170 mg cm^2 (no zone and heavy growth respectively).

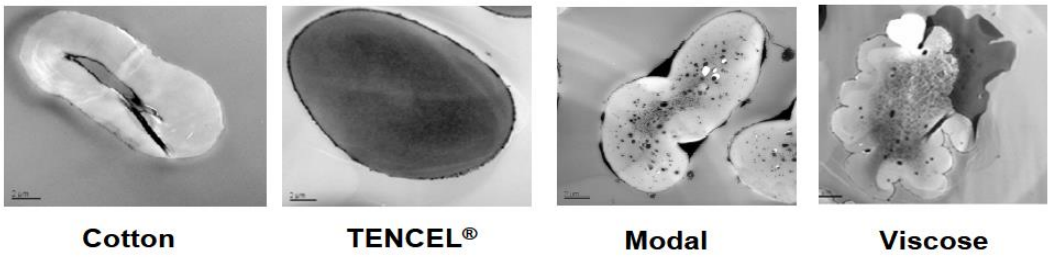

Figure 4.3: Transmission electron micrographs of different cellulosic fibres and their affinity for water. The water containing pores show up as dark areas (327, 328).

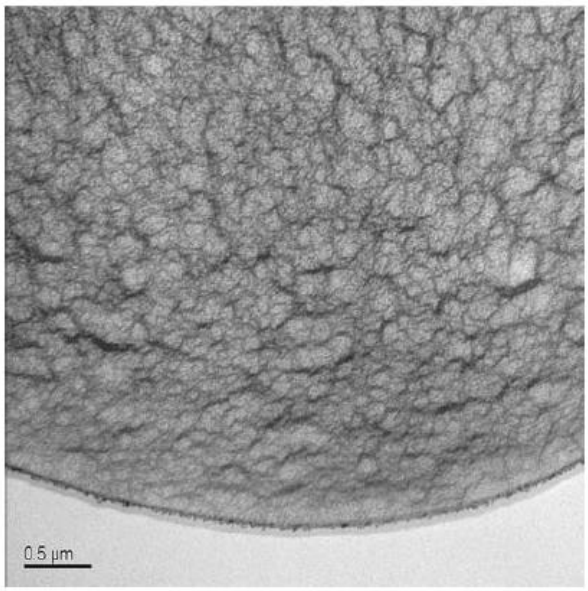

Figure 4.4: High resolution image of TENCEL® (lyocell) (328).

In Table 4.4 and 4.5 the effect of MGO concentrations between 0.1 mg cm^{-2} and 1.2 mg cm^{-2} on the growth of *E.coli* and *S.aureus* in contact with both Manuka honey and synthetic MGO shows a good antibacterial effect in all cases. Note it was not possible to prepare Manuka honey samples at concentrations above 0.2 mg cm^{-2} as the nonwoven samples became heavily saturated, due to the high density and viscose nature of the honey. However at these relatively low concentrations between 0.1 mg cm^{-2} and 0.2 mg cm^{-2} for the Manuka honey coatings, mean zones of inhibition were apparent against both *E.coli* and *S.aureus*, as seen in Fig. 4.5. A small mean zone of inhibition of 0.17 mm and 0.42 mm with a standard deviation of 0.31 mm and 0.24 mm was achieved against *E.coli* and *S.aureus* at a concentration of 0.1 mg cm^{-2}, respectively. Examples of this are shown in Fig. 4.5A and 4.5D. As the concentration of MGO doubled to 0.2 mg cm^{-2}, the mean zone of inhibition for *E.coli* increased by a factor of about four times to 1.58 mm with a standard deviation of 0.42 mm,

Fig. 4.5C shows an example of this. The mean zone of inhibition for *S.aureus* increased to a far greater level by an approximate factor of eighteen to 3.08 mm, with a standard deviation of 0.42 mm, see Fig. 4.5F.

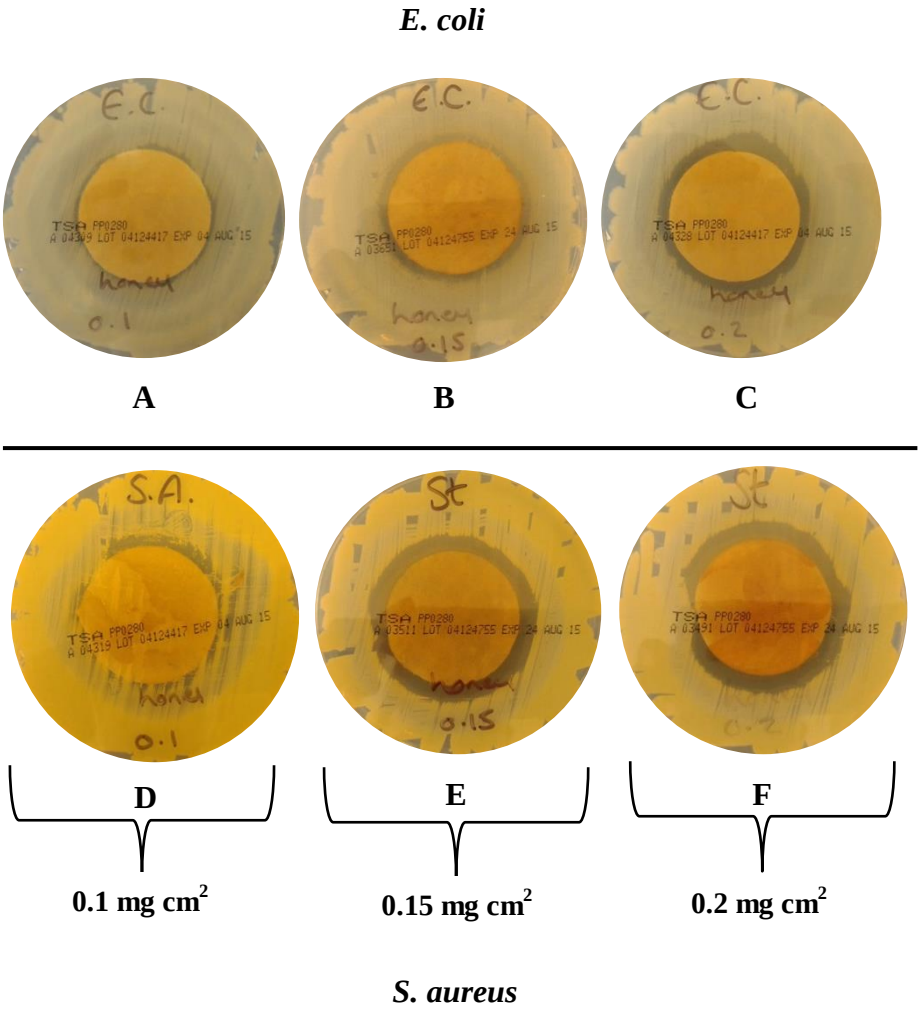

Figure 4.5: Examples of mean zones of inhibition produced (mm) from MGO concentrations (0.1 mg cm^{-2} to 0.2 mg cm^{-2}) in Manuka honey coatings against *E.coli* (A, B & C) and *S. aureus* (D, E & F).

Conversely, for the synthetic MGO coatings, no zone of inhibition was apparent below a concentration of 0.2 mg cm^{-2} for *E.coli* and 0.4 mg cm^{-2} for *S.aureus*, as seen in Fig. 4.6. However, upon removal of the samples from the agar, no growth was observed at a concentration of 0.1 mg cm^{-2} for both *E.coli* and *S.aureus*, which corresponds to a good antibacterial effect. It was observed that an unclear zone was formed for synthetic MGO concentrations of 0.2 mg cm^{-2} for and *E.coli* (Fig. 4.6A) and 1.5 mg cm^{-2} to 0.4 mg cm^{-2} for *S.aureus* (Fig. 4.6E-6G). Repeating the experiment at the same concentrations, led to the same observations. As reported previously, limited diffusion of the Manuka honey and synthetic MGO from the lyocell nonwovens was achieved at the lower concentrations of

0.0054 mg cm^{-2} to 0.0170 mg cm^{-2} (Fig. 4.2). The Manuka honey coatings produced a clear zone of inhibition at concentrations between 0.1 mg cm^{-2} to 0.2 mg cm^{-2} (Fig. 4.5). At these concentrations, the Manuka honey coatings became extremely viscous when compared with the synthetic MGO coatings at the same MGO concentration. The synthetic MGO coatings still maintained a viscous nature, similar to water, which was likely to be absorbed and retained by the lyocell fibres. Fig. 4.7 shows images of the dry lyocell fibres (Fig. 4.7A), MGO coated lyocell fibres (Fig. 4.7B) and the Manuka coated lyocell fibres (Fig. 4.7C&D), obtained by an FEI Quanta 200F Field Emission Scanning Electron Microscope (FEGSEM). It can be seen that the MGO coated lyocell fibres (Fig 4.7B) retain a similar nature to the dry lyocell fibres as seen in Fig. 4.7A, with no obvious sign of any coating, confirming that the coating has been absorbed and retained by the fibres. However, the Manuka honey coated lyocell fibres, appear mainly occluded by the honey coating (Fig 4.7C&D), and some protruding fibres with a globular like structure, assumed to be the honey coating. This image provided further evidence that the Manuka honey coating is more freely available on the surface of the lyocell fibres to permit contact with the bacteria agar.

Upon incubation of the Manuka honey samples at 37ºC during testing, the Manuka honey coating is likely to soften and allow greater diffusion into the bacteria seeded agar from the fibres. Previous studies have shown that temperature has a direct influence on the viscosity of honey (330-332), as the temperature increases the viscosity falls due to reduced hydrodynamic forces and a lesser amount of molecular friction (332). A viscosity measurement of Manuka honey at 37ºC ± 2ºC and ambient room temperature of 25 ± 2ºC using the procedure outlined in section 3.2.1, found that a relatively low viscosity of 17800 cP was obtained at 37ºC ± 2ºC when compared with a higher measurement of 21800 cP at 25 ± 2ºC. This confirms that the Manuka honey coating is likely to migrate more freely into the bacteria seeded agar due to the reduced viscosity at 37ºC.

In contrast, the synthetic MGO coatings did not show a clear zone of inhibition until a concentration of 0.4 mg cm^{-2} was reached for *E.coli* (Fig. 4.6B) and 0.8 mg cm^{-2} for *S.aureus* (Fig. 4.6H). Below these concentrations an unclear zone was observed and it is likely the lyocell fibres retained much of the synthetic MGO and subsequently only partial inhibition of the bacteria could be achieved. As the addition of synthetic MGO solution became greater, the lyocell fibres approach their absorbent capacity and their ability to retain the synthetic MGO solution may be reduced. This would encourage greater diffusion of MGO into the agar to create a clear zone of inhibition. Due to the calibration limits of the viscometer, a viscosity measurement of the synthetic MGO coatings was not possible.

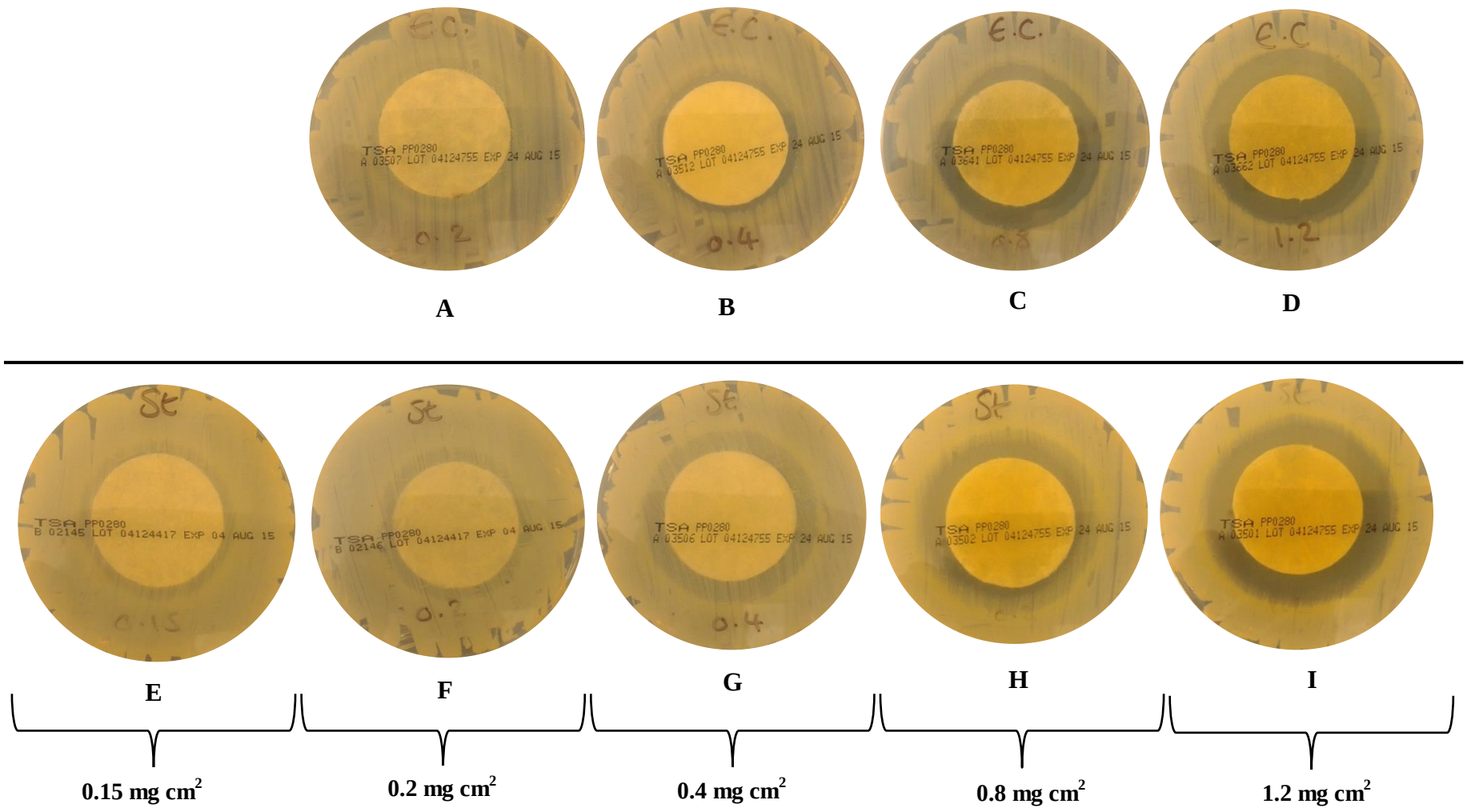

E. coli

S. aureus

Figure 4.6: Zones of inhibition produced from MGO concentrations (0.15 mg cm^2 to 1.2 mg cm^2) in the synthetic MGO coatings against *E.coli* and *S.aureus*. A & F = 0.2 mg cm^2, B & G = 0.4 mg cm^2, C & H = 0.8 mg cm^2, D and I = 1.2 mg cm^2 and E = 0.15 mg cm^2.

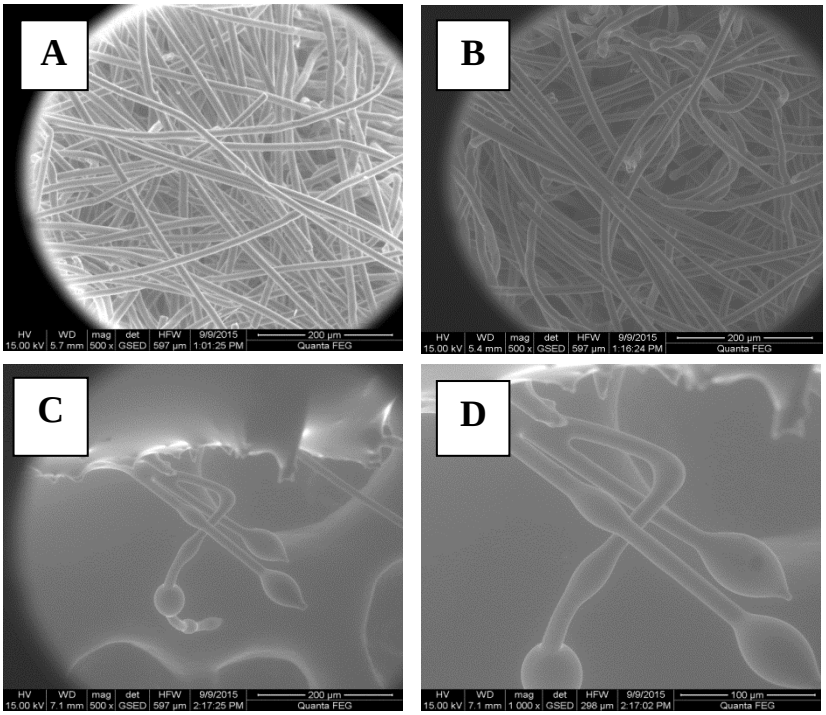

Figure 4.7: FEGSEM of dry lyocell fibres (A), synthetic MGO coated fibres (B) and Manuka honey coated fibres (C&D). Taken at a magnification of 500 (A, B & C) and 1000 (D).

Another study which explored the antibacterial activity of Manuka honey and MGO in a liquid form reported that higher levels of MGO alone were required to inhibit the growth of P.aeroginosa when compared with Manuka honey, which contained equivalent MGO concentrations. It was proposed that MGO may be enhanced when in the Manuka honey solution (183). There is also the probability that the hydrogen peroxide present in the Manuka honey may heighten the antibacterial effect (164, 168, 169).

Comparing the results obtained using BS EN ISO 20743:2007, where quantitative results were obtained, and BS EN ISO 20645:2004, the concentration of MGO required to produce an antibacterial effect was found to be slightly different. For BS EN ISO 20743:2007, a low concentration of 0.0054 mg cm^{-2} for both Manuka honey and synthetic MGO showed 100% reduction in bacteria for both *S.aureus* and *K. pneumonia*. For BS EN ISO 20645:2004, a good antibacterial effect was achieved at slightly higher concentrations between 0.0170 mg cm^{-2} and 0.1 mg cm^{-2} for *E.coli* and *S.aureus*. In the results from BS EN ISO 20743:2007, a likely explanation for the antibacterial effect at a concentration of 0.0054 mg cm^{-2} may be attributed to the addition of 20 ml of SCDLP (used to simulate wound exudate) solution to the test specimens in the jars (314). In this case, the lyocell fibres were exposed to a high moisture content, which would encourage hydration of the fibres and facilitate extraction of the MGO from the fibres, allowing 100% reduction in bacteria. In the case of BS EN ISO 20645:2004, an insufficient moisture content was available to initiate the diffusion of the

MGO from the fibres (329). It is only when the nonwoven samples became increasingly saturated that the moisture content during the test heightened and allowed for the diffusion of MGO into the agar.

4.3 MIC and MBC of MGO against common wound pathogens

To determine the MIC and MBC of MGO against three common wound pathogens, a standard laboratory assay was carried out in the Leeds Pathology Microbiology department according to 3.2.8.3. A 40 wt % MGO solution was diluted to concentrations between 1 mg L^{-1} to 1026 mg L^{-1} based on similar concentrations reviewed in the current literature (183) and tested against three bacterial strains including *S.aureus, P.aeruginosa* and *E.faecalis*. Two separate strains were collected from patients following ethical approval, and an American type culture collection (ATCC) standard of each was also used. The MIC was determined as the lowest concentration of MGO that was found to completely inhibit the growth of the organism in the microdilutions, as detected by the unaided eye. The MBC was determined as the lowest MGO concentration at which there was no growth upon subculture.

4.3.1 Results and Discussion

Table 4.6 shows the results of the MIC and MBC of MGO in liquid form against each bacterial strain. For *P.aeruginosa* the MIC against the ATCC strain and patient 1 strain was found to be 512 mg L^{-1}. The patient 2 strain required twice the concentration (1024 mg L^{-1}) to inhibit the growth. Upon subculture of all three isolates, the MBC required to kill *P.aeruginosa* ATCC strain was doubled to 1024 mg L^{-1}, while the two patient strains remained the same as the MIC. These concentrations were the highest among each bacterium species tested, as the MIC and MBC for *S.aureus* and *E. faecalis* did not reach above 512 mg L^{-1}. The relatively high concentrations required to inhibit or kill *P.aeroginosa* are not surprising, given that *P.aeruginosa* is one of the most problematic multidrug-resistant strains that is increasingly being isolated in clinical environments (183). It is important because *P.aeroginosa* is now showing resistance to common antibiotics, including ciprofloxacin (132), amikacin and imipenem (333). Limited work has been previously published on the MBC of MGO against *P.aeruginosa*. One previous study reported the MBC of both *MRSA* and *P.aeruginosa* in a planktonic and biofilm state. The MBC for *P.aeruginosa* in a planktonic state was found to range between 600 mg L^{-1} to 1200 mg L^{-1}, while in the biofilm state the MBC was much higher ranging from 1800 mg L^{-1} to 7600 mg L^{-1}(334). It can be expected that a raised concentration of MGO would be required in a biofilm state, as the polysaccharide (Psl) in *P.aeruginosa* biofilms has been shown to

provide a physical barrier against various antibiotics at the beginning stages of biofilm development (120). In the current study, the MBC was only tested in the planktonic state and shows a slightly lower MBC between 512 mg L^{-1} and 1024 mg L^{-1} than in the previous study.

S.aureus, reportedly the most common bacterium species found in a chronic wound environment (6), showed the lowest MIC and MBC for all three bacteria species. The ATCC strain showed the lowest MIC of 128 mg L^{-1}, while the two patient strains did not exceed 256 mg L^{-1} for both the MIC and MBC. A previous study (172) reported a lower MIC of 79.3 mg L^{-1} (1.1mM) for *S.aureus* while another reported a biocidal effect of MGO in Manuka honey with an MGO concentration of 530 mg L against $biofilms^{-1}$ (335). In the same study, the concentration of MGO alone required to achieve a biocidal effect against biofilms was >1050 mg L^{-1}, which is four times higher than the concentration reported in the current study (256 mg L^{-1}).

The effect of MGO concentration on *E.faecalis* has, to the author's knowledge not been previously reported. One study has reported the effect of Activon Manuka honey dressing against vancomycin-resistant *Enterococcus faecalis* (*VRE*), stating that that a 5% (w/v) concentration was needed to initiate an antibacterial effect against the biofilm. No reference was made throughout the study in relation to MGO. Therefore, it was of interest to understand the MIC and MBC of MGO concentration against *E.faecalis*, as the literature has previously revealed (section 2.2.2) it is the second most prevalent bacteria to be found in a chronic wound environment (6). In the current study, equivalent MIC and MBC were shown to be effective for the ATCC strain at a concentration of 256 mg L^{-1} and the two patient strains with a concentration of 512 mg L^{-1}.

Table 4.6: MIC and MBC (mg L^{-1}) of MGO in liquid form against three common wound pathogens.

Test organism	MIC (mg L^{-1})	MBC (mg L^{-1})
Pseudomonas aeruginosa ATCC27853	512	1024
Pseudomonas aeruginosa patient 1	512	512
Pseudomonas aeruginosa patient 2	1024	1024
Staphylococcus aureus ATCC29213	128	256
Staphylococcus aureus patient 1	256	256
Staphylococcus aureus patient 2	256	256
Enterococcus faecalis ATCC21292	256	256
Enterococcus faecium (VRE) patient 1	512	512
Enterococcus faecium (VRE) patient 2	512	512

The results of this experiment were particularly important because they provided an indication of the bactericidal concentration or the MBC of MGO when compared with the bacteriostatic concentration or the MIC (336). The previously conducted antibacterial test BS EN ISO 20743:2007 could not indicate if the antibacterial effect was attributed to a bactericidal or bacteriostatic effect. The results from BS EN ISO 20645:2004, showed only an inhibitory (bacteriostatic) effect. In this experiment the bactericidal concentration of MGO has been successfully identified for the three most prevalent chronic wound pathogens, and for the first time the effect of MGO on *E.faecalis* has been established.

4.4 Summary

In accordance with BS EN ISO 20743:2007, it was found that when Manuka honey or synthetic MGO are applied as a coating to a nonwoven fabric, a concentration of 0.0054 mg cm^{-2} of MGO was sufficient to achieve 100% reduction in bacteria using *S.aureus* and *K.peunomia*. Further experiments, using BS EN ISO 20645:2004 and the same nonwoven coated fabrics, revealed that higher concentrations of MGO between 0.0170 mg cm^{-2} and 0.1 mg cm^{-2} were required to produce a good antibacterial effect against *E.coli* and *S.aureus*. Zones of inhibition were apparent at relatively low MGO concentrations between 0.1 mg cm^{-2} and 0.2 mg cm^{-2} for the Manuka honey coated nonwovens and were shown to increase with an increasing MGO concentration. However, clear zones of inhibition were not achieved with the synthetic MGO coated nonwovens until a concentration of 0.4 mg cm^{-2} of MGO

was achieved for *E.coli* and 0.8 mg cm^{-2} of MGO for *S.aureus*. The moisture content that was present during the BS EN ISO 20743:2007 and BS EN ISO 20645:2004 methods and the affinity of the lyocell fibres for water may account for the differing antibacterial concentrations in both tests. The MIC and MBC results revealed the concentrations of MGO in liquid form to have bacteriostatic and bactericidal effects on three of the most common chronic wound pathogens. Most importantly the bactericidal concentration of MGO, required to provide a functional effect has been established.

Chapter 5 Evaluation of Needle Electrospun Fibres Containing Poly(vinyl alcohol) and Synthetic Methylglyoxal

5.1 Introduction

In section 4.2.4.1, it was found that nonwoven webs containing 0.0054 mg cm^{-2} of synthetic methylglyoxal (MGO) had an antibacterial effect against both Gram positive *S.aureus* and Gram negative *K.pneumonia* when assessed in accordance with BS EN ISO 20743:2007. A 100% reduction in bacteria was observed comparable in performance to the equivalent concentration of MGO in the coated nonwoven Manuka honey samples. Further experiments using BS EN ISO 20645:2004 found that the synthetic MGO coated nonwovens, required a concentration between 0.0170 mg cm^{-2} and 0.1 mg cm^{-2} for *E.coli* and *S.aureus* respectively, to inhibit the bacteria and achieve a good antibacterial effect (section 4.2.4.2). The results from the minimum inhibitory concentration (MIC) and minimum bactericidal concentration (MBC) tests for MGO in liquid form against three bacterial wound pathogens also confirmed low antimicrobial efficiency results against three common chronic wound pathogens (section 4.3.1).

As reported in section 2.8.4.2, electrospinning of inherently antibacterial materials for wound care is an area of new interest. Electrospun polymeric materials have been shown to mimic the extracellular matrix of the (ECM) of tissues (58) as well as to provide a suitable matrix for the controlled release of antimicrobials and their inclusion within a composite wound dressing. Hydrogel forming polymers are particularly useful in wound care as they provide a moist environment at the wound bed, which is essential for healing (18, 19). In a wound contact layer they also facilitate a low adherent surface that is less likely to disturb new tissue when removed. Poly(vinyl alcohol) (PVA) is a hydrogel-forming polymer that has received significant attention in the literature and in particular electrospinning studies for medical applications (54, 65, 66).

Given the antibacterial efficacy of MGO and the hydrogel formation properties of PVA, the aim of this chapter was to investigate the feasibility of combining MGO with PVA in a one-step manufacturing process to produce fibres and webs via needle electrospinning. This was explored using aqueous solutions of PVA doped with synthetic MGO. To determine the presence of MGO in the electrospun webs, Fourier transform infra-red spectroscopy (FTIR) and proton nuclear magnetic resonance (^{1}H-NMR) were employed. The antibacterial activity of the webs was then determined by means of the protocol set out in BS EN ISO 20645: 2004. Firstly, suitable concentrations of PVA in aqueous solutions of synthetic MGO and distilled water were investigated to determine the optimum spinning solution, providing fibres free from defects. The degree of PVA hydrolysis, molecular weight (274) and concentration (337) can all be expected to contribute to the morphological features of the fibres. For PVA, previous studies have reported the use of molecular weights between 9,000-10,000 and 58,000-85,000 and a degree of hydrolysis between 97-99% contribute to fibres free from beads. At a lower molecular weight of 13,000 - 23,000 a concentration of at least 21 wt % was required to electrospin fibres free from beads. In contrast, at higher molecular weights of 58,000 - 85,000, a reduced

concentration of only 9 wt % was required to facilitate spinning (242). Other studies have reported electrospinning with concentrations of PVA between 5 wt % and 20 wt % (272, 274, 338, 339). At concentrations between 5 wt % and 8 wt % the morphology of the fibres consists mainly of beads, merging areas or fibres that form junctions. As the concentration is increased to 10 wt % beads and defects become less frequent and elongated fibres are observed (274). A study by Santos et al. (338) reported that at concentrations below 10% (w/w), electrospraying was observed without fibre formation. At concentrations of 12% (w/w) and 20% (w/w) fibres free from defects were produced due to the viscous and conductive properties. An increase in the viscosity enabled the solution to withstand the columbic stretching force in the charged jet resulting in the formation of uniform fibres (338).

5.1.1 Preparation of PVA and PVA/MGO solutions for needle electrospinning.

Prior to electrospinning with PVA/MGO solutions, initial trials were carried out to check the spinning ability of PVA with a molecular weight of 31,000-50,000 in distilled water at concentrations of 8% (w/v), 12% (w/v) and 16% (w/v). To evaluate and determine if PVA/MGO solutions could form fibres using needle electrospinning, PVA concentrations of 8% (w/v), 12% (w/v) and 16% (w/v) were prepared in a 40 wt % MGO solution and in a further three aqueous dilutions of the 40 wt % MGO solution. The concentrations of MGO in each solution were calculated to be 40 wt %, 21.57 wt %, 14.76 wt % and 11.22 wt %.The prepared solutions were kept under constant agitation at 80ºC ± 2ºC for 24 h in a glass conical flask, sealed with a glass stopper. After 24 h all the PVA had dissolved and the solutions appeared clear.

5.1.2 Needle Electrospinning

The prepared PVA/MGO solutions were electrospun to determine the spinning ability of each solution using needle electrospinning. The method of electrospinning was described in section 3.2.4.1. Needle electrospinning was performed inside a fume cupboard using a Glassman high voltage power supply and a Kd Scientific syringe pump. The syringe pump flow rate was set to run at 0.1 ml h^{-1}. Initial results revealed that a voltage below 7 kV was insufficient to maintain a continuous electrospinning jet and a voltage above 18 kV gave rise to electrostatic sparks, which again interrupted the process. A previous study has also reported that using a voltage below 5.5kV leads to difficulties in initiating a polymer jet (276). A higher voltage is required to induce the necessary charges on the polymer solution enabling the columbic repulsive force in the solution to overcome the surface tension and stretch the viscoelastic solution (267). For this reason a series of voltages between 7 kV to 18 kV was applied. Aluminium foil measuring 10 cm x 10 cm was used as the web collector and tip to collector distances from 5 cm to 15 cm were employed following the initial trials.

5.1.3 Spinning solution properties: Viscosity, surface tension and conductivity

As previously reported in section 2.8.3.1, the viscosity (272, 276) is known to have an influence on electrospinning performance and the morphological features of the resultant webs. To determine any correlations between the solution properties and the spinning ability, measurements of viscosity, surface tension and conductivity of each prepared spinning solution were made. Measurements were taken according to the procedures outlined in section 3.2.1. Prior to recording the measurements, all spinning solutions were initially incubated at 25ºC for 24 h. This temperature was chosen, to reflect the average ambient room temperature recorded during needle electrospinning of 25ºC ± 2ºC.

Initial tests on the prepared spinning solutions confirmed that because of the variation in the viscosity of the prepared solutions, it was not possible to measure the viscosity of all the solutions with the same spindle and speed. Therefore direct comparisons were not always possible. It was therefore decided that extra solutions should be prepared for polymer concentrations between the experimental range of 8% (w/v), 12% (w/v) and 16% (w/v). Accordingly, additional solution concentrations of 10% (w/v), 14% (w/v), 18% (w/v) and 20% (w/v) were prepared and measured to determine their viscosity where possible with the same spindle and speed. The surface tension and conductivity of the additional solution concentrations was also measured. This provided an indication of the relative differences between the experimental solutions.

5.1.4 Results and Discussion

5.1.4.1 Needle Electrospinning performance

A summary of the needle electrospinning performance of each polymer solution is given in Table 5.1. Visual observations were also recorded as shown in Fig. 5.1.

Table 5.1: Needle electrospinning performance of each spinning solution.

Solvent	MGO concentrations (wt %)	PVA concentration (% w/v)	Electrospinning performance	Behaviour of polymer solutions
Distilled water	0	8 &12	Merging fibres that form junctions	Wet polymer on the collector
	0	16	Fibres	Steady jet stream
40 wt % MGO	40	8, 12 & 16	Solution not spinnable	Formed a gel after 24 hours stirring
40 wt % MGO (aqueous solution) diluted with distilled water	21.57	8 & 16	Merging fibres that form junctions or solution not spinnable	Wet polymer on the collector or polymer dried at needle tip
	21.57	12	Beads	Intermittent stream or a bowing Taylor cone
	14.76	8, 12 &16	Merging fibres that form junctions or solution not spinnable	Wet polymer on the collector or polymer dried at needle tip
	11.22	8 & 12	Merging fibres that form junctions	Wet polymer on the collector
	11.22	16	Fibres	Steady jet stream

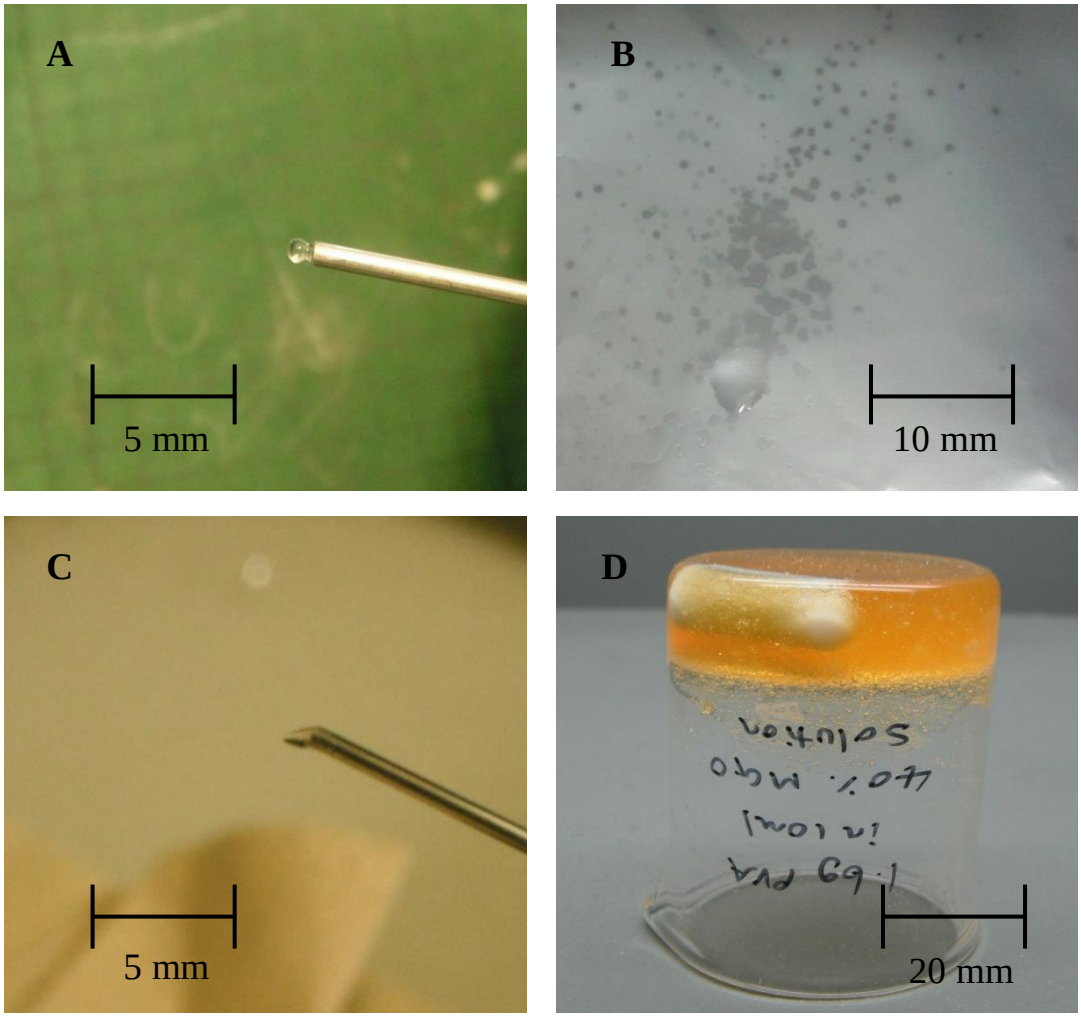

Figure 5.1: Observations of polymer solutions before & during electrospinning. A = polymer drying at the needle tip, B = wet spots on the aluminium foil collector, C = bowing Taylor cone & D = gel formation

The viscosity of the spinning solutions was found to greatly influence the needle electrospinning ability. Fig. 5.2 displays the viscosity results obtained for the experimental solutions and additional concentrations as described in section 5.1.3. With an MGO concentration of 21.57 wt % and polymer concentrations between 8% (w/v) and 12% (w/v), the viscosity was found to be relatively low between 260 cP and 435 cP. At an MGO concentration of 14.76 wt % and a polymer concentration of 12% (w/v) the viscosity was also relatively low at 374 cP. Concentrations below 12% (w/v) for an MGO concentration of 14.76 wt % were not measurable using the same spindle and speed. Similarly for an MGO concentration of 11.22 wt %, polymer concentrations below 14% (w/v) were not measurable. However, it is apparent from the points on the curves that the viscosity of the unmeasurable PVA concentrations would have been lower than the recorded measurements with a 21.57 wt % MGO concentration and PVA concentrations between 8% (w/v) to 12% (w/v). At these low polymer concentrations between 8% (w/v) and 12% (w/v), the chain entanglement in the polymer solution was insufficient to

sustain and stabilise an electrospinning jet, resulting in the breakup of the electrically driven jet into droplets (275, 340) that formed upon the collector, as observed in Fig. 5.1B.

SEM micrographs were taken using a Carl Zeis EVO MA15 at a magnification of 11.00 K to provide an initial examination of the morphological characteristics of the spun webs as shown in Fig. 5.3. At the relatively low viscosities between 260 cP and 374 cP, wet polymer droplets formed upon the collector resulting in merging fibres that formed junctions or flat ribbon-like fibres (Fig. 5.3A to 5.3D). A previous study reported that for an 8.1 wt % concentration of Nylon 6,6 in formic acid, the fibre formation changed from elongated fibres to fibres that formed junctions when the distance from the tip of the needle to the collector was reduced from 2 cm to 0.5 cm. At the shorter distance of 0.5 cm, wet polymer landing upon the substrate was observed (275) and can be attributed to the solvent having insufficient time to evaporate. However, in the present study an increase in distance from 5 cm to 15 cm made no difference to the deposition of wet polymer accumulating on the collector and subsequently resulting in flat ribbon like fibres. Another study reported that PVA with a lower degree of hydrolysis (80%) also gave rise to flat ribbon-like fibres (272). However, in the present study the degree of hydrolysis remained constant at a relatively high magnitude of 98-99% and therefore results did not follow the same trend.

Many previous studies have also reported that low viscosities contribute to the formation of beads (268, 270, 272, 273, 276, 341-343). At a low viscosity, a greater number of free solvent molecules are available as well as fewer chain entanglements, which results in the surface tension of the solution having a dominant influence on the electrospinning jet causing beads to form along the fibre (267).

Beads were observed in the present study (Fig. 5.3E) at relatively low viscosity of 435 cP, as seen in Fig. 5.2. At a higher polymer concentration of 16% (w/v) in an MGO concentration of 11.22 wt %, the viscosity increased to 605 cP, as seen in Fig. 5.2, and fibres free from beads and defects were observed (Fig. 5.3F). At this concentration sufficient chain entanglement in the polymer solution was apparent to prevent the breakup of the electrically charged jet, allowing the electrostatic charges to elongate the jet (275) and create fibres free from beads.

Comparatively, for a polymer concentration of 16% (w/v) in distilled water, a viscosity of a similar order of 635 cP was recorded and elongated fibres free from beads and defects were observed (Fig. 5.3G). Conversely at a polymer concentration of 16% (w/v) in an MGO concentration of 14.76 wt % and 21.57 wt %, the viscosity was shown to increase to 1421 cP and 3864 cP respectively. At these relatively high viscosities the polymer was found to dry at the needle tip, as seen in Fig. 5.1A, and subsequently an electrospinning jet was not formed.

Zong et al. also reported this observation for poly(D,L-lactic acid) at a concentration higher than 40 wt % in dimethyl formamide (268).

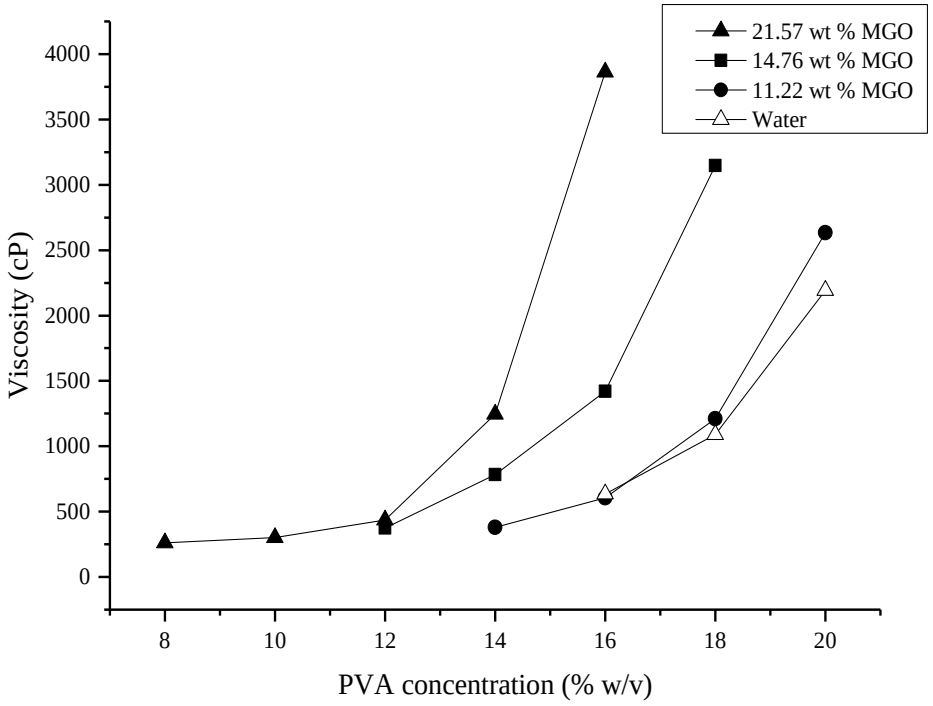

Figure 5.2: The effect of MGO concentration (wt %) and PVA concentration (% w/v) on the viscosity (cP) of the needle electrospinning and additional solutions. Measured using a Brookfield LV DV- E viscometer with a spindle size of 31 and a speed of 6 r min^{-1} at a temperature of 25˚C ± 2˚C.

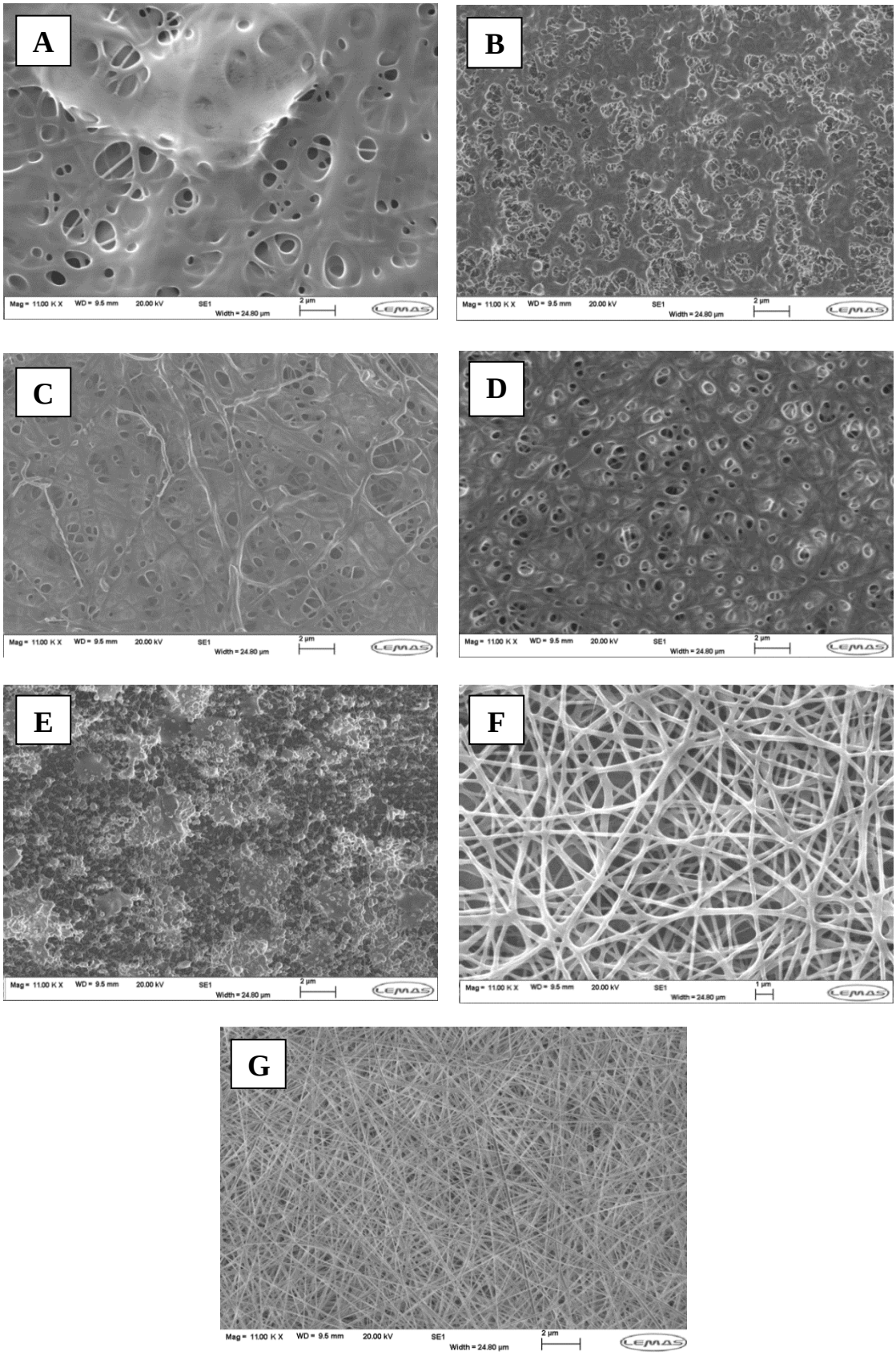

Figure 5.3: SEM micrographs produced from: A & B = 21.57 wt % MGO with an 8% and 12% (w/v) PVA concentration respectively, C = 14.76 wt % MGO with 8% (w/v) PVA, D = 11.22 wt % MGO with 8% (w/v) PVA, E = 14.76 wt % MGO with 12% (w/v) PVA, F = 11.22 wt % MGO with 16% (w/v) PVA and G = distilled water with 16% (w/v) PVA.

The surface tension and conductivity of the polymer solutions are also known to have an effect on the electrospinning ability and have a strong link to the viscosity. Fig. 5.4 displays the surface tension and conductivity results obtained for the experimental solutions and additional concentrations as described in section 5.1.3. The surface tension of the solutions with a relatively low viscosity (260 cP to 435 cP), which were shown to create merging fibres or beads (Fig. 5.3D to 3E), was found to be at the highest range between 50.2 mN m^{-1} and 48.4 mN m^{-1} (Fig. 5.4A).

A higher solution surface tension is generally known to suppress the electrospinning process because of instability in the electrospinning jet causing the creation of sprayed droplets on the collector (344), as was observed in the present study. In the case of bead formation as seen in Fig. 5.3E, when there is a high concentration of free solvent molecules in the polymer solution, there is a greater tendency for the solvent molecules to group together and create spherical bead shapes along the electrospinning jet (267). When the polymer concentration was increased to 16% (w/v) in a 11.22 wt % MGO concentration, the surface tension decreased to 45.96 mN m^{-1} as seen in Fig. 5.4A, and fibres free from beads were produced (Fig. 5.3F and 3G). This is not surprising given that the main solvent in the solution is distilled water, which is known to have a high surface tension of 72.8 mN m^{-1}. As the polymer concentration in the solutions is increased, the ratio of water molecules to polymer decreases, resulting in a decreasing surface tension. Other studies have also reported that reducing the surface tension results in smoother fibres (267, 341).

The conductivity of the electrospinning solutions also correlates with the transformation from merging areas that form fibres or beads to elongated fibres. The concentration of PVA in each MGO solution has minimum effect on the conductivity values. For example at a 21.57 wt % MGO concentration for any given concentration of PVA (% w/v), the conductivity is shown to stay at relatively low values between 0.364 mS cm^{-1} and 0.465 mS cm^{-1} (Fig. 5.4B). However, as the MGO concentration was decreased to 11.22 wt %, the conductivity rises to values between 1.033 mS cm^{-1} and 1.260 mS cm^{-1}. At a value of 1.234 mS cm^{-1} smooth fibres are achieved (Fig. 5.3F). Previous studies, have also reported that solutions with a higher conductivity yielded fibres free from beads (271-273). At a higher conductivity the charges in the solution will be greater which in turn increases the stretching of the polymer jet resulting in fibres free from beads (267).

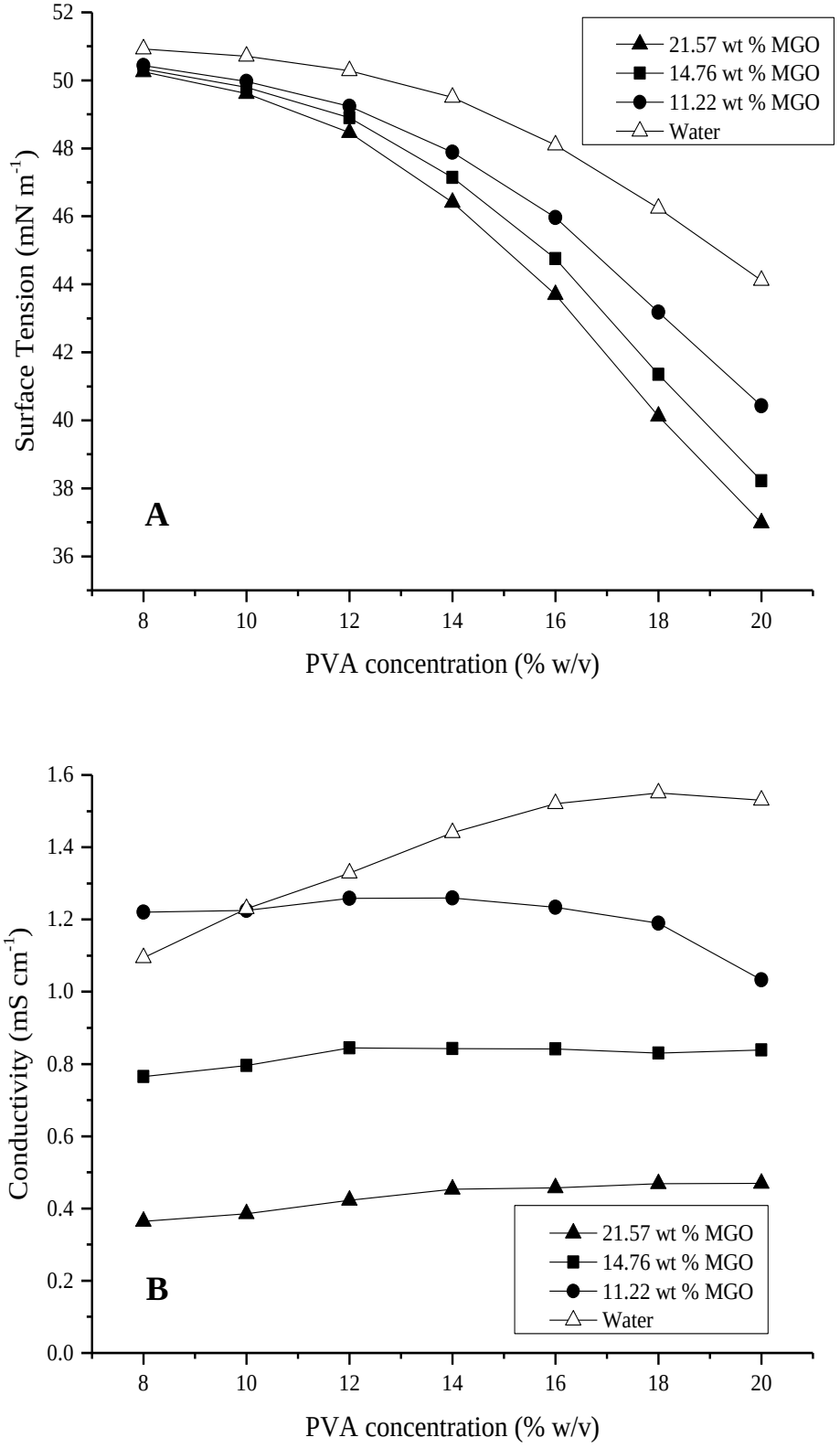

Figure 5.4: The effect of MGO concentration (wt %) and PVA concentration (% w/v) on the surface tension (mN m^{-1}) (A) and the conductivity (mS cm^{-1}) (B) of the needle electrospinning and additional solutions, at a temperature of 25°C ± 2°C.

SEM micrographs over the full range of voltages from 7 kV to 18 kV and distances from 5 cm to 15 cm can be seen in Fig. 5.5 and 5.6 for a 21.57 wt % MGO concentration with a 12% (w/v) PVA concentration and a 11.22 wt % MGO concentration with a 16% (w/v) PVA concentration respectively. The initial SEM images revealed that bead formation (Fig. 5.3E) occured for a 21.57 wt % MGO concentration with a 12% (w/v) PVA concentration. However it was of interest to understand if the bead formation transformed to smooth fibres with increasing distance and voltage, as this solution showed no evidence of wet polymer landing upon the collector during electrospinning.

Images were taken using a Jeol JSM-6610LV at a magnification of 2500. Fig. 5.5 shows that for a 21.57 wt % MGO concentration and a 12% (w/v) PVA concentration only 14 out of a possible 25 combinations of voltages and distances achieved web formation upon the collector. It was noted that as the distance increased a higher voltage was needed to initiate a polymer jet. At a greater distance there will be a decrease in the electrostatic field strength at the same voltage and so a greater voltage is required to initiate the polymer jet (274). The varied distances and voltages had no effect on the transformation from beads to fibres and no fibres were observed. However the size of the beads was shown to grow in size at a short distance of 5 cm and increasing voltage from 7 kV to 15 kV. Previous studies have also observed bead formation with an increasing voltage from 5 kV to 9 kV for a polymer concentration of 7 wt % polyethylene oxide in water (276). A receding electrospinning solution droplet to within the needle can explain this observation. As the voltage is increased the size of the droplet will decrease as the droplet resides within the needle and around the needle edge (276). In the present study an intermittent jet stream occurred, which resulted in short repellent bursts of the polymer jet towards the collector.

.

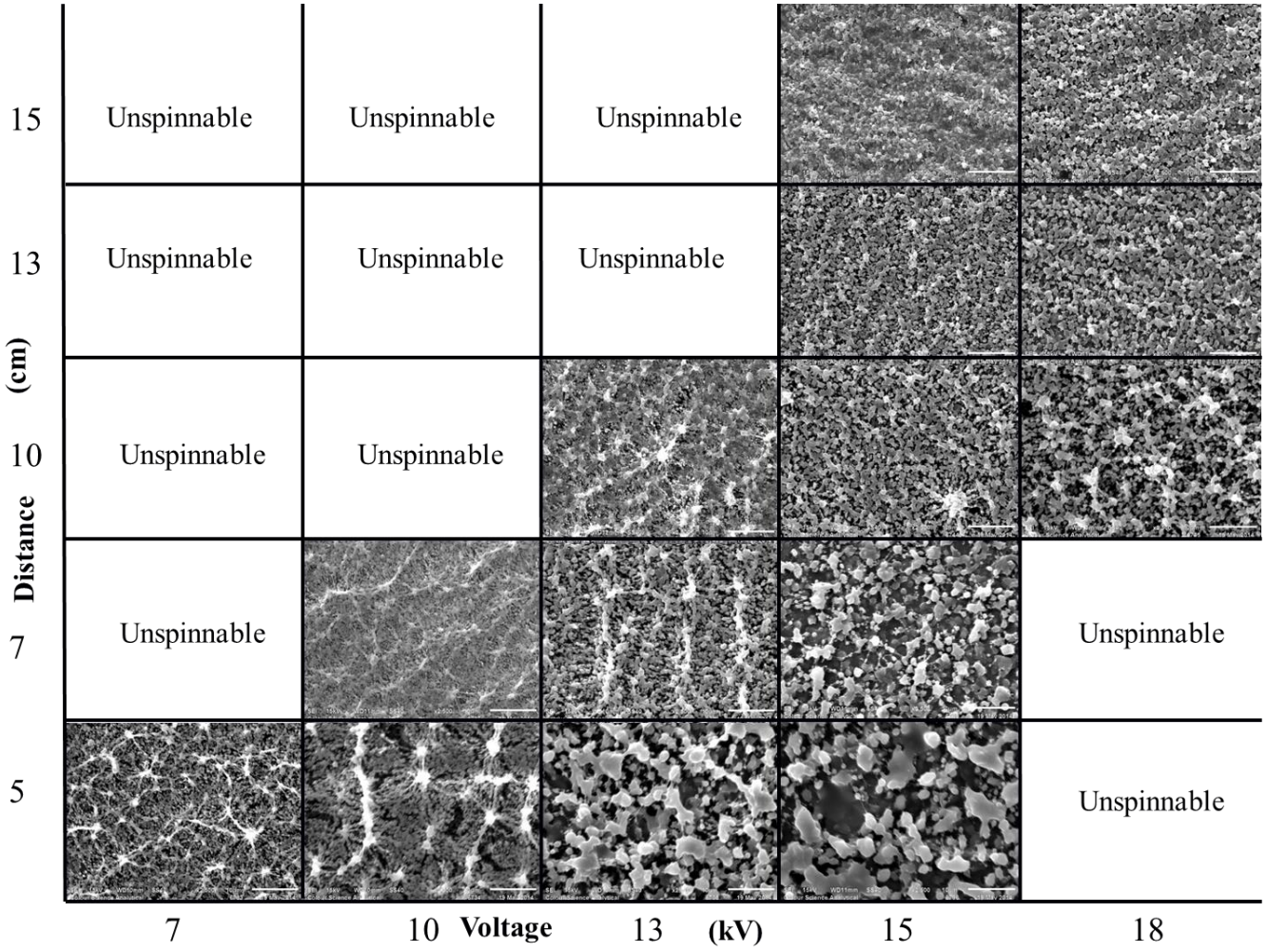

Figure 5.5: SEM micrographs of webs produced using needle electrospinning at different combinations of tip to collector distance and voltage, using a 21.57 wt % MGO concentration with a 12% (w/v) PVA concentration

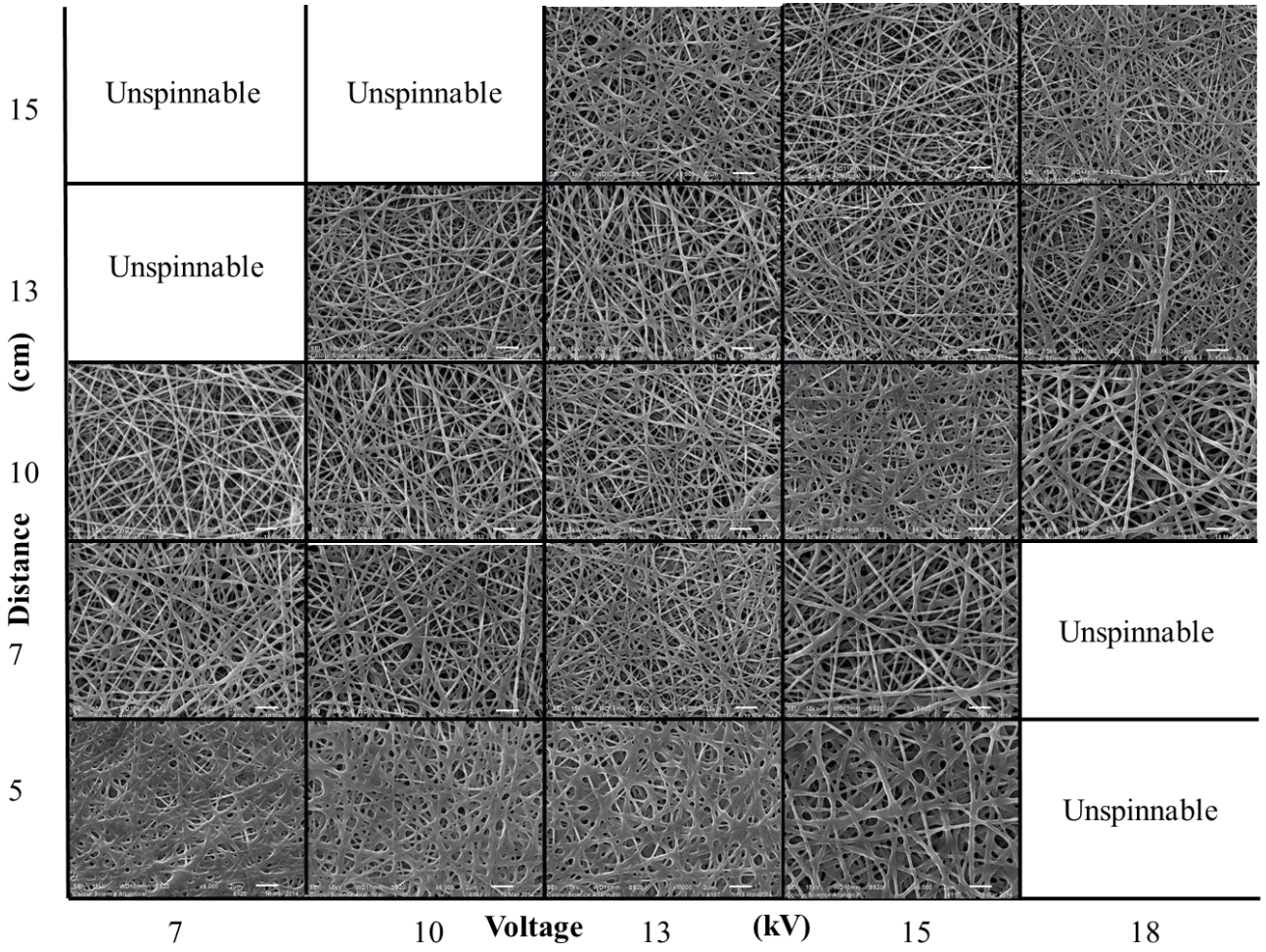

Figure 5.6: SEM micrographs of webs produced using needle electrospinning, from an 11.22 wt % MGO concentration with a 16% (w/v) PVA concentration

For the SEM micrographs shown in Fig. 5.6, for an 11.22 wt % MGO concentration with a 16% (w/v) PVA concentration, 19 out of 25 possible combinations between voltage and distance achieved web formation. The range of fibre diameters was recorded for each distance and voltage and the mean fibre diameter was calculated and can be seen in Table 5.2. In general, as the distance and voltage increased, the average fibre diameter decreased. A higher voltage will initiate a greater stretching of the solution due to the strong columbic forces in the electrospinning jet and a higher electric field (267). This also encourages faster solvent evaporation, which in turn yields drier fibres upon the collector (345).

A larger mean fibre diameter between 237 nm and 314 nm was associated with a short distance of 5 cm and an increasing voltage from 7 kV to 13 kV. The merging of fibres and fibres that form junctions was also evident using these parameters. Previous studies have also observed merging of fibres at short distances, which can be attributed to the solvent having less time to evaporate before arriving at the collector (275, 343). As the distance and voltage are increased, the average fibre diameter is shown to decrease. A study by Lee et al, also confirmed that a decrease in PVA fibre diameter is observed with an increase in voltage (274). Similarly Buchko et al. also reported a decrease in fibre diameter as the applied electric field was increased (275).

For each applied voltage and distance, the standard deviation of the fibre diameter from the mean was also calculated and is shown in Table 5.3. Examination of these results shows that the smallest mean fibre diameter (157 nm) is achieved at a distance of 15 cm and a voltage of 15 kV, which also coincides with the lowest standard deviation of 31 nm. At a smaller distance of 5 cm and a voltage of 10 kV the highest standard deviation was observed (141 nm), which corresponds with a relatively large mean fibre diameter of 291 nm, nearly double that of the smallest mean fibre diameter. The fibre distribution for the smallest and largest mean fibre diameters can be seen in Fig. 5.7.

Table 5.2: Mean fibre diameters (nm) achieved for a 11.22 wt % MGO concentration with a 16% (w/v) PVA concentration at different voltages (kV) and distances (cm). *n/s = not spinnable.

	Distance (cm)				
	5	**7**	**10**	**13**	**15**
Voltage (kV)	**Mean Fibre diameter (nm)**				
7	n/s*	241	188	n/s*	n/s*
10	238	244	205	192	192
13	291	196	201	193	212
15	314	300	209	170	157
18	n/s*	n/s*	240	192	166

Table 5.3: Standard deviation (nm) of the fibre diameters for a 11.22 wt % MGO concentration with a 16% (w/v) PVA concentration at different voltages (kV) and distances (cm). *n/s = not spinnable.

	Distance (cm)				
	5	**7**	**10**	**13**	**15**
Voltage (kV)	**Standard deviation (nm)**				
7	n/s	86	38	n/s	n/s
10	83	107	65	56	56
13	141	66	60	59	76
15	90	117	77	47	31
18			52	77	66

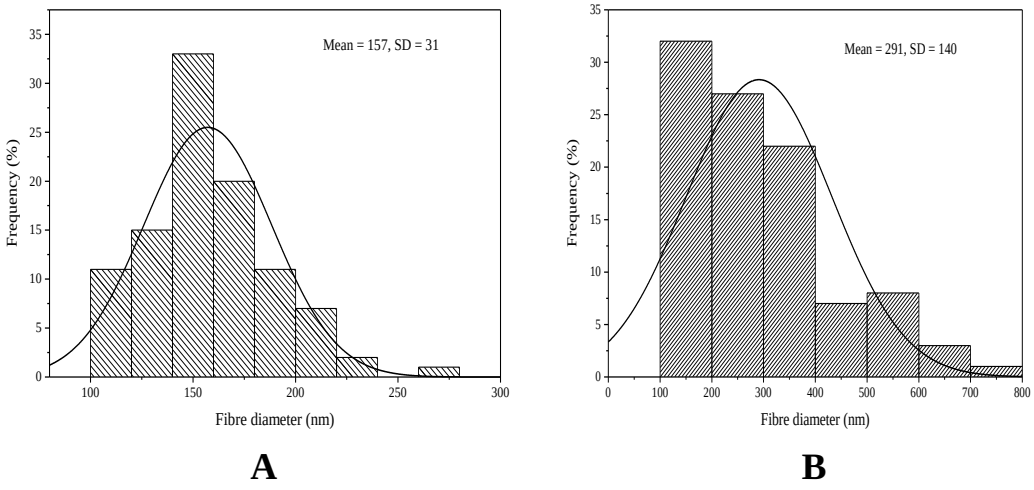

Figure 5.7: Fibre diameter distributions for an 11.22 wt % MGO concentration with a 16% (w/v) PVA concentration: A = sample spun at a distance of 15 cm and a voltage of 15 kV, B = sample spun at distance of 5 cm and voltage of 10 kV.

5.2 Identification of MGO in the PVA/MGO fibres

Both Fourier transform infra-red spectroscopy (FTIR) and proton nuclear magnetic resonance (^{1}H-NMR) were employed to determine the presence of MGO within the as-spun PVA/MGO fibres, as described in sections 3.2.6 and 3.2.7 respectively. Electrospun fibres produced from a spinning solution with a concentration of 11.22 wt % MGO with 16% (w/v) PVA, were assessed to verify if the MGO was present within the fibres after needle electrospinning. Prior to the analysis of the PVA/MGO fibres, FTIR spectra's of a 40% wt MGO solution and PVA granules (31-50,000Mw) were obtained to decipher the characteristic absorption bands found in both compounds. Similar to the FTIR analysis, measurements of both compounds were also taken using ^{1}H-NMR to establish the characteristic resonance peaks.

5.2.1 Results of Fourier Transform Infra-Red spectroscopy (FTIR)

Fig. 5.8 displays the FTIR results obtained for all three separate samples. As reported in section 2.5, MGO has two distinct carbonyl groups, a ketone and an aldehyde which are possible to detect using an FTIR system. A spectra of 40 wt % MGO solution (Fig. 5.8A) shows a characteristic vibrational absorption peak at 1728 cm^{-1}, which is attributed to the C=O stretching vibration in the aldehyde carbonyl. A peak at 1386 cm^{-1} was also observed and can be assigned to CH_3 bending in the methyl group of MGO (275). In Fig. 5.8B the spectra of PVA is displayed, the broad band centred at 3282 cm^{-1} is due to hydrogen-bonded O–H stretching vibration and the peak at 2905 cm^{-1} is attributed to C–H stretching in the polymer backbone. The peak at 1419 cm^{-1} is the result of in-plane O–H bending, while the peak at 1089 cm^{-1} is indicative of C–O stretching. Fig. 5.8C shows the spectra obtained for the PVA/MGO fibres.

Two small peaks were detected at 1720 cm^{-1} and 1379 cm^{-1} and coincide with similar peaks detected for the pure MGO. It can be assumed that the peak at 1720 cm^{-1} is attributed to the ketone carbonyl, while the small peak at 1379 cm^{-1} is indicative of the CH_3 bending.

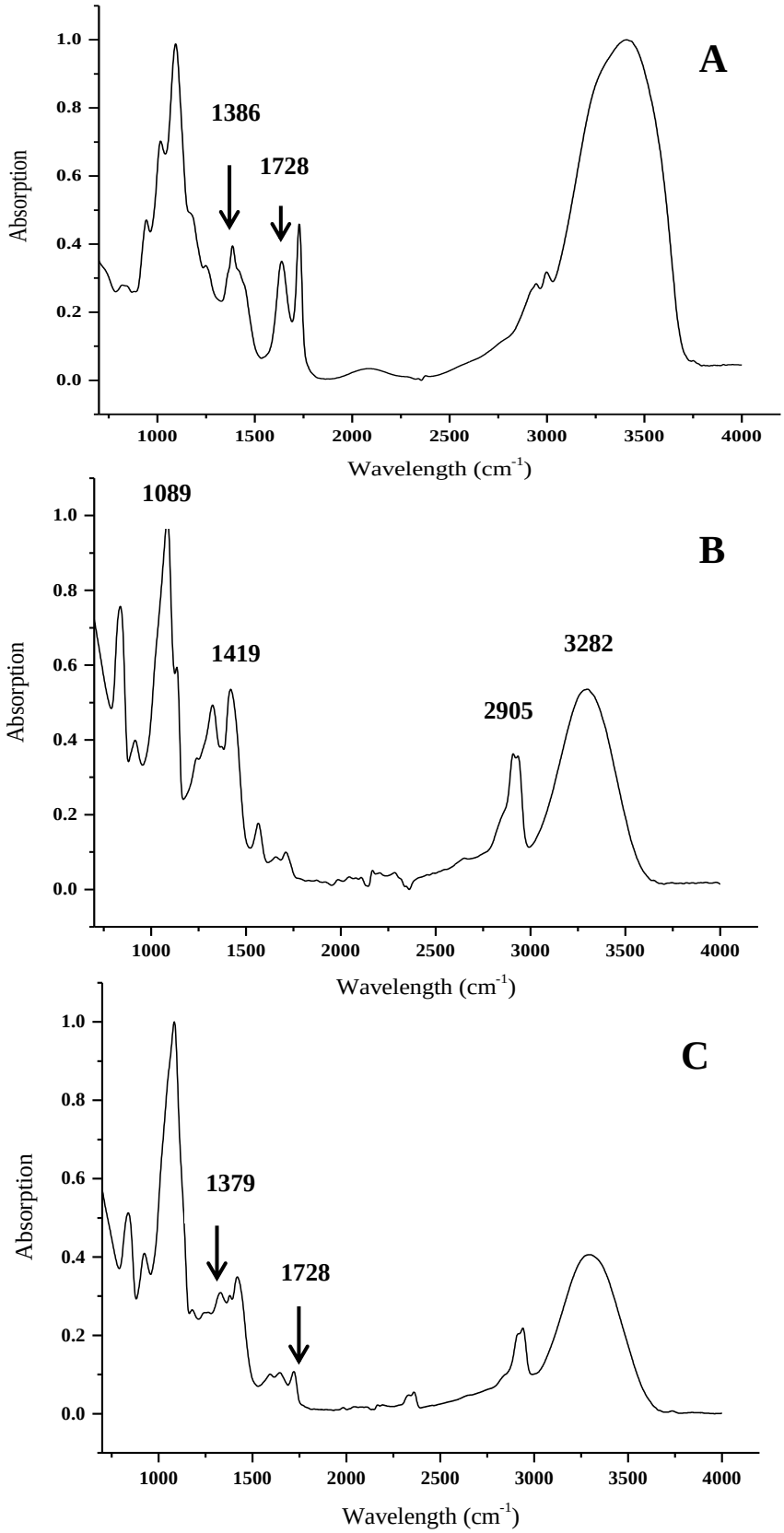

Figure 5.8: FTIR spectra of 40 wt % MGO solution (A), PVA powder (B) measured using the diamond ATR attachment with 64 repeat scans & PVA/MGO fibres in KBR pellets measured with 16 repeat scans(C).

5.2.2 Identification of MGO using proton nuclear magnetic resonance (^{1}H-NMR)

Similar to the FTIR analysis, a 40 wt % MGO solution and PVA granules (31-50,000Mw) were measured using ^{1}H-NMR to establish the characteristic resonance peaks of both compounds. The PVA/MGO fibres were then measured to establish if the MGO was detectable. Fig. 5.9 displays the ^{1}H-NMR spectra's obtained for all samples. In Fig. 5.9A the chemical formulas of MGO, MGO mono-hydrate and di-hydrate are shown. The hydrogen protons that are detectable for each chemical formula are indicated. Two singlet peaks at 1.403 ppm and 2.338 ppm can be assigned to the methyl protons present in the MGO di-hydrate and monohydrate respectively. The peak seen at 5.309 ppm is attributed to the alkyl proton of MGO monohydrate. These three peaks are in agreement with a previous study, which reported singlet peaks at 1.378 ppm, 2.306 ppm and 5.287 ppm for MGO (346). In Fig. 5.9B the spectra of dissolved PVA granules is displayed. The chemical formula of PVA and the hydrogen atoms, which are detectable, are shown. The resonance peaks observed at 1.751 ppm and 4.075 ppm can be assigned to the protons of CH_2 and the CH proton of the PVA, respectively (347). The spectra for the PVA/MGO fibres is seen in Fig. 5.9C. Resonance peaks for both MGO and PVA are detectable and coincide with the peaks detected in the pure compounds found in Fig. 5.9A and 5.9B. This data gives further confirmation that MGO is encapsulated within the resulting needle electrospun PVA fibres, with solvent evaporation having a limited effect.

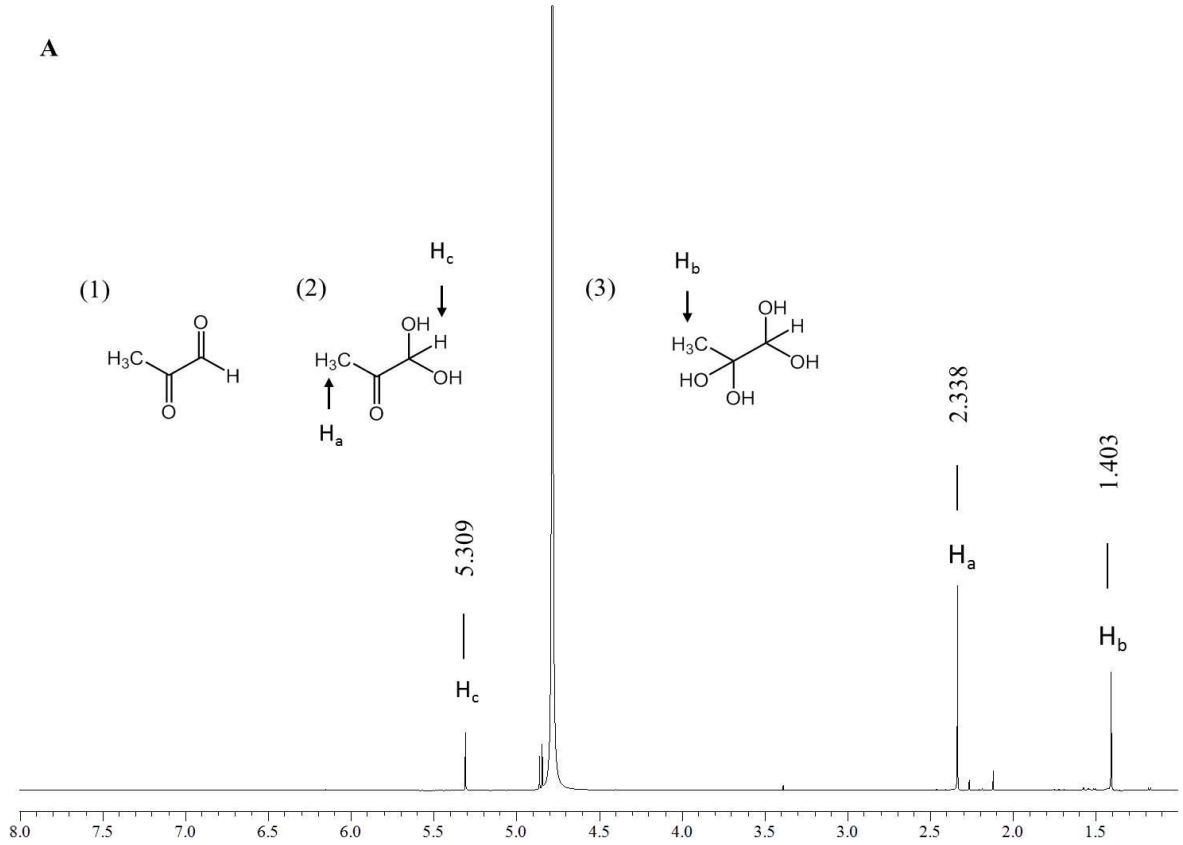

1, 2 and 3 indicate the chemical formulas of MGO, MGO mono-hydrate and MGO di-hydrate respectively.

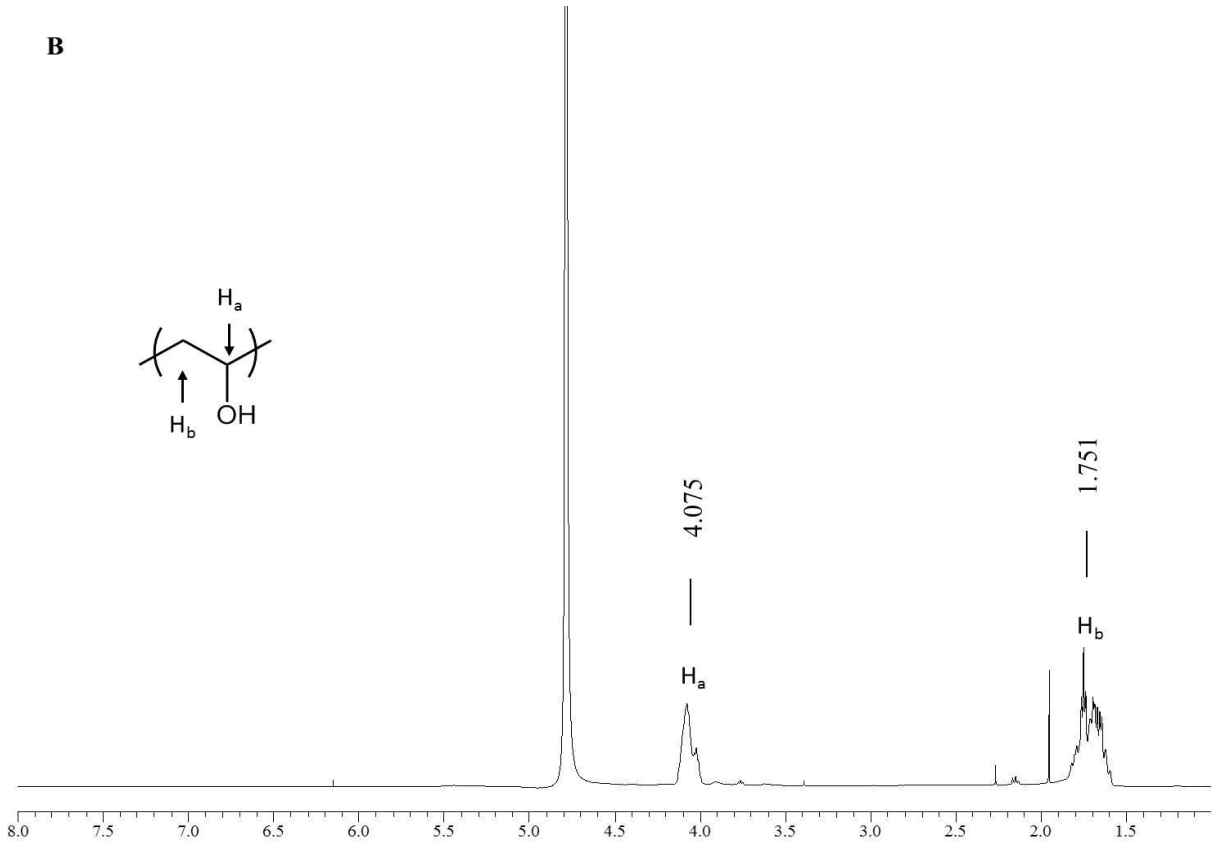

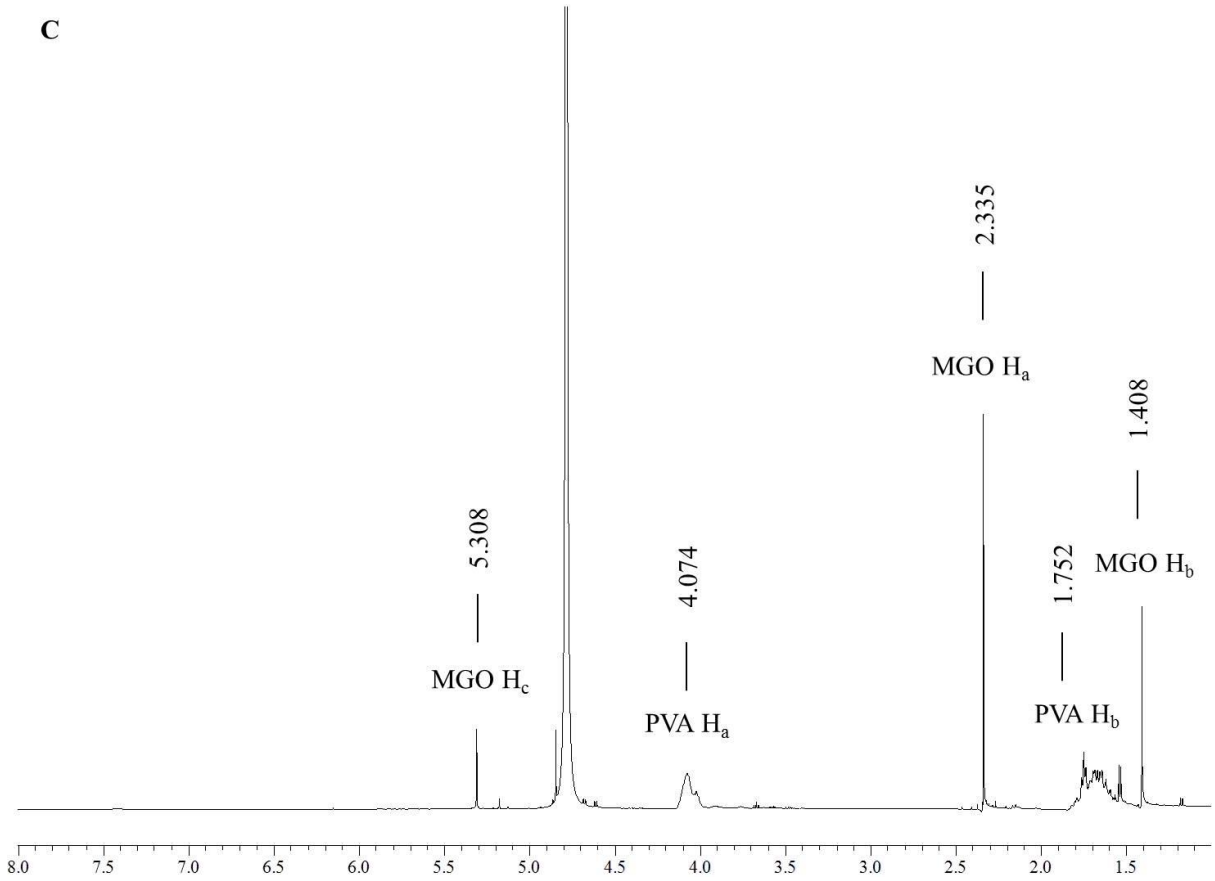

Figure 5.9: ^{1}H-NMR spectra's of 40 wt % MGO (A), PVA granules (B) and PVA/MGO fibres (C) all dissolved in 1ml of deuterium oxide (99.9 % atom). ^{1}H-NMR spectra were recorded with 1024 repetitions.

5.3 Antibacterial evaluation of PVA/MGO fibres

To evaluate the antibacterial behaviour of the fibres produced from needle electrospinning, BS EN ISO 20645:2004, Textile fabrics, determination of antibacterial activity, agar diffusion plate test, described in section 3.2.8.2 was followed. The electrospun fibres which were spun onto an inert nonwoven polypropylene spunbond substrate (SPB) were tested against two types of common wound pathogens: *S.aureus* and *E.coli*. As control specimens, PVA was electrospun onto SPB and SPB alone was used. The antibacterial activity of the samples was assessed by the absence or presence of bacterial growth in the contact zone between the agar and the specimen and the appearance of an inhibition zone around the specimen. The calculated width of the inhibition zone was recorded.

5.3.1 Preparation of PVA/MGO fibres for antibacterial testing

PVA/MGO fibres were prepared for antibacterial testing via needle electrospinning. An electrospinning solution made from an 11.22 wt % MGO concentration with 16% (w/v) PVA was prepared. For the control sample a 16% (w/v) concentration of PVA in distilled water was also prepared. SPB measuring 4 cm x 4 cm was used as the collector for the fibres to form a composite material. The SPB was placed over a piece of aluminium foil measuring 4 cm x 4 cm, to enable the attraction of the fibres to the SPB substrate. Based on the previous findings, a flow rate of 0.1 ml h^{-1}, a distance of 15 cm and voltage of 15 kV was utilised. The concentration of MGO in this solution was calculated to be 105 mg ml^{-1}. To determine the minimum concentration of MGO in the spun sample (mg cm^{-2}) required to have an antibacterial effect, electrospinning was carried out for various lengths of time between 0.5 h to 4 h. As the spinning time increased it was expected that there would be an increase in MGO concentration. Assuming that all of the MGO in the spun solution is in the spun fibres, the concentration of MGO in the spun sample (mg cm^{-2}) is given by the following equation:

Eq.5.1

$$\text{Concentration of MGO in the spun sample} = MGOc\ Fr\ T\ /\ Sa$$

where,

MGOc is the calculated concentration of MGO in the prepared spinning solution (105 mg ml^{-1})

Fr is flow rate of 0.1 ml h^{-1}

T is the spinning time (h)

Sa is the area of the spun sample (cm^2)

Note: The spun sample was normally a circle of approximately 3 cm in diameter. An area of 7 cm^2 (*Sa*) was therefore used.

Table 5.4 shows the calculated concentrations of MGO in the spun samples for each spinning time based on *Eq.5.1*.

Table 5.4: Calculated concentration of MGO in the electrospun samples (mg cm^{-2}).

Time spun (h)	MGO concentration (mg cm^{-2})
0.5	0.75
1	1.50
2	3.00
3	4.50
4	6.00

5.3.2 Results for antibacterial testing

Table 5.5 displays the results achieved for the needle electrospun PVA/MGO against *E.coli* and *S.aureus*. Fig. 5.10 and 5.11 show a visual representation of the effect of the control samples (PVA/SPB and SPB) and the PVA/MGO electrospun samples on the growth of *S.aureus* and *E.coli* after 24 h *in-vitro*, respectively. In Fig. 5.10, for the control samples, no zone of inhibition was present. Upon removal of the control samples from the surface of the agar, the contact zone between the sample and the agar presented heavy bacterial growth. This would be expected, given that no MGO was present.

The effect of MGO concentration on the growth of each bacterial species can clearly be seen in Fig. 5.11 and further confirms that MGO is the sole agent responsible for antibacterial activity. No zone of inhibition was apparent for an MGO concentration at 0.75 mg cm^{-2} for both *S.aureus* and *E.coli*, and slight bacterial growth was observed under the sample, showing a limited antibacterial efficiency (Table 5.5). At a concentration of 1.50 mg cm^{-2} a small mean zone of inhibition measuring 1 mm for both *S.aureus* and *E.coli* was apparent. Upon removal of the sample from the agar no growth was observed, showing a good antibacterial effect. In this case it can be assumed that the minimum concentration required to have an antibacterial effect against *S.aureus* and *E.coli* is 1.50 mg cm^{-2}. However, there may be a point between a spinning time of 0.5 h and 1 h, where the concentration of MGO (mg cm^{-2}) becomes great enough to initiate the development of a zone of inhibition or all bacteria is inhibited under the sample, further work would need to be carried out to determine this.

A previous study which evaluated the antibacterial activity of MGO in liquid and hydrogel form reported concentrations between 1.25 mg ml^{-1} (0.14 mg cm^{-2}) and 15 mg ml^{-1} (1.72 mg cm^{-2}) were found to have an antibacterial effect against *S.aureus* and multi-resistant *S. epidermidis* (*MRSE*) respectively. At the lower concentration of 0.14 mg cm^{-2} a zone of inhibition measuring approximately 20 mm for *S.aureus* and 16 mm for *MRSE* were recorded. While at the higher concentration of 1.72 mg cm^{-2} a larger zone of inhibition was observed at 40 mm for both strains (45). The concentration of MGO in the liquid or gels shows that for a concentration of approximately one-tenth (0.14 mg cm^{-2}) than that present in the PVA/MGO fibre webs (1.50 mg cm^{-2}) a zone of inhibition 16 to 20 times the size can be achieved. This difference can be attributed to the initial encapsulation of MGO within the fibre, which is not freely available on direct contact with the bacteria, as it is in a liquid or gel state.

On contact with the agar, the PVA fibres are shown to form a gel, which then prompts the diffusion of MGO from the fibres into the surrounding bacterial strain, preventing bacterial growth (290). In accordance with a previous study in which the concentration of MGO in liquid form required to inhibit *S.aureus* was found to be 0.14 mg cm^{-2} (45), the concentration of MGO identified in section 4.2.4.2 on the coated nonwoven samples was similar with a concentration of 0.1 mg cm^{-2} for *S.aureus*. In both these cases the synthetic MGO is not restricted by the initial encapsulation within a fibre, as it is in the needle electrospun PVA fibres, and as such a relatively lower concentration of MGO is required to inhibit the bacteria.

Table 5.5:Effect of MGO concentration (mg cm^{-2}), in the PVA/MGO needle electrospun webs, on the growth of *E.coli* and *S.aureus*.

MGO concentration (mg cm^{-2})	Mean inhibition zone (mm)	Growth under sample	Assessment
E.coli			
0.75	0.00	Slight	Limit of efficiency
1.50	1.00	No growth	Good effect
3.00	2.75	No growth	Good effect
4.50	6.50	No growth	Good effect
6.00	9.00	No growth	Good effect
S.aureus			
0.75	0.00	Slight	Limit of efficiency
1.50	1.00	No growth	Good effect
3.00	4.25	No growth	Good effect
4.50	6.25	No growth	Good effect
6.00	7.75	No growth	Good effect

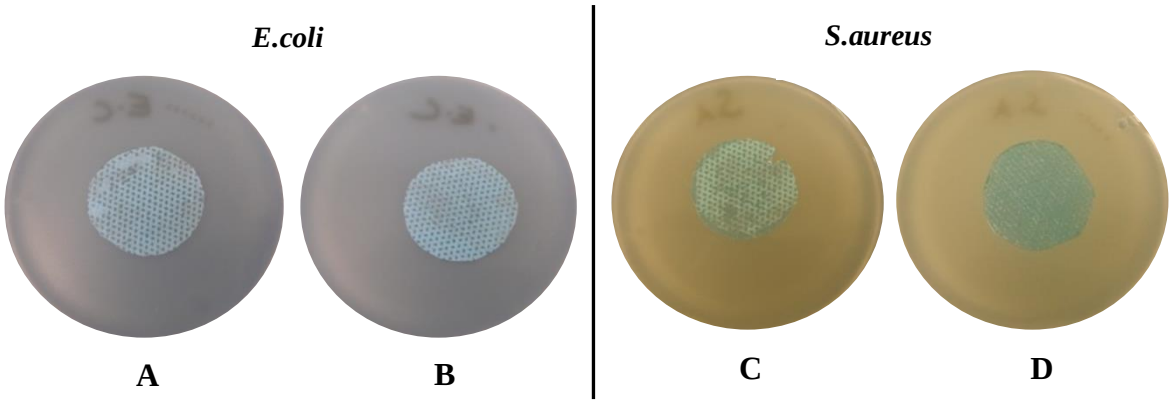

Figure 5.10: Effect of control samples on the growth of *E.coli*; A = PVA/SPB, B = SPB & *S.aureus*; C = PVA/SPB and D = SPB.

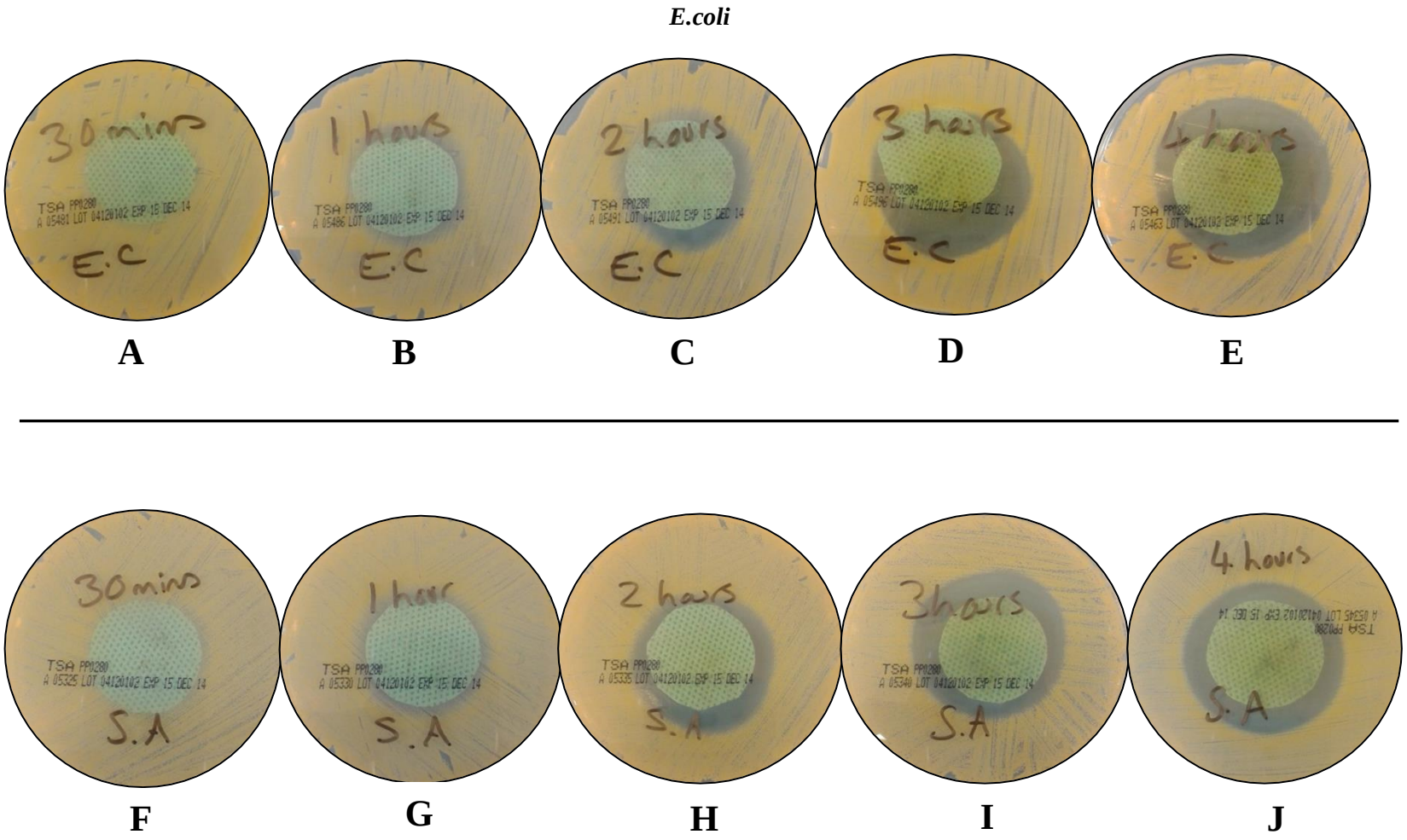

Figure 5.11: The effect of MGO concentration in the PVA/MGO fibres on the growth of *E.coli* and *S.aureus* after electrospinning for 0.5 h (A & F), 1 h (B & G), 2 h (C & H), 3 h (D & I) and 4 h (E & J).

5.4 Summary

It has been established that an 11.22 wt % MGO concentration with a 16% (w/v) PVA concentration was most favourable for producing smooth fibres free from defects. The smallest mean fibre diameter of 157 nm with the lowest standard deviation of 31 nm was achieved with a distance of 15 cm and a voltage of 15 kV on an aluminium foil collector. The successful encapsulation of MGO within the PVA fibres was confirmed using both FTIR and ^{1}H-NMR, which highlighted the carbonyl groups associated with MGO's keto-aldeyde groups. The presence of MGO was further confirmed by the evident antibacterial performance when compared with two control samples free from MGO, which showed no antibacterial effect. The antibacterial evaluations also confirmed that a minimum MGO concentration of 1.50 mg cm^{-2} was required to provide a bactericidal effect against both *S.aureus* and *E.coli in-vitro*. This concentration was substantially higher than that required on coated nonwovens to produce an antibacterial effect, where concentrations between 0.0170 mg cm^{-2} and 0.1 mg cm^{-2} of MGO were needed to inhibit *E.coli* and *S.aureus* respectively. The higher concentration of 1.50 mg cm^{-2} can be attributed to the encapsulation of MGO within the PVA fibres and the slower diffusion rate into the agar.

Chapter 6 Properties of Free Surface (Needleless) Electrospun Fibres Containing Poly(vinyl alcohol) and Synthetic Methylglyoxal

6.1 Introduction

In Chapter 5 the production of poly(vinyl alcohol) (PVA)/ methylglyoxal (MGO) fibres was successfully carried out via needle electrospinning. However, this method of electrospinning has some limitations if the intended purpose is to upscale the production of electrospun webs for commercial use. As reported in sections 2.8.1 and 2.8.2, free surface (needleless) electrospinning is available on an industrial scale. In this form of spinning, no needles are required and multiple electrostatic jets are produced along the surface of a rotating electrode immersed within a polymer bath (264). The advantage of this method is the continuous production of electrospun webs, potentially up to 50 million m^2 per year using PVA (348).

Although both needle and free surface (needleless) electrospinning exploit the same mechanism for stretching the jet, the mode of spinning is quite different and it cannot be assumed that spinning solutions can be easily interchanged between the two methods. Accordingly, the aim of this chapter was to explore and determine the feasibility of electrospinning commixed PVA and synthetic MGO using free surface electrospinning. As previously identified in Chapter 5, the optimisation and development of PVA/MGO fibres, via needle electrospinning was successfully established with a spinning solution containing 16% (w/v) PVA in a synthetic MGO aqueous solution (11.22 wt %). At these concentrations, fibres free from defects were obtained and the antibacterial properties of the PVA/MGO fibres were confirmed using BS EN ISO 20645:2004. Previous studies, which have explored the spinning ability of PVA in distilled water using free surface needle electrospinning have found that lower polymer concentrations between 6% (w/v) and 11% (w/v) have successfully produced fibres free from beads (266, 349). It was therefore of interest to determine if an 8% (w/v) PVA solution in 11.22 wt % MGO could form fibres free from defects, when using free surface electrospinning. Higher PVA concentrations of 16% (w/v) and 20% (w/v) in an 11.22 wt % aqueous MGO solution were also considered. The machine employed during these experiments was an Elmarco NS Lab (section 3.2.4.2). Two different collector substrates, an aluminium foil and a polypropylene spunbond (SPB) were used to collect the electrospun webs; this is to determine if the collector had any effect on the fibre morphology. Fourier transform infra-red spectroscopy (FTIR) and proton nuclear magnetic resonance (^{1}H-NMR) were employed to determine the presence of MGO within the spun webs. The antibacterial activity of the spun webs was determined by means of BS EN ISO 20645: 2004.

6.1.1 Preparation of PVA/MGO solutions for free surface (needleless) electrospinning

8% (w/v), 16% (w/v) and 20% (w/v) PVA (31-50,000 Mw) solutions in synthetic MGO (11.22 wt % aqueous solution) were prepared for spinning. Thus, a wide range of PVA concentrations were studied. The prepared solutions were kept under constant agitation, at 80ºC ± 2ºC for 24 h in a glass conical flask, sealed with a glass stopper. After 24 h all the PVA had dissolved and the solutions appeared clear.

6.1.2 Free surface electrospinning

Free surface electrospinning was performed using an Elmarco Nanospider NS LAB. A detailed description of this procedure is outlined in section 3.2.4.2. After initial investigation with both the roller and wire cylindrical electrode, it was found that the wire cylindrical electrode produced an even distribution of electrospinning jets, when compared to the roller electrode where, limited jet formation was observed. Therefore the wire cylindrical electrode was chosen for the following experiments and set to run at a speed of 6.0 r min^{-1}. During the initial investigation, it was also found that a voltage below 65 kV was unable to produce stable jet formation and therefore higher voltages between 65 kV and 75 kV were employed. Aluminium foil and SPB were used separately to collect the spun webs. Distances of 163 mm, 173 mm and 183 mm between the collector and the spinning electrode were applied. These calculated distances were obtained based on the following equation (350):

Eq.6.1

$$\text{Distance between collector and electrode} = Y + 13$$

where

Y is the height displayed on the collection head ruler (mm)

6.2 Results and Discussion

6.2.1 Free surface (needleless) electrospinning performance

A summary of the free-surface electrospinning performance of each polymer solution is given in Table 6.1.

Table 6.1: Summary of free surface electrospinning performance.

Solvent	MGO concentration (wt %)	PVA concentration (% w/v)	Electrospinning performance	Behaviour of polymer solutions
40 wt % MGO (aqueous solution) diluted with distilled water	11.22	8	Beads	Intermittent burst of polymer rising from the electrode/ some wet polymer on the collectors
		16	Fibres and beads	Consistent polymer jets rising from the electrode/dry polymer web on the collectors
		20	Fibres	Consistent polymer jets rising from the electrode/dry polymer web on the collectors

Initial SEM micrographs were taken using a Jeol JSM-6610LV at a magnification of 2500 in order to assess the morphological features of the electrospun webs collected on the foil and SPB substrates, as shown in Fig. 6.1.

For samples spun with 8% (w/v) PVA solution, the SEM micrographs showed that only beads were formed in the electrospun webs on both the foil and SPB collector, see Fig. 6.1A and Fig. 6.1B respectively. During spinning it was noted that the material landing upon the collector was still wet at voltages between 65 kV and 75 kV and distances from 163 mm to 183 mm. This finding is expected, given that wet material was also observed upon the aluminium foil during needle electrospinning at the same concentration, resulting in merging areas which formed junctions within the web. However, previous papers that have explored the free surface electrospinning of PVA, have reported that concentrations of PVA between 6% (w/v) and 11% (w/v) produced fibres free from defects in a distilled water solution (266, 349).

Notably, one study by Sinah et al. (349) did not report the molecular weight of the PVA used, and so no direct comparison can be made. In another study, the molecular weight was reported to be 72,000 (266). It has been previously documented that, for different molecular weights, a minimum polymer concentration is required to stabilise the electrospinning jets (242, 351). As the molecular weight of PVA in this experiment was 31-50,000, a relatively low concentration of 8% (w/v) provided insufficient chain entanglement to prevent the breakup of the polymer jet,

resulting in wet material forming upon both substrates which lead to the formation of beads. However, in the study where a 72,000 Mw was used, an 8% (w/v) PVA concentration provided sufficient entanglement between the polymer chains to avoid the breakup of the electrospinning jets (266).

In the present work, as the PVA concentration was increased to 16% (w/v), the morphology of the fibres in the spun webs improved, such that fibres together with some beads were formed on both the foil and SPB substrates, as seen in Fig. 6.1C and 6.1D respectively. Similar to the findings obtained for fibres produced via needle electrospinning, as the concentration of PVA was doubled from 8% (w/v) to 16% (w/v), the viscosity increased (section 5.1.4.1, Fig.5.2) and the polymer chain entanglement became sufficient to prevent the breakup of the electrically charged jet. When compared to the morphology of the fibres produced at a 16% (w/v) PVA concentration using needle electrospinning over a series of voltages between 7 kV and 18 kV and distances between 5 cm to 15 cm, no beads appeared (section 5.1.4.1, Fig. 5.6). However when using free surface electrospinning, some beads were apparent. Notably, the voltages used with free surface electrospinning were necessarily higher (65 kV to 75 kV) when compared with needle electrospinning (7 kV to 18 kV) to ensure continuous spinning could be maintained. This substantial increase in voltage can be expected to heighten the electrostatic field, leading to instabilities in the electrospinning jets, which has been reported to lead to an increase in bead formation (268, 276). It is also known that an increase in voltage can reduce the flight time of the polymer jets to the collector. This results in insufficient crystallisation in the fibre as the molecular chains have less time to align themselves before reaching the collector (352).

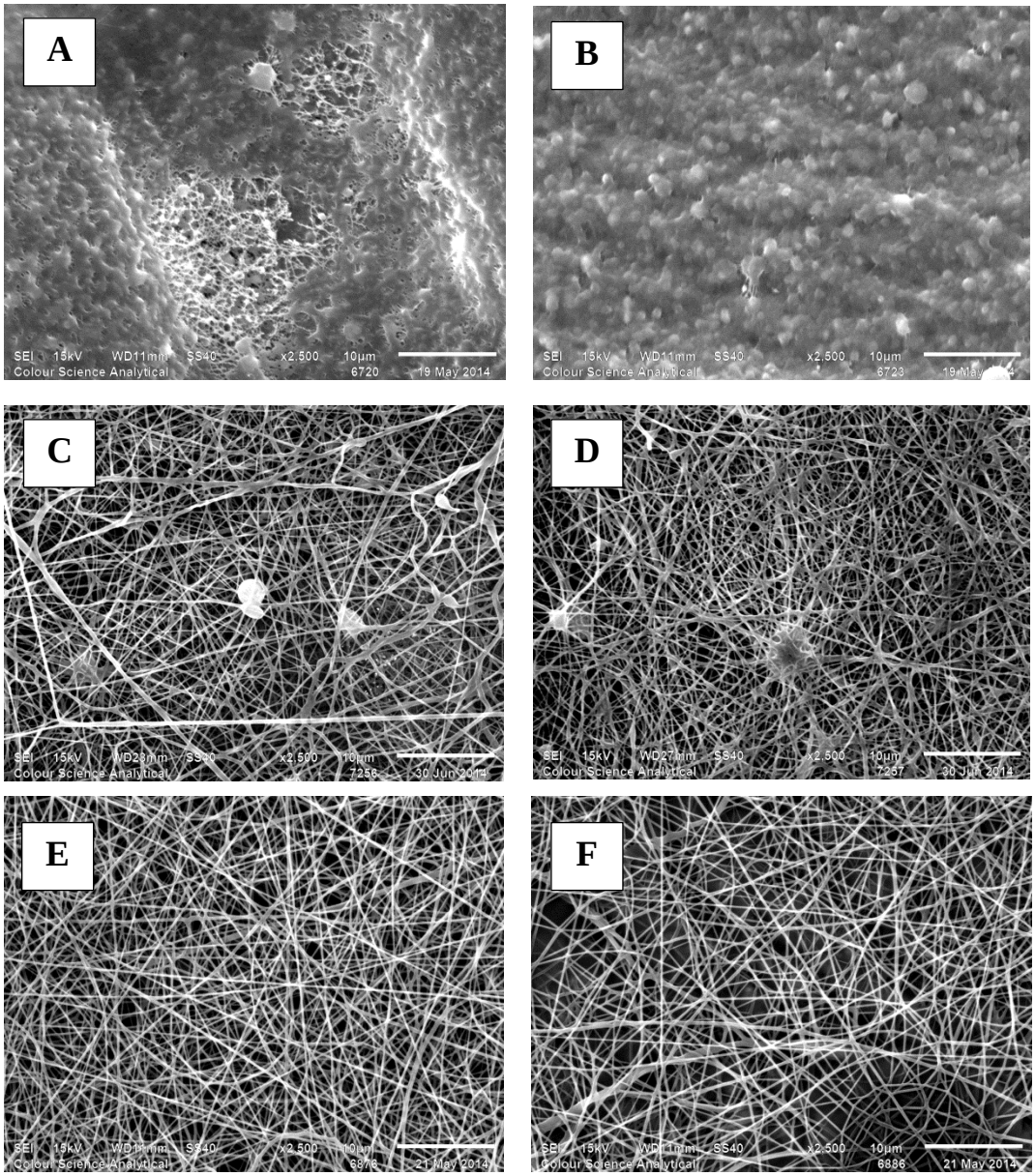

Figure 6.1: SEM micrographs of free surface (needleless) electrospun webs produced from different PVA concentrations on aluminium foil and SPB substrates. A & B = 8% (w/v) PVA on foil and SPB respectively, C & D = 16% (w/v) PVA on foil and SPB respectively and E & F = 20 % (w/v) on foil and SPB respectively.

Owing to the formation of some beads at a 16% (w/v) PVA concentration, a 20% (w/v) PVA solution was also prepared, with the intention of eliminating any beads in the web due to the increase in viscosity (2634 cP, as seen in section 5.1.4.1, Fig.5.2). Fig. 6.1E and 6.1F present micrographs of the morphology of the fibres produced at a 20% (w/v) PVA concentration on the foil and SPB substrates respectively. No beads were observed on either substrate. Interestingly, when the viscosity of the polymer solutions used in needle electrospinning was increased to 1421 cP and above, as discussed in section 5.1.4.1, the polymer was found to dry at the needle tip and subsequently there was no initiation of an electrospinning jet. A possible explanation as to why such a comparatively high viscosity of 2634 cP was capable of producing fibres using free surface electrospinning, may be due to the constant agitation of the polymer solution (6 r

min^{-1}). The continuous agitation of the fluid allowed the polymer chains to move freely, maintaining the viscoelastic nature of the polymer solution, which can be easily stretched via the electrostatic attraction between rotating electrode and collector.

When using needle electrospinning, the relatively slow flow rate of 0.1 ml hr^{-1} allows only a small volume of polymer solution to be exposed at the needle tip to the ambient conditions. The relatively slow flow rate at the point of electrification of the polymer allowed sufficient time for the solvent to evaporate, allowing the polymer to dry out quickly at the needle tip. However if the flow rate of the polymer from the needle tip was increased, this may give less time for the solvent to evaporate and allow the stretching of the polymer solution to elongate and form fibres on the collector (267).

Notably, after one hour of spinning time when using free surface electrospinning, the 20% (w/v) PVA solution in the polymer bath visually began to thicken as a result of solvent evaporation. This led to infrequent and intermittent formation of the polymer jets forming along the spinning electrode, at which point free surface electrospinning was inhibited.

In Fig 6.2 and 6.3, the morphology of the fibres produced from a 20% (w/v) PVA concentration over the series of voltages between 65 kV and 75 kV and distances of 163 mm to 183 mm are shown. In all cases, no beads were observed in the collected webs. The mean fibre diameter in each electrospun web produced at different voltages and distances is given in Table 6.2. Examples of the fibre distributions on both collector substrates are given in Fig 6.4.

The smallest mean fibre diameter (155 nm) and lowest standard deviation (35 nm) was achieved on the foil substrate at a voltage of 65 kV and a distance of 183 mm. The mean fibre diameters of the electrospun webs produced on the aluminium foil were all lower than any of the mean diameters fabricated on the SPB substrates. The increased electrical field when using a conductive aluminium foil collector compared with a non-conducting fibrous SPB material may explain this. A conductive collector allows the electrical charges on the fibres to be dissipated, thus allowing an increased electrical field, which may act upon the stretching and elongation of the polymer jet (353). In the case where a non-conductive SPB collector was used, the electrical charges on the polymer jets will accumulate on the non-conducting material and exert a repulsive force on the subsequent fibres landing on the collector. These repulsive forces may be inclined to reduce the stretching of the polymer solution (353, 354) such that there could be an increase in the mean fibre diameter of the collected fibres.

A previous study, which evaluated the morphology of PVA fibres on up to seven different substrates, when using free surface electrospinning, also reported a smaller mean fibre diameter using an aluminium foil substrate when compared to a polypropylene SPB substrate. The previous work related to experiments conducted at a lower voltage (60 kV) and distance (130 mm) (266) compared with that studied herein.

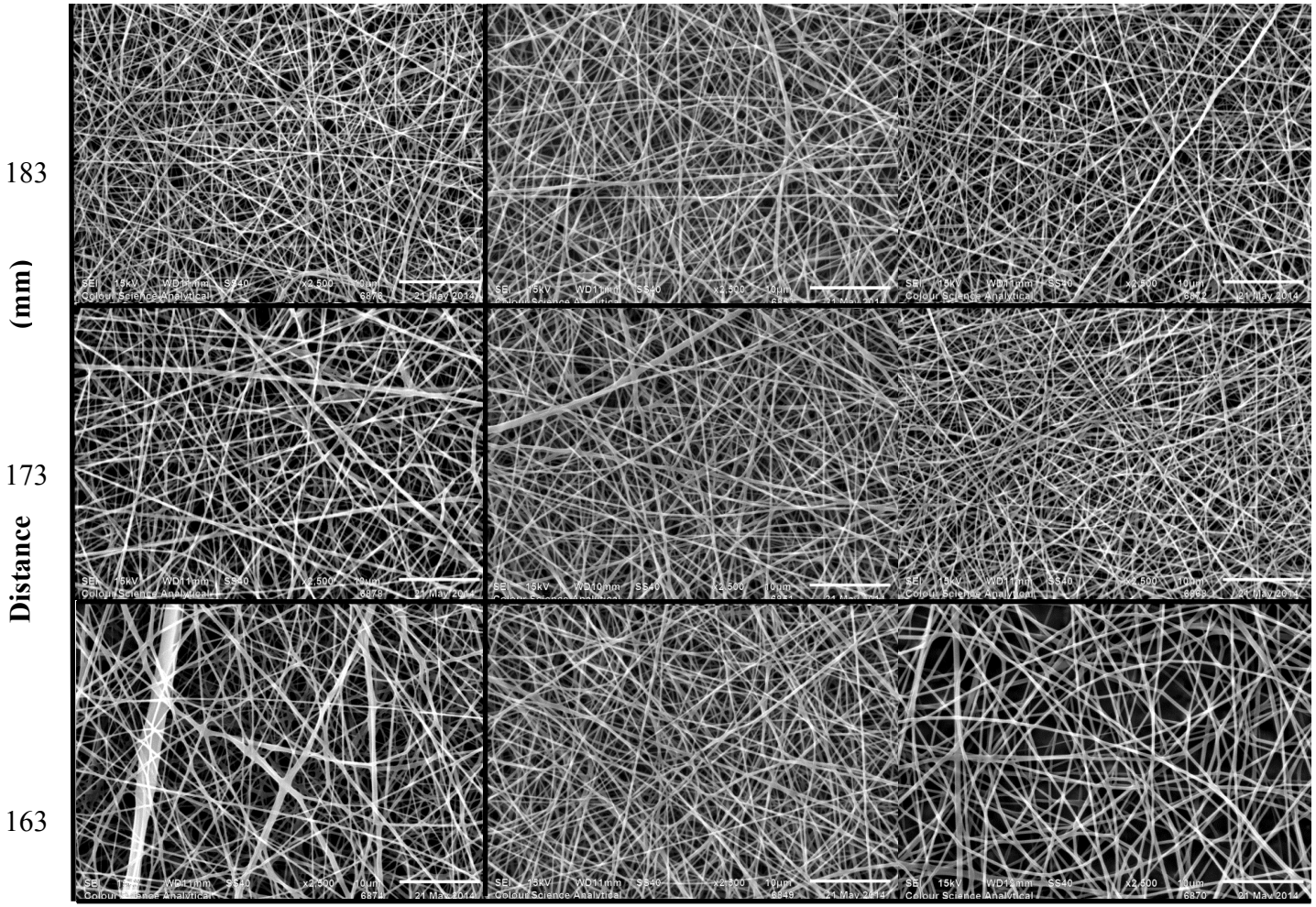

Figure 6.2: SEM micrographs of free surface (needleless) electrospun webs produced on an aluminium foil substrate from a 20% (w/v) PVA concentration over a series of voltages and distances.

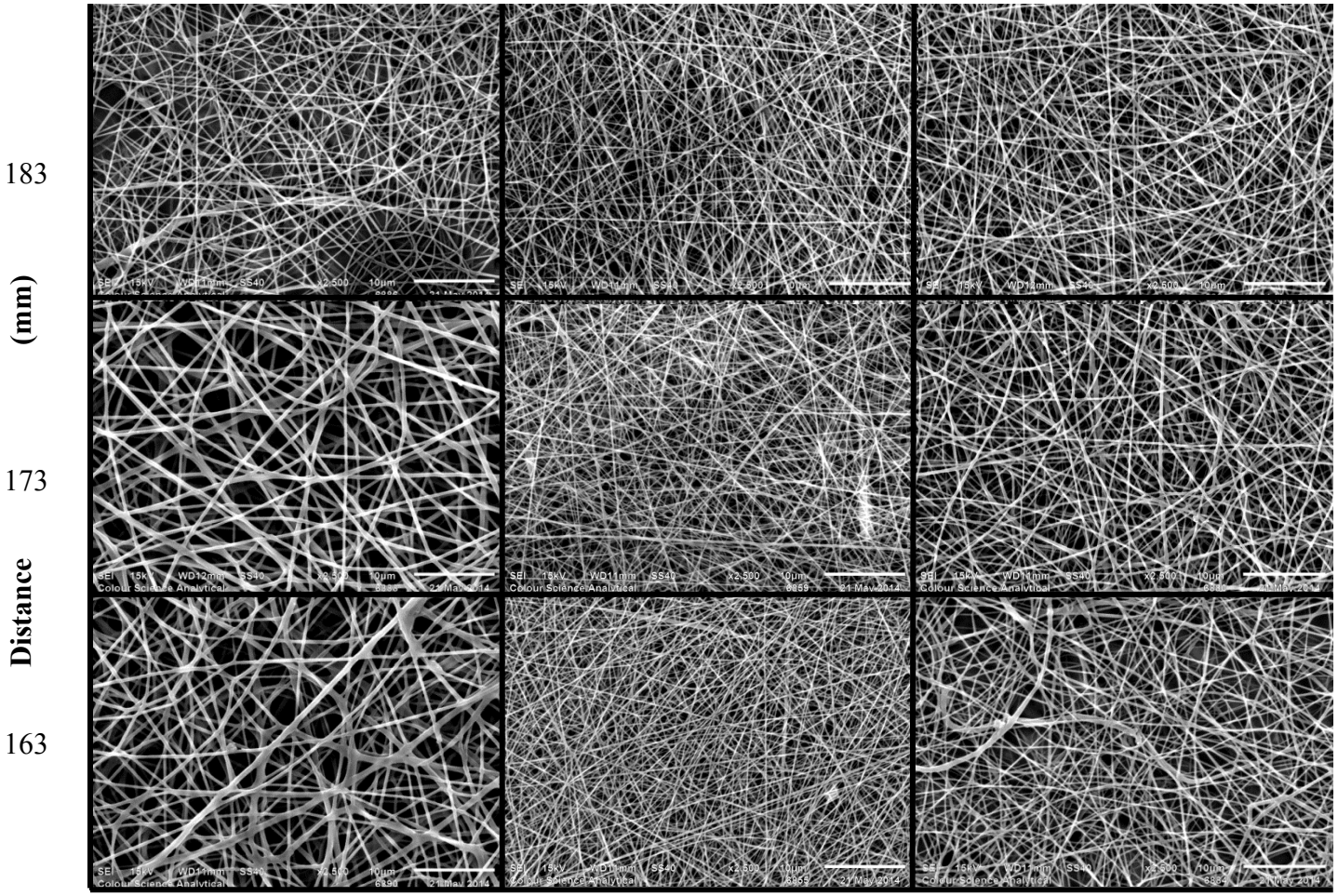

Figure 6.3: SEM micrographs of free surface electrospun webs on a SPB substrate from a 20% (w/v) PVA concentration over a series of voltages and distances.

Table 6.2: Mean fibre diameters and standard deviation (nm) of electrospun webs produced on both an aluminium foil and SPB substrate from a 20% (w/v) PVA concentration, over a series of voltages (kV) and distances (mm).

Substrate	Aluminium foil			Spunbond		
Voltage (kV)	**65**			**65**		
Distance (mm)	**163**	**173**	**183**	**163**	**173**	**183**
Mean (nm)	211	195	155	402	427	219
STD (nm)	93	66	35	160	131	113
Voltage (kV)	**70**			**70**		
Distance (mm)	**163**	**173**	**183**	**163**	**173**	**183**
Mean (nm)	161	172	175	226	247	239
STD (nm)	47.3	50.1	47.0	77.6	87.1	60.2
Voltage (kV)	**75**			**75**		
Distance (mm)	**163**	**173**	**183**	**163**	**173**	**183**
Mean (nm)	249	161	167	251	242	226
STD (nm)	74	47	61	107	81	57

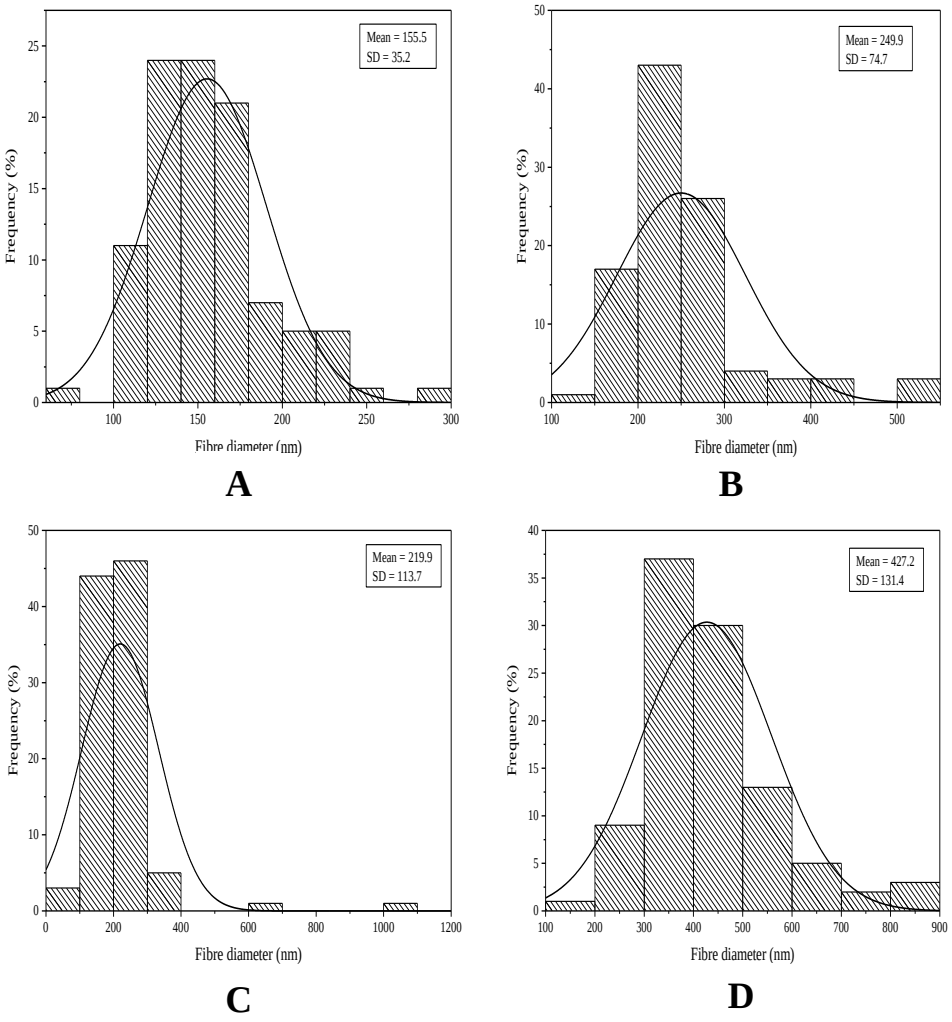

Figure 6.4: Examples of the fibre diameter distributions and mean fibre diameters and standard deviations (nm) of the free surface electrospun fibres on the aluminium foil and SPB substrates, produced from a 20% (w/v) PVA solution. A = 65 kV, 183 mm Foil, B = 75 kV, 163mm Foil, C = 65kV, 183mm SPB & D = 65kV 173mm SPB.

6.2.2 Identification of MGO in the free surface (needleless) electrospun PVA/MGO fibres

Both Fourier transform infra-red spectroscopy (FTIR) and proton nuclear magnetic resonance (^{1}H-NMR) were employed to determine the presence of MGO within the PVA/MGO fibres, as described in sections 3.2.6 and 3.2.7 respectively. Electrospun fibres produced from a spinning solution with a concentration of 20% (w/v) PVA in an 11.22 wt % synthetic MGO solution were assessed to verify the presence of MGO within the fibres after free surface electrospinning. The electrospun webs were produced at a voltage of 65 kV and a distance of 183 mm on an aluminium foil substrate, using a wire cylindrical electrode at a speed of 6.0 r min^{-1}, as these parameters were previously found to produce the smallest mean fibre diameter.

6.2.2.1 Identification of MGO using Fourier transform infra-red spectroscopy (FTIR)

Fig 6.5 displays the FTIR results obtained for the free surface (needleless) electrospun PVA/MGO fibres. As previously reported in section 5.2.1 the detection of MGO in the needle electrospun fibres was shown to have two small peaks which could be attributed to the two distinct carbonyl groups in MGO, a ketone and an aldehyde group. In Fig. 6.5 the detection of these two small peaks was also observed. A peak at 1717 cm^{-1} is attributed to the C=O stretching vibration in the aldehyde carbonyl and the small peak at 1345 can be assigned to CH_3 bending in the methyl group of MGO (275). The larger peaks in the spectra are attributed to the PVA. The broad band centred at 3410 cm^{-1} is due to hydrogen-bonded O–H stretching vibration and the peak at 2929 cm^{-1} is attributed to C–H stretching in the polymer backbone. The peak at 1438 cm^{-1} is the result of in-plane O–H bending, while the peak at 1094 cm^{-1} is indicative of C–O stretching.

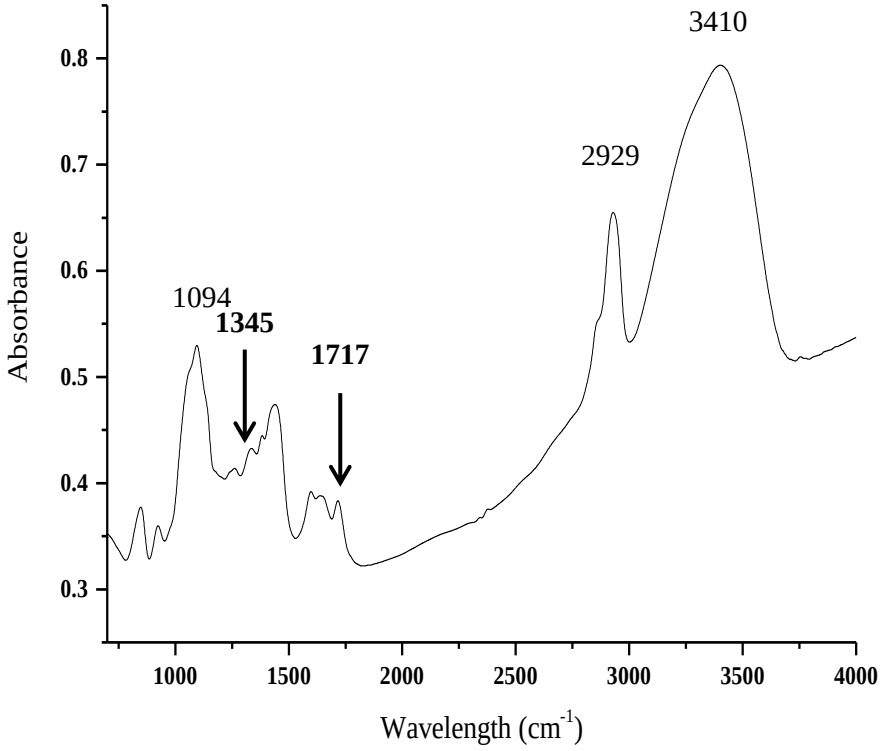

Figure 6.5: FTIR spectra of the free surface (needleless) electrospun PVA/MGO webs ground into KBr pellets and measured with 16 repeat scans.

6.2.2.2 Identification of MGO using proton nuclear magnetic resonance (^{1}H-NMR)

Fig 6.6 displays the ^{1}H-NMR spectra obtained. As previously reported in section 5.2.2 (Fig 5.9A) the chemical formulas of MGO, MGO mono-hydrate and di-hydrate are shown. The hydrogen protons, which are detectable for each chemical formula are indicated. In Fig. 6.6, the two singlet peaks at 1.335 ppm and 2.144 ppm can be assigned to the methyl protons present in the MGO di-hydrate and monohydrate respectively. The peak observed at 4.998 ppm is attributed to the alkyl proton of MGO monohydrate. The resonance peaks observed at 1.560 ppm and 3.886 ppm can be assigned to the protons of CH_2 and the CH proton of the PVA respectively (347). This data gives further confirmation that MGO was encapsulated within the free surface electrospun PVA fibres, with solvent evaporation having a limited effect.

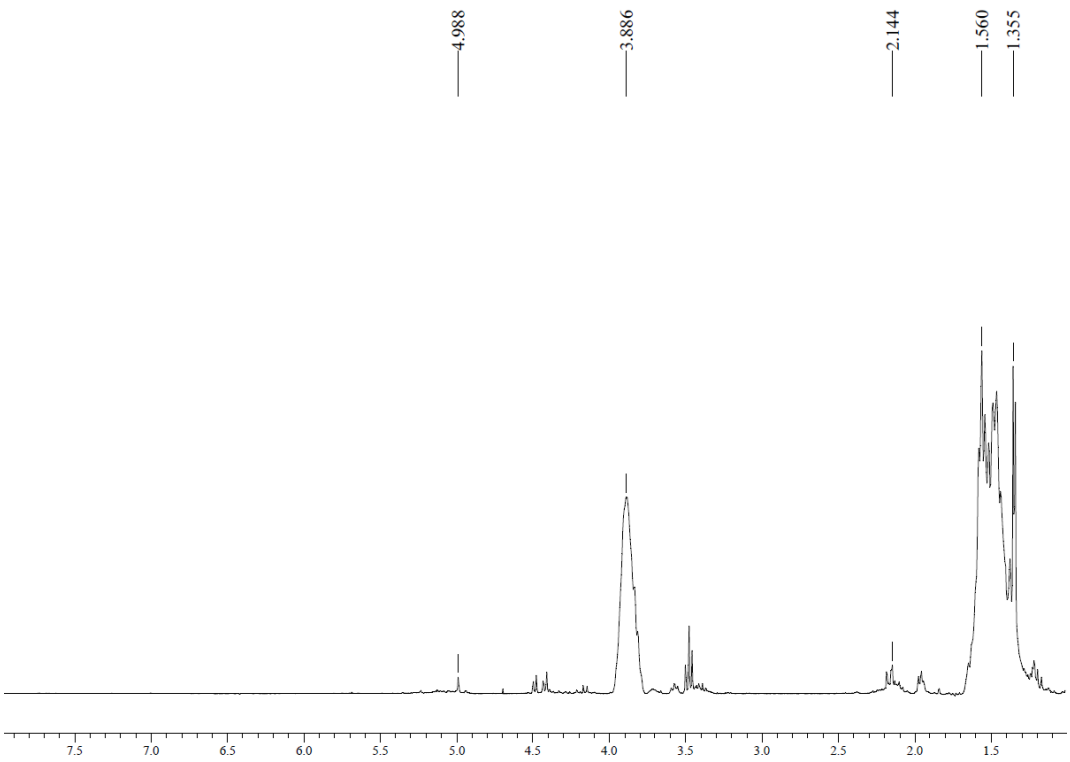

Figure 6.6: ^{1}H-NMR spectra's of PVA/MGO free surface (needleless) electrospun webs dissolved in 1ml of deuterium oxide (99.9 % atom) recorded with 1024 repetitions

6.2.3 Antibacterial Evaluation of PVA/MGO fibres

6.2.3.1 Free surface (needleless) electrospinning and calculated mass of MGO

PVA/MGO fibres were prepared for antibacterial testing via free surface (needleless) electrospinning. An electrospinning solution containing 20% (w/v) PVA in an 11.22 wt % synthetic MGO solution was prepared. The electrospinning solution was spun onto an aluminium foil substrate at a voltage of 65 kV and a distance of 183 mm using a wire cylindrical electrode, as these parameters were previously found to provide the smallest mean fibre diameter. To determine the minimum concentration of MGO required to produce an antibacterial effect, free surface electrospinning was carried out for various lengths of time between 2.5 and 30 min. Similar to the results found in section 5.1.8, it was expected that as the spinning time was increased, there would be an increase in the amount of MGO available within the spun web. However, as there is no control over the flow rate or the amount of jets produced along the spinning electrode, the weight of the spun webs was recorded after spinning. Initial experiments revealed that with an increasing spinning time, the weight of the spun webs did not increase proportionally. This may be due to the variable amount of electrospinning jets forming along the wire electrode during spinning, resulting in variable deposition of fibres on the collector. Therefore, electrospun samples were prepared with an increasing collected weight

from 10 mg to 150 mg. To determine the mass of MGO in the spun webs, a calculation was made using the initial ratio of PVA and MGO in the spinning solution as follows:

Eq. 6.2

$$Mass\ of\ MGO\ in\ spun\ web = Mass\ of\ sample \times R_{MGO}$$

where R_{MGO} is the ratio of MGO to MGO + PVA in the spinning solution, which in this experiment was 0.369.

In order to validate this assumption, three PVA/MGO webs produced via free surface electrospinning were dispersed in distilled water at 37ºC for 30 min, 3 days and 1 week. The samples were shown to disintegrate on direct contact with the water, due to the poor stability of PVA without the addition of any crosslinking. Therefore, it was of interest to understand if all the MGO was released instantaneously with no change over 1 week. Measurements of the water containing the dispersed PVA/MGO were assessed using reverse phase high performance liquid chromatography (RV- HPLC), as described in section 3.2.9 to determine the mass of MGO in each sample and can be seen in Table 6.3. The amount of MGO released from the electrospun webs was found to be 93.7% of that assumed from *Eq. 6.2*. The reason for this may be that some of the MGO remained in the spinning bath or that not all of the MGO was released from the fibres during dispersion. Based on this result the mass of MGO available for release, in an aqueous environment was calculated using *Eq. 6.3.* It should be noted that this equation is probably only valid for samples with the exact spinning specifications outlined in section 6.2.3.1.

Table 6.3: Amount of MGO released during dispersion test (mg), assessed via HPLC.

Dispersion time	**Weight of spun web (mg)**	**Calculated Mass of MGO in fibres based on *Eq. 6.2* (mg)**	**Mass of MGO found in dispersion test (mg)**	**Proportion of MGO found by HPLC compared to *Eq. 6.2***
30 min	173.00	63.85	59.8	0.937
3 days	154.00	56.84	51.3	0.903
1 week	67.20	24.80	24.1	0.972
			Mean	**0.937**

Eq.6.3

$$Mass\ of\ MGO\ available\ in\ spun\ web = Mass\ of\ sample \times R_{MGO} \times 0.937$$

6.2.3.2 Sample preparation for antibacterial testing

The delicate and frail nature of the electrospun webs prepared in section 6.2.3.1, presented a difficult task when preparing the samples to the same diameter in each case. A circular tube with a diameter of 20 mm was used to prepare the samples. All samples were prepared in line with the standards specifications of 25 ± 5 mm diameters, with the exception of one, which had a mean diameter of 32 mm. This was due to the fibrous webs overhang after removal of the tube. Four measurements were taken across the diameter of each sample to determine the mean diameter. From the mean diameter, the area of the sample was established. Based on the sample area and *Eq. 6.3,* the concentration of MGO per unit area (mg cm^{-2}) was calculated and can be seen in Table 6.4.

Table 6.4: Calculated mass of MGO in the spun webs (mg) and the concentration of MGO per unit area (mg cm^{-2}) for the samples tested against *E.coli* and *S.aureus*.

Weight of spun web (mg)	Mass of MGO in the spun web (mg)	Mean sample diameter (mm)	Concentration of MGO (mg cm^{-2})
E.coli			
10	3.46	26.0	0.65
20	6.92	25.0	1.41
50	17.29	24.0	3.82
100	34.58	29.0	5.24
150	51.87	30.0	7.34
S.aureus			
10	3.46	23.0	0.83
20	6.92	20.0	2.20
50	17.29	28.5	2.71
100	34.58	32.0	4.30
150	51.87	30.0	7.34

6.2.4 Results of Antibacterial testing

Table 6.5 displays the results achieved for the PVA/MGO webs tested against *E.coli* and *S.aureus*. The zones of inhibition and the effect of the sample on the growth of each bacteria species as per the standard requirements are shown. Fig 6.7 shows a visual representation of the PVA/MGO samples on the growth of *E.coli* and *S.aureus* after 24 h *in-vitro*. The dotted black line indicates the original mean sample size before testing. In all cases the PVA/MGO samples have decreased in size during the test, as seen in Fig. 6.7. This occurrence can be explained by the hydrophilic nature of the PVA fibres (65, 355). During incubation at 37ºC the fibres would have absorbed any moisture available from the agar and the surrounding environment, forming a hydrogel, which was then dissolved into the agar, releasing the MGO.

In Fig. 6.7A, 6.7E & 6.7F, where the concentration of MGO ranged from 1.41 mg cm^{-2} to 2.71 mg cm^{-2}, the original mean diameter of the sample was found to be slightly larger than the zone created by the shrunken hydrogel PVA/MGO fibres. In these cases no zone of inhibition was actually formed and is referred to here as zero in Table 6.5. However it is still apparent that the growth of bacteria was inhibited where the original sample was laid and no growth was observed upon removal of the remaining sample from the agar. In accordance with the standard requirements, a good antibacterial effect was still achieved at concentrations between 1.14 mg cm^{-2} to 2.71 mg cm^{-2}.

At MGO concentrations between 0.65 mg cm^{-2} and 0.83 mg cm^{-2} the majority of the sample had dissolved and moderate to heavy growth was apparent upon removal of the samples from the agar. In all other cases where the concentration was 3.92 mg cm^{-2} or above, a zone of inhibition was apparent. Upon removal of these samples from the agar, no growth was observed and a good antibacterial effect was achieved.

Table 6.5: Effect of MGO concentration (mg cm^{-2}), in the free surface (needleless) electrospun webs on the growth of *E.coli* and *S.aureus*.

MGO concentration (mg cm^2)	Mean inhibition zone (mm)	Growth under sample	Assessment
E.coli			
0.65	0	Moderate	Insufficient
1.41	0*[1]	No growth	Good effect
3.82	0.63	No growth	Good effect
5.24	2.25	No growth	Good effect
7.34	3.25	No growth	Good effect
S.aureus			
0.83	0	Slight to moderate	Insufficient
2.20	0*[1]	No growth	Good effect
2.71	0*[1]	No growth	Good effect
4.30	1.25	No growth	Good effect
7.34	2.00	No growth	Good effect

*[1] The absence of growth, even without an inhibition zone, may be regarded as a good effect, as the formation of such an inhibition zone may have been prevented by a low diffusion of the active substance (315). However, in this case the original sample size was larger than the apparent zone of inhibition, indicated by the dotted lines in Fig.6.7.

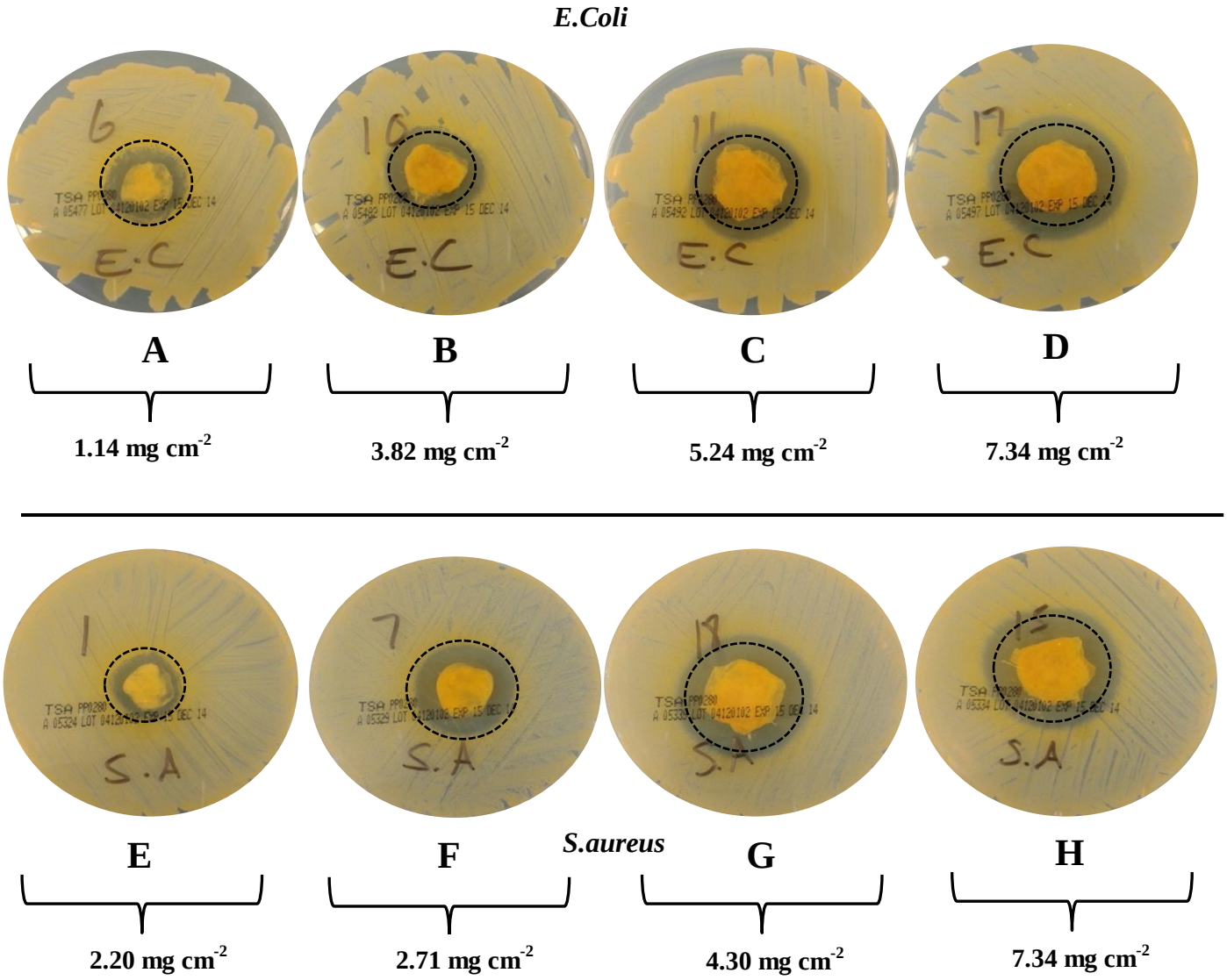

Figure 6.7: The effect of MGO concentration (mg cm^{-2}) on the growth of *E.coli* (A to D) and *S.aureus* (E to H). The dotted lines indicate the original sample size before incubation for 24 h.

6.2.5 Comparison between needle and free surface electrospinning

When comparing the electrospinning ability of PVA/MGO webs using needle and free surface (needleless) electrospinng techniques, it was found that different conditions were required to initiate the formation of electrospinning jets and produce fibres of differing morphology. Table 6.6 shows the parameters required for each electrospinning technique to produce fibres with the smallest mean fibre diameter.

A range of synthetic MGO solution concentrations between 40 wt % 11.22 wt %, with varying PVA concentrations between 8% (w/v) and 16% (w/v) were initially prepared and trialled using needle electrospinning. It was found that an 11.22 wt % MGO solution and a PVA concentration of 16% (w/v) were favoured for producing fibres free from beads. At lower PVA concentrations of 8% (w/v) and 12% (w/v), wet polymer was shown to land upon the collector, resulting in merging fibres. In contrast, a larger PVA concentration of 20% (w/v) for free surface electrospinning was required to produce fibres free from beads, when compared with 16% (w/v) where beads were observed in the as-spun webs over a series of voltages and distances. The viscosity of the polymer solutions was shown to increase with increasing PVA concentration for all synthetic MGO solutions. At a viscosity of 605 cP, the polymer solution moved freely through the needle at a speed of 0.1 ml h^{-1} and was found to initiate an electrospinning jet, resulting in dry bead free fibres on the collector. At a viscosity of 1421 cP and above, the polymer solution was found to dry at the needle tip and no fibres were formed. However, at a viscosity of 605 cP when using free surface electrospinning, beads were observed in the electrospun webs. At a higher PVA concentration of 20% (w/v) with a viscosity of 2634 cP, no beads were apparent in the free surface electrospun webs. The rotation of the wire electrode during free surface electrospinning, was able to maintain the viscoelastic nature of the polymer solution.

Notably, a larger voltage was used for free surface electrospinning of 65 kV in order to initiate electrospinning jets along the wire electrode, when compared with 15 kV for needle electrospinning, where sparks were shown to occur between the collector and the needle tip at a voltage above 18 kV. This may be attributed to the conductive nature of the bare metal needle tip when compared with the wire electrode, which is immersed in the less conductive polymer solution, allowing greater voltages to be used without sparking.

When using needle electrospinning, distances between the needle and collector showed that an increase in distance resulted in a finer mean fibre diameters for each voltage with the exception of 13 kV. No correlation was found between distance and fibre diameter for free surface electrospinning over a series of voltages. However, at a larger distance of 183 mm and a voltage

of 65 kV, a small mean fibre diameter was achieved when compared with a lower distance of 163 mm at the same voltage.

Table 6.6: Differing parameters required for needle and free surface electrospinning, to produce the smallest mean fibre diameter (nm) on an aluminium foil collector.

Parameters	**Needle electrospinning (smallest mean diameter = 157 nm)**	**Free surface (needleless) electrospinning (smallest mean fibre diameter = 155 nm)**
PVA concentration (% w/v)	16	20
Viscosity (cP)	605	2634
Surface tension mN m^{-1}	45.96	40.43
Conductivity mS cm^{-1}	1.234	1.033
Voltage (kV)	15	65
Distance (mm)	150	183
Flow rate (ml h^{-1})	0.1	n/a
Speed of electrode (r min^{-1})	n/a	6.0

6.3 Summary

In this chapter it was found that a spinning solution containing 16% (w/v) PVA in a synthetic MGO solution with a concentration of 11.22 wt %, produced fibres with some beads via free surface (needleless) electrospinning. When the polymer concentration was increased to 20% (w/v), fibres free from beads were produced over a series of voltages between 65 kV to 75 kV and distances from 163 mm to 183 mm. The smallest mean fibre diameters were found in all cases when using the aluminium foil substrate. The lowest mean fibre diameter of 155 nm and standard deviation of 35 nm was achieved at a voltage of 65 kV and distance of 183 mm. The presence of MGO within the PVA fibres was confirmed using both FTIR and ^{1}H-NMR. The antibacterial study revealed that MGO concentrations between 0.65 mg cm^{-2} and 0.83 mg cm^{-2} were unable to inhibit the growth of *E.coli* and *S.aureus* and slight to moderate bacteria growth was observed, resulting in limited antibacterial efficiency. As the MGO concentration was increased to 1.14 mg cm^{-2} and above, the bacteria growth under the samples was inhibited and a good antibacterial effect was achieved. This result also corresponds with the findings of the antibacterial work in section 5.3.2, where a similar MGO concentration of 1.50 mg cm^{-2} and above was found to inhibit the growth of bacteria. At a lower concentration of 0.75 mg cm^{-2}, slight bacteria growth was observed with a limited antibacterial efficiency.

Chapter 7 Effect of Crosslinking with Glutaraldehyde on the Release of Methylglyoxal from PVA/MGO Fibres

7.1 Introduction

The release behaviour and kinetics of other antibacterial agents or drugs, from electrospun PVA fibres or hydrogels, has been explored in numerous studies as previously discussed in sections 2.7.1.3 and 2.8.4.2. Although PVA is able to form a hydrogel upon contact with fluid, its ability to retain rigidity in water remains poor, as previously shown in section 6.2.3.1. Consequently, all of the encapsulated MGO was quickly released from the PVA/MGO webs into the water at 37ºC within the first 30 min, with no change in the amount of MGO detected over a period of one week. To overcome this problem, crosslinking techniques may be expected to assist in maintaining the fibrous structure as well as delay the release of the antibacterial agent, as discussed in section 2.7.1.3. Of these methods, crosslinking PVA with glutaraldehyde (GA) has been demonstrated to be effective, particularly when using GA in a vapour phase (66, 254), since this reduces the potential for loss of fibre morphology in aqueous conditions.

Additionally, plasma technology may also offer a potential method to provide crosslinks at the PVA fibre surfaces. The plasma technique is described in section 3.2.10. Plasma technology in the textile field has become increasingly popular since the 1980s in many research laboratories around the world, showing encouraging results for the improvement in various functional properties of the fabric. The environmental and energy saving potential of plasma technology has many advantages over wet chemistry based textile processing, where large amounts of water, energy and effluent are used. Therefore plasma technology has the potential to offer many benefits if development to a commercial level is intended (321).

A number of property enhancements can be achieved via plasma treatment, including imparting hydrophilic, hydrophobic or oleophobic properties, increasing adhesion, changing the electronic conductivity, application of antibacterial agents or fire retardants, anti-shrinkage to wool, sterilisation and desizing of cotton. These functions are achieved by the addition or removal of materials or chemistry to or from the intended sample via the plasma treatment. Where something may be added to a textile, activation of the surface energy may be achieved via the introduction of reactive species such as oxygen atoms, which can react with hydrocarbons, leading to the formation of chemicals such as H_2O and CO_2 (322, 356).

Functionalisation of the textile may also be employed via the permanent grafting of functional groups on the surface (356). Finally, a very thin film or coating may also be deposited on the surface by plasma polymerisation. In this case reactive precursor gases that can polymerise can be introduced into the plasma chamber. These gases are broken into radicals that react with each other on the surface of the textile sample (322).

As plasma technology offers the potential to add functionalisation to the surface of a textile, there is a possibility that the introduction of crosslinks on the surface of PVA/MGO electrospun webs may also be achieved by employing a GA gas into the plasma chamber to react with the hydroxyl groups in the PVA.

The aim of this chapter was therefore to investigate the effect of crosslinking PVA with GA vapour and with the aid of plasma, and to alter the release rate of synthetic MGO from the electrospun PVA/MGO webs. Where GA vapour crosslinking was employed, the effect of crosslinking time on the release of MGO over a period of 24 h was investigated for different crosslinking times between 1 h to 48 h.

The swelling behaviour of the GA vapour crosslinked PVA/MGO webs was also investigated. Scanning electron microscopy (SEM) was employed to examine the effect of GA vapour crosslinking on the morphology of the electrospun webs. As a novel technique, a preliminary experimental study using GA plasma treatment on the PVA/MGO webs over a period of 1 h was also introduced as a potential new crosslinking system. FTIR analysis was used to confirm the presence of GA on the surface of PVA/MGO webs after treatment with GA plasma. In both crosslinking systems, the detection of MGO released from the PVA/MGO webs was confirmed by reverse phase-high performance liquid chromatography (RV-HPLC).

7.1.1 Preparation of PVA/MGO electrospun webs

An electrospinning solution containing 20% (w/v) PVA and 11.22 wt % synthetic MGO was prepared as described in section 6.1.1. Free surface (needleless) electrospinning was carried out using an Elmarco Nanospider Lab as described in section 3.2.4.2. A voltage of 65 kV and a distance of 183 mm was utilised. Spinning was carried out for 30 min each time to enable the sufficient build up of fibres on an aluminium foil collector.

7.1.2 Crosslinking of PVA/MGO electrospun webs with GA

Crosslinking of the PVA/MGO electrospun webs was carried out via two methods of crosslinking described below. Prior to crosslinking with each method, all samples were contained within a sealed polythene bag to minimise exposure to variations in ambient moisture. Before the samples were subjected to GA vapour treatment, the sample weight was recorded.

7.1.2.1 GA vapour crosslinking using a desiccator chamber

A 40 ml glass beaker was filled with a 25 wt % GA solution and placed inside the desiccator chamber. The chamber was then sealed with a lubricated lid to provide an air tight environment, and left inside a fume cupboard for 24 h at room temperature. This allowed enough time for the GA vapour to saturate the desiccator chamber. The electrospun webs were then attached to a

metal frame, which was placed inside the desiccator chamber and suspended above the 40 ml beaker of GA. Care was taken to avoid any direct contact between the sample and the GA solution. The desiccator chamber was sealed once again to provide an air tight environment. Separate electrospun webs were left exposed in the saturated chamber for 1, 8, 24 and 48 h. Upon removal of the sample from the desiccator chamber, the sample was placed directly into a vacuum oven at 50ºC for 24 h to remove any unreacted GA and then contained within a sealed polythene bag.

7.1.2.2 GA crosslinking using plasma treatment

Plasma treatment with GA was investigated as a potential new crosslinking mechanism, as described in section 3.2.10. Only preliminary work was carried out via this experimental method due to time constraints in the study. As this was a new technique, preliminary experiments were initially performed to decide upon suitable experimental parameters. These initial parameters and observations are given in Table 7.1.

The initial experiments were done for 1 h. The valve connecting the GA solution with the plasma machine operates in a 10 s time cycle. For the initial experiments (Table 7.1), the valve was opened for 2 s (20 % time on) and closed for 8 s during the 10 s time cycles. After exposure to plasma power levels between 30 W and 150 W for 1 h, the PVA/MGO webs were shown to disintegrate or decrease in weight. This was due to an increase in temperature inside the plasma chamber at the higher power levels, causing the PVA/MGO webs to soften and deteriorate. From these preliminary findings, a power level of 15 W was identified as being suitable to permit further experiments.

Table 7.1: Initial experimental parameters using plasma GA treatment.

Power (W)	Time cycle (s)	Time on (%)	Sample weight prior to plasma treatment (mg)	Sample weight after plasma treatment (mg)	Percentage weight loss (%)	Sample observation after plasma treatment
150	10	20	825.1	n/a	n/a	Complete disintegration
90	10	20	987.4	256.9	73.9	Partial disintegration
30	10	20	151.32	100.02	33.9	Sample shrinkage
15	10	20	243.92	232.82	4.6	Minor decrease in weight (mg)

7.1.2.3 Characterisation of the GA plasma treated PVA/MGO webs

To detect the presence of GA in the electrospun webs after plasma treatment, ATR-FTIR analysis was employed as outlined in section 3.2.6. Electrospun webs were exposed to the plasma treatment for 1 h. The treatment was performed with 15 W power and the vaporiser was opened for 4 s (in a 10 s time cycle) to allow a greater density of GA. A control sample with no plasma treatment was also prepared.

7.1.3 Release study of MGO from the GA crosslinked PVA/MGO webs

The GA vapour crosslinked PVA/MGO webs and the GA plasma treated samples were placed in a 100ml conical flask containing 20 ml of distilled water at 37ºC. Each conical flask was then placed inside a Grant-Bio ES-20 orbital shaker incubator maintained at 37ºC and set to run at a speed of 250 r min^{-1}. The conical flask was sealed with a rubber stopper to avoid any loss of water during shaking. Individual samples crosslinked via GA vapour were allowed to disperse for 2, 8 and 24 h. As only limited samples were prepared for the GA plasma treatment, a dispersion time of only 8 h was used for these samples. RV-HPLC was used in this study to detect the presence of MGO when released from the GA vapour crosslinked PVA/MGO webs and the GA plasma treated webs. A detailed description of the RV-HPLC technique can be found in section 3.2.9. A calibration curve was obtained for synthetic MGO in aqueous solutions by using 0.1 mg ml^{-1}, 1 mg ml^{-1}, 10 mg ml^{-1} and 20 mg ml^{-1} solutions.

Fig. 7.1 shows the calibration curve obtained. The detectable HPLC retention times of synthetic MGO, PVA and GA were all confirmed and can be observed in Table 7.2. It was also important to determine that any unreacted GA was not present in the PVA/MGO electrospun webs after

exposure to the vacuum oven. Note that GA is employed as a disinfectant in hospital environments (128) and would cause unnecessary complications in a patient should this remain in a wound dressing material. During the HPLC analysis, any detection of GA was noted.

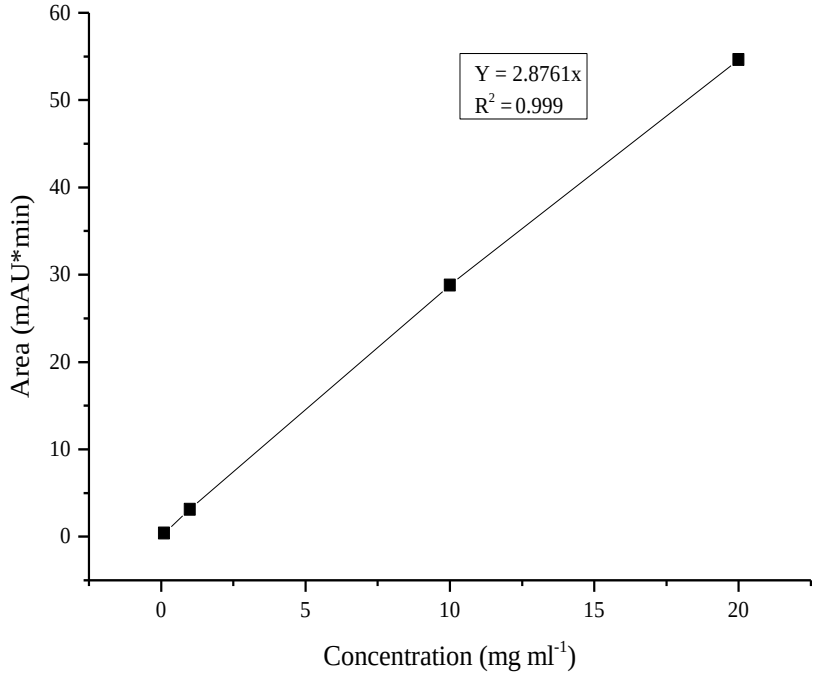

Figure 7.1: Calibration curve of MGO using RV-HPLC.

Table 7.2: Retention times of MGO, PVA and GA when using RV-HPLC.

Compound	Retention Time (min)
MGO	3.51 to 3.52
PVA	5.50 to 5.55
GA	5.17 to 5.20

7.1.4 Swelling behaviour of the GA vapour crosslinked PVA/MGO webs

The swelling behaviour of the GA vapour crosslinked fibres was studied, based on similar methods outlined in the current literature (255, 357). PVA/MGO webs crosslinked with GA vapour for 1, 8, 24 and 48 h were prepared and the weight of each sample was recorded. The sample webs were placed in separate conical flasks containing 20 ml of distilled water at 37ºC for 24 h. After removal from the distilled water, the samples were lightly blotted with Whatman blotting paper to remove any excess water on the surface. The wetted samples were then immediately weighed and the swelling percentage was calculated using the following equation:

Eq. 7.1

$$Swelling\ \% = 100\ (Ws - Wd) / Wd$$

where

Wd is the weight of the fibres after crosslinking and,

Ws is the weight of the swollen fibres after removing any excess water on the surface with blotting paper.

7.1.5 Results and Discussion

7.1.5.1 The effect of crosslinking with GA vapour on the PVA/MGO webs

The crosslinking reaction between the GA and the PVA is shown in Fig. 7.2. Acetal bridges are formed between the hydroxyl groups in the PVA and the difunctional aldehyde molecule of the GA (254, 255). The crosslinking reaction between PVA and GA can consist of intramolecular and/or intermolecular crosslinks (251, 253). Synthetic MGO will not react with the PVA during crosslinking, as the aldehyde group of MGO reacts with water when in solution, forming two compounds, methylglyoxal monohydrate and methylglyoxal dihydrate (216) as seen in Fig. 7.3 (358). Therefore the MGO will remain freely available within the crosslinked PVA fibres.

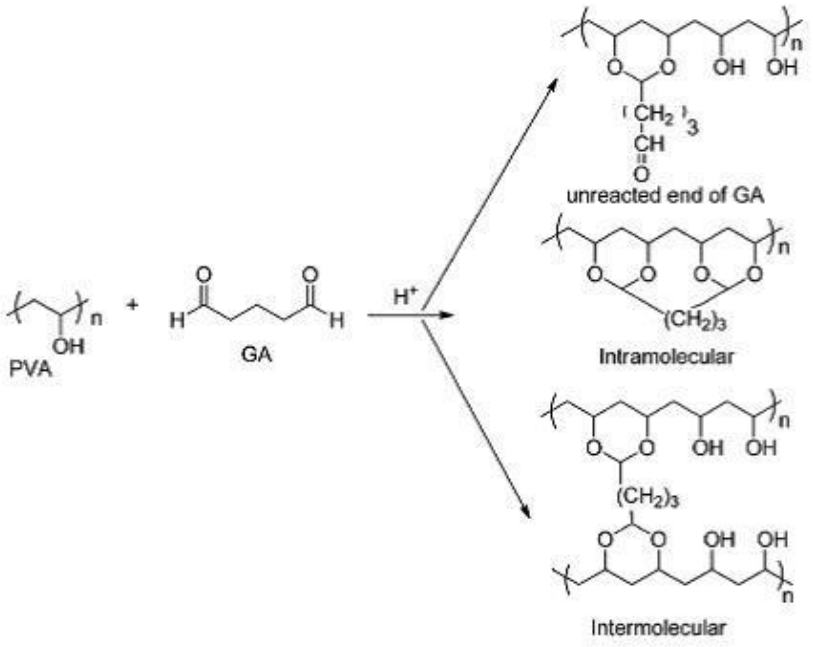

Figure 7.2: Reaction of PVA with GA(254)

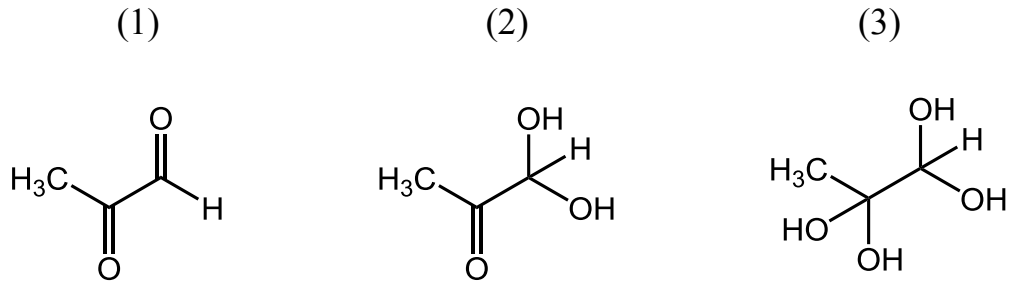

Figure 7.3: Chemical structure of methylglyoxal (1), methylglyoxal monohydrate (2) and methylglyoxal dihydrate (3).

7.1.5.2 Release behaviour of MGO from the GA vapour crosslinked fibres

Fig. 7.4 shows the percentage of MGO released from the fibres over a period of 24 h after crosslinking times of 1, 8, 24 and 48 h. The percentage release of MGO from the crosslinked fibres is based on the calculated mass of MGO available in the fibres prior to crosslinking, using *Eq.* 6.3 in section 6.2.3.1.

To understand the release profile of the MGO from the electrospun webs, SEM micrographs of the crosslinked samples before dispersion were taken using a Jeol JSM-6610LV at a magnification of 6000, as shown in Fig. 7.5.

It can clearly be observed in Fig. 7.4 that the percentage of MGO released after all crosslinking times, increases over a period of 24 h. Interestingly, the sample crosslinked for 8 h showed the highest percentage of MGO released between 2 h and 24 h, with a maximum release of 75%. The sample crosslinked for only 1 h showed the lowest percentage of MGO released, 35% after 2 h and 40% after 8 h. The release of MGO after 24 h crosslinking, showed a similar percentage release to 8 h crosslinking, with a slight decrease of approximately 5% over 24 h. After 48 h crosslinking time the percentage release of MGO has decreased to similar values to the sample crosslinked for only 1 h. However, the final amount released at 24 h was 6% less than the sample crosslinked for 1 h.

This unusual release profile may be explained by the change in fibre morphology of the electrospun webs, as seen in Fig 7.5. Fig. 7.5A shows a PVA/MGO sample with no crosslinking. The mean fibre diameter was found to be 155 nm. As the crosslinking time increased from 0 h to 1 h the mean fibre diameter increased to 434 nm as is evident in Fig. 7.5B. After 8 h crosslinking time, the morphology of the PVA fibres on the surface showed intersecting areas where the fibres had merged together (Fig 7.5C). As the crosslinking time increased to 24 h, little change in the morphology was obseved (Fig. 7.5D). However, after 48 h crosslinking, the fibres appeared to have fused together still further and no visual pores between interbonded fibres could be obverved on the surface (Fig. 7.5E).

The reason for this substantial change in fibre morphology, and subsequent release profile of MGO from the PVA fibres, may be explained by the high water content present in the 25 wt % gluatarldehyde solution during vapour crosslinking. As the crosslinking time increased from 1 h to 8 h, the hydrophilic PVA fibres softened and swelled, forming intersecting points and interfibre bonding (254). This created a larger surface area in contact with the water during dispersion, allowing an increased rate of MGO to diffuse out into the water. As there was little difference in the release of MGO at 24 h crosslinking and the morphology of the fibres remained similar to those after 8 h crosslinking, the same explanantion may be given.

However, as the crosslinking time increased to 48 h, the percentage release of MGO was decreased. This may be attributed to an increase in the amount of crosslinking between hydroxyl groups in the PVA and the difunctional aldehyde molecule of the GA. This will restrict the amount of swelling and subsequently reduce the diffusion of MGO into the water.

In a clinical situation, a wound dressing may be expected to sustain a controlled release of antibacterial agent into a bacteria critically colonised wound for up to one week . This avoids the unnecessary need to change the dressing (21). In this study, after 24 h the amount of MGO released for the sample crosslinked for 1 h, where a fibrous structure remained, showed that just over half of the MGO (56%) was released. Therefore further testing would need to be carried out in future work, in order to determine the percentage release after one week.

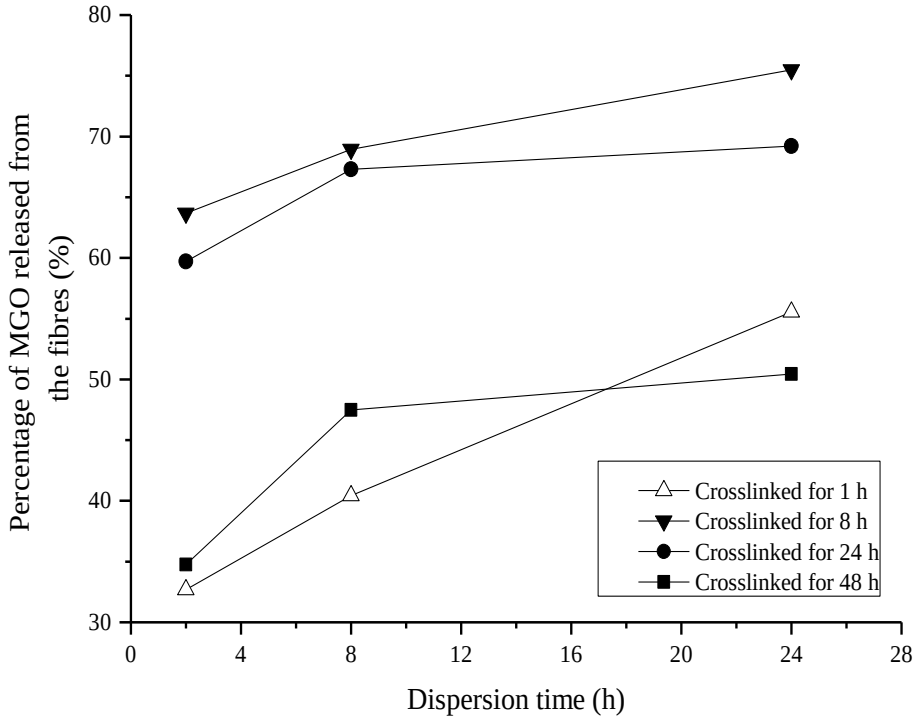

Figure 7.4: Percentage (%) of MGO released from the GA vapour crosslinked PVA/MGO webs for different crosslinking times.

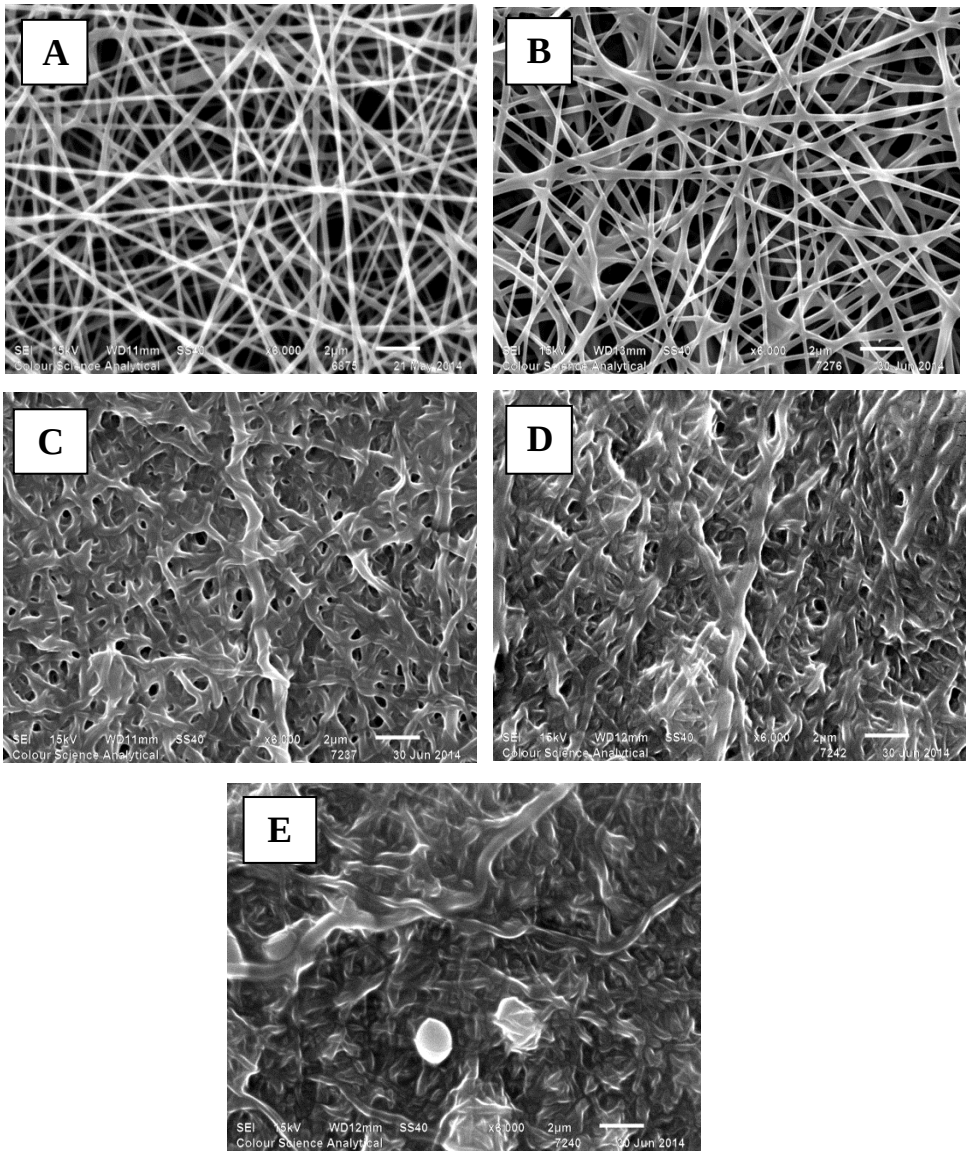

Figure 7.5: SEM micrographs of PVA/MGO fibres after crosslinking with GA vapour for different times. A = no crosslinking, B = 1 h, C = 8 h, D = 24 h and E = 48 h.

7.1.6 Swelling behaviour of the GA vapour crosslinked PVA/MGO webs

As described above, the morphology of the crosslinked samples for 8, 24 and 48 h showed only intersecting areas and inter-fibre bonding, allowing for a greater release of MGO in a quicker time frame and would be impractical for potential use as part of a controlled delivery system. For this reason the swelling of these samples was measured after only 24 h and can be seen in Table 7.3. The swelling of the samples crosslinked for 1 h, where the morphology of the web had retained a fibrous structure, were studied over a period of 10 days and can be observed in Table 7.4.

The results presented in Table 7.3 show that the samples crosslinked for only 1 h, had a mean swelling of 124% after 24 h. This was the lowest swelling percentage, when compared with the samples crosslinked for 8, 24, and 48 h. As the crosslinking time was increased to 8 h the largest swelling percentage was observed with a mean of 405%. This is unusual as previous studies have shown that when increasing the crosslinking time, the swelling decreases, due to an increased amount of acetal bridges formed between hydroxyl groups in the PVA and the difunctional aldehyde molecule of the GA (256). However, in this case, the larger surface area in contact with the water after 8 h crosslinking may have facilitated an increase in the amount of water into the PVA fibres, allowing for a higher swelling percentage. This also correlates with the largest percentage release of MGO for the 8 h crosslinked sample (Fig. 7.4). After 24 h crosslinking time the swelling percentage was reduced to a mean of 238% and after 48 h crosslinking time the swelling percentage remained similar, with a mean of 256%.

Interestingly the swelling of the samples crosslinked for 1, 8, 24 h, followed a similar relationship to the percentage release of MGO and can be seen in Fig. 7.6. This gave further evidence that at an increase in crosslinking time between 8 h and 48 h increased the amount of crosslinking, resulting in the reduced swelling. The results presented in Table 7.4, show that the mean swelling percentage of the PVA/MGO web crosslinked for only 1 h increased from 124% after 1 h in water to a mean swelling of 335% after 1 week. After 10 days the negligible increase in the mean swelling to 346% confirmed that the GA vapour crosslinked PVA/MGO fibres had reached saturation.

Table 7.3: Swelling % of GA vapour crosslinked PVA/MGO webs after 24 h in water.

Crosslinking time (h)	Wd (Weight after crosslinking) (g)	Ws (Weight after swelling for 24 h) (g)	Swelling (%)	Mean (%)	STD
1	0.08961	0.16375	82		
1	0.12475	0.2619	109		
1	0.0968	0.35094	262		
1	0.1472	0.20952	42	**124**	83
8	0.03263	0.15694	380		
8	0.04539	0.18912	316		
8	0.0648	0.37648	480		
8	0.04783	0.25894	441	**405**	62
24	0.05723	0.22202	287		
24	0.0537	0.1354	152		
24	0.04939	0.1646	233		
24	0.05369	0.20385	279	**238**	53
48	0.04587	0.13841	201		
48	0.1259	0.40111	218		
48	0.15374	0.59424	286		
48	0.2064	0.86554	319	**256**	48

Table 7.4: Swelling (%) of PVA/MGO webs after 10 days in water, for 1 h GA vapour crosslinking time.

Time in water	Mean swelling (%)	SD
1 h	124	83
3 days	291	45
7 days	335	64
10 days	346	66

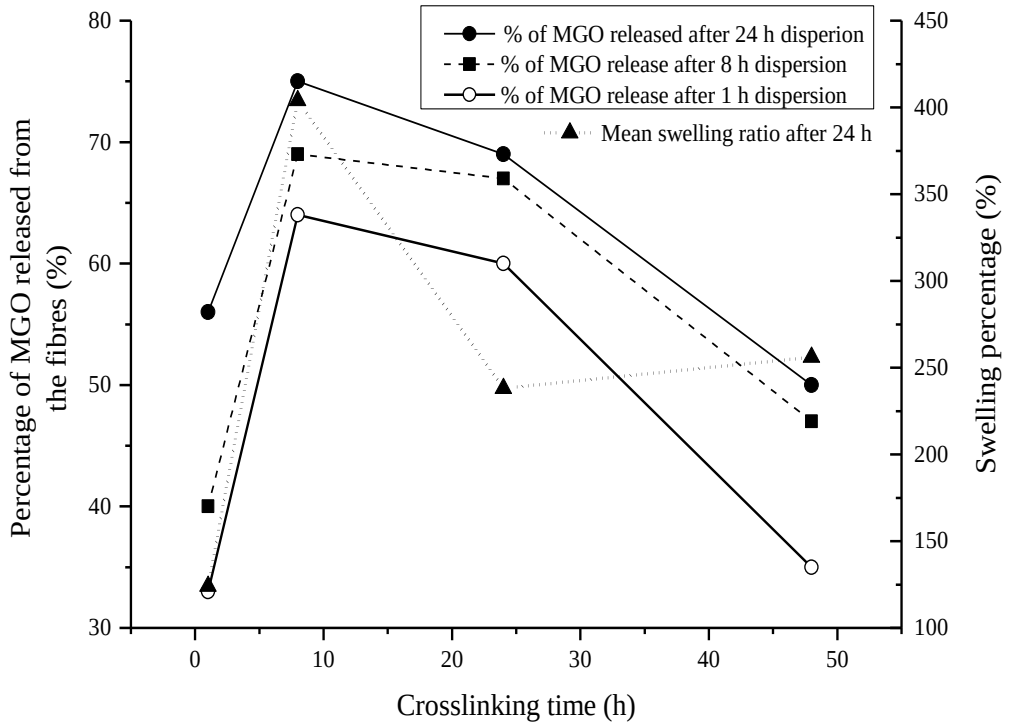

Figure 7.6: Relationship between the percentage release of MGO (%), mean swelling (%) and crosslinking time (h).

7.1.6.1 Effect of GA plasma treatment on the PVA/MGO fibres

Fig. 7.7 shows the percentage of MGO released from the GA plasma treated samples after 8 h dispersion in water. The plasma treatments were done for 1 h at 15 W power. The valve connecting the vaporiser to the plasma chamber operates at a 10 s time cycle where the opening time of the vaporiser could be varied. In this work, the opening time was varied from 20% (2 s) to 80% (8 s). The results indicate that the GA plasma treatment effectively introduced crosslinking to the PVA/MGO webs, as the samples did not disintegrate on direct contact with water, as the non-crosslinked samples did. The release of MGO from the GA plasma treated samples indicated a percentage MGO release of between 47% and 62% after a period of 8 h in water. The effect of time on, during plasma treatment had a limited effect on the amount of MGO released and further work would need to be carried out to study this further.

Fig. 7.8 shows the FTIR spectra obtained for the PVA/MGO samples exposed to GA plasma treatment for 1 h (time on 40%), when compared with a non-crosslinked sample. The large broad band observed between 3100 cm^{-1} and 3700 cm^{-1} (region 3) is associated with the stretching vibration of the hydroxyl group arising from intermolecular and intramolecular hydrogen bonds. The decrease in intensity of this broad band is shown for the GA plasma

treated sample, indicating the formation of acetal bridges between the hydroxyl groups in the PVA and the difunctional aldehyde molecule of the GA (254, 256). The bands between 1600 cm^{-1} and 1750 cm^{-1} (region 2) can be assigned to the C=O stretching of the unreacted end of the aldehyde in the PVA/MGO GA plasma treated sample (256). The heightened peak observed at 1185 cm^{-1} (region 1) for the plasma treated sample, may be attributed to the C-O-C vibration of the acetal group (256). Two other studies, which looked at the crosslinking of PVA with GA vapour, also reported similar spectra with a decrease in band intensity observed at 3330-3350 cm^{-1} (256) and 3200-3650 cm^{-1} (254) due to the formation of acetal bridges. Peaks were also observed between 1700 and 1750 cm^{-1} attributed to the C=O stretching (254) and broadening of peaks between1000-1140 cm^{-1} were attributed to C-O-C vibration of the acetal group (254, 256). This FTIR spectra gave further confidence that GA was successfully introduced to the PVA/MGO webs during treatment with GA plasma and further confirmed the delay in the release of MGO from the GA plasma treated samples as seen in Fig 7.7, when compared to a non-crosslinked sample referred to in section 6.2.3.1.

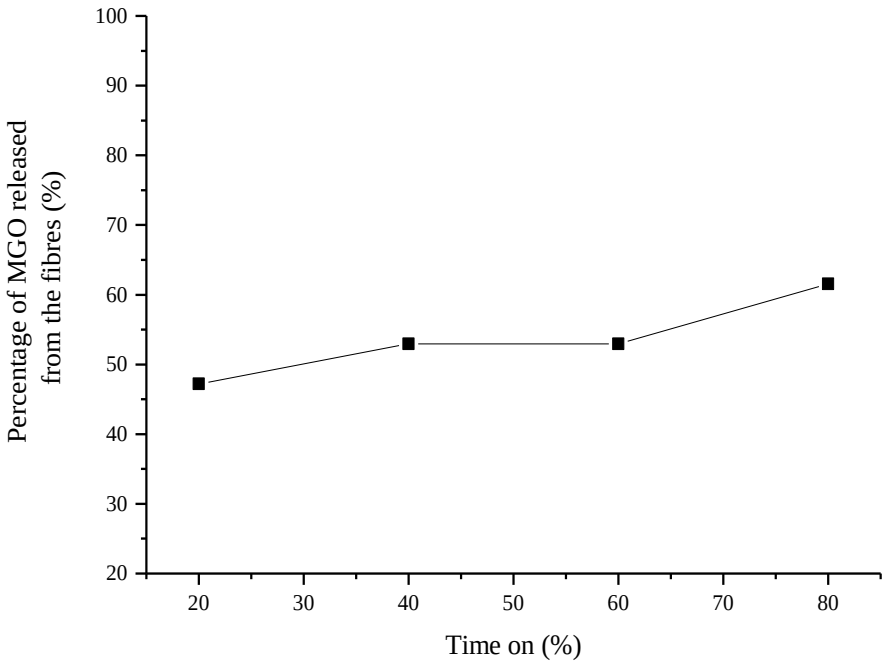

Figure 7.7: Percentage (%) of MGO released from the GA plasma treated samples after 8 h dispersion in water.

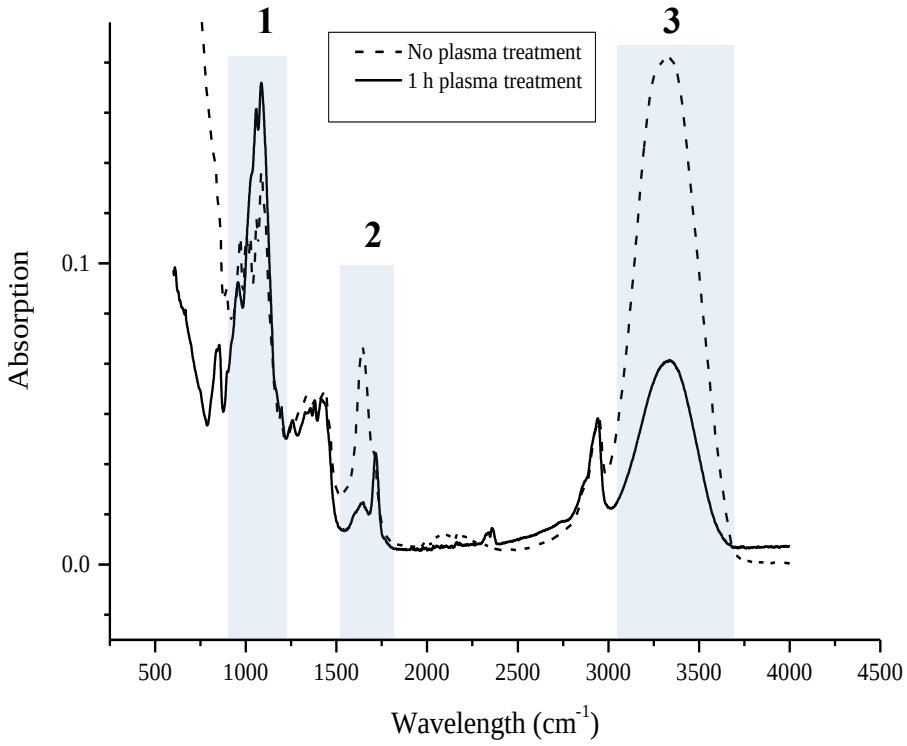

Figure 7.8: FTIR spectra of the GA plasma treated PVA/MGO webs, power of 15 W, treatment duration 1 h, valve opening time 4 s.

7.2 Summary

The stability of PVA/MGO electrospun fibre webs in water was considerably improved after crosslinking using two different approaches, namely a 25 wt % GA vapour and a GA plasma treatment. The non-crosslinked samples disintegrated instantly on contact with water, as reported in Chapter 6. The overall percentage release of MGO from the GA vapour crosslinked PVA/MGO webs progressively increased over a period of 24 h for each crosslinking time, with the largest percentage release after 8 h crosslinking time. The SEM images of the GA vapour crosslinked PVA/MGO webs revealed an increase in fibre diameter after 1 h crosslinking time and inter-fibre bonding and merging was apparent after 8 h crosslinking time. This was due to the high water content available in the 25 wt % GA vapour, allowing the fibres to swell and provide a larger surface area in contact with the water. The swelling studies also showed a similar relationship with the release study, showing the highest swelling percentage to be achieved at 8 h crosslinking time. As the crosslinking time was increased to 48 h, the percentage of MGO released and the swelling percentage was reduced due to an increase in the acetal bridge formation in the PVA fibres.

A small number of experiments were done with the novel GA plasma treatment. The experiments showed promising results, with a decrease in the percentage of MGO released when compared with a non-crosslinked sample. FTIR analysis provided additional confirmation that crosslinking had occurred in the PVA/MGO webs via GA plasma treatment. Although the GA plasma experiment was a preliminary study, the results confirmed that this is a promising technique for controlling the release rate of MGO from PVA/MGO samples. It is believed that this is the first time crosslinking with GA plasma treatment has been employed with a successful outcome. Further work is required to explore the effect of different operating parameters using plasma technology on crosslinking and MGO release behaviour.

Chapter 8 Conclusions and Future Work

8.1 Conclusions

Electrospun polymeric materials possess valuable properties as potential wound healing materials, as a result of their nano to sub-micron fibre diameters which closely mimic the topographical extra cellular matrix (ECM) of the skin, while providing conformability to the wound site and a scaffold for cellular growth. The high surface and small interfaces promote haemostasis to occur naturally, and a high porosity coupled with small pore size provides a semi-permeable environment offering protection from external bacteria and breathability. Additionally the ability to incorporate antibacterial agents into a polymer matrix also exists.

Manuka honey, a current antibacterial agent utilised in wound dressing materials, provides a well documented antibacterial effect owing in part to one of its constituents, methylglyoxal (MGO). Previously, Manuka honey has been coated or impregnated on to nonwoven substrates for use in wound care, and this mode of application has been clinically utilised for some time. However, this is not a particularly convenient means of delivery given the viscosity and adhesiveness of the native material. It also complicates packaging during manufacture as well as storage, prior to use. The encapsulation of Manuka honey or MGO within synthetic fibres is notionally a more convenient method of delivery, since it involves topical application of a dry substrate during wound care, followed by diffusion or release in to the surrounding wound environment. The feasibility of this approach has been studied herein as a potentially new approach for preparing a wound dressing component. It was established that poly(vinyl alcohol) (PVA) a hydrophilic polymer, approved by the FDA for use in humans, has the ability to provide a favourable moist wound environment, due to its ability to form a hydrogel on contact with water. Accordingly this research investigated the antibacterial properties of synthetic MGO as a sole antibacterial compound, and the feasibility of incorporating MGO into polymeric electrospun webs using PVA as a carrier.

To provide an understanding of the antibacterial properties of Manuka honey and MGO, experiments were first conducted in which both materials were evaluated as coatings onto a preformed nonwoven fabric and then after encapsulation in the form of PVA/MGO nano-fibrous electrospun webs.

Although there have been previous reports on the antibacterial activity of Manuka honey and MGO in liquid form or in the form of a Manuka honey dressing, none of them have expressed the concentration of MGO required to have an antibacterial effect in terms of unit area, which is particularly important in the design and development of a wound dressing material. This study provided the first comparison of equivalent MGO concentrations per unit area to provide an antibacterial effect when applied as a coating to a nonwoven fabric in the form of Manuka honey and synthetic MGO. The antibacterial efficiency was investigated using both BS EN ISO

20743:2007 (314) and BS EN ISO 20645:2004 (315) to determine if synthetic MGO provided a comparable antibacterial effect to Manuka honey. In the first instance, the bacteria inoculated samples were immersed in 20 ml of simulated wound exudate fluid where a relatively high moisture content was available to facilitate the diffusion of MGO. It was found that an MGO concentration of 0.0054 mg cm^{-2} for both Manuka honey and synthetic MGO was sufficient to achieve 100% reduction in bacteria when tested against Gram positive *S.aureus* and Gram negative *K.pneumonia*.

Experiments using bacteria seeded agar plates, found that higher concentrations of MGO between 0.0170 mg cm^{-2} and 0.1 mg cm^{-2} were required to produce a good antibacterial effect against *E.coli* and *S.aureus*. The variation in moisture content in each method of test and the affinity of lyocell fibres for water, is believed to be responsible for the differing MGO concentrations needed to produce an antibacterial effect. In the case of BS EN ISO 20743:2007, a high moisture content is available due to the addition of 20 ml of SCDLP, which is likely to encourage the hydration of the lyocell fibres and facilitate MGO diffusion, when compared to BS EN ISO 20645:2004, where limited moisture content is available from the agar plates.

The Manuka honey coated nonwovens were shown to produce zones of inhibition at relatively low MGO concentrations between 0.1 mg cm^{-2} and 0.2 mg cm^{-2}, when compared with the synthetic MGO coated nonwovens, where clear zones of inhibition were not apparent until a concentration of 0.4 mg cm^{-2} of MGO was achieved for *E.coli* and 0.8 mg cm^{-2} of MGO for *S.aureus*. This difference was attributed to the incubation of the samples at 37ºC during testing, where the Manuka honey coating is likely to soften and allow greater diffusion into the bacteria seeded agar from the fibres, when compared to the less viscous synthetic MGO coating, which is retained by the lyocell fibres. Manuka honey also contains hydrogen peroxide, which may also heighten the antibacterial effect, when compared with synthetic MGO.

Assessment of the minimum inhibitory concentrations (MIC) and minimum bactericidal concentrations (MBC) of MGO in liquid form, was achieved via a standard laboratory protocol in accordance with the Clinical and Laboratories Standards Institute (CLSI). Three of the most common bacterial strains found in chronic wounds, including *S.aureus*, *P.aeuroginosa* and *E.faecalis* were assessed. Limited studies have previously been reported on the MIC and MBC of MGO. In this study the MIC and MBC against *P.aeuroginosa* were found be lower than that previously reported in the current literature when in a planktonic state. The MIC and MBC for S.aureus was found comparable to previous studies with the exception of one, where a concentration of approximately four times higher than that found in this study, had a bactericidal effect. Notably in this study, the MIC and MBC of MGO against *E.faecalis* was reported for the first time.

The production of the electrospun webs was explored using both needle and free surface (needleless) electrospinning technologies, where the parameters of each process was governed to determine the most favourable conditions in producing fibres free from defects. Synthetic MGO was successfully encapsulated in PVA electrospun webs using both electrospinning techniques. It could not be assumed that the conditions required for optimal needle-based electrospinning of PVA/MGO fibres could be directly translated to free surface electrospinning because of the substantial differences in the design of the electrodes used by each method. The different conditions required by each system are rarely reported in the literature. Therefore, the spinning of PVA/MGO was explored by both methods for the first time.

A number of synthetic MGO and PVA concentrations in water were initially examined to determine the optimum spinning solution. In the case of needle electrospinning, an 11.22 wt % MGO solution with a 16% (w/v) PVA concentration was most favourable for producing fibres free from defects, observed via scanning electron microscopy (SEM). It was found that a voltage of 15 kV and a distance of 15 cm between the needle tip and an aluminium foil collector, produced the smallest mean fibre diameter of 157 nm. At a concentration of 20% (w/v) PVA, needle blockage occurred due to a high viscosity of 2634 cP and slow flow rate of 0.1 ml h^{-1} allowing the polymer to dry at the needle tip.

When using free surface needle electrospinning, a PVA concentration of 20% (w/v) was found to be needed to eliminate any beads in the resultant fibres when compared to a 16% (w/v) PVA concentration, where some beads were observed. During free surface electrospinning, unlike in needle based electrospinning, the 20% (w/v) PVA solution was kept under constant agitation because of the rotation of the electrode, allowing the polymer chains to move freely and become easily stretched by the electrostatic force. Larger voltages between 65 kV and 75 kV were required to initiate electrospinning jets from the wire electrode, when compared with needle electrospinning, where a voltage above 18 kV produced sparking due to the highly conductive nature of the aluminium collector and metal needle tip. It is thought that the larger voltage of 65 kV, when using free surface electrospinning was achieved due to the immersion of the wire electrode in a less conductive polymer solution. The smallest mean fibre diameter of 155 nm was produced at a voltage of 65 kV and a distance of 183 mm between the wire electrode and an aluminium foil collector.

For practical assembly of a wound dressing component as part of a continuous process it is important to establish conditions that will allow fibres to be directly deposited on to a preformed nonwoven substrate, rather than on to metal foil, which is the most commonly used collector reported in the literature. Therefore, direct deposition on to a preformed nonwoven substrate

was also explored in the current work. It was established that use of an aluminium foil substrate produced fibres with a smaller mean fibre diameter due to an increased electric field when compared with a non-conducting nonwoven substrate (polypropylene spunbond), where repulsive forces act upon the resultant fibres during deposition, reducing the stretching of the viscoelastic jet. The findings were found to be consistent with the results of previous studies, in which up to eight different collector substrates were examined for their effect on resultant fibre morphology.

FTIR and ^{1}H-NMR confirmed the successful incorporation of MGO within the PVA fibres, which highlighted the carbonyl groups associated with MGO's keto-aldeyde groups. The antibacterial evaluation of the PVA/MGO electrospun webs, further confirmed the presence of MGO using BS EN ISO 20645:2004 when compared to a PVA only electrospun web, where no antibacterial activity was observed.

It was also established that the composition of the polymer substrate used to deliver the MGO or Manuka honey is likely to affect the concentration needed to produce an antibacterial effect. The antibacterial evaluation of both needle and free surface PVA/MGO electrospun webs confirmed that similar MGO concentrations of 1.50 mg cm^{-2} and 1.14 mg cm^{-2} respectively, provided a good antibacterial effect *in-vitro*. These concentrations were found to be noticeably higher when compared to the coated nonwoven samples due to the encapsulation of MGO within the PVA fibres allowing for a slower diffusion rate into the agar.

Depending on their molecular structure, water soluble PVA fibres can dissolve within a few hours, or instantaneously on contact with water, as they did so in this study. It is an important requirement for a bioactive wound dressing material to be able to maintain a stable structure, while providing a controlled and sustained release of antibacterial agent into the wound bed up to a period of one week. To overcome the instability of PVA in water, crosslinking with GA in previous studies has shown the potential to control the stability of PVA and reduce the release of any supplementary compounds within the fibre matrix. In this study crosslinking with GA was successfully carried out via two different processes including vapour crosslinking and a novel technique with plasma technology, which to the author's knowledge has not been previously reported in the literature.

The percentage release of MGO from the GA vapour crosslinked PVA/MGO webs was detected using reverse phase high performance liquid chromatography (RV-HPLC). 93.7% MGO of that assumed in the PVA/MGO webs was released within 30 minutes from the non-crosslinked samples. A considerable reduction in the percentage release of MGO from the crosslinked PVA/MGO webs was observed over a period of 24 h. A noticeable change in the fibre

morphology was shown with an increase in crosslinking time, resulting in an enlarged mean fibre diameter after 1 h crosslinking time when compared to a non-crosslinked sample.

An increased surface area was observed between 8 h and 48 h crosslinking time where merging and inter-fibre bonding occurred. This was attributed to the swelling of the PVA/MGO fibres in the GA vapour, where a high water content was available. The swelling percentage of the vapour crosslinked fibres showed a similar relationship to the percentage release of MGO after different crosslinking times, where the highest swelling was shown to provide the highest percentage release of MGO.

Initial experiments with GA plasma treatment were shown to effectively crosslink the PVA/MGO webs, where confirmation with FTIR analysis showed elevated and reduced peaks as a result of GA plasma treatment, when compared to a non-plasma treated sample. The stability of the PVA/MGO webs in water was shown to improve, slowing the release of MGO when compared to the non-crosslinked sample. To the authors knowledge this is the first time that GA plasma technology has been employed as a novel crosslinking technique, and provides a promising new approach to controlling the release of MGO from PVA electrospun webs.

8.2 Suggestions for future work

A number of additional areas of study can be identified for future work, that will help in the further understanding of MGO as an antibacterial agent as well as providing greater understanding of the release kinetics of MGO from electrospun PVA webs.

- The antibacterial evaluation of MGO against multiple bacteria organisms, when applied as a coating to a nonwoven fabric and when incorporated within electrospun PVA webs would provide further insight into the bacteriostatic and bactericidal performance of MGO as an antibacterial agent in wound care. BS EN ISO 20743:2007 and BS EN ISO 20645:2004 could be modified to provide this data.
- Electrospinning of co-polymer solutions with differing mechanical and physical properties, suitable for wound healing applications, may provide an alternative approach in the controlled release of MGO into a wound site.
- GA vapour crosslinking times between 1 h and 8 h and variations in GA concentration would give further insight into the conditions at which the fibrous morphology of spun webs transforms to merging and inter-bonding areas.

- The vapour crosslinking study provided a release profile of MGO after 24 h. Clinically, a dressing could potentially extend beyond the 3-4 day maximum that is often encountered in practice. A release profile up to 7-10 days would be valuable to explore.
- The current study involved a preliminary experiment in which a novel GA plasma approach was explored. Extensive research could be employed in this area, to further understand the effects of different operating parameters and GA concentration on the crosslinking and release of MGO from PVA/MGO fibres. There is also the potential to assess a variety of crosslinking agents and polymeric materials.
- A release study of MGO from the crosslinked PVA/MGO electrospun webs using BS EN ISO 20645:2004 or BS EN ISO 20743:2007 over a period of one week, would offer a useful insight into the effect of differing antibacterial conditions on the delivery of the MGO into a wound environment.
- On the understanding that Manuka honey contains MGO and additional antibacterial compounds, such as hydrogen peroxide, a study into the electrospinning of Manuka honey/PVA fibres and their antibacterial properties compared to PVA/MGO fibres would be of interest.
- Study the adherence properties of the PVA/MGO webs via a simulated wound model.

References

1. Czajka R. Development of medical textile market. Fibres & Textiles in Eastern Europe. 2005;13(1):13-15.
2. Economist. T. Don't Panic: The Economist; 2014 [29-01-15]. Available from: http://www.economist.com/news/international/21619986-un-study-sparks-fears-population-explosion-alarm-misplaced-dont-panic.
3. Haub C. World Population Aging: Clocks Illustrate Growth in Population Under Age 5 and Over Age 65. 2011 [cited 29-01-15 29-01-15]. Available from: http://www.prb.org/Publications/Articles/2011/agingpopulationclocks.aspx.
4. Posnett J, Franks PJ. The cost of skin breakdown and ulceration in the UK. 2007. In: Skin breakdown: the silent epidemic [Internet]. Hull, UK: Smith and Nephew Foundation; [6-12].
5. Arthur S, Harding KG. Chapter 1 Wound managment and dressings. In: Rajendran S, editor. Advanced textiles for wound care. Boca Ranton, USA: Woodhead Publishing Ltd; 2009. p. 3-19.
6. Gjodsbol K, Christensen JJ, Karlsmark T, Jorgensen B, Klein BM, Krogfelt KA. Multiple bacterial species reside in chronic wounds: a longitudinal study. International Wound Journal. 2006;3(3):225-231.
7. Tenover FC. Mechanisms of Antimicrobial Resistance in Bacteria. American Journal of Infection Control. 2006;34(5):S3-S10.
8. Howell-Jones RS, Wilson MJ, Hill KE, Howard AJ, Price PE, Thomas DW. A review of the microbiology, antibiotic usage and resistance in chronic skin wounds. Journal of Antimicrobial Chemotherapy. 2005;55(2):143-149.
9. Fletcher J. Antimicrobial dressings in wound care. Nurse Prescribing. 2006;4(8):320-326.
10. Lansdown ABG. Chapter 8 The toxicology of silver. In: Lansdown ABG, editor. Silver in healthcare: its antimicrobial efficacy and safety in use.Cambridge, England: Royal society of chemistry; 2010. p. 164 -170.
11. Vincent KM, Burd A. In vitro cytotoxity of silver: implication for clinical wound care. Burns. 2004 30:140–147.
12. Burd A, Kwok CH, Hung SC, Chan HS, Gu HL, Wai KL, et al. A comparative study of the cytotoxicity of silver-based dressings in monolayer cell, tissue explant, and animal models. Wound Repair and Regeneration. 2007;15:94-104.
13. Landsdown ABG, Williams A. Bacterial resistance to silver in wound care and medical devices. Journal of Wound Care. 2007;16(1):15-19.
14. Percival SL, Bowler PG, Russell D. Bacterial resistance to silver in wound care. Journal of Hospital Infection. 2005;60(1):1-7.
15. Elsner JJ, Egozi D, Ullmann Y, Berdicevsky I, Shefy-Peleg A, Zilberman M. Novel biodegradable composite wound dressings with controlled release of antibiotics: results in a guinea pig burn model. Burns 2011;3 7 896-904.
16. Elsne JJ, Berdicevsky I, Zilberman M. In vitro microbial inhibition and cellular response to novel biodegradable composite wound dressings with controlled release of antibiotics Acta Biomaterialia 2011;7:325–336.
17. Schoukens G. Chapter 5 Bioactive dressing to promote healing. In: Rajendran S, editor. Advanced textiles for wound care. Boca Raton, USA: CRC Press and Woodhead Publishing Ltd; 2009. p. 114-152.
18. Winter GD. Formation of the scab and the rate of epithelisation of superficial wounds in the skin of the young domestic pig. Nature. 1962;4(8):366-367.
19. Winter GD, Scales JT. Effect of air drying and dressings on the surface of a wound. Nature. 1963;197(4862):91-92.

20. Wiegand C, Hipler U-C. Polymer-based Biomaterials as Dressings for Chronic Stagnating Wounds. In: Heinze TJMKA, editor. Utilization of Lignocellulosic Materials. Macromolecular Symposia. 294-II2010. p. 1-13.
21. Boateng JS, Matthews KH, Stevens HNE, Eccleston GM. Wound healing dressings and drug delivery systems: a review. Journal of Pharmaceutical Science. 2008;97(8):2892-2923
22. Weller C. Chapter 4 Interactive dressings and their role in moist wound management. In: Rajendran S, editor. Advanced textiles for wound care. Boca Raton, USA: CRC Press and Woodhead Publishing Ltd; 2009. p. 97-113.
23. White RJ, Cooper R, Kingsley A. Section 2 A topical issue: the issue of antibacterials in wound pathogen control. In: White RJ, editor. Trends in wound care. Wiltshire, UK.: Mark Allen Publishing Ltd; 2003. p. 16-36.
24. Vowden P, Vowden K, Carville K. Antimicrobial dressings made easy. Wounds International (Made Easys). 2011;2(1):1-6.
25. Flores A, Kinsgley A. Topical antimicrobial dressings: an overview. Wound Essentials. 2007(2):182-185.
26. Lipsky BA, Hoey C. Topical antimicrobial therapy for treating chronic wounds. Clinical Infectious Diseases. 2009;49(10):1541-1549.
27. Best Practice Statement: the use of topical antiseptic/antimicrobial agents in wound management. Wounds UK, Aberdeen, 2010.
28. Palmieri TL, Greenhalgh DG. Topical treatment of pediatric patients with burns: a practical guide. American Journal of Clinical Dermatology. 2002;3(8):529-534.
29. Patel PP, Vasquez SA, Granick MS, Rhee ST. Topical antimicrobials in pediatric burn wound management. Journal of Craniofacial Surgery. 2008;19(4):913-922.
30. Percival SL, Slone W, Linton S, Okel T, Corum L, Thomas JG. The antimicrobial efficacy of a silver alginate dressing against a broad spectrum of clinically relevant wound isolates. International Wound Journal. 2011;8(3):237-243.
31. Toy LW, Macera L. Evidence-based review of silver dressing use on chronic wounds. Journal of the American Academy of Nurse Practitioners. 2011;23(4):183-192.
32. Smith&newphew. DURAFIBER Ag 2015 [08-02-15]. Available from: http://www.smith-nephew.com/uk/products/wound_management/product-search/durafiber/further-product-information/durafiber-ag/.
33. Fan K, Tang J, Escandon J, Kirsner RS. State of the art in topical wound-healing products. Plastic and Reconstructive Surgery. 2011;127(1):44S-59S.
34. Atiyeh BS, Costagliola M, Hayek SN, Dibo SA. Effect of silver on burn wound infection control and healing: review of the literature. Burns. 2007;33(2):139-148.
35. Agrawal P, Soni S, Mittal G, Bhatnagar A. Role of Polymeric Biomaterials as Wound Healing Agents. International Journal of Lower Extremity Wounds. 2014;13(3):180-190.
36. Salcido R. Complementary and alternative medicine in wound healing. Advances in Skin and Wound Care. 2011;24(5):200.
37. Molan PC. The role of honey in the management of wounds. Journal of Wound Care. 1999;8(8):415-418.
38. Molan PC, Betts JA. Clinical usage of honey as a wound dressing: an update. Journal of Wound Care. 2004;13(9):353-356.
39. Mavric. E WS, Barth. G and Henle. T. Identification and quantification of methylglyoxal as the dominant antibacterial constituent of Manuka (Leptospermum scoparium) honeys from New Zealand. Molecular Nutrition and Food Research. 2008;52(4):483-489.
40. Talukdara. D, Raja. S, Dasb. S, Jainb. A K, Kulkarnic. A, Raya. M. Treatment of a number of cancer patients suffering from different types of malignancies by methylglyoxal-based formulation: a promising result. Cancer Therapy. 2006;4:205-222.
41. Ayoub FM, Allen RE, Thornalley PJ. Inhibition of proliferation of human leukemia 60 cells by methylglyoxal in vitro. Leukemia Research. 1993;17(5):397-401.
42. Apple MA, Greenberg DM. Inhibition of cancer growth in mice by a normal metabolite. Life Sciences. 1967;6(20):2157-2160.
43. Anderson EL, Casey JE, Jr., Emas M, Force EE, Jensen EM, Matz RS, et al. Antiviral activity of glyoxals and derivatives. Journal of Medicinal Chemistry. 1963;6(6):787-791.
44. Wright JB, Lincoln EH, Heinzelman RV. Antiviral compounds. III. derivatives of β-aminolactaldehyde. Journal of the American Chemical Society. 1957;79:1690-1694.

45. Fidaleo M, Zuorro A, Lavecchia R. Methylglyoxal: a new weapon against staphylococcal wound infections. Chemistry Letters. 2010;39:322-323.
46. Fidaleo M, Zuorro A, Lavecchia R. Antimicrobial efficacy of hydrogels containing methylglyoxal and hyaluronan against wound pathogens. Journal of Biotechnology. 2010;150:S1-S576.
47. Ghosh S, Chakraborty P, Saha P, Acharya S, Ray M. Polymer based nanoformulation of methylglyoxal as an antimicrobial agent: efficacy against resistant bacteria. RSC Advances. 2014;4:23251-23261.
48. Breteler MRT, Nierstrasz VA, Warmoeskerken MMCG. Textiles slow release systems with medical applications. AUTEX Research Journal. 2002;2(4):175-189.
49. Jing X, Mi H-Y, Peng J, Peng X-F, Turng L-S. Electrospun aligned poly(propylene carbonate) microfibers with chitosan nanofibers as tissue engineering scaffolds. Carbohydrate Polymers. 2015;117:941-949.
50. He X, Cheng L, Zhang XM, Xiao Q, Zhang W, Lu CH. Tissue engineering scaffolds electrospun from cotton cellulose. Carbohydrate Polymers. 2015;115:485-493.
51. Meinel AJ, Germershaus O, Luhmann T, Merkle HP, Meinel L. Electrospun matrices for localized drug delivery: current technologies and selected biomedical applications. European Journal of Pharmaceutics and Biopharmaceutics. 2012;81(1):1-13.
52. Sohrabi A, Shaibani PM, Etayash H, Kaur K, Thundat T. Sustained drug release and antibacterial activity of ampicillin incorporated poly(methyl methacrylate)-nylon6 core/shell nanofibers. Polymer. 2013;54(11):2699-2705.
53. Agarwal S, Wendorff JH, Greiner A. Use of electrospinning technique for biomedical applications. Polymer. 2008;49(26):5603-5621.
54. Jannesari M, Varshosaz J, Morshed M, Zamani M. Composite poly(vinyl alcohol)/poly(vinyl acetate) electrospun nanofibrous mats as a novel wound dressing matrix for controlled release of drugs. International Journal of Nanomedicine. 2011;6:993-1003.
55. Chena JP, Chang GY, Chen JK. Electrospun collagen/chitosan nanofibrous membrane as wound dressing. Colloids and Surfaces: A Physiochemical and Engineering Aspect. 2008;313-314:183-188.
56. Kim SE, Heo DN, Lee JB, Kim JR, Park SH, Jeon S, et al. Electrospun gelatin/polyurethane blended nanofibers for wound healing. Biomedical Materials. 2009;4(4):044106.
57. Myung-Seob K, Dong-Il C, Hak-Yong K, K I-S, Narayan B. Electrospun nanofibrous polyurethane membrane as wound dressing. Journal of Biomedical Materials Research Part B: Applied Biomaterials. 2003;15;67(2):675-679.
58. Sill TJ, von Recum HA. Electro spinning: applications in drug delivery and tissue engineering. Biomaterials. 2008;29(13):1989-2006.
59. Flemming RG, Murphy CJ, Abrams GA, Goodman SL, Nealey PF. Effects of synthetic micro- and nano-structured surfaces on cell behavior. Biomaterials. 1999;20(6):573-588.
60. Langer R. Polymeric delivery systems for controlled drug release. Chemical Engineering Communications. 1980;6(1-3):1-48.
61. Chong. SF SAaZA. Microstructured, functional PVA hydrogels through bioconjugation with oligopeptides under physiological conditions.Small.2013;9:942-950.
62. Don TM, King CF, Chiu WY, Peng CA. Preparation and characterization of chitosan-g-poly (vinyl alcohol)/poly (vinyl alcohol) blends used for the evaluation of blood-contacting compatibility. Carbohydrate Polymers. 2006;63(3):331-339.
63. Moretto A, Tesolin L, MarsilioF, Schiavon M, Berna M, Veronese FM. Slow release of two antibiotics of veterinary interest from pva hydrogels. Farmaco (Lausanne) 2003;59(1):1-5.
64. Pal K, Banthia AK, Majumdar DK. Preparation and characterization of polyvinyl alcohol-gelatin hydrogel membranes for biomedical applications. Aaps Pharmscitech. 2007;8(1):E1-E5.
65. Sakai S, Tsumura M, Inoue M, Koga Y, Fukanob K, Taya M. Polyvinyl alcohol-based hydrogel dressing gellable on-wound via a co-enzymatic reaction triggered by glucose in the wound exudate. Journal of Materials Chemistry B. 2013;1(38):5067-5075.
66. Abdelgawad AM, Hudson SM, Rojas OJ. Antimicrobial wound dressing nanofiber mats from multicomponent (chitosan/silver-NPs/polyvinyl alcohol) systems. Carbohydrate Polymers. 2014;100:166-178.

67. Liu X, Lin T, Fang J, Yao G, Zhao H, Dodson M, et al. In vivo wound healing and antibacterial performances of electrospun nanofibre membranes. Journal of Biomedical Materials Research, Part A. 2010;94A:499-508.
68. Collins F, Hampton S, White R. A-Z dictionary of wound care. Wiltshire: Mark Allen Publishing Ltd; 2002.
69. Robson MC. Wound Infection: a failure of wound healing, caused by an imbalance of bacteria. Surgical Clinics of North America. 1997;77:637-650.
70. Lazarus GS, Cooper DM, Knighton DR, Margolis DJ, Pecoraro RE, Rodeheaver G, et al. Definitions and guidelines for the assessment of wounds and evaluation of healing. Archives of Dermatology. 1994;130:489-493.
71. Attinger C, Janis E, Jeffrey J, Steinberg J, Schwartz J, Al-Attar A, et al. Clinical approach to wounds: débridement and wound bed preparation including the use of dressings and wound-healing adjuvants. Plastic and Reconstructive Surgery. 2006;117(supplement 7):72S-109S.
72. Brunner L, Suddarth D. Textbook of adult nursing. London: Chapman and Hall; 1992.
73. Bale S, Harding K, Leaper D. Chapter 1 History of wounds and the healing process. An introduction to wounds. London: Emap Healthcare Ltd; 2000. p. 3-14.
74. Russell L. Section 1 Understanding physiology of wound healing and how dressings help. In: White R, Harding K, editors. Trends in wound care. Wiltshire: Mark Allen Publishing Ltd.; 2002. p. 3-15.
75. Dealey C. Chapter 1 The phyisology of wound healing. In: Dealey C, editor. The care of wounds a guide for nurses.Oxford: Blackwell Publishing Ltd; 2005. p. 1-12.
76. Hart J. Inflammation 1: Its role in the healing of acute wounds. Journal of Wound Care. 2002;11(6):205-209.
77. Timmons J. Skin function and wound healing physiology. Wound Essentials [Internet]. 2006 25/01/2012; 1:[8-17 pp.]. Available from: http://www.wounds-uk.com/wound-essentials.
78. Kerstein MD. The scientific basis of healing. Advances in Wound Care. 1997;10(2):30-36.
79. Silver IA. The physiology of wound healing. Journal of Wound Care. 1994;3(2):106-109.
80. Rhoads DD, Wolcott RD, Percival SL. Biofilms in wounds: management strategies. Journal of Wound Care. 2008;17(11):502-508.
81. Fazli M, Bjarnsholt T, Kirketerp-Moller K, Jorgensen A, Andersen CB, Givskov M, et al. Quantitative analysis of the cellular inflammatory response against biofilm bacteria in chronic wounds. Wound Repair and Regeneration. 2011;19(3):387-391.
82. Bjarnsholt T, Kirketerp-Moller K, Jensen PO, Madsen KG, Phipps R, Krogfelt K, et al. Why chronic wounds will not heal: a novel hypothesis. Wound Repair and Regeneration. 2008;16(1):2-10.
83. Trostrup H, Thomsen K, Christophersen LJ, Hougen HP, Bjarnsholt T, Jensen PO, et al. Pseudomonas aeruginosa biofilm aggravates skin inflammatory response in BALB/c mice in a novel chronic wound model. Wound Repair and Regeneration. 2013;21(2):292-299.
84. Tankersley A, Frank MB, Bebak M, Brennan R. Early effects of staphylococcus aureus biofilm secreted products on inflammatory responses of human epithelial keratinocytes. Journal of Inflammation. 2014;11:11-17.
85. Jones V, Bale S, Harding K. Chapter 5 Acute and chronic wound healing. In: Baranoski S, Ayello EA, editors. Wound care essentials practice principles. Ambler USA: Lippincott Williams and Wilkins; 2004. p. 61-78.
86. Iocono JA, Ehrlich HP, Gottrup F, Leaper DJ. Chapter 3 The biology of healing. In: Leaper DJ, Harding KG, editors. Wound biology and management. Oxford: Oxford University Press; 1998. p. 11-22.
87. Eaglestein WH, Alvarez OM, Mertz PM. The effect of occlusive dressings on collagen synthesis and re-epithelialisation in superficial wounds. Journnal of Surgical Research 1983;35(2):142-148.
88. Schultz GS, Sibbald GR, Falanga V, Ayello EA, Dowsett C, Harding K, et al. Wound bed preparation: a systematic approach to wound management. Wound Repair and Regeneration. 2003;11(2):S1-S28.

89. Field C, Kerstein M. Overview of wound healing in a moist environment. American Journal of Surgery. 1994;167(1a):25-65.
90. Posthauer ME, Thomas DR. Chapter 10 Nutrition and wound care. In: Baranoski S, Ayello EA, editors. Wound care essentials practice principles. Ambler USA: Lippincott Williams & Wilkins; 2004. p. 157-186.
91. Patel S. Understanding wound infection and colognisation. Wound Essentials. 2007;2:132-142.
92. Pinchcosfsky-Devon G. Nutrition and wound healing. Journal of Wound Care. 1994;3(5):231-234.
93. Dealey C. Chapter 2 The management of patients with wounds. In: Dealey C, editor. The care of wounds; a guide for nurses.Oxford: Blackwell Publishing Ltd; 2005. p. 13-55.

94. Kingsley A. A proactive approach to wound infection. Nursing standard Royal College of Nursing (Great Britain). 2001;15(30):50-58.
95. Williams REO. Benefit and mischief from commensal bacterias. Journal of Clinical Pathology. 1973;26:811-818.
96. Qin Y. Chapter 7 Antimicrobial textile dressings in managing wound infection. In: Rajendran S, editor. Advanced textiles for wound care. Boca Raton, USA: CRC Press and Woodhead Publishing Ltd; 2009. p. 179-197.
97. Stotts NA. Wound infection: diagnosis and mananagement. In: Stotts NA, Morison MJ, Ovington LG, Wilkie K, editors. Chronic wound care a problem-based learning approach.London: Mosby Elsevier Limited; 2004. p. 101-116.

98. Baranoski S, Ayello EA. Chapter 4 Skin an essential organ. In: Baranoski S, Ayello EA, editors. Wound care essentials practice principles. Ambler USA: Lippincott Williams & Wilkins; 2004. p. 47-60.
99. Gardner SE, Frantz RA. Chapter 7 Wound bioberden. In: Baranoski S, Ayello EA, editors. Wound care essentials practice principles. Ambler USA: Lippincott Williams & Wilkins; 2004. p. 91-116.
100. Mulder GD, Brazinsky BA, Harding KG, Agren MS. Factors influencing wound healing. In: Leaper DJ, Harding KG, editors. Wounds biology and management. Oxford: Oxford University Press; 1998. p. 52-70.
101. Wilson J. Infection control in clinical practice 2nd edition. London: Bailliere Tindall; 2001.
102. GA P, Sabath LD. Clinical relevance of bacteriostatic versus bactericidal mechanisms of action in the treatment of gram-positive bacterial infections. Clinincal Infectious Disease. 2004;38(6):864-870.
103. Cruse PJE, Foord R. Five year prospective study of 23,649 surgical wounds. Archives of Surgery. 1973;107(2):206-210.
104. Mangram AJ, Horan TC, Pearson ML, Silver LC, Jarvis WC. Guidelines for prevention of surgical site infections 1999. American Journal of Infection Control. 1999;27(2):97-134.
105. Siana E, Frankild S, Gottrupt E. The effect of smoking on tissue function. Jounal of Wound Care. 1992, ;1(2):37-41.
106. Jorgensen LN, Kallehave F, Christensen E, Siana JE, Gottrupt F. Less collagen production in smokers. Surgery. 1998;123(4):450-455.
107. Kiecolt- Glaser JK, Marucha PT, Malarkey WB, Mercado AM, Glaser R. Slowing of healing by psychological stress. Lancet. 1995;346(8984):1194-1196.
108. Cole-King A, Harding KG. Psychological factors and delayed healing in chronic wounds. Psychomatic Medicine. 2001;63:216-220.
109. Singleton P. Chapter 1 The bacteria: an introduction. In: Singleton P, editor. Bacteria in biology, biotechnology and medicine. Chichester, England: John Wiley and Sons Ltd; 1997 p. 1-5.
110. Russell AD, Chopra I. Understanding antibacterial action and resistance, 2nd edition. Hemel Hempstead, England: Ellis Horwood Ltd; 1996.
111. Singleton P. Chapter 11 Bacteria in medicine. In: Singleton P, editor. Bacteria in biology, biotechnology and medicine, 4th edition. Chichester, England: Wiley and Sons, Inc; 1997 p. 232-266.

112. Hentges DJ. Chapter 17 Anaerobes: general characteristics. 1996. In: Medical microbiology 4th edition [Internet]. Galvestan,Texas: University of Texas Medical Branch Available from: http://www.ncbi.nlm.nih.gov/books/NBK7638/.
113. Bowler PG, Davies BJ. The microbiology of infected and noninfected leg ulcers. International Journal of Dermatology. 1999;38(8):573-578.
114. Singleton P. Chapter 2 The Bacteria cell. In: Singleton P, editor. Bacteria in biology, biotechnology and medicine. Chichester, England: John Wiley and Sons Ltd; 1997. p. 6-34.
115. Percival S L, Hill KE, Williams DW, Hooper SJ, Thomas DW, Costerton JW. A review of the scientific evidence for biofilms in wounds. Wound Repair and Regeneration. 2012;20:647-657.
116. Davis SC, Ricotti C, Cazzaniga A, Welsh E, Eaglstein WH, Mertz PM. Microscopic and physiologic evidence for biofilm-associated wound colonization in vivo. Wound Repair and Regeneration. 2008;16(1):23-29.
117. Percival SL, Thomas JG, Williams DW. Biofilms and bacterial imbalances in chronic wounds: anti-Koch. International Wound Journal. 2010;7(3):169-175.
118. Cooper RA, Bjarnsholt T, Alhede M. Biofilms in wounds: a review of present knowledge. Journal of Wound Care. 2014;23(11):570-582.
119. Donlan RM, Costerton JW. Biofilms: Survival mechanisms of clinically relevant microorganisms. Clinical Microbiology Reviews. 2002;15(2):167-193.
120. Billings N, Millan MR, Caldara M, Rusconi R, Tarasova Y, Stocker R, et al. The extracellular matrix component Psl provides fast-acting antibiotic defense in pseudomonas aeruginosa biofilms. PLOS Pathogens. 2013;9(8):E10032526.
121. Bjarnsholt T, Kirketerp-Moller K, Kristiansen S, Phipps R, Nielsen AK, Jensen PO, et al. Silver against pseudomonas aeruginosa biofilms. Apmis. 2007;115(8):921-928.
122. Wolcott RD, Rhoads DD. A study of biofilm-based wound management in subjects with critical limb ischaemia. Journal of Wound Care. 2008;17(4):145-8, 150-2, 154-5.
123. Wolcott RD, Rhoads DD, Bennett ME, Wolcott BM, Gogokhia L, Costerton JW, et al. Chronic wounds and the medical biofilm paradigm. Journal of Wound Care. 2010;19(2):45-53.
124. James GA, Swogger E, Wolcott R, Pulcini Ed, Secor P, Sestrich J, et al. Biofilms in chronic wounds. Wound Repair and Regeneration. 2008;16(1):37-44.
125. Percival SL, Emanuel C, Cutting KF, Williams DW. Microbiology of the skin and the role of biofilms in infection. International Wound Journal. 2012;9(1):14-32.
126. Kohanski MA, Dwyer DJ, Hayete B, Lawrence CA, Collins JJ. A common mechanism of cellular death induced by bactericidal antibiotics. Cell (Cambridge, MA, U S). 2007;130(5):797-810.
127. Cooper R, Gray D. Is Manuka honey a credible alternative to silver in wound care? Wounds UK. 2012;8(4):54-64.
128. McDonnell G, Russell AD. Antiseptics and disinfectants: activity, action, and resistance. Clinical Microbiolgy Reviews. 1999;12(1):147-179.
129. Russell AD. Antibiotic and biocide resistance in bacteria: comments and conclusions. Journal of Applied Microbiology. 2002;92 Suppl:171S-173S.
130. Russell AD. Antibiotic and biocide resistance in bacteria: introduction. Journal of Applied Microbiology. 2002;92 Suppl:1S-3S.
131. Hiramatsu K, Hanaki H, Ino T, Yabuta K, Oguri T, Tenover FC. Methicillin-resistant Staphylococcus aureus clinical strain with reduced vancomycin susceptibility. Journal of Antimicrobial Chemotherapy. 1997;40(1):135-136.
132. Colsky AS, Kirsner RS, Kerdel FA. Analysis of antibiotic susceptibilities of skin wound flora in hospitalized dermatology patients. The crisis of antibiotic resistance has come to the surface. Archives of Dermatology. 1998;134(8):1006-1009.
133. McHugh GL, Moellering RC, Hopkins CC, Swartz MN. Salmonella typhimurium resistant to silver nitrate, chloramphenicol, and ampicillin. Lancet. 1975;1(7901):235-240.
134. Lowbury EJ, Babb JR, Bridges K, Jackson DM. Topical chemoprophylaxis with silver sulphadiazine and silver nitrate chlorhexidine creams: emergence of sulphonamide-resistant Gram-negative bacilli. British Medical Journal. 1976;1(6008):493-496.
135. Bridges K, Kidson A, Lowbury EJ, Wilkins MD. Gentamicin- and silver-resistant pseudomonas in a burns unit. British Medical Journal. 1979;1(6161):446-449.

136. Modak SM, Fox CL, Jr. Sulfadiazine silver-resistant pseudomonas in burns. new topical agents. Archives of Surgery. 1981;116(7):854-857.
137. Hendry AT, Stewart IO. Silver-resistant enterobacteriaceae from hospital patients. Canadian Journal of Microbiology. 1979;25(8):915-921.
138. Gupta A, Matsui K, Lo J-F, Silver S. Molecular basis for resistance to silver cations in Salmonella. Nature Medicine. 1999;5(2):183-188.
139. Gilbert P, Das J, Foley I. Biofilm susceptibility to antimicrobials. Advances in Dental Research. 1997;11(1):160-167.
140. Cooper RA, Jenkins L, Henriques AFM, Duggan RS, Burton NF. Absence of bacterial resistance to medical-grade manuka honey. European Journal of Clinical Microbiology & Infectious Diseases. 2010;29(10):1237-1241.
141. Campeau MEM, Paatel R. Antibiofilm activity of manuka honey in combination with antibiotics. International Journal of Bateriology [Internet]. 2014:[1-7 pp.].
142. Finley PJ, Huckfeldt RE, Walker KD, Shornick LP. Silver dressings improve diabetic wound healing without reducing bioburden. Wounds-Compend Clin Res Pract. 2013;25(10):293-301.
143. Bowler P, Jones S, Towers V, Booth R, D P, Walker M. Dressing conformability and silver-containing wound dressings. Wounds UK. 2010;6(2):14-20.
144. Morris C. Wound management and dressing selection. Wound Essentials. 2006;1:178-183.
145. Jones SA, Bowler PG, Walker M, Parsons D. Controlling wound bioburden with a novel silver-containing Hydrofiber((R)) dressing. Wound Repair and Regeneration. 2004;12(3):288-294.
146. Thomas S, McCubbin P. An in vitro analysis of the antimicrobial properties of 10 silver-containing dressings. Journal of Wound Care. 2003;12(8):305-308.
147. Thomas S, McCubbin P. A comparison of the antimicrobial effects of four silver containing dressings on three organisms. Journal of Wound Care. 2003;12(3):101-107.
148. Fisher NM, Marsh E, Lazova R. Scar-localized argyria secondary to silver sulfadiazine cream. Journal of the American Academy of Dermatology. 2003;49(4):730-732.
149. Bleehen SS, Gould DJ, Harrington CI, Durrant TE, Slater DN, Underwood JCE. Occupational argyria - light and electron-microscopy studies and x-ray-microanalysis. British Journal of Dermatology. 1981;104(1):19-26.
150. Sato S, Sueki H, Nishijima A. Two unusual cases of argyria: the application of an improved tissue processing method for x-ray microanalysis of selenium and sulphur in silver-laden granules. British Journal of Dermatology. 1999;140(1):158-163.
151. Buckley WR, Oster CF, Fassett DW. Localized argyria. II. chemical nature of silver containing particles. Archives of Dermatology. 1965;92(6):697-705.
152. Tanita Y, Kato T, Hanada K, Tagami H. Blue macules of localized argyria caused by impanted acupuncture needles-electron microscopy and roentgenogrphic microanalysis of deposited metal. Archives of Dermatology. 1985;121(12):1550-1552.
153. Gaul LE, Staud AH. Clinical spectroscopy - Quantitative distribution of silver in the body or its physiopathologic retention as a reciprocal of the capillary system. Archives of Dermatology and Syphilology. 1935;32(5):775-780.
154. Crane E. Honey, a comprehensive survey. London: William Heinemann; 1975.
155. British Pharmacopoeia 1993 London : H.M.S.O.
156. Austrailian Government Department of Health TGA. Honey scientific report 1998 [22-09-13]. Available from: http://www.tga.gov.au/pdf/archive/report-honey-9812.pdf.
157. Loveridge J. Chemical composition of honey [20-06-12]. Available from: http://www.chm.bris.ac.uk/webprojects2001/loveridge/index-page3.html.
158. Kramer SN. Levey an older pharmacopoeia. Journal of American Medical Association. 1954;155(1):26.
159. Mullick NP. Honey and beekeeping in the scriptures and after. Indian Bee Journal 1944;6 108-114.
160. Zumla A, Lulat A. Honey - a remedy rediscovered. Journal of the Royal Society of Medicine. 1989;82(7):384-385.
161. Crane E. Chapter 47 History of the uses of honey. In: Crane E, editor. The world history of beekeeping and honey hunting. London: Gerald Duckworth & Co Ltd; 1999. p. 502-512.

162. Haynes JS, Callaghan R. Properties of honey: its mode of action and clinical outcomes. Wounds UK. 2011;7(1):50-57.
163. Dold H, Du DH, Dziao ST. The antibacterial, heat- and light-sensitive inhibiting substance, inhibine, in natural honey (flower honey). Zeitschrift für Hygiene und Infektionskrankheiten. 1937;120:155-167.
164. White JW, Schepartz AI, Subers MH. Identification of inhibine, antibacterial factor in honey, as hydrogen peroxide and its origin in a honey glucose-oxidase system. Biochimica Et Biophysica Acta. 1963;73(1):57-70.
165. Aurongzeb M, Kamran AM. Antimicrobial properties of natural honey: a review of literature. Pakistan Journal of Biochemical Molecular Biology. 2011;44(3):118-124
166. Bang LM, Buntting C, Molan P. The effect of dilution on the rate of hydrogen peroxide production in honey and its implications for wound healing. Journal of Alternative and Complement Medicine. 2003;9(2):267-273.
167. Lusby PE, Coombes A, Wilkinson JM. Honey: a potent agent for wound healing? Journal of Wound Ostomy & Continence Nursing. 2002;29(6):295-300.
168. Weston RJ. The contribution of catalase and other natural products to the antibacterial activity of honey: a review. Food Chemistry. 2000;71:235-239.
169. Kwakman PHS, Zaat SAJ. Antibacterial components of honey. IUBMB Life. 2012;64(1):48-55.
170. Molan PC. The antibacterial activity of honey. 1. the nature of the antibacterial activity. Bee World. 1992;73:5-28.
171. White JW. Composition of Honey. In: Crane E, editor. Honey: A comprehensive survey. London: William Heinemann Ltd; 1975. p. 157-205.
172. Mavric E, Wittmann S, Barth G, Henle T. Identification and quantification of methylglyoxal as the dominant antibacterial constituent of manuka (leptospermum scoparium) honeys from New Zealand. Molecular Nutrition and Food Research. 2008;52:483-489.
173. Molan PC, Russell KM. Non-peroxide antibacterial activity in some new zealand honeys. Journal of Apicultural Research. 1988;27(1):62-67.
174. Allen KL, Molan PC, Reid GM. A survey of the antibacterial activity of some new zealand honeys. Journal of Pharmacology and Pharmacotherapeutics. 1991;43(12):817-822.
175. McDonald Counsell SJ. The factors responsible for the varying levels of UMF® in mānuka (leptospermum scoparium) honey [Ph.D. thesis]: University of Waikato; 2006.
176. Russell KM. The antibacterial properties of honey [MS.c Thesis]: University of Waikato; 1983.
177. Molan PC, Smith IM, Reid GM. A comparison of the antibacterial activities of some new zealand honeys. Journal of Apicultural Research. 1988;27(4):252-256.
178. Russell KM, Molan PC, Wilkins AL, Holland PT. Identification of some antibacterial constituents of new zealand manuka honey. Journal of Agricultural and Food Chemistry. 1990;38(1):10-13.
179. Wilkins AL, Lu Y, Molan PC. Extractable organic substances from new zealand unifloral manuka. Journal of Apicultural Research. 1993;32(1):3-9.
180. Steeg E, Montag A. Aromatic carbonic-acids of honey. Zeitschrift Fur Lebensmittel-Untersuchung Und-Forschung. 1987;184(1):17-19.
181. Weston RJ, Mitchell KR, Allen KL. Antibacterial phenolic components of new zealand manuka honey. Food Chemisty. 1998;64(3):295-301.
182. Weigel KU, Opitz T, Henle T. Studies on the occurrence and formation of 1,2-dicarbonyls in honey. European Food Reseach and Technology. 2004;218(2):147-151.
183. Hayashi K, Fukushima A, Hayashi-Nishino M, Nishino K. Effect of methylglyoxal on multidrug-resistant pseudomonas aeruginosa. Frontiers in Microbiology. 2014;5(180):1-6.
184. Adams CJ, Manley-Harris M, Molan PC. The origin of methylglyoxal in new zealand manuka (leptospermum scoparium) honey. Carbohydrate Research. 2009;344(8):1050-1053.
185. Natarajan S, Williamson D, Grey J, Harding KG, Cooper RA. Healing of an MRSA-colonized, hydroxyurea-induced leg ulcer with honey. Journal of Dermatological Treatment. 2001;12(1):33-36.
186. Van der Weyden EA. Treatment of a venous leg ulcer with a honey alginate dressing. British Journal of Community Nursing. 2005;Supplement:S21-S27.

187. Gethin G, Cowman S. Case series of use of manuka honey in leg ulceration. International Wound Journal. 2005;2(1):10-15.
188. Gethin G, Cowman S. Bacteriological changes in sloughy venous leg ulcers treated with manuka honey or hydrogel: an RCT. Journal of Wound Care. 2008;17(6):241-247.
189. Hampton S, Coulborn A, Tadej M, Bree-Aslan C. Using a superabsorbent dressing and antimicrobial for a venous ulcer. British Journal of Nursing 2011;20(15):S40-S43.
190. Molan PC, Betts JA. Using honey to heal diabetic foot ulcers. Advances in skin & wound care. 2008;21(7):313-316.
191. Kamaratos AV, Tzirogiannis KN, Iraklianou SA, Panoutsopoulos GI, Kanellos IE, Melidonis AI. Manuka honey-impregnated dressings in the treatment of neuropathic diabetic foot ulcers. International Wound Journal. 2014;11(3):259-263.
192. Cooper RA, Halas E, Molan PC. The efficacy of honey in inhibiting strains of pseudomonas aeruginosa from infected burns. Journal of Burn Care & Rehabilitation. 2002;23(6):366-370.
193. Bischofberger AS, Dart CM, Perkins NR, Kelly A, Jeffcott L, Dart AJ. The effect of short- and long-term treatment with manuka honey on second intention healing of contaminated and noncontaminated wounds on the distal aspect of the forelimbs in horses. Vetenary Surgery. 2013;42:154-160.
194. Cooper RA, Molan PC, Krishnamoorthy L, Harding KG. Manuka honey used to heal a recalcitrant surgical wound. European Journal of Clinical Microbiology & Infectious Diseases. 2001;20:758-759.
195. Chopra I, Hesse L, O'Neill AJ. Exploiting current understanding of antibiotic action for discovery of new drugs. Society of Applied Microbiology Symposium Series. 2002;31(Antibiotic and biocide resistance in bacteria):4S-15S.
196. Jenkins R, Burton N, Cooper R. Manuka honey inhibits cell division in methicillin-resistant staphylococcus aureus. Journal of Antimicrobial Chemotherapy.2011;66(11):2536-2542.
197. Cooper R, Jenkins L, Rowland R. Inhibition of biofilms through the the use of manuka honey. Wounds UK. 2011;7(1):24-32.
198. Sherlock O, Dolan A, Athman R, Power A, Gethin G, Cowman S, et al. Comparison of the antimicrobial activity of ulmo honey from chile and manuka honey against methicillin-resistant staphylococcus aureus, escherichia coli and pseudomonas aeruginosa. BMC Complement and Alternative Medicine. 2010;10(47):2-5.
199. Majtan J, Bohova J, Horniackova M, Klaudiny J, Majtan V. Anti-biofilm effects of honey against wound pathogens proteus mirabilis and enterobacter cloacae. Phytotherapy Research. 2014;28(1):69-75.
200. Cooper R, Hooper S, Jenkins L. Inhibition of biofilms of pseudomonas aeruginosa by medihoney in vitro. Journal of Wound Care. 2014;23(3):93-6, 98-100.
201. Henriques AF, Jenkins RE, Burton NF, Cooper RA. The effect of manuka honey on the structure of pseudomonas aeruginosa. European Journal of Clinical Microbiology & Infectious Diseases. 2011;30(2):167-171.
202. Maddocks SE, Lopez MS, Rowlands RS, Cooper RA. Manuka honey inhibits the development of streptococcus pyogenes biofilms and causes reduced expression of two fibronectin binding proteins. Microbiology 2012;158(3):781-790.
203. Lin SM, Molan PC, Cursons RT. The controlled in vitro susceptibility of gastrointestinal pathogens to the antibacterial effect of manuka honey. European Journal of Clinical Microbiology & Infectious Diseases. 2011;30(4):569-574.
204. Badet C, Quero F. The in vitro effect of manuka honeys on growth and adherence of oral bacteria. Anaerobe. 2011;17:19-22.
205. Hammond EN, Donkor ES, Brown CA. Biofilm formation of clostridium difficile and susceptibility to manuka honey. Bmc Complementary and Alternative Medicine [Internet]. 2014 Sep 3; 14(329):[2-6 pp.]. Available from: <Go to ISI>://WOS:000342102500001.
206. Camplin AL, Maddocks SE. Manuka honey treatment of biofilms of pseudomonas aeruginosa results in the emergence of isolates with increased honey resistance. Annals of Clinical Microbiology and Antimicrobials. 2014;13(19):1-5.
207. Derma Sciences. Antibacterial dressing medihoney with with active leptospermum honey 2015 [08/10/15]. Available from: http://outside-us.dermasciences.com/medihoney.

208. Advancis Medical. Product range: activon manuka honey dressings 2014 [08/10/15]. Available from: http://www.advancismedical.com/products/activon-manuka-honey.
209. L-Mestitran. Products 2015 [08/10/15]. Available from: http://www.l-mesitran.com/en/products.
210. Nemet I, Varga-Defterdarovic L, Turk Z. Methylglyoxal in food and living organisms. Molecular Nutrition and Food Research. 2006;50(12):1105-1117.
211. Kalapos MP. Methylglyoxal in living organisms. chemistry, biochemistry, toxicology and biological implications. Toxicology Letters. 1999;110(3):145-175.
212. Barros A, Rodrigues JA, Almeida PJ, Oliva-Teles MT. Determination of glyoxal, methylglyoxal, and diacetyl in selected beer and wine, by HPLC with UV spectrophotometric detection, after derivatization with o-phenylenediamine. Journal of Liquid Chromatography and Related Technologies. 1999;22(13):2061-2069.
213. Hayashi T, Shibamoto T. Analysis of methyl glyoxal in foods and beverages. Journal of Agricultural and Food Chemistry. 1985;33(6):1090-1093.
214. Nagao M, Wakabayashi K, Fujita Y, Tahira T, Ochiai M, Sugimura T. Mutagenic compounds in soy sauce, chinese cabbage, coffee and herbal teas. Progress in Clinical and Biological Research. 1986;206:55-62.
215. Creighton DJ, Migliorini M, Pourmotabbed T, Guha MK. Optimization of efficiency in the glyoxalase pathway. Biochemistry. 1988;27(19):7376-7384.
216. Nemet Ina, Vikic-Topic Drazen, Varga-Defterdarovic Lidija. Spectroscopic studies of methylglyoxal in water and dimethylsulfoxide. Bioorganic Chemistry. 2004;32(6):560-570.
217. Goswami P. Chemical structure of methylglyoxal. Powerpoint 2007. University of Leeds.2013.
218. Tiffany BD, Wright JB, Moffett RB, Heinzelman RV, Strube RE, Aspergren BD, et al. Antiviral compounds. I. aliphatic glyoxals, α-hydroxyaldehydes, and related compounds. Journal of American Chemical Society. 1957;79:1682-1687.
219. French FA, Freedlander BL. Carcinostatic action of polycarbonyl compounds and their derivatives. I. 3-ethoxy-2-ketobutyraldehyde and related compounds. Cancer Research. 1958;18:172-175.
220. Bhattacharyya N, Pal A, Patra S, Haldar AK, Roy S, Ray M. Activation of macrophages and lymphocytes by methylglyoxal against tumor cells in the host. International Immunopharmacol. 2008;8(11):1503-1512.
221. Kang YB, Edwards LG, Thornalley PJ. Effect of methylglyoxal on human leukaemia 60 cell growth: modification of DNA, G(1) growth arrest and induction of apoptosis. Leukemia Research. 1996;20(5):397-405.
222. Egyud LG, Szentgyo A. Cancerostatic action of methylglyoxal Science. 1968;160(3832):1140.
223. Jiang D, Liang J, Noble PW. Hyaluronan in tissue injury and repair. Annual Review of Cell and Developmental Biology. Annual Review of Cell and Developmental Biology. 232007. p. 435-461.
224. Shipanova IN, Glomb MA, Nagaraj RH. Protein modification by methylglyoxal: Chemical nature and synthetic mechanism of a major fluorescent adduct. Archives of Biochemistry and Biophysics. 1997;344(1):29-36.
225. Lo TWC, Westwood ME, McLellan AC, Selwood T, Thornalley PJ. Binding and modifaction of proteins by methylglyoxal binding and modification of prtoeins by methylglyoxal under physiological conditions - a kinetic and mechanistic study with n-alpha-acterylarginnie, n-alpha-acetycysteine, and n-alpha-acetyllysine, and bovine serum-albumin. Journal of Biological Chemistry. 1994;269(51):32299-32305.
226. Baynes JW. Chemical modification of proteins by lipids in diabetes. Clinical Chemistry and Laboratory Medicine. 2003;41(9):1159-1165.
227. Yamagishi S-i, Maeda S, Matsui T, Ueda S, Fukami K, Okuda S. Role of advanced glycation end products (AGEs) and oxidative stress in vascular complications in diabetes. Biochimica Et Biophysica Acta-General Subjects. 2012;1820(5):663-671.
228. Yap FYT, Kantharidis P, Coughlan MT, Slattery R, Forbes JM. Advanced glycation end products as environmental risk factors for the development of type 1 diabetes. Current Drug Targets. 2012;13(4):526-540.

229. Rabbani N, Thornalley PJ. Glyoxalase in diabetes, obesity and related disorders. Seminars in Cell Development & Biology. 2011;22(3):309-317.
230. Sassi-Gaha. S LD, Kappler. F, Schwartz. ML, Su. B, Tobia. AM and Artlett. CM. Two dicarbonyl compounds, 3-deoxyglucosone and methylglyoxal, differentially modulate dermal fibroblasts. Matrix Biology. 2010;29(2):127-134.
231. Majtan J. Methylglyoxal-a potential risk factor of manuka honey in healing of diabetic ulcers. Evidence-Based Complementary and Alternative Medicine. 2011:1-5.
232. Seghal PK, Sripriya R, Senthikuma M. Chapter 9 Drug delivery dressings. In: Rajendran S, editor. Advanced textile for woundcare. Boca Raton, USA: CRC Press, Woodhead Publishing Limited; 2009. p. 223-253.
233. Yang D, Li Y, Nie J. Preparation of gelatin/pva nanofibers and their potential application in controlled release of drugs. Carbohydrate Polymers. 2007;69(3):538-543.
234. Hoare TR, Kohane DS. Hydrogels in drug delivery: progress and challenges. Polymer. 2008;49(8):1993-2007.
235. Abrigo M, McArthur SL, Kingshott P. Electrospun nanofibers as dressings for chronic wound care: advances, challenges, and future prospects. Macromolecular Bioscience. 2014;14(6):772-792.
236. Moody A. Use of a hydrogel dressing for management of a painful ulcer. British Journal of Community Nursing. 2006;11:S12-S17.
237. Kamoun EA, Chen X, Mohy EMS, Kenawy E. Crosslinked poly(vinyl alcohol) hydrogels for wound dressing applications: A review of remarkably blended polymers. Arabian Journal of Chemistry. 2015;8(1):1-14.
238. Giusti P, Lazzeri L, Barbani N, Narducci P, Bonaretti A, Palla M, et al. Hydrogels of poly(vinyl alcohol) and collagen as new bioartificial materials. Journal of Materials Science: Materials in Medicine. 1993;4(6):538-542.
239. Jiang S, Liu S, Feng W. PVA hydrogel properties for biomedical application. Journal of the Mechanical Behavior of Biomedical Materials. 2011;4(7):1228-1233.
240. Lay-Flurrie K. The properties of hydrogel dressings and their impact on wound healing. Professional Nurse 2004;19(5):269-273.
241. Jones V, Grey JE, Harding KG. ABC of wound healing: wound dressings. British Medical Journal. 2006;332:777-780.
242. Koski A, Yim K, Shivkumar S. Effect of molecular weight on fibrous pva produced by electrospinning Materials Letters. 2004;58:493– 497.
243. Supaphol P, Chuangchote S. On the electrospinning of poly(vinyl alcohol) nanofiber mats: a revisit. Journal of Applied Polymer Science. 2008;108:969–978
244. DeMerlis CC, Schoneker DR. Review of the oral toxicity of polyvinyl alcohol (pva). Food and Chemical Toxicology. 2003;41(3):319-326.
245. Cascone MG, Sim B, Sandra D. Blends of synthetic and natural polymers as drug delivery systems for growth hormone. Biomaterials. 1995;16(7):569-574.
246. Kim JO, Park JK, Kim JH, Jin SG, Yong CS, Li DX, et al. Development of polyvinyl alcohol–sodium alginate gel-matrix-based wound dressing system containing nitrofurazone. International Journal of Pharmaceutics. 2008;359(1–2):79-86.
247. Suzuki Y, Tanihara M, Nishimura Y, Suzuki K, Kakimaru Y, Shimizu Y. A new drug delivery system with controlled release of antibiotic only in the presence of infection. Journal of Biomedical Materials Research. 1998;42(1):112-116.
248. Chiellini E, Corti A, D'Antone S, Solaro R. Biodegradation of poly (vinyl alcohol) based materials. Progress in Polymer Science. 2003;28(6):963-1014.
249. Yu HJ, Xu XY, Chen XS, Hao JQ, Jing XB. Medicated wound dressings based on poly(vinyl alcohol)/poly(N-vinyl pyrrolidone)/chitosan hydrogels. Journal of Applied Polymer Science. 2006;101(4):2453-2463.
250. Bolto B, Tran T, Hoang M, Xie Z. Crosslinked poly(vinyl alcohol) membranes. Progress in Polymer Science. 2009;34(9):969-981.
251. Wang YH, Hsieh YL. Crosslinking of polyvinyl alcohol (pva) fibrous membranes with glutaraldehyde and peg diacylchloride. Journal of Applied Polymer Science. 2010;116(6):3249-3255.
252. M'Barki O, Hanafia A, Bouyer D, Faur C, Sescousse R, Delabre U, et al. Greener method to prepare porous polymer membranes by combining thermally induced phase

separation and crosslinking of poly (vinyl alcohol) in water. Journal of Membrane Science. 2014;458:225-235.
253. Tang C, Saquing CD, Harding JR, Khan SA. In situ cross-linking of electrospun poly(vinyl alcohol) nanofibers. Macromolecules. 2010;43(2):630-637.
254. Destaye AG, Lin C-K, Lee C-K. Glutaraldehyde vapor cross-linked nanofibrous pva mat with in situ formed silver nanoparticles. ACS Applied Materials & Interfaces. 2013;5(11):4745-4752.
255. Wang XF, Chen XM, Yoon K, Fang DF, Hsiao BS, Chu B. High flux filtration medium based on nanofibrous substrate with hydrophilic nanocomposite coating. Environmental Science & Technology. 2005;39(19):7684-7691.
256. Mansur HS, Sadahira CM, Souza AN, Mansur AAP. FTIR spectroscopy characterization of poly (vinyl alcohol) hydrogel with different hydrolysis degree and chemically crosslinked with glutaraldehyde. Materials Science & Engineering C-Biomimetic and Supramolecular Systems. 2008;28(4):539-548.
257. Formhals A, inventor*Process and apparatus for preparing artificial threads*. US 1975504 A patent US 1975504 A. 1934.
258. Taylor G. Disintegration of water droplets in an electric field. Proceedings of the Royal Society of London, series A, mathematical and physical sciences. 1964;280(1382):383-397.
259. Teo WE, Ramakrishna S. A review on electrospinning design and nanofibre assemblies. Nanotechnology. 2006;17:R89–R106
260. Li D, Xia Y. Electrospinning of nanofibers: reinventing the wheel? Advanced Materials. 2004;16(14):1151-1170.
261. Wang X, Nui H, Lin T, Wang X. Needleless electrospinning of nanofibers with a conical wire coil. Polymer Engineering and Science. 2009;49(8):1582-1586.
262. Han W, Nurwaha D, Li C, Wang X. Free surface electrospun fibers: the combined effect of processing parameters. Polymer Engineering and Science. 2014;54(1):189-197.
263. Jirsak O, Sanetrink F, Lukas D, Kotek V, Martinova L, Chaloupek J, inventors*A method of nanofibres production from a polymer solution using electrostatic spinning and a device for carrying out the method*. US 7585437 B2.2005.
264. Petrik S, Maly M. Production nozzle-less electrospinning nanofibre technology: Elmarco s.r.o.; 2009 [14/06/12]. Available from: http://www.elmarco.cz/upload/soubory/dokumenty/66-1-1-mrs-fall-boston-09.pdf.
265. Lukas D, Sarkar A, Pokorny P. Self-organization of jets in electrospinning from free liquid surface: a generalized approach. Journal of Applied Physics. 2008;103(8):084309.
266. Adomaviciute E, Stanys S. Formation of electrospun pva mats on different types of support materials using various kinds of grounded electrodes. Fibres & Textiles in Eastern Europe. 2011;19(4):34-40.
267. Ramakrishna S, Fujihara K, Teo WE, Lim TC, Ma Z. Chapter 3 Electrospinning process. An introduction to electrospinning and nanofibres. Singapore: World Scientific Publishing Co. Pte. Ltd; 2005. p. 90-154.
268. Zong XH, Kim K, Fang DF, Ran SF, Hsiao BS, Chu B. Structure and process relationship of electrospun bioabsorbable nanofiber membranes. Polymer. 2002;43(16):4403-4412.
269. Shenoy SL, Bates WD, Frisch HL, Wnek GE. Role of chain entanglements on fiber formation during electrospinning of polymer solutions: good solvent, non-specific polymer-polymer interaction limit. Polymer. 2005;46(10):3372-3384.
270. Lee KH, Kim HY, Bang HJ, Jung YH, Lee SG. The change of bead morphology formed on electrospun polystyrene fibers. Polymer. 2003;44(14):4029-4034.
271. Choi JS, Lee SW, Jeong L, Bae SH, Min BC, Youk JH, et al. Effect of organosoluble salts on the nanofibrous structure of electrospun poly(3-hydroxybutyrate-co-3-hydroxyvalerate). International Journal of Biological Macromolecules. 2004;34(4):249-256.
272. Zhang CX, Yuan XY, Wu LL, Han Y, Sheng J. Study on morphology of electrospun poly(vinyl alcohol) mats. European Polymer Journal. 2005;41(3):423-432.
273. Uyar T, Besenbacher F. Electrospinning of uniform polystyrene fibers: the effect of solvent conductivity. Polymer. 2008;49(24):5336-5343.

274. Lee JS, Choi KH, Ghim HD, Kim SS, Chun DH, Kim HY, et al. Role of molecular weight of atactic poly(vinyl alcohol) (pva) in the structure and properties of pva nanofabric prepared by electrospinning. Journal of Applied Polymer Science. 2004;93(4):1638-1646.
275. Buchko CJ, Chen LC, Shen Y, Martin DC. Processing and microstructural characterization of porous biocompatible protein polymer thin films. Polymer. 1999;40:7397-7407.
276. Deitzel JM, Kleinmeyer J, Harris D, Tan NCB. The effect of processing variables on the morphology of electrospun nanofibers and textiles. Polymer. 2001;42(1):261-272.
277. Yuan XY, Zhang YY, Dong CH, Sheng J. Morphology of ultrafine polysulfone fibers prepared by electrospinning. Polymer International. 2004;53(11):1704-1710.
278. Huang L, Nhu-Ngoc B, Manickam SS, McCutcheon JR. Controlling electrospun nanofiber morphology and mechanical properties using humidity. Journal of Polymer Science Part B-Polymer Physics. 2011;49(24):1734-1744.
279. Demir MM, Yilgor I, Yilgor E, Erman B. Electrospinning of polyurethane fibers. Polymer. 2002;43(11):3303-3309.
280. Bhardwaj N, Kundu SC. Electrospinning: A fascinating fiber fabrication technique. Biotechnology Advances. 2010;28(3):325-347.
281. Huang Z-M, Zhang YZ, Kotaki M, Ramakrishna S. A review on polymer nanofibers by electrospinning and their applications in nanocomposites. Composites Science and Technology. 2003;63(15):2223-2253.
282. Gibson P, Schreuder-Gibson H, Rivin D. Transport properties of porous membranes based on electrospun nanofibers. Colloids and Surfaces A: Physicochemical and Engineering Aspects. 2001;187:469-481.
283. Wnek GE, Carr ME, Simpson DG, Bowlin GL. Electrospinning of nanofiber fibrinogen structures. Nano Letters. 2003;3(2):213-216.
284. Zhang Y, Lim C, Ramakrishna S, Huang Z-M. Recent development of polymer nanofibers for biomedical and biotechnological applications. Journal of Materials Science: Materials in Medicine. 2005;16(10):933-946.
285. Dabney SE. The use of electrospinning technology to produce wound dressings [Ph.D. thesis]: University of Akron; 2002.
286. Khil M-S, Cha D-I, Kim H-Y, Kim I-S, Bhattarai N. Electrospun nanofibrous polyurethane membrane as wound dressing. Journal of Biomedical Materials Research Part B: Applied Biomaterials. 2003;67B(2):675-679.
287. Maleki H, Gharehaghaji AA, Dijkstra PJ. A novel honey-based nanofibrous scaffold for wound dressing application. Journal of Applied Polymer Science. 2013;127:4086-4092.
288. Hong KH. Preparation and properties of electrospun poly (vinyl alcohol)/silver fiber web as wound dressings. Polymer Engineering and Science. 2007;47(1):43-49.
289. Taepaiboon P, Rungsardthong U, Supaphol P. Drug-loaded electrospun mats of poly(vinyl alcohol) fibres and their release characteristics of four model drugs. Nanotechnology. 2006;17(9):2317-2329.
290. Bulman SEL, Goswami P, Tronci G, Russell SJ, Carr C. Investigation into the potential use of poly(vinyl alcohol)/methylglyoxal fibres as antibacterial wound dressing components. Journal of Biomaterials Applications. 2015;29(8):1193-1200.
291. Kenawy E-R, Abdel-Hay FI, El-Newehy MH, Wnek GE. Controlled release of ketoprofen from electrospun poly(vinyl alcohol) nanofibers. Materials Science and Engineering: A Structural Materials: Properties, Microstructure and Processing. 2007;459(1-2):390-396.
292. Shalumon KT, Anulekha KH, Nair SV, Chennazhi KP, Jayakumar R. Sodium alginate/poly(vinyl alcohol)/nano zno composite nanofibers for antibacterial wound dressings. International Journal of Biological Macromolecules. 2011;49(3):247-254.
293. Tarun K, Gobi N. Calcium alginate/pva blended nanofibre matrix for wound dressing. Indian Journal of Fibre Textile Research. 2012;37:127-132.
294. Sirc J, Kubinova S, Hobzova R, Stranska D, Kozlik P, Bosakova Z, et al. Controlled gentamicin release from multi-layered electrospun nanofibrous structures of various thicknesses. International Journal of Nanomedicine. 2012;7:5315-5325.
295. Xu C, Xu F, Wang B, Lu TJ. Electrospinning of poly(ethylene-co-vinyl alcohol) nanofibres encapsulated with ag nanoparticles for skin wound healing. Journal of Nanomaterials. 2011;201834:1-7.

296. Kang YO, Yoon I-S, Lee SY, Kim D-D, Lee SJ, Park WH, et al. Chitosan-coated poly(vinyl alcohol) nanofibers for wound dressings. Journal of Biomedical Materials Research Part B: Applied Biomaterials. 2010;92B(2):568-576.
297. Zhou Y, Yang H, Liu X, Mao J, Gu S, Xu W. Electrospinning of carboxyethyl chitosan/poly(vinyl alcohol)/silk fibroin nanoparticles for wound dressings. International Journal of Biological Macromolecules. 2013;53:88-92.
298. Ranjbar-Mohammadi M, Bahrami SH, Joghataei MT. Fabrication of novel nanofiber scaffolds from gum tragacanth/poly(vinyl alcohol) for wound dressing application: In vitro evaluation and antibacterial properties. Materials Science and Engineering: C. 2013;33(8):4935-4943.
299. Goodwin JW, Hughes RW. Chapter 1: Introduction. 2 ed: RSC Publishing; 2008. 1-13
300. Munnik JN, editor Introduction to Dynamic Viscometry. Rheology & Methodology Seminar; 2012; Coventry.
301. Brookfield Engineering Laboratories. More solutions to sticky problems: a guide to getting more from your brookfield viscometer. Brookfield Engineering Lab, Inc.2014. Available from: http://www.brookfieldengineering.com/support/documentation/solutions-to-sticky-problems.asp.
302. Patterson C. Viscosity and stuff. Lecture at the University of Leeds, Chemistry Department.23rd October 2011.
303. Yuan Y, Lee TR. Contact Angle and Wetting Properties. In: Bracco G, Holst B, editors. Surface Science Techniques. Springer Series in Surface Sciences. 51: Springer Berlin Heidelberg; 2013. p. 3-34.
304. Kruss GmbH. Wilhelmy plate method Hamburg, Germany2014 [09/07/14]. Available from: http://www.kruss.de/services/education-theory/glossary/wilhelmy-plate-method/.
305. Eutech Instruments. Conductivity cell instruction guide 2010.
306. Golnabi H, Matloob MR, Bahar M, Sharifian M. Investigation of electrical conductivity of different water liquids and electrolyte solutions. Iranian Physical Journal. 2009; 3-2: 24-28
307. Semat H, Katz R. Electrical conduction in liquids and solids. Physics. 1958:524-538.
308. Speight JG. Lange's handbook of chemistry 16 edition. Speight JG, editor. New York: McGraw-Hill Professional; 2005.
309. Lawrence CA. Lecture 2, fibres and technical textiles.: University of Leeds; October 2010.
310. Mirau PA. A Practical Guide to Understanding the NMR of Polymers. Hoboken, New Jersey: John Wiley & Sons, Inc.; 2005.
311. Field LD. Introduction In: Field LE, Sternhell S, editors. Analytical NMR. Petersfield, UK: John Wiley and Sons Ltd; 1989. p. 1-3.
312. Lambert JB, Mazzola EP. Nuclear magnetic resonance spectroscopy 'an introduction to principles, applications and experimental methods. London: Pearson Educations Ltd; 2004.
313. Ault A, Dudek GO. NMR an introduction to proton magnetic resonance spectroscopy. San Francisco, California: Holden-Day, Inc.; 1976.
314. BS EN ISO 20743 Textiles —Determination of antibacterial activity of antibacterial finished products. 2007.
315. BS EN ISO 20645: Textile fabrics - determination of antibacterial activity - agar diffusion plate test. 2004.
316. Clinical and Laboratory Standards Institute. M07-A9. Methods for dilution antimicrobial susceptibility tests for bacteria that grow aerobically; approved standard - 9th edition. 2012.
317. Naushad M, Khan MR, Alothman ZA. Chapter 1 History and introduction of UPLC/MS. 2014. In: Ultra performance liquid chromatography mass spectrometry [Internet]. Boca Raton, USA: CRC Press Taylor and Francis Group LLC; [1-15]. Available from: http://www.crcnetbase.com/doi/abs/10.1201/b16670-2.
318. Riley CM. Chapter 2 Efficiency, retention, selectivity and resolution in chromatography. In: Lough WJ, Wainer IW, editors. High performance liquid chromatography: fundamental principles and practice. London, UK: Blackie Academic & Professional; 1995. p. 15-35.

319. Riley CM. Chapter 3 Modes of chromatography. In: Lough WJ, Wainer IW, editors. High performance liquid chromatography. London, UK: Blackie Academic & Professional 1995. p. 36-77.
320. Graham WG. Part 1: The physics and chemistry of plasmas for processing textiles and other materials. In: Shishoo R, editor. Plasma technologies for textiles. Roca Raton: Woodhead Publishing Limited and CRC Press LLC; 2007. p. 3-24.
321. Shahidi S, Ghoranneviss M, Moazzenchi B. New advances in plasma technology for textile. Journal of Fusion Energy. 2014;33(2):97-102.
322. Lippens P. Part 3: Low-pressure cold plasma processing technology. In: Shishoo R, editor. Plasma technologies for textiles. Boca Raton: Woodhead Publishing Limited and CRC Press LLC; 2007. p. 64-78.
323. Marcandalli B, Riccardi C. Part 11: Plasma treatments of fibre and textiles. In: Shishoo R, editor. Plasma technologies for textiles. Boca Raton: Woodhead Publishing Limited and CRC Press LLC; 2007. p. 282-300.
324. Willix DJ, Molan PC, Harfoot CG. A comparison of the sensitivity of wound-infecting species of bacteria to the antibacterial activity of manuka honey and other honey. Journal of Applied Bacteriology. 1992;73:388-394.
325. Visavadia BG, Honeysett J, Danford M. Manuka honey dressing: an effective treatment for chronic wound infections. British Journal of Oral and Maxillofac Surgery. 2008;46:696-697.
326. Männer J, Schuster KC, Suchomel F, Gürtler A, Firgo H. Higher performance with natural intellegence. Lenzinger Berichte. 2004;83:99-110.
327. Firgoa H, Schustera KC, Suchomela F, Männera J, Burrow T, Abu-Rousb M. The functional properties of Tencel ® - a current Update Lenzinger Berichte. 2006;85:22-30.
328. Abu-Rous M, Ingolic E, Schuster KC. Visualisation of the fibrillar and pore morphology of cellulosic fibres applying transmission electron microscopy. Cellulose. 2006;13(4):411-419.
329. Thomas ST. Chapter 2 Testing dressings and wound management materials. In: Rajendran S, editor. Advanced textiles for wound care. Cambridge: Woodhead Publishing Ltd; 2009. p. 20-47.
330. Gómez-Díaz D, Navaza JM, Quintáns-Riveiro LC. Effect of temperature on the viscosity of honey. International Journal of Food Properties. 2009;12(2):396-404.
331. Yoo B. Effect of temperature on dynamic rheology of korean honeys. Journal of Food Engineering. 2004;65(3):459-463.
332. Mossel B, Bhandari B, D'Arcy B, Caffin N. Use of an arrhenius model to predict rheological behaviour in some australian honeys. Lebensmittel-Wissenschaft Und-Technologie-Food Science and Technology. 2000;33(8):545-552.
333. Sekiguchi J-I, Asagi T, Miyoshi-Akiyama T, Kasai A, Mizuguchi Y, Araake M, et al. Outbreaks of multidrug-resistant pseudomonas aeruginosa in community hospitals in Japan. Journal of Clinical Microbiology. 2007;45(3):979-989.
334. Kilty SJ, Duval M, Chan FT, Ferris W, Slinger R. Methylglyoxal: (active agent of manuka honey) in vitro activity against bacterial biofilms. International Forum of Allergy & Rhinology. 2011;1(5):348-350.
335. Jervis-Bardy J, Foreman A, Bray S, Tan L, Wormald P-J. Methylglyoxal-Infused Honey Mimics the Anti-Staphylococcus aureus Biofilm Activity of Manuka Honey: Potential Implication in Chronic Rhinosinusitis. Laryngoscope. 2011;121(5):1104-1107.
336. Finberg RW, Moellering RC, Tally FP, Craig WA, Pankey GA, Dellinger EP, et al. The importance of bactericidal drugs: future directions in infectious disease. Clinical Infectious Diseases. 2004;39(9):1314-1320.
337. Liu Y, He J-H, Yu J-y, Zeng H-m. Controlling numbers and sizes of beads in electrospun nanofibers. Polymer International. 2008;57(4):632-636.
338. Santos C, Silva CJ, Buttel Z, Guimaraes R, Pereira SB, Tamagnini P, et al. Preparation and characterization of polysaccharides/pva blend nanofibrous membranes by electrospinning method. Carbohydrate Polymers. 2014;99:584-592.
339. Ding B, Kim HY, Lee SC, Shao CL, Lee DR, Park SJ, et al. Preparation and characterization of a nanoscale poly(vinyl alcohol) fiber aggregate produced by an electrospinning method. Journal of Polymer Science Part B-Polymer Physics. 2002;40(13):1261-1268.

340. Kenawy E-R, Layman JM, Watkins JR, Bowlin GL, Matthews JA, Simpson DG, et al. Electrospinning of poly(ethylene-co-vinyl alcohol) fibers. Biomaterials. 2003;24(6):907-913.
341. Fong H, Chun I, Reneker DH. Beaded nanofibers formed during electrospinning. Polymer. 1999;40:4585–4592.
342. Megelski S, Stephens JS, Chase DB, Rabolt JF. Micro-and nanostructured surface morphology on electrospun polymer fibers. Macromolecules. 2002;35(22):8456-8466.
343. Sukigara S, Gandhi M, Ayutsede J, Micklus M, Ko F. Regeneration of bombyx mori silk by electrospinning - part 1: processing parameters and geometric properties. Polymer. 2003;44(19):5721-5727.
344. Hohman MM, Shin M, Rutledge G, Brenner MP. Electrospinning and electrically forced jets. II. applications. Physics of Fluids. 2001;13(8):2221-2236.
345. Pawlowski KJ, Belvin HL, Raney DL, Su J, Harrison JS, Siochi EJ. Electrospinning of a micro-air vehicle wing skin. Polymer. 2003;44(4):1309-1314.
346. Pavia DL, Lampman GM, Kriz GS. Introduction to spectroscopy : a guide for students of organic chemistry Philadelphia: Saunders College; 1979.
347. Petit JM, Zhu XX. 1H and 13C NMR Study on local dynamics of poly(vinyl alcohol) in aqueous solutions. Macromolecules. 1996;29:2075-2081.
348. Elmarco s.r.o. Nanospider electrospinning technology 2015 [09/10/15]. Available from: http://www.elmarco.com/electrospinning/electrospinning-technology/.
349. Sinah MK, Das BR, Srivastava A, Saxena AK. Influence of process parameters on electrospun nanofibre morphology Asian Journal of Textile. 2013;3(1):8-14.
350. Rathod M, Wright T, Tausif M, Eaton J, Chetty V, Goswami P, et al. E: Setting the height on the collection head. NIRI operating procedures: standard operating procedure for nanospider electrospinner. University of Leeds.2012. p. 11-12.
351. Tao J. Effect of molecular weight and solution concentration on the electrospinning of pva [MSc. thesis]: Worcester polytechnic institute; 2003.
352. Zhao SL, Wu XH, Wang LG, Huang Y. Electrospinning of ethyl-cyanoethyl cellulose/tetrahydrofuran solutions. Journal of Applied Polymer Science. 2004;91(1):242-246.
353. Liu HQ, Hsieh YL. Ultrafine fibrous cellulose membranes from electrospinning of cellulose acetate. Journal of Polymer Science Part B-Polymer Physics. 2002;40(18):2119-2129.
354. Kessick R, Tepper G. Microscale polymeric helical structures produced by electrospinning. Applied Physics Letters. 2004;84(23):4807-4809.
355. Hassan C, Peppas N. Structure and applications of poly(vinyl alcohol) hydrogels produced by conventional crosslinking or by freezing/thawing methods. In: Chang JY, editor. Biopolymers pva hydrogels, anionic polymerisation nanocomposites. Advances in Polymer Science. 153. Berlin: Springer 2000. p. 37-65.
356. Buyle G. Nanoscale finishing of textiles via plasma treatment. Materials Technology. 2009;24(1):46-51.
357. Jagadish NH, Vishalakshi B. Effect of crosslinking on swelling behaviour of IPN hydrogels of guar gum & polyacrylamide. Journal for medical chemistry, pharmaceutical chemistry and computaitional chemistry [Internet]. 2012; 4(3):[946-955 pp.].
358. Donarski JA, Roberts DPT, Charlton AJ. Quantitative NMR spectroscopy for the rapid measurement of methylglyoxal in manuka honey.Analytical Methods. 2010;(2):1479-1483.

Appendix

Appendix A:

Supplementary data is given for Tables 4.4 and 4.5 in Chapter 4.

Table A.1: Zone of inhibition measurements for the Manuka honey coated samples, against *E.coli.*

	Zone Diameter Measurements (mm)						
MGO concentration on sample (mg cm^{-2})	1	2	3	4	Mean diameter across the sample and zone of inhibition (mm)	Calculated zone of inhibition based on *Eq. 3.5* (mm)	Mean zone of inhibition (mm)
0.20	32	32	31.5	32.5	32.0	1	1.58
	34	33	33.5	33.5	33.5	1.75	
	34	34	34	34	34.0	2	
0.15	30	30	30	30	30.0	0	0.75
	32	32	31.5	32.5	32.0	1	
	32	33	32.5	32.5	32.5	1.25	
0.10	31	31	31	31	31.0	0.5	0.42
	31	32	31.5	31.5	31.5	0.75	
	30	30	30	30	30.0	0	
0.0170	-----	-----	-----	-----	N/A	N/A	N/A
0.0054	-----	-----	-----	-----	N/A	N/A	N/A

Table A.2: Zone of inhibition measurements for the synthetic MGO coated samples, against *E.coli*.

	Zone Diameter Measurements						
MGO concentration on sample ($mgcm^2$)	1	2	3	4	Mean diameter across the sample and zone of inhibition (mm)	Calculated zone of inhibition based on *Eq. 3.5* (mm)	Mean zone of inhibition (mm)
1.20	41	38	40	39	39.5	4.75	4.50
	36	37	36.5	36.5	36.5	3.25	
	41	41	40.5	41.5	41.0	5.50	
0.80	32	33	32.5	32.5	32.5	1.25	2.17
	33	32	33	32	32.5	1.25	
	38	38	37.5	38.5	38.0	4.00	
0.40	31	31	31	31	31.0	0.50	1.00
	33	33	32.5	33.5	33.0	1.50	
	31	33	33	31	32.0	1.00	
0.20	-----	-----	-----	-----	N/A	N/A	N/A
0.15	-----	-----	-----	-----	N/A	N/A	N/A
0.10	-----	-----	-----	-----	N/A	N/A	N/A

Table A.3: Zone of inhibition measurements for the Manuka honey coated samples, against *S.aureus*.

	Zone Diameter Measurements (mm)						
MGO concentration on sample (mg cm^{-2})	1	2	3	4	Mean diameter across the sample and zone of inhibition (mm)	Calculated zone of inhibition based on *Eq. 3.5* (mm)	Mean zone of inhibition (mm)
0.20	36	37	36.5	36.5	36.5	3.25	3.08
	36	35	35.5	35.5	35.5	2.75	
	37	36	37	36	36.5	3.25	
0.15	31	31	31	31	31.0	0.5	1.58
	34	33	33.5	33.5	33.5	1.75	
	35	35	34.5	35.5	35.0	2.5	
0.10	31	31	31	31	31.0	0.5	0.17
	30	30	30	30	30	0	
	30	30	30	30	30	0	
0.0170	-----	-----	-----	-----	N/A	N/A	N/A
0.0054	-----	-----	-----	-----	N/A	N/A	N/A

Table A.4: Zone of inhibition measurements for the synthetic MGO coated samples, against *S.aureus*.

	Zone Diameter Measurements						
MGO concentration on sample (mg/cm^2)	1	2	3	4	Mean diameter across the sample and zone of inhibition (mm)	Calculated zone of inhibition based on *Eq. 3.5* (mm)	Mean zone of inhibition (mm)
1.20	38	41	39	40	39.5	4.75	4.50
	39	37	38.5	37.5	38.0	4	
	39	40	40	39	39.5	4.75	
0.80	37	38	37.5	37.5	37.5	3.75	3.08
	38	36	35.5	36.5	36.5	3.25	
	34	35	35	34	34.5	2.25	
0.40	-----	-----	-----	-----	N/A	N/A	N/A
	-----	-----	-----	-----	N/A	N/A	
	-----	-----	-----	-----	N/A	N/A	
0.20	-----	-----	-----	-----	N/A	N/A	N/A
0.15	-----	-----	-----	-----	N/A	N/A	N/A
0.10	-----	-----	-----	-----	N/A	N/A	N/A

Appendix B:

Supplementary data is given for Figure 5.2 in Chapter 5.

Table B.1: Viscosity measurements of PVA/MGO solutions at different concentrations. A spindle size of 31 was used with 9ml of fluid.

	PVA concentration (% w/v)															
	16	18	20	14	16	18	20	12	14	16	18	8	10	12	14	16
	MGO concentration (wt %)															
	No MGO			11.22				14.76				21.57				
Speed (r min^{-1})	**Viscosity (cP)**															
100	----	----	----	287	----	----	----	355	----	----	----	237	277	----	----	----
60	501	----	----	299	483	----	----	357	----	----	----	237	280	415	----	----
50	518	----	----	305	490	----	----	358	719	----	----	239	282	416	----	----
30	525	----	----	321	512	----	----	360	730	----	----	240	283	419	----	----
20	563	970	----	334	535	1063	----	362	749	1387	----	243	286	421	----	----
12	589	1011	----	355	575	1127	----	367	763	1401	----	250	291	427	1213	----
10	621	1030	2180	366	585	1146	2624	371	774	1415	----	258	295	432	1230	----
6	636	1089	2193	380	605	1210	2634	374	783	1421	3147	260	301	435	1245	3864
5	655	1131	2210	----	630	1242	2651	----	791	1441	3141	----	306	444	1257	3857
4	672	1147	2217	----	652	1282	2662	----	802	1480	3162	----	----	465	1261	3884
3	----	1179	2240	----	----	1320	2699	----	----	1490	3191	----	----	490	1273	3919
2.5	----	1213	2250	----	----	1340	2700	----	----	1501	3203	----	----	----	1290	3900
2	----	1245	2261	----	----	1380	2710	----	----	----	3215	----	----	----	----	3891
1.5	----	----	2266	----	----	----	2720	----	----	----	3275	----	----	----	----	3880
1	----	----	2272	----	----	----	2730	----	----	----	----	----	----	----	----	3840

Supplementary data is given for Figure 5.11 in Chapter 5.

Table B.2: Needle electrospun sample measurements and zone of inhibition measurements, against *Ecoli*.

		Sample Diameter Measurements					Zone Diameter Measurements					
Time spun (h)	Mass of MGO based on *Eq.5.1* (mg cm^{-2})	1	2	3	4	Mean sample diameter for testing (mm)	1	2	3	4	Mean diameter across the sample and zone of inhibition (mm)	Calculated zone of inhibition based on *Eq. 3.5* (mm)
0.5	0.75	30	30	30	30	30	30	30	30	30	30	0
1	1.50	30	30	30	30	30	32	32.5	31.5	32	32	1
2	3.00	30	29.5	30.5	30	30	34.5	35	35.5	37	35.5	2.75
3	4.50	30	32.5	32.5	35	32.5	43.5	43	42.5	43	43	5.25
4	6.00	30	30	30	30	30	49	48	48	47	48	9

Table B.3: Needle elctrospun sample measurements and zone of inhibition measurements, against *S.aureus*.

		Sample Diameter Measurements					Zone Diameter Measurements					
Time spun (h)	Mass of MGO based on *Eq.5.1* (mg cm^{-2})	1	2	3	4	Mean sample diameter for testing (mm)	1	2	3	4	Mean diameter across the sample and zone of inhibition (mm)	Calculated zone of inhibition based on *Eq. 3.5* (mm)
0.5	0.75	30	30	30	30	30	30	30	30	30	30	0
1	1.50	30	30	30	30	30	32	32.5	32	31.5	32	1
2	3.00	30	29.5	30.5	30	30	38	39	37.5	39.5	38.5	4.25
3	4.50	30	30.5	29.5	30	30	41.5	44	42	42.5	42.5	6.25
4	6.00	30	30	30	30	30	45	46	45.5	45.5	45.5	7.75

Appendix C:

Supplementary data is given for Figure 6.7 in Chapter 6.

Table C.1: Free surface (needleless) electrospun sample measurements and zone of inhibition measurements, against *Ecoli*.

	Sample Diameter Measurements					**Zone Diameter Measurements**							
Weight of spun web (mg)	1	2	3	4	Mean sample diameter for testing (mm)	1	2	3	4	Mean diameter across the sample and zone of inhibition (mm)	Calculated zone of inhibition based on *Eq. 3.5* (mm)	MGO in fibres based on *Eq.6.2* (mg)	MGO per unit area based on *Eq.6.3* (mg cm^{-2})
10	24	25	27	28	26.0	-----	-----	-----	-----	No Zone	-----	3.46	0.65
20	25	24	26	25	25.0	21.5	22	21	21.5	21.5	-1.75	6.92	1.41
30	24	24	25	23	24.0	25.5	24.5	26	25	25.3	0.63	17.29	3.82
40	29.5	30	28	28.5	29.0	33.5	34.5	35	31	33.5	2.25	34.58	5.24
50	32	31	29	28	30.0	36	37	37	36	36.5	3.25	51.87	7.34

Table C.2: Free surface (needleless) electrospun sample measurements and zone of inhibition measurements, against *S.aureus*.

	Sample Diameter Measurements					**Zone Diameter Measurements**							
Weight of spun web (mg)	1	2	3	4	Mean sample diameter for testing (mm)	1	2	3	4	Mean diameter across the sample and zone of inhibition (mm)	Calculated zone of inhibition based on *Eq. 3.5* (mm)	MGO in fibres based on *Eq.6.2* (mg)	MGO per unit area based on *Eq.6.3* (mg cm^{-2})
10	22	23	23	24	23.0	-----	-----	-----	-----	No Zone	-----	3.46	0.83
20	21	19	20	20	20.0	17	16	19	20	18.0	-1	6.92	2.20
30	30	27	28	29	28.5	28	28.5	27.5	28	28.0	-0.25	17.29	2.71
40	31	33	30.5	33.5	32.0	36.5	34	33.5	34	34.5	1.25	34.58	4.30
50	29	30	31	30	30.0	34	33	35.5	33.5	34.0	2	51.87	7.34

Appendix D:

Supplementary data is given for Figures 7.4 and 7.7 in Chapter 7.

Table D.1:Percentage of MGO released from the GA vapour crosslinked PVA/MGO webs for different crosslinking times .

Crosslinking time (h)	Dispersion time (h)	Weight of fibres before crosslinking (mg)	Amount of MGO in fibres based on *Eq. 6.3* (mg)	MGO released based on HPLC analysis (mg)	Percentage of MGO released from fibres (%)
1	2	565.40	195.52	63.89	33
1	8	1074.10	371.43	150.20	40
1	24	750.10	259.39	144.08	56
8	2	333.32	115.26	73.40	64
8	8	153.58	53.11	36.62	69
8	24	300.23	103.82	78.36	75
24	2	324.08	112.07	66.92	60
24	8	156.47	54.11	36.42	67
24	24	140.53	48.60	33.64	69
48	2	396.05	136.96	47.60	35
48	8	171.55	59.32	28.16	47
48	24	216.66	74.92	37.80	50

Table D.2:Percentage (%) of MGO release from the GA plasma treated PVA/MGO webs after 8 h in water.

Power (W)	Time cycle (sec)	Time on (%)	Crosslinking time (h)	Dispersion time (h)	Weight of fibres before crosslinking (mg)	Amount of MGO in fibres based on *Eq. 6.3* (mg)	MGO released based on HPLC analysis (mg)	Percentage of MGO released from fibres (%)
15	10	20	1	8	243.92	84.35	39.82	47
15	10	40	1	8	293.19	101.39	53.70	53
15	10	60	1	8	284.52	98.39	52.10	53
15	10	80	1	8	354.67	122.65	75.48	62